STATE OF CALIFORNIA • DEPARTMENT OF TRANSPORTATION

TECHNICAL REPORT DOCUMENTATION PAGE

TR0003 (REV 10/98)

ADA Notice

For individuals with sensory disabilities, this document is available in alternate formats. For alternate format information, contact the Forms Management Unit at (916) 445-1233, TTY 711, or write to Records and Forms Management, 1120 N Street, MS-89, Sacramento, CA 95814.

1. REPORT NUMBER	2. GOVERNMENT ASSOCIATION NUMBER	3. RECIPIENT'S CATALOG NUMBER
CA17-2693		

4. TITLE AND SUBTITLE

Development of Recommended Guidelines for Preservation Treatments for Bicycle Routes

5. REPORT DATE

January 2017

6. PERFORMING ORGANIZATION CODE

7. AUTHOR

H. Li, J. Buscheck, J. Harvey, D. Fitch, D. Reger, R. Wu, R. Ketchell, J. Hernandez, B. Hayne

8. PERFORMING ORGANIZATION REPORT NO.

UCPRC-RR-2016-02

9. PERFORMING ORGANIZATION NAME AND ADDRESS

University of California Pavement Research Center
Department of Civil and Environmental Engineering, UC Davis
One Shields Avenue
Davis, CA 95616

10. WORK UNIT NUMBER

11. CONTRACT OR GRANT NUMBER

65A0542

12. SPONSORING AGENCY AND ADDRESS

California Department of Transportation
Division of Research, Innovation and System Information
P.O. Box 942873
Sacramento, CA 94273-0001

13. TYPE OF REPORT AND PERIOD COVERED

Research Report, May 2015 - January 2016

14. SPONSORING AGENCY CODE

15. SUPPLEMENTARY NOTES

Additional author C. Thigpen

16. ABSTRACT

This project was a continuation of a previous study that focused on the effects of pavement macrotexture on bicycle ride quality using input from bicycle club members and their bicycles on state highways, and considered changes to Caltrans chip seal specifications that resulted in seals with larger maximum size stones being typically used. This second project included a wider range of bicycle riders and bicycle types, considered pavement roughness and distresses in addition to macrotexture, and included measurements on urban preservation treatments and city streets as well as on treatments on state highways and county roads. This study also examined preservation treatment aggregate gradations and the mechanistic responses of bicycles to pavement macrotexture and roughness. The results of both projects were used to prepare recommended guidelines for the selection of preservation treatments that are best suited to bicycle routes on California's state highways and local streets. Macrotexture, roughness, and pavement distresses were measured for different preservation treatments on 67 road sections distributed in five northern California and Nevada cities (Davis, Richmond, Sacramento, Reno, and Chico) and on a number of Caltrans highway sections and county roads. Bicycle ride quality surveys were conducted with a total of 155 participants. Correlations of the measurements and ride surveys were preliminarily explored. Models for bicycle ride quality and physical rolling resistance were also developed. Long-term monitoring of pavement macrotexture for larger stone seals on highway LA-2, SLO-1, and Mon-198.

17. KEY WORDS	18. DISTRIBUTION STATEMENT
chip seal, macrotexture, bicycle vibration, bicycle ride quality, MPD, IRI	No restrictions. This document is available to the public through the National Technical Information Service, Springfield, VA 22161

19. SECURITY CLASSIFICATION *(of this report)*	20. NUMBER OF PAGES	21. COST OF REPORT CHARGED
Unclassified	192	None

January 2017
Research Report: UCPRC-RR-2016-02

Development of Recommended Guidelines for Preservation Treatments for Bicycle Routes

Version 2

Authors:
H. Li, J. Buscheck, J. Harvey, D. Fitch, D. Reger, R. Wu, R. Ketchell, J. Hernandez, B. Haynes, and C. Thigpen

Part of Partnered Pavement Research Program (PPRC) Strategic Plan Element 4.57:
Development of Guidelines for Preservation Treatments for Bicycle Routes

PREPARED FOR:

California Department of Transportation
Division of Research, Innovation, and System Information
Office of Materials and Infrastructure

PREPARED BY:

University of California
Pavement Research Center
UC Davis, UC Berkeley

TABLE OF CONTENTS

LIST OF TABLES ..... **vi**
LIST OF FIGURES ..... **vii**
DISCLAIMER STATEMENT ..... **x**
ACKNOWLEDGMENTS ..... **xi**
PROJECT OBJECTIVES ..... **xiii**
EXECUTIVE SUMMARY ..... **xv**
LIST OF ABBREVIATIONS ..... **xxiii**
LIST OF TEST METHODS AND SPECIFICATIONS ..... **xxiii**
1 INTRODUCTION **1**
1.1 Background 1
1.2 Goal and Scope of the Study 2
1.3 Scope and Organization of This Report 3
2 LITERATURE REVIEW **5**
2.1 Pavement Texture Measurement and Ride Quality 5
2.2 Bicycle Vibration and Bicycle Ride Quality 6
2.3 Pavement Macrotexture and Bicycle Ride Quality 7
2.4 Correlations between Macrotexture and Treatment Specifications 8
2.5 Modeling for Bicycle Ride Quality 9
2.6 Modeling for Physical Rolling Resistance 10
2.6.1 A Model and Test Considerations for Physical Resistance 10
2.6.2 Test Considerations 12
3 METHODOLOGY FOR URBAN FIELD MEASUREMENTS AND SURVEYS **15**
3.1 Road Sections Used for Urban Texture Measurements and Bicyclist Surveys 15
3.2 Summary of Urban Pavement Sections for Bicyclist Surveys 16
3.3 Summary of Macrotexture Specification Comparison Sections and Rolling Resistance Measurement Sections 22
3.4 Macrotexture Measurement Methods 24
3.5 Bicycle Vibration Measurement Method 25
3.5.1 Instrumentation 25
3.5.2 Data Processing Procedure 31
3.5.3 Development of Data Collection 32
3.6 Bicycle Ride Quality Survey Method 32
3.6.1 Survey Sample of Surface Treatments and Participants 32
3.6.2 Survey Method for City Surveys 33
3.6.3 Participating Cycling Groups and Road Sections Used in the Survey 33
3.7 Macrotexture and Roughness Measurement Methods 34
3.8 Distress Survey Method 36
3.9 Methodology for Modeling Bicycle Ride Quality 36
3.10 Methodology for Measuring and Modeling Physical Rolling Resistance 36
3.10.1 Test Equipment 37
3.10.2 Test Procedure 37
3.10.3 Selection Criteria for Test Sections 40
3.10.4 Expansion of Power Meter Measurement Systems 40
4 MEASUREMENT AND SURVEY RESULTS AND ANALYSIS **43**
4.1 Macrotexture Results Measured with the Laser Texture Scanner (LTS) 43
4.2 Macrotexture Measured by Inertial Profiler 43
4.2.1 Continuous Macrotexture Results of Different Survey Sections Using IP 43
4.3 Correlation of Macrotexture Measurements with Inertial Profiler and Laser Texture Scanner 47

4.4 IRI Measurement Results 48
4.5 Bicycle Vibration Results 51
4.6 Bicycle Survey Results 58
4.6.1 Acceptability 58
4.6.2 Ride Quality 59
4.7 Correlations between Texture, Vibration, and Ride Quality 65
5 TRENDS BETWEEN PAVEMENT TEXTURE AND ROUGHNESS WITH PRESENCE OF DISTRESSES 73
5.1 City Section Distress Survey 73
5.1.1 Distress Results 73
5.2 Relationships between Pavement Roughness and Distresses 73
5.2.1 IRI and Distresses 73
5.2.2 MPD and Distresses 74
5.2.3 Correlations between Bicycle Vibration and Distresses 75
5.3 Preliminary Exploration of a Bicycle Ride Quality Index 75
5.3.1 Correlation of Bicycle Ride Quality Index and Rider Survey 75
5.3.2 Correlation of Bicycle Ride Quality Index and Distress 78
6 CORRELATIONS BETWEEN PAVEMENT MACROTEXTURE AND TREATMENT SPECIFICATIONS 81
6.1 Macrotexture Measurement Results from Caltrans Highway Sections 81
6.2 Analysis of Chip Seal Projects 88
6.2.1 Correlation of Macrotexture and Chip Seal Aggregate Gradation Specifications 92
6.2.2 Macrotexture versus Time 95
6.3 Analysis of Slurry Seal Sections 96
6.3.1 Correlation of Macrotexture and Slurry Seal Aggregate Gradation Specifications 96
7 MODELING FOR BICYCLE RIDE QUALITY 99
7.1 Data Exploration 99
7.2 Modeling the Acceptability of Pavement 99
7.2.1 Varying Intercept Model 99
7.2.2 Pavement Characteristic Model 100
7.2.3 Bicycle/Personal Characteristics Model 101
7.2.4 Full Model 101
8 MODELING FOR BICYCLE ROLLING RESISTANCE 107
8.1 Comparing Power Meters 107
8.2 Establishing a Baseline Aerodynamic Drag Area for Modeling 108
8.3 Field Backcalculated Coefficient of Rolling Resistance 110
8.4 Effects on Rider Fatigue 114
9 LONG-TERM MONITORING OF MACROTEXTURE CHANGE FOR DIFFERENT TREATMENTS 115
9.1 LA-2 115
9.2 SLO-1 117
9.3 Mon-198 118
9.4 Summary of Long-Term Monitoring Results 120
10 RECOMMENDED GUIDELINES FOR SELECTING PRESERVATION TREATMENT SPECIFICATIONS FOR BICYCLE RIDE QUALITY 123
10.1 Approach Used to Develop Recommended Guidelines 123
10.2 Use of the Recommended Guidelines 124
11 CONCLUSIONS AND RECOMMENDATIONS 131
11.1 Summary 131
11.2 Conclusions 131
11.3 Recommendations 132

REFERENCES **133**
Appendix A: Example Survey Form (Reno) **136**
Appendix B: Macrotexture Measured Using IP on Survey Sections **144**
Appendix C: Plots of Correlations between Texture, Vibration, and Ride Quality by Bicycle Type for This Study **163**
Appendix D: Texture Results of State Highway Sections **166**
Appendix E: Pavement Distress Survey Results **167**

LIST OF TABLES

Table 2.1: Summary of Results 9
Table 3.1: Summary of Road Sections and Surveys in the Study 17
Table 3.2: Summary of Cyclist Surveys 21
Table 3.3: Summary of Survey Sections 22
Table 3.4: Summary of Slurry Sections in the Study for MPD Analysis 22
Table 3.5: Summary of Chip Seal Sections in the Study for MPD Analysis 23
Table 3.6: Summary of Microsurfacing Sections in the Study for MPD Analysis 24
Table 3.7: Summary of State and Local Highway Sections in the Study for Rolling Resistance Measurement 24
Table 3.8: Summary of Measurement Methods for Pavement Surface Characteristics Used in This Study 25
Table 3.9: Road Bicycle Details 27
Table 3.10: Commuter Bicycle Details 29
Table 3.11: Mountain Bicycle Details 30
Table 3.12: Test Sequence Summary 39
Table 4.1: Summary Macrotexture (MPD, mm) Measurements Using the Inertial Profiler for All Survey Sections 46
Table 4.2: Summary Roughness (IRI, m/km) Measurements for All Survey Sections 50
Table 4.3: Summary Table of Bicycling Speed (mph) for Each Survey Section 56
Table 4.4: Summary of Bicycle Vibration Data[a] (*g*) for Each Survey Section 57
Table 4.5: Summary of Ride Quality Acceptability (0 or 1) for Each Survey Section Across All Cities 62
Table 4.6: Summary of Ride Quality (1 to 5) for Each Survey Section Across All Cities 64
Table 4.7: Summary of Values of Variables for Each Survey Section in All Groups 67
Table 5.1: Summary of Average Pavement Distress Survey Results by City 73
Table 5.2: Average IRI Results for Varying Conditions of Pavement 74
Table 5.3: Median MPD Results (mm) for Varying Conditions of Pavement 74
Table 5.4: Summary of Correlations (R^2) between Vibration and Percent of Sections with Cracking 75
Table 5.5: Summary of Correlations (R^2) between BRQI and Mean Survey Results (1 to 5) for Commuter Bicycle by City 76
Table 5.6: Summary of Correlations (R^2) between BRQI and Mean Survey Results (1 to 5) for Mountain Bicycle by City 76
Table 5.7: Summary of Correlations (R^2) between BRQI and Mean Survey Results (1 to 5) for Road Bicycle by City 76
Table 5.8: Summary of Correlations (R^2) between BRQI (events/km) and Mean Survey Results (1 to 5) for Commuter Bicycle by Surface Type 77
Table 5.9: Summary of Correlations (R^2) between BRQI (events/km) and Mean Survey Results (1 to 5) for Mountain Bicycle by Surface Type 77
Table 5.10: Summary of Correlations (R^2) between BRQI (events/km) and Mean Survey Results (1 to 5) for Road Bicycle by Surface Type 78
Table 6.1: Summary of MPD (mm) Results: Chip Seals 82
Table 6.2: Summary of MPD (mm) Results: Slurry Seals 84
Table 6.3: Summary of MPD (mm) Results: Microsurfacings 84
Table 6.4: Summary of Median MPD Results: Chip Seals 89
Table 6.5: Chip Seal Standard Specification Maximum Aggregate Size (first sieve with 100 percent passing) and #4 Sieve Bounds 92
Table 6.6: Summary of Laboratory Gradation Results for Reno Slurry Seal Treatments 96
Table 7.1: Coefficients Resulting from the Modeling for Acceptability 103
Table 8.1: Comparison of Power Meter Testing Results 107
Table 8.2: Summary of Inertial Profiler Testing Results 110
Table 8.3: Summary of Backcalculated Global Coefficient of Friction (μ) Values 111
Table 9.1: Summary of Long-Term Macrotexture Measurements on Test Sections 120
Table 10.1: Median and 25th Percentile (Q1) MPD Values for Each Treatment Specification 126

LIST OF FIGURES

Figure 2.1: Pavement surface texture components and their wavelengths *(3)*. 5
Figure 2.2: Influence of pavement surface texture components on functional performance of motorized vehicles *(3)*. 6
Figure 2.3: Pavement macrotexture (MPD) ranges for different HMA mixture types on California highways considering all ages from new to 16 years of service *(7)*. 7
Figure 2.4: Comparison of MPD values for four commonly used asphalt surface mix types in California for different initial age categories (age category, survey years) and for five years of data collection *(7)*. 8
Figure 3.1: Geographic distribution of the cities selected for the study. 21
Figure 3.2: Road bicycle instrumented with accelerometers (solid red circles) at the typical mounting locations and a GPS unit on the handlebar (circle of blue dashes). 26
Figure 3.3: Detail of front of road bicycle instrumented with accelerometer (solid red circle) at the stem mounting location and a GPS unit on the handlebar (circle of blue dashes). 27
Figure 3.4: Detail of rear of road bicycle instrumented with accelerometer (solid red circle) at the seatpost mounting location. 27
Figure 3.5: Commuter bicycle instrumented with accelerometers (solid red circles) at the typical mounting locations and a GPS unit on the handlebar (circle of blue dashes). 28
Figure 3.6: Detail of front of commuter bicycle instrumented with accelerometer (solid red circle) at the stem mounting location and a GPS unit on the handlebar (circle of blue dashes). 28
Figure 3.7: Detail of rear of commuter bicycle instrumented with accelerometer (solid red circle) at the seatpost mounting location. 28
Figure 3.8: Mountain bicycle instrumented with accelerometers (solid red circles) at the typical mounting locations and a GPS unit on the handlebar (circle of blue dashes). 29
Figure 3.9: Detail of front of mountain bicycle instrumented with accelerometer (solid red circle) at the stem mounting location and a GPS unit on the handlebar (circle of blue dashes). 30
Figure 3.10: Detail of rear of mountain bicycle instrumented with accelerometer (solid red circle) at the seatpost mounting location. 30
Figure 3.11: Example extract of bicycle speed with corresponding acceleration data. 31
Figure 3.12: UCPRC intertial profiler vehicle with rear-mounted high-speed laser (red circle), in the right wheelpath, and GPS unit (orange oval). 34
Figure 3.13: SSI lightweight inertial profiler with rear-mounted high-speed lasers, one in each wheelpath (red circle, shows laser in right wheelpath) and GPS unit (orange oval). 35
Figure 3.14: SSI lightweight inertial profiler with rear-mounted high-speed lasers in both wheelpaths (red circles) and GPS unit (orange oval). 35
Figure 3.15: Manufacturer A power meter crank, front. 38
Figure 3.16: Manufacturer A power meter crank, rear. 38
Figure 3.17: Bicycle instrumented with the Manufacturer A power meter (solid orange circle) and mobile weather station behind bicycle. 38
Figure 3.18: Test rider on baseline test section in upright riding position. 39
Figure 3.19: Manufacturer B cycling power meter left crank arm, front. 41
Figure 3.20: Manufacturer B cycling power meter left crank arm, rear. 41
Figure 4.1: Box plots of MPD from LTS measurements for bicycle lanes or the inside of the edge of traveled way (ETW). 44
Figure 4.2: Summary box plots of macrotexture measured using the inertial profiler for all survey sections of all groups. 45
Figure 4.3: Correlation of macrotexture measurements with the inertial profiler and laser texture scanner. 48
Figure 4.4: Summary box plots of IRI for all the survey sections in all groups. 49
Figure 4.5: Summary box plots of road bicycle vibration for survey sections across all cities. 52
Figure 4.6: Summary box plots of commuter bicycle vibration for survey sections across all cities. 53

Figure 4.7: Summary box plots of mountain bicycle vibration for survey sections across all cities. 54
Figure 4.8: Summary box plot of bicycle vibration for all bicycle types together for survey sections across all cities. 55
Figure 4.9: Summary plot of mean acceptability for each survey section across all cities. 60
Figure 4.10: Summary box plot of mean ride quality for each survey section across all cities. 61
Figure 4.11: Correlations between MPD, IRI, speed, vibration, ride quality level, and acceptability rate (first study [Phases I and II] on rural pavements). 69
Figure 4.12: Correlations between MPD, IRI, speed, vibration, ride quality level, and acceptability rate (second study on urban pavements). 70
Figure 4.13: Correlations between MPD, IRI, speed, vibration, ride quality level, and acceptability rate (first and second studies combined). 71
Figure 5.1: Acceleration BQRI (events/km) versus severity of cracking (1 to 3 scale), road bike, rear mount, 4 g event threshold. 79
Figure 6.1: Summary of state highway sections for comparison of specifications and MPD. 85
Figure 6.2: Ranges of MPD measured on chip seal sections. 86
Figure 6.3: Ranges of MPD measured on slurry seal sections. 87
Figure 6.4: Ranges of MPD measured on microsurfacing sections. 88
Figure 6.5: Distribution of median MPD results for all projects, chip seals. 90
Figure 6.6: Chip seal average of median MPD results by specification type. 91
Figure 6.7: Maximum aggregate size (smallest sieve with 100 percent passing allowed in the specification) versus average median MPD for each chip seal specification type. 93
Figure 6.8: Percent passing #4 sieve upper bound versus average median MPD for chip seal specification types. 93
Figure 6.9: Maximum aggregate size (smallest sieve with 100 percent passing allowed in the specification) versus median MPD for all chip seal sections. 94
Figure 6.10: Percent passing #4 sieve upper bound versus median MPD for all chip seal sections. 94
Figure 6.11: MPD results measured in fall 2015 plotted by project award date. 95
Figure 6.12: Correlations of percent passing the #4 sieve and median MPD (mm). 97
Figure 6.13: Correlations of percent passing the #8 sieve and median MPD (mm). 97
Figure 7.1: Correlations between MPD, IRI, vibration, speed, ride quality level, and acceptability level (all groups) from the first study. 100
Figure 7.2: Counterfactual plot of the simulated predicted probability of acceptance for a simulated rider independent of gender and other influencing personal characteristics. 104
Figure 7.3: Counterfactual plot of the simulated predicted probability of acceptance for the most discriminating rider (a female rider, with at least a BA in education level, who bicycles often). 105
Figure 8.1: Normalized plotted output speeds for three different riding efforts (150 watts, 250 watts, 350 watts). 109
Figure 8.2: Road bicycle power and speed plot of recorded data, given C_DA=0.383 m^2 and a similar standard road bicycle. 109
Figure 8.3: Backcalculated global coefficient of friction, μ, correlations to MPD (mm) with baseline value denoted in red. 111
Figure 8.4: Backcalculated global coefficient of friction, μ, correlations to IRI (inches/mile) with baseline value denoted in red. 112
Figure 9.1: MPD over time on LA-2 by direction. 116
Figure 9.2: Close-up photo of pavement on LA-2. 117
Figure 9.3: MPD over time on the SLO-1 subsections (by post mile and direction) on the shoulder (SHLD) and in the wheelpath (WP). 118
Figure 9.4: MPD over time on Mon-198. 119
Figure 10.1: Decision tree for MPD values. 125
Figure 10.2: MPD values of chip seals with different specifications. 127
Figure 10.3: MPD values of slurry seals with different specifications. 128

Figure 10.4: MPD values of microsurfacings with different specifications. 129
Figure B.1: Macrotexture measured using IP on Davis survey Sections 1 to 4. 145
Figure B.2: Macrotexture measured using IP on Davis survey Sections 5 to 8. 146
Figure B.3: Macrotexture measured using IP on Davis survey Section 9. 147
Figure B.4: Macrotexture measured using IP on Richmond survey Sections 1 to 4. 148
Figure B.5: Macrotexture measured using IP on Richmond survey Sections 5 to 8. 149
Figure B.6: Macrotexture measured using IP on Richmond survey Sections 9 to 12. 150
Figure B.7: Macrotexture measured using IP on Richmond survey Sections 13 to 15. 151
Figure B.8: Macrotexture measured using IP on Sacramento survey Sections 1 to 4 152
Figure B.9: Macrotexture measured using IP on Sacramento survey Sections 5 to 8 153
Figure B.10: Macrotexture measured using IP on Sacramento survey Sections 9 to 11 154
Figure B.11: Macrotexture measured using IP on Reno survey Sections 1 to 4. 155
Figure B.12: Macrotexture measured using IP on Reno survey Sections 5 to 8. 156
Figure B.13: Macrotexture measured using IP on Reno survey Sections 9 to 12. 157
Figure B.14: Macrotexture measured using IP on Reno survey Sections 13 to 16. 158
Figure B.15: Macrotexture measured using IP on Chico survey Sections 1 to 4. 159
Figure B.16: Macrotexture measured using IP on Chico survey Sections 5 to 8. 160
Figure B.17: Macrotexture measured using IP on Chico survey Sections 9 to 12. 161
Figure B.18: Macrotexture measured using IP on Chico survey Sections 13 to 16. 162
Figure C.1: Correlations between MPD, IRI, speed, vibration, ride quality level, and acceptability rate (second study, road bicycles). 163
Figure C.2: Correlations between MPD, IRI, speed, vibration, ride quality level, and acceptability rate (second study, commuter bicycles). 164
Figure C.3: Correlations between MPD, IRI, speed, vibration, ride quality level, and acceptability rate (second study, mountain bicycles). 165
Figure D.1: Summary of MPD of state highway sections. 166

DISCLAIMER STATEMENT

This document is disseminated in the interest of information exchange. The contents of this report reflect the views of the authors who are responsible for the facts and accuracy of the data presented herein. The contents do not necessarily reflect the official views or policies of the State of California or the Federal Highway Administration. This publication does not constitute a standard, specification or regulation. This report does not constitute an endorsement by the Department of any product described herein.

For individuals with sensory disabilities, this document is available in alternate formats. For information, call (916) 654-8899, TTY 711, or write to California Department of Transportation, Division of Research, Innovation and System Information, MS-83, P.O. Box 942873, Sacramento, CA 94273-0001.

ACKNOWLEDGMENTS

The authors would like to acknowledge the interest taken in this project and the assistance offered with it by the following groups and organizations:

Industry

- Dennis Scott, Nick Schaeffer, Ahren Verigin, and Mike Chadd of Surface Systems and Instruments (SSI) for technical support and for developing the lightweight inertial profiler vehicle
- Brian Harer of Lumos & Associates for providing aggregate gradation laboratory test results
- Mike Hall of SRM (Schoberer Rad Messtechnik GmbH) for providing an SRM PowerMeter unit
- Andy Lull of Stages Cycling for providing a power meter unit
- Robby Ketchell of Winning Algorithms for coordinating industry support

Cities and Universities

- Patrick Phelan and Tawfic Halaby of the City of Richmond for their support of the Richmond survey
- Scott Gibson of the Washoe County Regional Transportation Commission for supporting the Reno survey and Elie Hajj of the University of Nevada, Reno for organizing the Reno student volunteers
- Mark Brown of the city of Sacramento Facilities Management Department and Ian Sanders of the Butte County Office of Public Works for specification information
- Kenneth Derucher and Russell Mills of California State University, Chico, for organizing the Chico student volunteers and Janine Rood (Chico Velo) for supporting the Chico survey
- The Work Training Center, Inc. in Chico, California for use of their facilities

Students

- University of Nevada, Reno students: Dario Batioja, Farzan Kazemi, Luis Sibaja, Sandeep Pandey, Johnny Habbouche, Sara Pournoman, Nicholas Weitzel, Ye Yuan, Wadih Zaklit, Jared Herhewe, and Hadi Nabizadeh for staffing the Reno survey
- California State University, Chico: Pedro Valdivia, Jonathan Campos, Manuel Zavala, Janette Calvillo Solis, and Yuliana Calvillo Solis for staffing the Chico survey

Caltrans

- Joe Holland and Nick Burmas of the Caltrans Division of Research, Innovation and System Information for research support and coordination, and Sri Balasubramanian, Haiping Zhou, and Sri Holikatti of the Caltrans Office of Asphalt Pavements for direction and report reviews

UCPRC

- UCPRC friends, students and visiting scholars: Rita Harvey, Jessica Sales, Yong Peng, and UCPRC staff and students for their work administering the surveys
- UCPRC staff: Mark Hannum and Julian Brotschi for field testing, and David Spinner for editing the report

PROJECT OBJECTIVES

This project was a continuation of the work carried out in Caltrans/UCPRC Partnered Pavement Research Center Strategic Plan Element (PPRC SPE) 4.47. The objective of this second project was to propose or recommend guidelines for the design of preservation treatments suitable for bicycle routes on state highways and local streets in California. This was achieved through the following tasks:

1. Texture and roughness measurement for different preservation treatments to:
    a. Determine the typical ranges of texture and roughness for different preservation treatments, in particular for local streets that were not included in the first study;
    b. Determine what the relationships are between pavement texture (macrotexture or mean profile depth [MPD, 0.5 to 50 mm wavelength]) and treatment specifications; and
    c. Determine what the relationship is between pavement roughness (IRI, over 500 mm wavelength) and distresses (transverse cracking, patch, joint cracking/faulting for portland cement concrete [PCC], etc.).
2. Conduct long-term monitoring of texture and roughness change for different treatments on selected sections.
3. Conduct bicycle use surveys to cover a wide range of riders, bicycle types and treatment textures, and IRI, in particular including relatively low-speed commuter bicycles that were not included in the first study.
4. Determine if there are correlations between texture (macrotexture), roughness (IRI), bicycle vibration (frequency, amplitude, and duration), and the consequent ride quality and acceptability of pavement to riders.
5. Develop improved models to characterize the impact of texture, roughness, and vibration on bicycle ride quality and acceptability of pavement to riders.
6. Develop guidelines for selecting appropriate aggregate gradations for preservation treatments from existing Caltrans specifications.
7. Prepare a report documenting the study and study results.

This report includes the results of all of the tasks.

(This page left blank)

EXECUTIVE SUMMARY

The study described in this report is a continuation of an initial two-phase study (Strategic Plan Element 4.47) that the UCPRC performed in 2013 to address chip seal specifications and bicycle ride quality. The initial study included several surveys on bicycle ride quality in Central and Northern California assessing riders' views of what constituted acceptable and unacceptable road conditions in terms of the macrotexture of the surface and bicycle ride quality. The final report delivered in May 2014 incorporated the results from both the initial and subsequent surveys and completed the first study.

The first study examined a limited range of pavement surface treatment types, bicycle types, and bicycle riders. It lacked some of the treatments typically used in urban areas, and instead focused almost exclusively on long-distance, road-type bicycles, and included bicycle riders who were nearly all involved in organized, long-distance riding clubs. To address the surface treatment condition issue more fully, it was determined that the study needed to be extended so that it covered the different surface textures found statewide, included a larger sample of cyclists, used additional instrumentation on bicycles, encompassed urban bicycle routes and commuter-type bicycles, and developed recommended guidelines for the design of preservation treatments suitable for bicycle routes.

The second study, presented in this report, filled these following specific gaps that were identified in the first study:

1. The typical ranges of texture and roughness for different preservation treatments had not been established, particularly for local streets with relatively low-speed commuter bicycles;
2. No relationship had been identified between pavement texture and treatment specifications, specifically gradations;
3. No relationships had been identified between pavement roughness and distresses (that is, transverse cracking, patch, joint cracking/faulting, etc.);
4. The change of texture (macrotexture and megatexture) and roughness of different treatments over time was not understood;
5. The correlations between texture (macrotexture) and roughness (IRI) with bicycle vibration (frequency, amplitude, and duration) and consequent ride quality and rider perception of pavement acceptability had not been established;
6. Additional bicycle surveys were needed to cover a wider range of riders, bicycle types and treatment textures, and IRI, particularly for urban and suburban routes and for riders not using high-performance bicycles with high-pressure tires for long-distance rides;

7. Expanded instrumentation and data collection for bicycles and improved models were needed to characterize the impact of texture and roughness and vibration on bicycle ride quality; and
8. Recommended guidelines for the design and selection of preservation treatments for bicycle routes on state highways and local streets were needed.

The gaps mentioned were addressed by performing the following tasks:

1. Measure texture and roughness for different preservation treatments to:
    a. Determine the typical ranges of texture and roughness for different preservation treatments, in particular for local streets, which were not included in the first study;
    b. Determine what the relationships are between pavement texture (macrotexture or mean profile depth [MPD, 0.5 to 50 mm wavelength]) and treatment specifications; and
    c. Determine what the relationship is between pavement roughness (IRI, over 500 mm wavelength) and distresses (transverse cracking, patch, joint cracking/faulting for portland cement concrete [PCC], etc.).
2. Conduct long-term monitoring of texture and roughness change for different treatments on selected sections.
3. Conduct bicycle use surveys to cover a wide range of riders, bicycle types and treatment textures, and IRI, in particular including relatively low-speed commuter bicycles that were not included in the first study.
4. Determine if there are correlations between texture (macrotexture), roughness (IRI), bicycle vibration (frequency, amplitude, and duration), and the consequent ride quality and acceptability of pavement to riders.
5. Develop improved models to characterize the impact of texture, roughness, and vibration on bicycle ride quality and acceptability of pavement to riders.
6. Develop guidelines for selecting appropriate aggregate gradations for preservation treatments from existing Caltrans specifications.
7. Prepare a report documenting the study and study results.

This report includes the results of all of these tasks. Chapter 2 includes the results of a literature review and covers basic pavement surface texture concepts, typical texture characteristics, and the measured texture values for several types of asphalt surfaces built by Caltrans in the past. The chapter also includes a discussion of the available literature regarding pavement surface texture, bicycle ride quality, and physical rolling resistance. A few studies about bicycle vibration were found in the literature, but they mostly focused on the vibration-caused damage to bicycle frames and handlebars and on optimal frame designs for mountain bicycles and other off-road

bicycles. Many of the studies found investigated the interactions of human behavior and transportation mode choice (car versus bicycle). These studies indicated that variables affecting mode choice include typical vehicle speeds, vehicle traffic flow, road width, availability of bicycle paths, etc. However, no specific data were found in the literature regarding whether or how pavement macrotexture-related bicycle vibration or other factors related to pavement affected travelers' transportation mode choices. Despite the fact that pavement condition can affect both the physical and psychological stress of the rider, the effect of infrastructure on mode choice and ride quality has typically focused on the effects of different types of bicycle facilities. The effects of the pavement itself on bicyclists' perceptions of the acceptability of the level of service (functionality to the user), and mode choice, were only mentioned in a few studies.

Chapter 3 describes the test sections and experimental methods used for field measurements on the surface treatments, including the measurement methods for pavement macrotexture and bicycle vibration. This study conducted measurements of pavement texture and ride quality, and administered bicycle ride quality surveys in five cities (Davis, Richmond, Sacramento, Reno, and Chico). Pavement section selections for the city surveys were based on the following characteristics: uniformity of pavement surface within sections, age, pavement condition, and the logistics of bicycle travel between sections within each city to produce a combined route less than 15 miles long. The UCPRC traveled the sections on bicycle and by car to ascertain the range of surface treatments on the pavements as well as the macrotexture and roughness conditions, and also reached out to local government and nongovernmental bicycle organizations to help select routes in each city with a range of surface treatments and surface conditions. The bicycle surveys collected data from a total of 155 participants who rode on 67 road sections distributed across the five cities, resulting in a total of 2,194 observations.

A number of state and local roads were also measured for pavement texture to look for correlations between macrotexture, in terms of MPD, and treatment type, and between macrotexture and the specifications followed by Caltrans and local governments. Sections were selected based on the availability of documentation of the specifications used for the projects. Measurements of MPD, IRI, rolling resistance, and cycle power requirements were also collected on a small set of local roads for use in mechanistic modeling of bicycle/pavement interaction.

Chapter 4 presents the results and analyses of the pavement surface macrotexture measurements, including the results and correlations of the bicycle vibration and bicycle ride quality surveys in the five selected cities. The main observations from correlation of the combined results from both studies include the following:

a. Strong correlations were found between MPD, bicycle vibration, acceptability, and ride quality level.
b. Medium to weak correlations were found between IRI, bicycle vibration, acceptability, and ride quality level.
c. A relatively weak correlation was found between bicycle vibration and bicycle speed. No significant correlation was found between other variables and bicycle speed (small set of speeds).
d. Vibration appears to be somewhat more sensitive to MPD when MPD values are above 2 mm.
e. Vibration appears to be somewhat more sensitive to IRI when IRI values are above 317 inches/mile (5 m/km).
f. Stronger correlations were found between bicycle vibration with acceptability and ride quality than between MPD and IRI with acceptability and ride quality.
g. The relationship between MPD and ride quality is approximately linear.
h. The following are the approximate ranges of maximum MPD values for bicycle ride quality "acceptability" based on a straight line interpolation for the percentage of participants who rated sections as "acceptable":
    - 80 percent found 1.8 mm MPD acceptable.
    - 60 percent found 2.1 mm MPD acceptable.
    - 50 percent found 2.3 mm MPD acceptable.
    - 40 percent found 2.5 mm MPD acceptable.
i. The average ride quality level rating (on a scale of 1 to 5) is approximately:
    - 3.5 for an MPD of 1.0 mm
    - 3.0 for an MPD of 1.8 mm
    - 2.5 for an MPD of 2.2 mm
    - 1.5 for an MPD of 3.0 mm
j. Most riders rated a pavement as "acceptable" when the ride quality rating was 3 or greater, and the percentage of riders finding a pavement "acceptable" decreased approximately linearly for ride quality ratings below 3 to a point where almost no one found a pavement acceptable when its ride quality rating was about 1.

Chapter 5 presents the results of the exploration of trends between pavement roughness and distresses, and also explores a preliminary bicycle ride quality index (BRQI). Based on the results shown in this chapter, the relationships between distresses and MPD are unclear. On the other hand, a relationship between IRI and distresses was found, but how this affects cyclists is unknown as IRI was developed as a measure of vehicle ride quality. Correlations were explored between a preliminary BRQI based on the number of acceleration events above a threshold and bicycle ride quality. The comparisons of BRQI and mean survey results among pavement

surface types show the strongest correlations between the HMA surface and road bicycle (R^2 = 0.53 to 0.56), commuter bicycle (R^2 = 0.30 to 0.53), and mountain bicycle (R^2 = 0.30 to 0.53). The comparisons between BRQI and mean survey results showed lower R^2 correlations for both the chip seal and slurry seal surface types. The low correlations between the BRQI based on vibration events per kilometer and the survey results indicate that there are likely other characteristics of the pavement surface that can be better correlated to the mean survey results.

Chapter 6 presents the results of correlations between pavement texture and treatment specifications. Correlations were identified between pavement texture measured by MPD and surface treatment specifications. The data used to develop the correlations came from state highway sections selected because specification information was available, and from those city and county sections used for the rider survey analysis for which specifications were also available. The trends found for chip seals were between increasing maximum aggregate size and increasing MPD and between decreasing percent passing the No. 4 sieve (4.76 mm) and increasing MPD, although these correlations were very weak. Although it was found in this study that MPD can decrease as a chip seal is subjected to traffic, no correlation between age and macrotexture was found in this analysis.

Chapters 7 and 8 present the results of modeling of bicycle ride quality and physical rolling resistance, respectively, using the combined results of this study and the previous study. In Chapter 7, the results of the bicycle ride quality surveys, including riders' opinions of the sections and their demographic information, and the measurements of MPD and IRI were used to develop models for predicting the pavement ratings (1 to 5) and the acceptability of the pavement to cyclists. By simulating riders and pavement conditions and holding all other aspects constant, the full model was used to predict the percentage of the population that would rate a given segment as acceptable. The results of the simulations show that it is the combination of MPD and IRI which determines acceptability, and the personal characteristics of the riders also influence the riders' perceptions of acceptability. Results for 80 and 90 percent ratings of acceptability versus MPD and IRI were developed.

In Chapter 8, a physical model for bicycle rolling resistance that uses the global coefficient of friction (μ) as a measure of rolling resistance was calibrated using power meters installed on test bicycles that were ridden over a set of test sections. Correlations between pavement macrotexture measured in MPD and the backcalculated μ results had an R^2 value of 0.70.

Chapter 9 presents the results of long-term monitoring of pavement macrotexture on selected sections. Chapter 10 presents recommended guidelines for selecting macrotexture in terms of MPD for bicycle ride quality and summarizes the range of MPD for the slurry seal, microsurfacing, and chip seal specifications

measured as part of this study. The simulations were performed using two groups of riders: one group (Group 1) sampled across all ranges of personal characteristics and another group (Group 2) representing riders with the personal characteristics associated with the most discriminating opinions about section acceptability. Ranges of acceptable maximum MPD are given in the recommended guidelines, spanning the results of the simulations for Group 1 and Group 2. Controlling the level of IRI on chip seals, surface seals, and microsurfacing treatments as part of construction quality control is beyond an agency's or contractor's capacity, but an agency can chose a particular specification for MPD, as different surface treatments have been shown to yield different MPD ranges. Therefore, the results of the simulations were used to recommend a level of maximum MPD for a given level of IRI for a segment. To make the recommended guidelines workable, the desired IRI values were broken into three categories: <190 inches/mile, 190 to 380 inches/mile, and >380 inches/mile [<3 m/km, 3 to 6 m/km, and >6 m/km]). Estimation of IRI into these three broad ranges should not be difficult. Median and 25th percentile (more conservative) values of MPD for all of the different chip seal, slurry seal and microsurfacing specifications sampled in this study are included with the recommended guidelines, which allow the user to select the specification that meets the desired level of acceptability of the surface treatment to bicyclists.

The scope of these recommended guidelines for choosing a surface treatment specification are based solely on bicycle ride quality. The recommended guidelines also state that other criteria must be considered when selecting a surface treatment specification, including motor vehicle safety in terms of skid resistance under wet conditions, for which minimum MPD requirements should be considered, and the life-cycle cost of the treatment.

Chapter 11 presents conclusions and recommendations. The following conclusions have been drawn from the results and analyses presented:

- Both IRI and MPD are important parameters to determine whether riders find a particular section acceptable, and MPD is more important than IRI.
- The perception of bicycle ride quality appears to depend on the interaction of MPD and IRI; the MPD threshold at which riders will find a given segment unacceptable decreases as IRI increases.
- Considering simple rider demographics or pavement condition variables such as those used in this study does not completely capture the considerable variability among people and among sections that influences what riders consider acceptable or unacceptable pavement condition.
- Increased MPD and to a lesser extent increased IRI were found to correlate with the increased vibration and additional power required to move a bicycle, which matches the rider survey results.

- From the measurements and surveys completed in this study and its predecessor and without considering IRI, 80 percent of riders rated pavements with MPD values of 1.8 mm or less as acceptable and 50 percent rated pavements with MPD values of 2.3 mm or less as acceptable.
- Most treatments used in urban areas produced high acceptability across cities, however, there are some specifications that have a high probability of resulting in high percentages of "unacceptable" ratings from bicyclists.
- Pavement macrotexture generally tends to decrease over time under trafficking, with less reduction outside the wheelpaths than in the wheelpaths.
- The research was successful in identifying ranges of MPD for current Caltrans specifications for chip seals, slurry seals, and microsurfacings, however it was not possible to find useful correlations between MPD and individual sieve sizes within the gradations.
- From laboratory gradation data on aggregate screenings used on slurry seal sections in Reno, Nevada, correlations were found between the median MPD of a pavement surface and the percent passing the #4 (4.75 mm) and #8 (2.36 mm) screen sizes in the constructed gradation.
- The research was successful in developing recommended guidelines that allow pavement treatment designers and pavement managers to select treatment specifications for bicycle routes that will result in a high probability of being found "acceptable" by bicyclists. The scope of the recommended guidelines presented in this report for choosing a surface treatment specification only considers bicycle ride quality. The recommended guidelines also state that other criteria must be considered when selecting a surface treatment specification, including motor vehicle safety in terms of skid resistance under wet conditions, for which minimum MPD requirements should be considered, and the life cycle cost of the treatment.

Based on the results of this study, the following recommendations are made regarding pavement surfaces that will be used by bicyclists:

- Begin use of the recommended guidelines included in this report as part of the surface treatment selection process along with existing guidance that considers criteria other than bicycle ride quality such as motorist safety and treatment life cycle cost, and improve them as experience is gained. The recommendations are for the selection of existing surface treatment specifications based on different levels of bicycle ride quality satisfaction.
- In the recommended guidelines, consider using the 90 percent acceptable MPD level on routes with higher bicycle use as opposed to the 80 percent acceptable MPD level that is also included. Further confidence that the treatment will have an acceptable MPD level can be obtained by selecting treatments based on the 25th percentile MPD instead of the median MPD.

- As new treatment specifications are developed, collect MPD data on them so that they can be included in updated versions of the recommended guidelines.
- If greater precision in developing specifications is desired than is currently possible, consider additional research to develop methods of estimating MPD from gradations and aggregate shape (such as flakiness index).

LIST OF ABBREVIATIONS

AR	Asphalt rubber
ASTM	American Society for Testing and Materials
BRQI	Bicycle Ride Quality Index
C_DA	Coefficient of drag area
C_{RR}	Coefficients of rolling resistance
Caltrans	California Department of Transportation
ConnDOT	Connecticut Department of Transportation
CSU	California State University
CTM	Circular Texture Meter
EMTD	Estimated Mean Texture Depth
ETD	Estimated Texture Depth
ETW	Edge of Traveled Way
HMA	Hot mix asphalt
IFI	International Friction Index
IRB	Institutional Research Board
IRI	International Roughness Index
IP	Inertial Profiler
LTS	Laser Texture Scanner
MCMC	Markov chain Monte Carlo
MPD	Mean Profile Depth
MTD	Mean Texture Depth
PCC	Portland cement concrete
PMAR/RAB	Polymer-modified asphalt rubber/Rubberized asphalt binder
PPRC	Partnered Pavement Research Center
RTC	Regional Transportation Commission
SP	Sand Patch method
SSI	Surface Systems & Instruments
UCPRC	University of California Pavement Research Center
UNR	University of Nevada, Reno
WAIC	Widely Applicable Information Criteria

LIST OF TEST METHODS AND SPECIFICATIONS

ASTM E965-96 (2006)	Standard Test Method for Measuring Pavement Macrotexture Depth Using a Volumetric Technique
ASTM E2157-09	Standard Test Method for Measuring Pavement Macrotexture Properties Using the Circular Track Meter (referenced but not used in this study)
ASTM E2380-09	Standard Test Method for Measuring Pavement Texture Drainage Using an Outflow Meter (referenced but not used in this study)
ASTM E1845-09	Standard Practice for Calculating Pavement Macrotexture Mean Profile Depth
ASTM E1926-08	Standard Practice for Computing International Roughness Index of Roads from Longitudinal Profile Measurements

SI* (MODERN METRIC) CONVERSION FACTORS

APPROXIMATE CONVERSIONS TO SI UNITS

Symbol	When You Know	Multiply By	To Find	Symbol
		LENGTH		
in	inches	25.4	Millimeters	mm
ft	feet	0.305	Meters	m
yd	yards	0.914	Meters	m
mi	miles	1.61	Kilometers	Km
		AREA		
in^2	square inches	645.2	Square millimeters	mm^2
ft^2	square feet	0.093	Square meters	m^2
yd^2	square yard	0.836	Square meters	m^2
ac	acres	0.405	Hectares	ha
mi^2	square miles	2.59	Square kilometers	km^2
		VOLUME		
fl oz	fluid ounces	29.57	Milliliters	mL
gal	gallons	3.785	Liters	L
ft^3	cubic feet	0.028	cubic meters	m^3
yd^3	cubic yards	0.765	cubic meters	m^3
		NOTE: volumes greater than 1000 L shall be shown in m^3		
		MASS		
oz	ounces	28.35	Grams	g
lb	pounds	0.454	Kilograms	kg
T	short tons (2000 lb)	0.907	megagrams (or "metric ton")	Mg (or "t")
		TEMPERATURE (exact degrees)		
°F	Fahrenheit	5 (F-32)/9 or (F-32)/1.8	Celsius	°C
		ILLUMINATION		
fc	foot-candles	10.76	Lux	lx
fl	foot-Lamberts	3.426	$candela/m^2$	cd/m^2
		FORCE and PRESSURE or STRESS		
lbf	poundforce	4.45	Newtons	N
lbf/in^2	poundforce per square inch	6.89	Kilopascals	kPa

APPROXIMATE CONVERSIONS FROM SI UNITS

Symbol	When You Know	Multiply By	To Find	Symbol
		LENGTH		
mm	millimeters	0.039	Inches	in
m	meters	3.28	Feet	ft
m	meters	1.09	Yards	yd
km	kilometers	0.621	Miles	mi
		AREA		
mm^2	square millimeters	0.0016	square inches	in^2
m^2	square meters	10.764	square feet	ft^2
m^2	square meters	1.195	square yards	yd^2
ha	Hectares	2.47	Acres	ac
km^2	square kilometers	0.386	square miles	mi^2
		VOLUME		
mL	Milliliters	0.034	fluid ounces	fl oz
L	liters	0.264	Gallons	gal
m^3	cubic meters	35.314	cubic feet	ft^3
m^3	cubic meters	1.307	cubic yards	yd^3
		MASS		
g	grams	0.035	Ounces	oz
kg	kilograms	2.202	Pounds	lb
Mg (or "t")	megagrams (or "metric ton")	1.103	short tons (2000 lb)	T
		TEMPERATURE (exact degrees)		
°C	Celsius	1.8C+32	Fahrenheit	°F
		ILLUMINATION		
lx	lux	0.0929	foot-candles	fc
cd/m^2	$candela/m^2$	0.2919	foot-Lamberts	fl
		FORCE and PRESSURE or STRESS		
N	newtons	0.225	Poundforce	lbf
kPa	kilopascals	0.145	poundforce per square inch	lbf/in^2

*SI is the symbol for the International System of Units. Appropriate rounding should be made to comply with Section 4 of ASTM E380 (Revised March 2003).

1 INTRODUCTION

1.1 Background

In late 2012, the Caltrans Division of Maintenance in District 5 asked the Division of Maintenance Office of Asphalt Pavement and the Division of Research, Innovation and System Information to evaluate the impact of different chip seal treatments on bicycle ride quality. In January 2013, the Office of Asphalt Pavement and District 5 prepared a scoping document titled "Chip Seals for Highways Including Bicycle Users." Caltrans then requested that the University of California Pavement Research Center (UCPRC), through the Caltrans/UCPRC Partnered Pavement Research Center program, prepare a research work plan in response to the scoping document. The UCPRC developed a work plan titled "Impact of Chip Seal on Bicyclists." Caltrans approved a final version of the work plan in March 2013 but it was updated in July 2013 to include a second phase with additional pavement sections and cyclist surveys. The initial two-phase study (Strategic Plan Element 4.47) that the UCPRC performed in 2013 to address chip seal issues included several surveys on bicycle ride quality in Central and Northern California, assessing riders' views of what constituted acceptable and unacceptable road conditions. A technical memorandum delivered in November 2013 completed the scope of the first study and included the results from the initial survey *(1)*. The final report *(2)* delivered in May 2014 incorporated the results from both the initial and subsequent surveys and completed Phase II of the first study.

The results of the first two-phase study examined a limited range of pavement surface treatment types, bicycle types, and bicycle riders. It lacked some of the treatments typically used in urban areas, and instead focused almost exclusively on long-distance, road-type bicycles, and included bicycle riders who were nearly all involved in organized, long-distance riding clubs. To address the surface treatment condition issue more fully, it was determined that the study needed to be extended so that it covered the different surface textures found statewide, included a larger sample of cyclists, used additional instrumentation on bicycles, encompassed urban bicycle routes and commuter-type bicycles, and developed recommended guidelines for the design of preservation treatments suitable for bicycle routes. The second study, presented in this report, filled these following specific gaps that were identified in the first study:

1. The typical ranges of texture and roughness for different preservation treatments had not been established, particularly for local streets with relatively low-speed commuter bicycles;
2. No relationship had been identified between pavement texture and treatment specifications, specifically gradations;
3. No relationships had been identified between pavement roughness and distresses (that is, transverse cracking, patch, joint cracking/faulting, etc.);

4. The change of texture (macrotexture and megatexture) and roughness of different treatments over time was not understood;
5. The correlations between texture (macrotexture) and roughness (IRI) with bicycle vibration (frequency, amplitude, and duration) and consequent ride quality and rider perception of pavement acceptability had not been established;
6. Additional bicycle surveys were needed to cover a wider range of riders, bicycle types and treatment textures, and IRI, particularly for urban and suburban routes and for riders not using high-performance bicycles with high-pressure tires for long-distance rides;
7. Expanded instrumentation and data collection for bicycles and improved models were needed to characterize the impact of texture and roughness and vibration on bicycle ride quality; and
8. Recommended guidelines for the design and selection of preservation treatments for bicycle routes on state highways and local streets were needed.

1.2 Goal and Scope of the Study

This project was a continuation of the work carried out in Caltrans/UCPRC Partnered Pavement Research Center Strategic Plan Element (PPRC SPE) 4.47. The objective of this second project was to prepare recommended guidelines for the design of preservation treatments suitable for bicycle routes on state highways and local streets in California. This was achieved by performing the following tasks:

1. Measure texture and roughness for different preservation treatments to:
    a. Determine the typical ranges of texture and roughness for different preservation treatments, in particular for local streets, which were not included in the first study;
    b. Determine what the relationships are between pavement texture (macrotexture or mean profile depth [MPD, 0.5 to 50 mm wavelength]) and treatment specifications; and
    c. Determine what the relationship is between pavement roughness (IRI, over 500 mm wavelength) and distresses (transverse cracking, patch, joint cracking/faulting for portland cement concrete [PCC], etc.).
2. Conduct long-term monitoring of texture and roughness change for different treatments on selected sections.
3. Conduct bicycle use surveys to cover a wide range of riders, bicycle types and treatment textures, and IRI, in particular including relatively low-speed commuter bicycles that were not included in the first study.

4. Determine if there are correlations between texture (macrotexture), roughness (IRI), bicycle vibration (frequency, amplitude, and duration), and the consequent ride quality and acceptability of pavement to riders.
5. Develop improved models to characterize the impact of texture, roughness, and vibration on bicycle ride quality and acceptability of pavement to riders.
6. Develop guidelines for selecting appropriate aggregate gradations for preservation treatments from existing Caltrans specifications.
7. Prepare a report documenting the study and study results.

This report includes the results of all of these tasks.

1.3 Scope and Organization of This Report

This research report documents the results from all the tasks in this study combined with results from the previous study. The report also presents recommendations on how to improve the selection of pavement surface treatments for use by bicycles.

Chapter 2 includes the results of a literature review and covers basic pavement surface texture concepts, typical texture characteristics, and the measured texture values for several types of asphalt surfaces built by Caltrans in the past. The chapter also includes a discussion of the available literature regarding pavement surface texture, bicycle ride quality, and physical rolling resistance. Chapter 3 describes the test sections and experimental methods used for field measurements on the surface treatments, including the measurement methods for pavement macrotexture and bicycle vibration. Chapter 4 presents the results and analyses of the pavement surface macrotexture measurements, including the results and correlations of the bicycle vibration and bicycle ride quality surveys in five selected cities. Chapters 5 presents the results of the exploration of trends between pavement roughness and distresses, and also explores a preliminary bicycle ride quality index. Chapter 6 presents the results of correlations between pavement texture and treatment specifications. Chapters 7 and 8 present the results of modeling of bicycle ride quality and physical rolling resistance, respectively, using the combined results of this study and the previous study. Chapter 9 presents the results of long-term monitoring of pavement macrotexture on selected sections. Chapter 10 presents recommended guidelines for selecting macrotexture in terms of MPD for bicycle ride quality and summarizes the range of MPD for the slurry seal, microsurfacing, and chip seal specifications measured as part of this study. Chapter 11 presents conclusions and recommendations. The appendixes contain the forms used in the bicycle surveys (Appendix A), detailed results of field macrotexture measurements using the inertial profilometer (Appendix B), texture, vibration and ride quality correlations (Appendix C), texture results of state highway sections (Appendix D), and pavement distress survey results (Appendix E).

(This page left blank)

2 LITERATURE REVIEW

The literature review presented in Section 2.1 through Section 2.3 was conducted as part of the earlier study (PPRC Strategic Plan Element 4.47) and was reported in Reference *(2)*.

2.1 Pavement Texture Measurement and Ride Quality

Pavement surface texture is an important characteristic that influences ride quality. There are four components of pavement surface texture that are defined based on the maximum dimension (wavelength) of their deviation from a true planar surface: roughness (unevenness), megatexture, macrotexture, and microtexture. The definition of each component is shown in Figure 2.1 *(3)*.

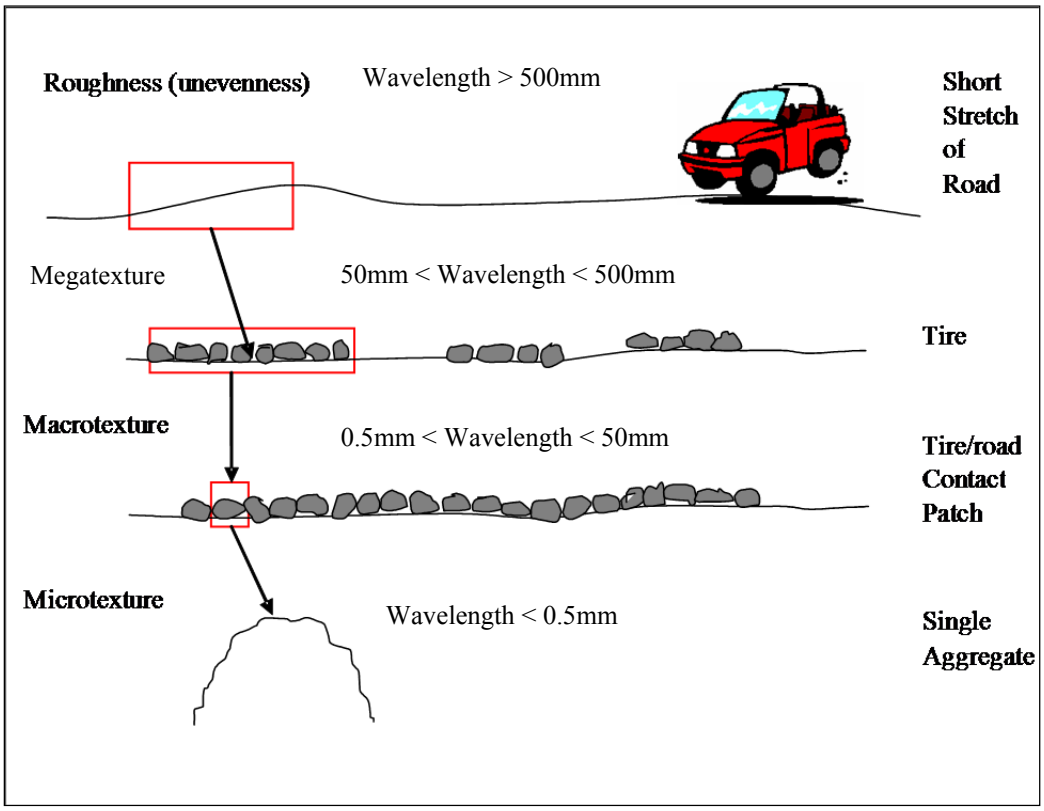

Figure 2.1: Pavement surface texture components and their wavelengths *(3)*.

***(Note:* 500 mm = 1.64 ft, 50 mm = 0.164 ft or 2.0 in., 0.5 mm = 0.02 in.)**

Figure 2.2 shows the relationship among the four components and their influence on the functional performance of pavement. Although the figure notes that vehicle ride quality is primarily affected by megatexture and roughness, for bicycles an examination of macrotexture may be more influential as vibrations caused by this range of wavelengths in the surface texture are most likely to directly affect ride quality. The figure and the

literature *(4-6)* also note that macrotexture is important for vehicle skid resistance and that macrotexture values that are too small can lead to greater risk of wet weather skidding and hydroplaning.

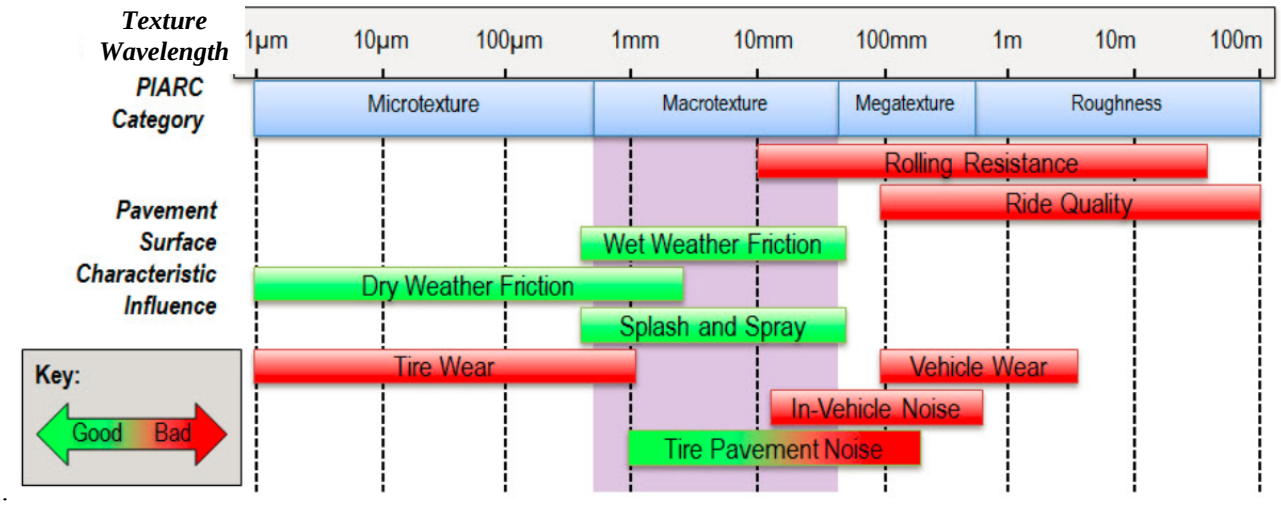

Figure 2.2: Influence of pavement surface texture components on functional performance of motorized vehicles *(3)*.

Macrotexture is typically measured in terms of mean profile depth (MPD) or mean texture depth (MTD), two closely related parameters. Ways to measure them include use of the sand patch method (SP, ASTM E965), the outflow meter (OM, ASTM E2380), the laser texture scanner (LTS, ASTM E2157/ASTM E1845), or the inertial profiler (IP, ASTM E1845).

As is shown in Figure 2.3, MPD values for most hot mix asphalt (HMA) materials historically used on California state highways typically range from approximately 0.019 in. (0.5 mm) to 0.059 in. (1.5 mm), with the macrotexture of some large-stone open-graded materials (F-mixes) that were used for a time on the North Coast going as high as approximately 2.0 mm *(7)*. Generally, the surface macrotexture of in-service asphalt pavements with hot mix asphalt surfaces increases with time *(7)* due to raveling (loss of fines around large aggregates) from traffic, oxidation of the asphalt, and rainfall, as shown in Figure 2.4. This figure also shows that for some materials there may be an initial reduction in MPD after construction due to embedment and the polishing of surface aggregates.

2.2 Bicycle Vibration and Bicycle Ride Quality

A few studies about bicycle vibration were found in the literature. However, these studies mostly focused on the vibration-caused damage to bicycle frames and handlebars and on optimal frame designs for mountain bicycles and other off-road bicycles *(8-12)*.

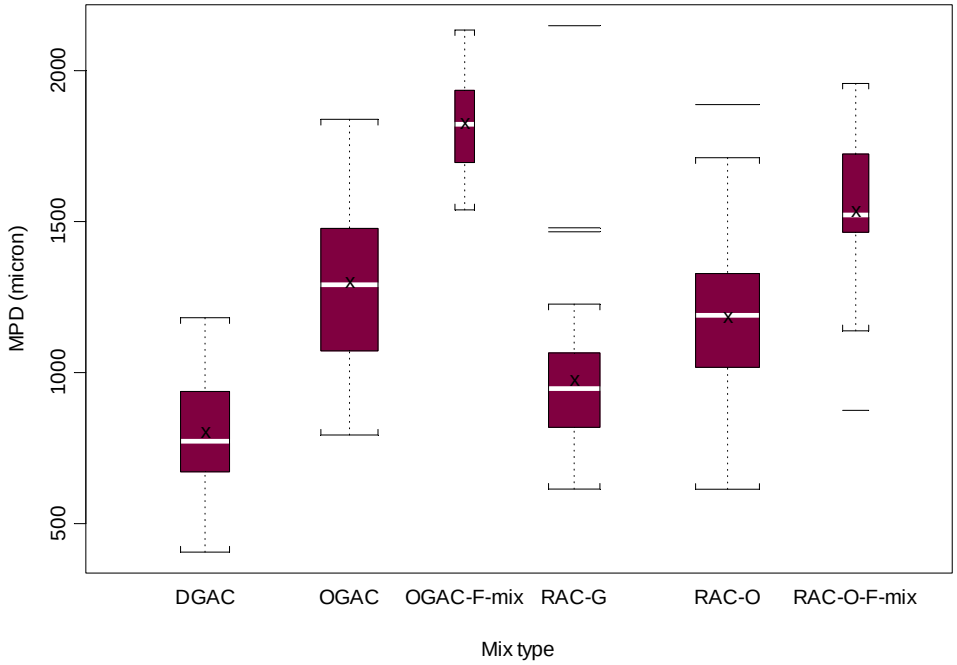

Figure 2.3: Pavement macrotexture (MPD) ranges for different HMA mixture types on California highways considering all ages from new to 16 years of service *(7).*
***(Note:* 1,000 microns = 1 mm = 0.039 inches)**

Notes on Figure 2.3:

1. DGAC is conventional dense-graded asphalt concrete (currently called hot mix asphalt, HMA), OGAC is conventional or polymer-modified open-graded asphalt concrete, OGAC-F mix is large-aggregate Oregon F-type open-graded asphalt concrete, RAC-G is rubberized gap-graded asphalt concrete (currently called RHMA-G), RAC-O is rubberized open-graded asphalt concrete (currently called RHMA-O), and RAC-O-F is rubberized F-type open-graded asphalt concrete.
2. 1,000 microns = 1 millimeter. Both units are typically used for MPD.
3. MPD measurements were made with an inertial profiler measuring in the right wheelpath.
4. The center line is the median value, the "x" close to the center line is the mean value, the colored box indicates the 25th and 75th percentiles (first and third quartiles, Q1 and Q3), the brackets are the minimum and maximum values except for outliers, and the additional lines are outliers defined as being more than 1.5 x (Q3-Q1).

2.3 Pavement Macrotexture and Bicycle Ride Quality

Many of the studies found investigated the interactions of human behavior and transportation mode choice (car versus bicycle). These studies indicated that variables affecting mode choice include typical vehicle speeds, vehicle traffic flow, road width, availability of bicycle paths, etc. *(13-15)*. No specific data were found in the literature regarding whether or how pavement macrotexture-related bicycle vibration or other factors related to pavement affected travelers' transportation mode choices.

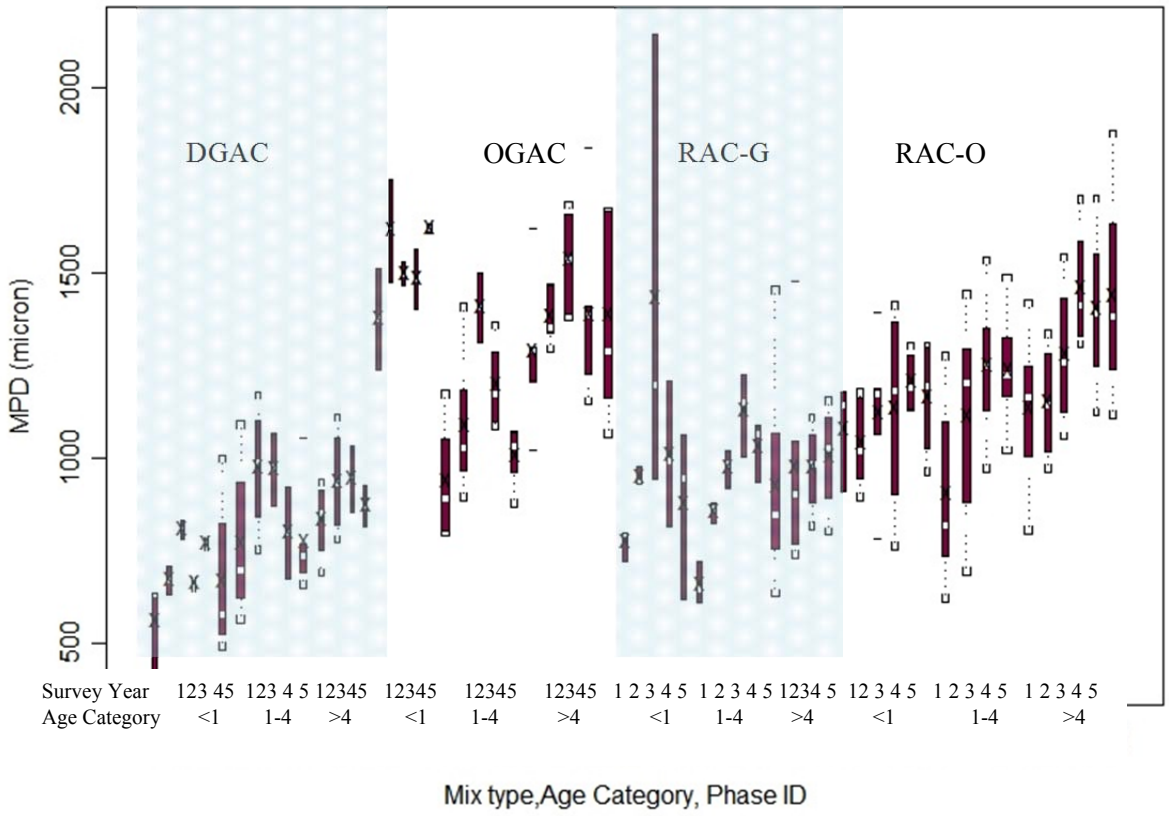

Figure 2.4: Comparison of MPD values for four commonly used asphalt surface mix types in California for different initial age categories (age category, survey years) and for five years of data collection *(7).*
***(Note*: 1,000 microns = 1 mm = 0.039 inches)**

Notes on Figure 2.4:

1. The Survey Year is the year of measurement, and five surveys were performed over the past eight years.
2. The Age category represents the number of years that the surface type was in service at the time of the first-year survey.

2.4 Correlations between Macrotexture and Treatment Specifications

No studies were found in the available literature regarding the relationship between macrotexture and maintenance treatment specifications.

One report had characterized the pavement macrotexture of four different Connecticut Department of Transportation (ConnDOT) Superpave HMA pavement designs with the following nominal maximum size aggregates: 0.187 in. (4.75 mm), 0.25 in. (6.3 mm), 0.375 in. (9.5 mm), and 0.5 in. (12.5 mm) *(16).* The correlation of MPD with aggregate size for the four different pavement designs is shown in Table 2.1.

Results of the study also showed that the MPD for HMA pavements generally increases as less material passes the #4 and #8 (4.75 and 2.36 mm) sieves, creating a coarser gradation.

Table 2.1: Summary of Results

Variable 1	Variable 2	R^2 correlation Value
MPD	Nominal maximum aggregate size	0.8078
MPD	percent passing #4 sieve	0.9555
MPD	percent passing #8 sieve	0.9003

The ConnDOT study used the sand patch method to evaluate MTD, a circular track meter (CTM) to find MPD, and a high-speed laser profiler to also measure MPD along the wheelpath. The study concluded that MPD is the best measure for characterizing HMA pavement macrotexture using the CTM or laser profiler testing equipment. The research recommended further testing on portland cement concrete (PCC) pavements, open-graded friction courses, and various surface treatments.

2.5 Modeling for Bicycle Ride Quality

A growing body of research shows that a number of factors influence someone's decision to bicycle, whether for recreation or as a mode of transportation. Recent studies show that this choice is affected by whether the person enjoys bicycling as well as their perceived safety and comfort *(17, 18).* Studies attempting to determine the phenomena of safety and comfort have typically considered rider safety in terms of potential conflicts with motorized vehicles, and rider comfort in psychological terms based on a cyclist's perceived level of safety. However, pavement condition can also potentially affect a rider's comfort and perceived safety. High levels of texture or roughness cause changes in rolling resistance, forcing a rider to work harder and to possibly experience increased physical discomfort. The pain- or discomfort-inducing vibration a rider may be subject to is transferred upward from the pavement through the cycle's wheels to the handlebars and seats. A rider's psychological discomfort may come about from a worry that poor pavement condition increases the likelihood of a crash or of damage to the bicycle.

Despite the fact that pavement condition can affect both the physical and psychological stress of the rider, the effect of infrastructure on mode choice and ride quality has typically focused on the effects of different types of bicycle facilities *(19, 20).* The effects of the pavement itself on bicyclists' perceptions of the acceptability of the level of service (functionality to the user), and mode choice, were only mentioned in a few studies. A study in London by Parkin et al. found that as the condition of a pavement worsened, the percentage of people who chose a bicycle as their mode of transportation to work decreased *(21)*. Landis et al. *(18)* determined that poor pavement condition is a determining factor in the bicycle level of service. One further important aspect to note is the conclusion by Landis et al. that only by placing bicyclists in the actual conditions where they can feel their cycle's response to the pavement condition (such as the conditions for this study) can a level of service be obtained with confidence. That said, the study also concluded that infrastructure changes alone are insufficient

to cause changes in bicycling mode share. This means that even maintaining pavements in perfect condition does not mean that bicyclists will find the road acceptable if other factors such as interactions with vehicle traffic are still poor.

2.6 Modeling for Physical Rolling Resistance

Modeling of physical rolling resistance provides a means to explain the pavement surface characteristics that affect bicyclist perception of ride quality in addition to vibration. Rolling resistance increases the power required of the rider to move forward, and this can lead to a dissatisfaction that is different than that associated with discomfort from vibration. Studies about modeling a bicycle at steady state and sprint conditions were both found in the literature. Among these was a model by Martin et al. for predicting a cyclist's aerodynamic drag under two different idealized conditions, on a closed circuit track and in the field on open roads; this model is based on a known set of environmental, equipment, and physiological inputs. Proper construction of a field-based model of a bicycle at both steady state and sprint conditions requires considering all the known inputs. A summary of this model and of related work, as they contribute to a physical model for predicting the pavement-rolling resistance of various surface types, is shown below.

2.6.1 A Model and Test Considerations for Physical Resistance

Accurate methods for calculating cycling power rely on precise measurements of aerodynamic drag determined using a wind tunnel *(22)*, and both rolling resistance *(23)* and drivetrain and bearing friction *(24)*, as measured by laboratory equipment. Alternatively, physical and engineering principles can be used to model speed and power during steady state and sprint cycling events when the parameters to the following equation are known *(22, 25)*.

$$P\ x\ E - \frac{\Delta PE}{\Delta t} - \frac{\Delta KE}{\Delta t} = C_D A \frac{1}{2} \rho S_a^2 S_g + \mu S_g \cos[tan^{-1}(G_R)]$$

Where P = Power
E = Efficiency of the bicycle drive system
PE = Potential Energy
KE = Kinetic Energy
T = Time
C_D = Coefficient of drag
A = Frontal area
P = Air density
S_a = Air speed
S_g = Ground speed
μ = Global coefficient of friction
G_R = Road grade
m_T = Total mass of the system (rider + equipment)
g = Gravitational constant

The parameters include the power required to overcome aerodynamic drag, rolling resistance and bearing friction, drive train resistance, and changes in potential and kinetic energy. Aerodynamic drag can account for up to 90 *(26)* to 96 percent *(27)* of the power required on flat surfaces during steady state efforts. The coefficient of drag area (C_DA) and global coefficient of friction in the above equation were derived by multiple linear regression from field test results and did not differ ($P = 0.53$) from measured values in a laboratory wind tunnel *(27)*. The drivetrain efficiency on a bicycle has been measured to be 97.7 percent *(25)*, with the remainder of the power produced by the cyclist being used to overcome changes in kinetic and potential energy and friction caused by the tire-to-road surface interface (C_{rr}) and by bearings in the bicycle wheels. A global coefficient of friction that encapsulates both the coefficient of rolling resistance and bearing friction was used by Martin et al. to accurately predict cycling speed by forward integration with a strong correlation ($r^2 = 0.989$) during non-steady state sprint cycling.

Aerodynamic Drag

The power required to overcome aerodynamic drag is the product of the frontal area and shape of the bicycle and rider, air density, and air and ground speed *(28)*.

$$P_{aero} = C_D A \frac{1}{2} \rho S_a^2 S_g$$

Because the wind direction can change the drag area *(25)*, wind velocity must be corrected for its tangential vector component as a result of wind speed (S_w) and wind direction (D_w), and the ground speed (S_g) and ground direction (D_g) of the rider.

$$S_a = S_w \cos(D_w - D_g) + S_g$$

Rolling Resistance

When a cyclist rides in a straight line, rolling resistance is the product of the combined mass of the cyclist and the bicycle (m_T), tire pressure and construction, and road surface and gradient (G_R) *(29)*. Previously, a reported coefficient of rolling resistance (C_{rr}) for silk tires on a smooth surface was 0.0016 *(23)*. The global coefficient of friction on a track has been calculated as 0.0025 and as 0.0043 on a taxiway *(27)*.

$$P_{rr} = C_{rr}\, S_g\, mT\mathrm{g} \cos[tan^{-1}(G_R)]$$

Turning

When cycling through a turn, a cyclist's center of mass travels at a reduced speed, so the wheels and the center of aerodynamic pressure may not have the same position as the center of mass. The centripetal force (F_c) acts along the longitudinal axis of the cyclist and augments the force acting against the road surface. In addition, there is side loading of each tire that could increase rolling resistance via scrubbing *(25)*. To account for this additional resistance from scrubbing during turns, the equation for calculating the power needed to overcome rolling resistance was updated to include centripetal force (F_c):

$$P_{rr} = S_g\ (\mathrm{mg} + F_c)\cos[tan^{-1}(G_R)]$$

Kinetic and Potential Energy

When a cyclist accelerates from a standing start or is cycling up a steep grade, changes in potential (ΔPE) and kinetic energy (ΔKE) outweigh aerodynamic forces *(30)*. The power to overcome changes in potential energy is related to the combined mass of the rider and bicycle and to the vertical velocity *(22)*.

$$P_{PE} = \frac{\Delta PE}{\Delta t} = S_g\ mg\ \sin[tan^{-1}(G_R)]$$

When a cyclist accelerates, work is done by the system to increase the velocity of the rider and bicycle mass from an initial speed (S_{gi}) to a final speed (S_{gf}). There is also additional kinetic energy stored in the rotation of the wheels. The moment of inertia (I) calculated from the weight about the radius of the wheels (r) is added to the total mass of the rider bicycle system *(25)*.

$$P_{KE} = \frac{\Delta KE}{\Delta t} = \frac{1}{2}\left(m + \frac{I}{r^2}\right)\frac{\left(S_{gf}^2 - S_{gi}^2\right)}{\left(t_f - t_i\right)}$$

2.6.2 Test Considerations

Martin et al. have provided a test protocol for measuring aerodynamic drag area on a closed circuit track and in the field on open roads. This protocol recommends a minimum of five to ten trials per test at constant speeds ranging from 7 $\frac{\mathrm{m}}{s}$ to 12 $\frac{\mathrm{m}}{s}$ to produce a stable global coefficient of friction considering rolling resistance and bearing friction. This information was used to determine the number of replicates when measuring the power required to ride down a pavement test section in this study.

Body Position

The size and shape of a cyclist's body represents the majority of the coefficient of drag area of the total cyclist-bicycle system. Handlebar type *(31)* can decrease C_DA by 68 percent *(25)*. The position of the rider on the handlebar (upright or dropped) also affects aerodynamic drag *(26)*. These results stress that replicating the cyclist's position is paramount for reproducing accurate results and backcalculating rolling resistance.

Equipment

The accuracy of a rolling resistance model is limited by the correctness of the measured power. The SRM™ PowerMeter has previously been validated to +/-2.5 percent, although environmental conditions such as temperature can influence the strain gauges and affect the power readings by 5.2 percent *(32)*. Special consideration needs to be given to ensure correct calibration and recording when environmental conditions such as temperature change.

Track

The protocol by Martin et al. was tested on both an oval, closed circuit track and in the field on a taxiway. These two surface conditions are considered to be ideal baseline conditions to develop the model. Field testing occurred on a straight roadway 472 m long. Neither test accounted for rapid changes in speed or power. It was not proven whether shorter or longer tracks would give similar results, although with less than six trials at 472 m in length *(27)*, the evidence suggests that μ will be unstable.

Air Density

Other considerations when measuring power in the field are barometric pressure, relative humidity, and air temperature at the testing site *(33)*. The formula to calculate the density of moist air, the CIPM 81/91 equation, was revised in 2007 *(34)* based on values for the molar gas constant and density of moist air.

$$\rho_{(10^{-3}kg/m^3)} = \left\{3.48374 + 1.446\left(x_{co_2} - 0.0004\right)\right\}\frac{P}{ZT}(1 - 0.3780x_v)$$

Wind

Aerodynamic forces are also related to the square of air speed. Weather forecasts generally predict wind speeds and direction 30 to 70 m above the effective ground level *(35)*. The effective ground level varies depending on topographical features such as trees and buildings. Prominent features can affect air speed and direction. To correct for these features, wind speed measurements should be taken at the site of testing.

Summary

To date, no one has measured the bicycle rolling resistance values of the surface treatments (different types of chip seals, microsurfacings, slurry seals, cape seals) used on California state highways. The aerodynamic drag field protocol presented by Martin et al. is commonly used within the cycling industry to analyze a rider's aerodynamics and efficiency and was followed in this study when measuring the influence of pavement on bicycle power requirements. These protocols can be applied to calculate a rider's coefficient of drag area on a baseline asphalt pavement road and to backcalculate relative rolling resistance values for pavements with various surface treatments.

3 METHODOLOGY FOR URBAN FIELD MEASUREMENTS AND SURVEYS

The methodology used for the field measurements and surveys in the previous study are described in the report from that study *(2)*. That methodology was updated for this study of urban pavements.

This study conducted measurements of pavement texture and ride quality, and administered bicycle ride quality surveys in five cities. A number of state and local roads were also measured for pavement texture to look for correlations between macrotexture, in terms of MPD, and treatment type, and between macrotexture and the specifications followed by Caltrans and local governments. Measurements of MPD, IRI, rolling resistance and cycle power requirements were also collected on a small set of local roads for use in mechanistic modeling of bicycle/pavement interaction.

3.1 Road Sections Used for Urban Texture Measurements and Bicyclist Surveys

Pavement section selections for the city surveys were based on the following characteristics: uniformity of pavement surface within sections, age, pavement condition, and the logistics of bicycle travel between sections within each city to produce a combined route less than 15 miles long. The UCPRC traveled the sections on bicycle and by car to ascertain the range of surface treatments on the pavements as well as the macrotexture and roughness conditions, and also reached out to local government and nongovernmental bicycle organizations to help select routes in each city with a range of surface treatments and surface conditions.

In Davis, the UCPRC selected an 8.5 mile route with nine sections. In Richmond, the city engineering services department provided the UCPRC with a treatment map that included recently maintained sections in the city. With advice from city staff, a 9.3 mile route with 15 sections was selected. In south Sacramento, the Franklin Neighborhood Development Corporation provided the UCPRC with a community map and guidance on cycling routes within the city based on their initial survey; the UCPRC followed that survey up with one of its own and the result was a 5.7 mile route with 11 sections. In Reno, Nevada, the Washoe County Regional Transportation Commission (RTC) provided the UCPRC with a treatment map that included recently maintained and reconstructed sections. With advice from RTC staff, a 14.5 mile route with 16 sections was selected. In Chico, the Chico Velo Cycling Club provided the UCPRC with local advice on popular cycling routes. After adding input from the club's executive director, a 10.9 mile route with 16 sections was selected.

Table 3.1 lists the road sections used for the urban cyclist surveys, including the measurement methods and the timing of the measurements. The general geographic locations of the cities are shown in Figure 3.1.

3.2 Summary of Urban Pavement Sections for Bicyclist Surveys

With the permission of the UC Davis Institutional Research Board (IRB) administration, which reviews protocols for studies involving human subjects, on-road surveys of bicycle ride quality and surveys of demographics, bicycling habits, and bicycle set-up were conducted in each of the cities. Table 3.2 lists the number of cyclists surveyed, the number of sections they surveyed, and the number observations obtained in the study.

Table 3.1: Summary of Road Sections and Surveys in the Study

City	Sect.	Route Street and Start/ End Cross Streets	Approx. Length (ft)	Pavement Type	Profile Measurements and Dates	Bicycle Vibration Measurements and Dates	Bicyclist Survey Participants and Dates
Davis	1	Portage Bay East from Russell Blvd. to West End	1,850	Polymer-modified asphalt rubber/ Rubberized asphalt binder (PMAR/RAB) Double chip seal	MPD using LTS on Aug 27, 2015 and Aug. 28,2015, profile using IP on Sep. 14, 2015, profile using Smart Car on Sep. 14, 2015	Bicycle vibration using road bicycle on Aug. 13, 2015 and Nov. 18, 2015, bicycle vibration using commuter bicycle on Oct. 23, 2015, bicycle vibration using mountain bicycle on Oct. 23 ,2015	8 riders on May. 23, 2015
Davis	2	Portage Bay West from Arlington Apartment parking lot to Lake Blvd.	750	Slurry seal			
Davis	3	Danube Ave. from Bienville St. to Hudson St.	775	Slurry seal			
Davis	4	Sycamore Ln. from W. 8th to Purdue Dr.	1,180	Asphalt overlay			
Davis	5	Catalina Dr. from Alvarado Ave. to Anza Ave.	650	Slurry seal			
Davis	6	Fiesta/Encina Ave. from Catalina Dr. to Catalina Dr.	2,040	PMAR chip seal			
Davis	7	Del Oro/Cabrillo Ave. from Catalina Dr. to Catalina Dr.	2,040	PMAR chip seal			
Davis	8	8th St. from Oak St. to Anderson Rd.	1,700	HMA			
Davis	9	Anderson Rd. from W. 8th St. to Sunset Ct.	650	Dense-graded HMA overlay			
Richmond	1	8th St. from MacDonald Ave. to Barrett Ave.	850	Slurry over chip seal	MPD using LTS on Aug. 19, 2015 and Sep. 23, 2015, profile using IP on	Bicycle vibration using road bicycle on Nov. 18, 2015, bicycle vibration using commuter	25 riders on Jul. 18, 2015
Richmond	2	Barrett Ave. from 6th St. to A St.	1,600	Slurry seal			
Richmond	3	Richmond Pkwy. from Barrett Ave. to W. Ohio Ave.	2,400	Slurry seal			
Richmond	4	Richmond Pkwy. from W. Cutting Blvd. to Wharf St.	2,600	Slurry seal			
Richmond	5	Richmond Pkwy. from Wharf St. to W. Cutting Blvd.	2,600	Slurry seal			

Richmond	6	W. Cutting Blvd. from Richmond Pkwy. to S. 2nd St.	2,800	Slurry seal	Sep. 22, 2015, profile using Smart Car on Sep. 22, 2015	bicycle on Nov. 24, 2015, bicycle vibration using mountain bicycle on Nov. 24, 2015	
Richmond	7	S. 2nd St. from W. Cutting Blvd. to W. Ohio Ave.	2,000	Slurry seal			
Richmond	8	W. Ohio Ave. from 2nd St. to Harbour Way S.	2,100	Slurry seal w/ HMA patching			
Richmond	9	W. Ohio Ave. from Harbour Way S. to S. 23rd St.	3,350	Slurry seal w/ HMA patching			
Richmond	10	S. 23rd St. from W Ohio Ave. to Virginia Ave.	1,400	Slurry seal			
Richmond	11	Marina Way S. from Cutting Blvd. to Hoffman Blvd.	850	Slurry seal			
Richmond	12	Marina Way S. from Weight Ave. to Regatta Blvd.	1,400	Slurry seal			
Richmond	13	Regatta Blvd. from West End to Melville Sq.	2,500	Slurry seal			
Richmond	14	Regatta Blvd. from Marina Bay Pkwy. to North End	3,000	Slurry seal			
Richmond	15	Meade St. from Regatta Blvd. to E. Montgomery Ave.	2,400	HMA			
Sacramento	1	28th Ave. from 24th St. to 24th St.	850	Cape seal, medium prep	MPD using LTS on Aug. 13, 2015 & Aug. 14, 2015, Profile using IP on Sep. 18, 2015,	Bicycle vibration using road bicycle on Nov. 20, 2015 & Nov. 30, 2015, bicycle vibration using commuter bicycle on Nov. 24, 2015;	41 riders on Aug. 1, 2015
Sacramento	2	26th Ave. from 24th St. to 24th St.	1,330	Cape seal, medium prep			
Sacramento	3	24th St. from 26th Ave. to 16th Ave.	2,900	Slurry seal, Type III			
Sacramento	4	Attawa Ave. from 16th St. to 24th Ave.	2,900	Cape seal, rubberized			
Sacramento	5	23rd St. from 22nd Ave. to 15th Ave.	1,500	Slurry seal, Type II light prep			
Sacramento	6	Wilmington Ave./Deebie St. from W. Pacific Ave. to W. Pacific Bypass	2,000	HMA			
Sacramento	7	10th Ave. from Sutterville Rd. Overpass to Crocker Rd.	1,800	Dense-graded HMA			
Sacramento	8	10th Ave./W. Curtis Dr/9th Ave. from 24th St. to 24th St.	600	Slurry seal Type II medium prep			

Sacramento	9	24th St. from 9th St. to Curtis Way	1,050	HMA	Profile using Smart Car on Sep. 18, 2015	bicycle vibration using mountain bicycle on Oct. 29, 2015	
Sacramento	10	Curtis Way/E. Curtis Dr. 9th Ave.	1,450	HMA			
Sacramento	11	9th Ave./Franklin Blvd./10th Ave. from E. Curtis Dr.to E. Curtis Dr.	450	Slurry seal, Type II medium prep			
Reno	1	Mill St. from Sinclair St. to Holocomb Ave.	820	Slurry seal, Type III	MPD using LTS on Oct. 8, 2015 & Oct/9/2015, Profile using IP on Oct. 8, 2015, Profile using Smart Car on Oct. 8, 2015	Bicycle vibration using road bicycle on Oct. 9, 2015, bicycle vibration using commuter bicycle on Nov. 20, 2015, bicycle vibration using mountain bicycle on Oct. 9, 2015	41 riders on Sep. 26, 2015
Reno	2	Holocomb Ave. from E. Liberty St. to Burns St.	3,000	Slurry seal, Type III			
Reno	3	Holocomb Ave. from Burns St. to Vassar St.	750	Slurry seal, Type III			
Reno	4	Lakeside Dr. from Mt. Rose St. to W. Plumb Ln.	1,400	Slurry seal, Type III modified			
Reno	5	Lakeside Dr. from W. Plumb Ln. to Brinkby Ave.	3,600	HMA			
Reno	6	Plumas St. from Berrum Ln. to Urban Rd.	2,900	Slurry seal, Type III			
Reno	7	S. Arlington Ave. from Urban Rd. to Mt. Rose St.	2,600	Slurry seal, Type II			
Reno	8	S. Arlington Ave. from Mt. Rose St. to California Ave.	3,800	Slurry seal, Type II			
Reno	9	California Ave. from S. Arlington to Memory Ln.	5,700	Slurry seal, Type II			
Reno	10	Mayberry Dr. from Hunter Lake Dr. to S. McCarran Blvd.	6,700	Slurry seal, Type III modified			
Reno	11	Mayberry Dr. from S. McCarran Blvd. to Idlewild Dr	2,500	Slurry seal, Type II			
Reno	12	Mayberry Dr. from Idlewild Dr. to Livermore Dr.	410	Test slurry			
Reno	13	Mayberry Dr. from Livermore Dr. to Aspen Glen Dr.	4,800	Slurry seal, Type III modified			
Reno	14	W 4th St. from Mayberry Dr. to 1,500 ft before S. McCarran Blvd.	7,500	Slurry seal, Type III			
Reno	15	W. 4th St. from S. McCarran Blvd. to Stoker Ave.	6,900	Slurry seal, Type III			

Reno	16	W 1st St. from Vine St. to Ralson St.	1,300	HMA			
Chico	1	Oak Lawn Ave. from W. Sacramento Ave. to Bidwell Ave.	1,270	Unknown	MPD using LTS on Nov. 5, 2015 & Nov. 6, 2015; Profile using IP on Oct. 14, 2015; Profile using Smart Car on Oct. 14, 2015	Bicycle vibration using road bicycle on Nov. 19, 2015; bicycle vibration using commuter bicycle on Nov. 23, 2015; bicycle vibration using mountain bicycle on Nov. 23, 2015	40 riders on Oct. 18, 2015
Chico	2	Bidwell Ave. from Oak Lawn Ave. to Lazy Trail Ave.	3,220	Unknown			
Chico	3	Rose Ave. from Bidwell Ave. to Oak Park Ave.	1,270	Unknown			
Chico	4	Oak Park Ave. from Rose Ave. to Rosenthal Ln.	2,060	Unknown			
Chico	5	Oak Park Ave. from Rosenthal Ln. to W. 1st St.	790	Dense-graded HMA			
Chico	6	W 5th St. from Oak St. to Chico River Rd.	1,480	Chip seal			
Chico	7	North Graves Ave. from Chico River Rd. to Oak St.	1,690	Chip seal			
Chico	8	Miller Ave. from Butte Ave. to Ponoma Ave.	1,900	Unknown			
Chico	9	W. 5th from Chico River Road to Oak St.	1,370	Unknown			
Chico	10	But-32 from Normal Ave. to Orange St.	1,750	Chip seal			
Chico	11	But-32 from Cypress St. to Bartlett St.	2,750	Chip seal			
Chico	12	But-32 from Barlett St. to Cypress St.	2,750	Chip seal			
Chico	13	But-32 from Orange St. to Normal Ave.	1,750	Chip seal			
Chico	14	Mulberry St. from E. 14th St. to E. 19th St.	1,690	Unknown			
Chico	15	Elm St. from E. 21st to E. 23rd St.	1,210	Unknown			
Chico	16	E. 23rd St. from Elm St. to Mulberry St.	530	Unknown			

[a.] *Note:* MPD macrotexture measurement method: IP = inertial profiler (ASTM E1845); LTS = laser texture scanner (ASTM 2157/ASTM E1845).

Figure 3.1: Geographic distribution of the cities selected for the study.

A total of 2,194 observations were collected in the urban pavement cyclist surveys, as shown in Table 3.2. The survey sections are summarized in Table 3.3.

Table 3.2: Summary of Cyclist Surveys

City	No. of Sections	No. of Riders	No. of Observations
Davis, CA	9	8	72
Richmond, CA	15	25	375
Sacramento, CA	11	41	451
Reno, NV	16	41	656
Chico, CA	16	40	640
Total	**67**	**155**	**2,194**

Table 3.3: Summary of Survey Sections

City	Number of Sections for Each Surface Type				
	HMA	Chip Seal	Slurry Seal	Cape Seal	Unknown
Davis	3	3	3	0	0
Richmond	1	0	14	0	0
Sacramento	4	0	4	3	0
Reno	2	0	14	0	0
Chico	1	6	0	0	9
Total	**11**	**9**	**35**	**3**	**9**

3.3 Summary of Macrotexture Specification Comparison Sections and Rolling Resistance Measurement Sections

State highway sections with slurry seals, microsurfacings, and chip seals with known specifications were selected for texture testing. State highway test sections for slurry seal treatments are shown in Table 3.4, for chip seal sections are shown in Table 3.5, and for microsurfacing treatments are shown in Table 3.6. Sections were found using the project search function on the Caltrans Office Engineer *Project Bucket* database at the url *www.dot.ca.gov/hq/esc/oe/planholders/projects_archive.php*. General specification information, begin and end locations, and project milestone dates for each section were obtained from the Caltrans Office Engineer database. The UCPRC intended to collect as-built aggregate gradations for each project and laboratory test data on the screening gradations for each section. But due to the scope of this project and limited resources available, these documents were not obtained. Without laboratory test results from the screenings of each project, the actual gradation for each surface treatment section is unknown. Gradation bands were found by referencing the relevant specification information for each section.

The UCPRC high-speed profile vehicle operator visually verified the start and end location for each section.

Table 3.7 shows a summary of state and local highway sections used for field rolling-resistance testing.

Table 3.4: Summary of Slurry Sections in the Study for MPD Analysis

Section ID	EA	Location	Specification Year	Construction Year	Aggregate Type
Slurry Seal-1	02-3E9404	02-Plu-70-0.0/33.0	2006	2012	Type III
Slurry Seal-4	06-0N3004	06-Tul-201-0.0/14.0	2006	2012	Type III
Slurry Seal-5	07-1W7004	07-LA-66-0.0/3.0	2010	2015	Type II
Slurry Seal-2	03-0G1804	03-Yol-128-7.8/10.0	2010	2015	Type II
Slurry Seal-8	08-0P7904	08-Riv-95-L0.0/36.2	2006	2013	Type III
Slurry Seal-11	11-2M4104	11-SD-94, 188-30.0	2010	2013	Type III

Table 3.5: Summary of Chip Seal Sections in the Study for MPD Analysis

Section ID	EA	Location	Specification Year	Construction Year	Binder Type	Aggregate Type
Chip Seal-15	06-0N2804	06-Kin-33-8.0/19/0	2006	2012	Asphaltic emulsion (polymer-modified)	3/8" medium screenings
	06-0N2804	06-Kin-41-33.0/28.5	2006	2012		
	06-0N2804	06-Mad-145-6.8/0.2	2006	2012		
Chip Seal-44	11-2M2104	11-Imp-78-62.9/80.7	2006	2012	Asphalt rubber binder	1/2" medium precoated screenings
Chip Seal-2	02-3E9004	02-Sis-97-34.5/40.0	2006	2012		
Chip Seal-43	09-354504	09-Mno-395-40.1/44.9	2006	2013	Asphalt rubber binder	3/8" precoated screenings
Chip Seal-8	06-0P7504	06-Ker-46-37.5/49.0	2010	2014	Asphaltic emulsion (polymer-podified)	Coarse 1/2" max. precoated screenings
Chip Seal-13	06-0S2404	06-Fre-33-72.8/R83.0	2010	2015		
	06-0S2404	06-Fre-33-R63.0/69.1	2010	2015		
Chip Seal-7	03-0G1404	03-Yol-16-0.0/18.9	2010	2015	Asphaltic emulsion polymer-modified)	3/8" medium maximum screenings
Chip Seal-10	06-0Q8404	06-Ker-223-10.9/20.0	2010	2014		
	06-0Q8404	06-Ker-223-1.9/4.0	2010	2014		
	06-0Q8404	06-Ker-58-15.4/27.2	2010	2014		
	06-0Q8404	06-Ker-43-16.3/24.1	2010	2014		
Chip Seal-12	06-0S2304	06-Mad-49-1.3/9.3	2010	2015		
	06-0S2304	06-Mad,Mpa-41-40.9/45.7,0.0/4.9	2010	2015		
Chip Seal-31	03-4M5504	03-Gle-162-76.3/84.6	2010	2013		
	03-4M5504	03-Gle-162-67.2/76.3	2010	2013		
Chip Seal-38	06-0Q8504	06-Ker-119-0.0/r9.5	2010	2014		
Chip Seal-41	08-0Q5004	08-SBd,Riv-62-66.0/91.0	2010	2015		
Chip Seal-39	07-2W8304	07-LA-2-26.4/82.3-WB	2010	2012	Asphalt rubber binder	1/2" medium maximum screenings
	07-2W8304	07-LA-2-26.4/82.3-EB		2012		
Chip Seal-6	03-0G1904	03-Sac-104-4.6/17.7		2015		
Chip Seal-9	06-0Q7904	06-Ker-46-54.0/57	2010	2014	Asphalt rubber binder	Coarse 1/2" max. precoated screenings
	06-0Q7904	06-Ker-65-0.7/6.1	2010	2014		
Chip Seal-14	06-0S2504	06-Ker-166, 178-9.0/24.5, 27.2/57.1	2010	2015		
	06-0S2504	06-Ker-178-27.2/57.1-WB	2010	2015		
	06-0S2504	06-Ker-178-27.2/57.1-EB	2010	2015		
Chip Seal-3	02-4E9604	02-Teh-172-0.0/8.9	2010	2013	Asphalt rubber binder	Fine 3/8" max. screenings
Chip Seal-4	02-4F1604	02-Sis-3-R48.3/53.1	2010	2013		
Chip Seal-5	02-4G1704	02-Mod-395-23.3/40.0	2010	2014		
Chip Seal-26	02-4E9704	02-Teh-36-55.2/67.5	2010	2013		
Chip Seal-27	02-4F1304	02-Sha-44-46.3/43.2	2010	2013		
	02-4F1304	02-Sha-44-57.0/48.2	2010	2013		
	02-4F1304	02-Las-139-40.0-30.0	2010	2013		
Chip Seal-28	02-4F1504	02-Sis-97-0.5/R11.5	2010	2013		
	02-4F1504	02-Sis-3-27.0/36.0	2010	2013		
Chip Seal-29	02-4F1804	02-Tri-3-69.0/74.5	2010	2013		
	02-4F1804	02-Teh-36-11.5/6.0	2010	2013		
Chip Seal-30	02-4G9704	02-Sis-3-6.9/23.0	2010	2014		
Chip Seal-42	09-358504	09-Mno-6-26.5/32.3	2010	2014		

Table 3.6: Summary of Microsurfacing Sections in the Study for MPD Analysis

Section ID	EA	Location	Specification Year	Construction Year	Aggregate Type
Microsurfacing-1	02-4E9804	02-Plu-70-37.5/46.2	2010	2013	Microsurfacing Type III
Microsurfacing-2	03-0G1704	03-Pla-28-0.8/5.9	2010	2015	Microsurfacing Type III
	03-0G1704	03-Pla-28-10.5/11.1	2010	2015	Microsurfacing Type III
Microsurfacing-5	03-4M8004	03-ED-89-0.0/8.6	2010	2013	Microsurfacing Type III
Microsurfacing-6	03-4M3404	03-ED-49-15.7/24.0	2006	2012	Microsurfacing Type II
	03-4M3404	03-ED-153-0.0/0.6	2006	2012	Microsurfacing Type II
Microsurfacing-10	08-0P3804	08-SBd-83, 210-R0.0/7.2, R30.2/R33.2	2006	2013	Microsurfacing Type III

Table 3.7: Summary of State and Local Highway Sections in the Study for Rolling Resistance Measurement

Section ID	Route	Start	End	Pavement Description	Length (mi.)	Grade (%)	Approximate Age (years)
1	Yol-RD98	Yol-RD28	Yol-RD29	HMA	0.95	0.1	1 to 5
2	Yol-RD90	38.552282, -121.953750	38.545115, -121.953462	Chip seal	0.52	0.1	10+
3	Sol-Sievers Rd.	38.488945, 121.806407	38.488996, -121.818038	Chip seal	0.53	0.4	0 to 1
4	Sol-Sparlng Rd.	Tremnot Rd.	38.489014, -121.802814	HMA	0.51	0.0	0 to 1
5	UCD-Hopkins Rd.	Hutchinson Rd.	Apiary Rd.	HMA	0.51	0.2	5 to 10
6	UCD-Levee Rd.	Hopkins Rd.	Brooks Rd.	HMA	0.30	0.0	5 to 10
7	Sol-Putah Creek Rd.	38.530862, -121.932791	38.529383, -121.942984	HMA	0.54	0.0	1 to 5
8	Sol-Putah Creek Rd.	38.526193, -121.905949	38.522875, -121.915176	Chip seal	0.53	0.2	5 to 10

Note: Yol = Yolo, Sol = Solano, UCD = UC Davis campus

3.4 Macrotexture Measurement Methods

In this study, macrotexture was measured using both the laser texture scanner (LTS) and the inertial profiler (IP).

LTS tests are performed on a small patch of pavement less than 8 inches by 8 inches square (200 mm by 200 mm). The LTS consists of a laser mounted in a small box that moves back and forth over the surface and provides a three-dimensional image used for calculating macrotexture in terms of mean profile depth (MPD) and mean texture depth (MTD). The inertial profiler (IP) measurement is performed using a high-speed spot laser mounted on a vehicle operating at highway speed. The IP provides a two-dimensional measure of the pavement

surface in the wheelpath measured at high speed (approximately 64 Hz) that is used to calculate macrotexture in terms of MPD. Table 3.8 summarizes the measurement equipment and the standards used.

Table 3.8: Summary of Measurement Methods for Pavement Surface Characteristics Used in This Study

Method	Equipment	Standard	Index	Operational Notes	Sample Size Notes
Laser Texture Scanner	Moving laser	ASTM E1845/ ASTM E2157	MPD/MTD	Requires traffic closure, takes about 20 minutes for one test	Single location measurement
Inertial Profiler	High-speed laser	ASTM E1845	MPD/ MTD	Performed using equipment mounted on vehicle operating at highway speeds	Continuous measurement

Note: MPD is mean profile depth, MTD is mean texture depth.

3.5 Bicycle Vibration Measurement Method

3.5.1 Instrumentation

The procedure used to obtain bicycle vibration measurements in the first study is summarized below (Table 3.9, Table 3.10, and Table 3.11, respectively, list the component details of this study's road, commuter, and mountain bicycles). In this study, a similar procedure was used with the following modifications.

In this study, each bicycle used to measure bicycle vibration was instrumented with two three-axis accelerometers (Model X16-1C, Golf Coast Data Concepts) and a GPS bicycle computer (Garmin™ Edge 510 and Garmin Edge 520). One accelerometer was mounted to the seatpost and the other on the stem with its base normal to the ground in various configurations. The objective was to have one of the three axes measuring acceleration in the direction normal to the ground. The accelerometer took samples at 200 Hz, while the GPS bicycle computer was set to record the location, speed, cadence (revolutions of the wheel per minute), and elevation of the bicycle every second.

The data from the accelerometer and GPS were synchronized using their respective time stamps. Riders made frequent stops between test sections, which permitted accurate synchronization of accelerometer data and GPS data even if the time stamp on the accelerometer was off by several seconds.

Modifications from Initial Study:

1. Data recording was performed with a Garmin Edge 510 and Garmin Edge 520 bicycle computer.
2. GPS collection settings were set to GPS+GPS GLONASS and one-second recording intervals.
3. Speed and cadence were recorded from on-bicycle magnetic sensor measuring systems.

4. The vibration measurements were collected continuously for each city and bicycle type. UCPRC staff utilized the lapping function in the Garmin software to mark the beginning and end locations of the sections. GPS data were reviewed later to verify location.
5. Accelerometers were mounted in two locations, and were unique for each bicycle. Their placement on a road bicycle is shown in Figure 3.2, Figure 3.3, and Figure 3.4, on a commuter bicycle in Figure 3.5, Figure 3.6 and Figure 3.7, and on a mountain bicycle in Figure 3.8, Figure 3.9, and Figure 3.10.

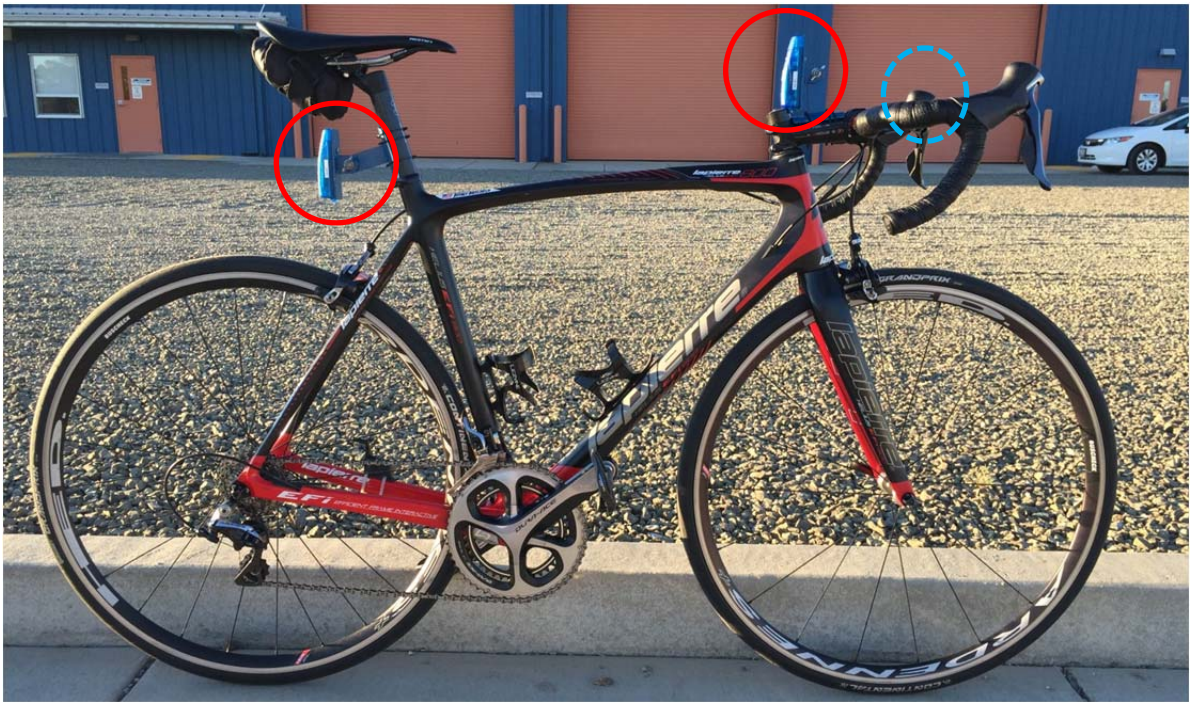

Figure 3.2: Road bicycle instrumented with accelerometers (solid red circles) at the typical mounting locations and a GPS unit on the handlebar (circle of blue dashes).

Figure 3.3: Detail of front of road bicycle instrumented with accelerometer (solid red circle) at the stem mounting location and a GPS unit on the handlebar (circle of blue dashes).

Figure 3.4: Detail of rear of road bicycle instrumented with accelerometer (solid red circle) at the seatpost mounting location.

Table 3.9: Road Bicycle Details

Component	Type	Component	Type
Frame	Carbon Fiber Lapierre Xelius 800	Cassette	Shimano Ultegra 6800
Fork	Carbon Fiber Lapierre Xelius 800	Chain	Shimano Dura Ace 9000
Headset	FSA	Crankset	Shimano Dura Ace 9000, Std.
Stem	Aluminum Easton EA90	Bottom bracket	Shimano Press Fit
Handlebar	Carbon Fiber 3T Ergonova, 42mm	Pedals	Shimano Dura Ace 9000
Grip	Fizik 3mm	Rims	HED Belgium 32 Spoke
Front Brake	Shimano Dura Ace 9000	Spokes	DT Swiss
Rear Brake	Shimano Dura Ace 9000	Hubs	Shimano Ultegra 6800
Front Derailleur	Shimano Dura Ace 9000	Tires	Continental GP4000S II, width = 0.9 in. (23 mm), tire pressure = 115 psi (792 kPa)
Rear Derailleur	Shimano Dura Ace 9000	Saddle	Specialized Romin Expert
Levers	Shimano Dura Ace 9000	Seatpost	Carbon Fiber 3T Stylus

Figure 3.5: Commuter bicycle instrumented with accelerometers (solid red circles) at the typical mounting locations and a GPS unit on the handlebar (circle of blue dashes).

Figure 3.6: Detail of front of commuter bicycle instrumented with accelerometer (solid red circle) at the stem mounting location and a GPS unit on the handlebar (circle of blue dashes).

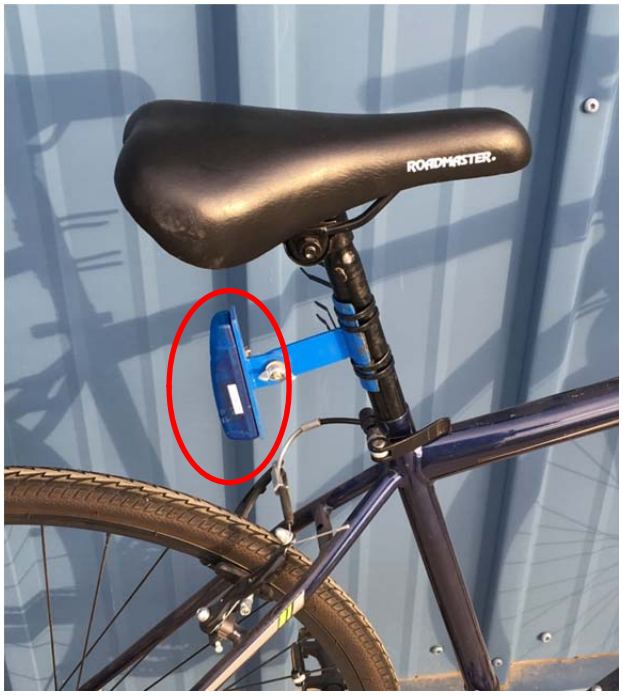

Figure 3.7: Detail of rear of commuter bicycle instrumented with accelerometer (solid red circle) at the seatpost mounting location.

Table 3.10: Commuter Bicycle Details

Component	Type	Component	Type
Frame	Steel Roadmaster Adventures	Cassette	OEM 18-speed
Fork	Steel Roadmaster Adventures	Chain	OEM 18-speed
Headset	OEM	Crankset	OEM 18-speed
Stem	OEM	Bottom bracket	OEM
Handlebar	OEM	Pedals	OEM Platform
Grip	OEM	Rims	OEM 36 spoke
Front Brake	OEM	Spokes	OEM
Rear Brake	OEM	Hubs	OEM
Front Derailleur	OEM 18-speed	Tires	OEM, width = 2 in. (50 mm), tire pressure = 30 psi (207 kPa)
Rear Derailleur	OEM 18-speed	Saddle	OEM
Levers	OEM 18-speed	Seatpost	OEM

Figure 3.8: Mountain bicycle instrumented with accelerometers (solid red circles) at the typical mounting locations and a GPS unit on the handlebar (circle of blue dashes).

Figure 3.9: Detail of front of mountain bicycle instrumented with accelerometer (solid red circle) at the stem mounting location and a GPS unit on the handlebar (circle of blue dashes).

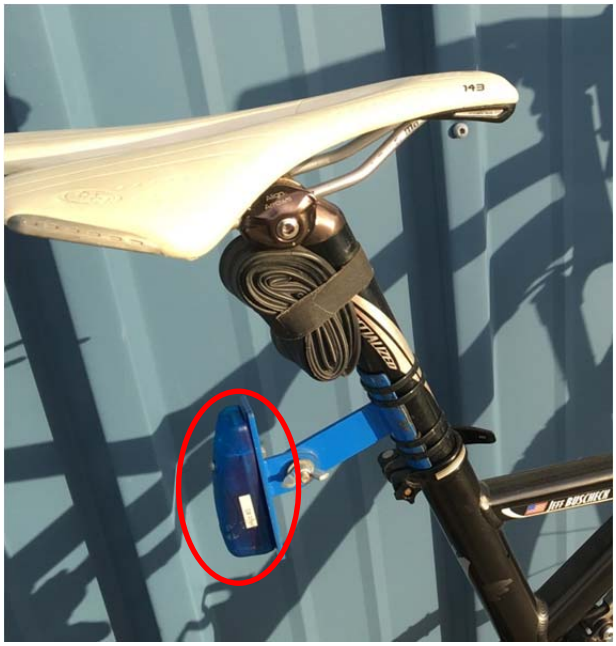

Figure 3.10: Detail of rear of mountain bicycle instrumented with accelerometer (solid red circle) at the seatpost mounting location.

Table 3.11: Mountain Bicycle Details

Component	Type	Component	Type
Frame	Aluminum Specialized Epic Expert	Cassette	Shimano HG61
Fork	Rockshock SID Race, 100 mm Travel	Chain	SRAM PC-971
Rear Shock	Specialized AFR w/ Brain Inertia Valve	Crank	Shimano FC-M762
Headset	Specialzied OEM	Bottom bracket	Shimano M762
Stem	Aluminum Specialized	Pedals	VP Pedal Platform
Handlebar	Aluminum Specialized	Rims	DT Swiss X420SL (26")
Grip	Specialized OEM	Spokes	DT Swiss
Front Brake	Avid Elixir R Carbon SL	Front Hub	Specialized Disc Brake
Rear Brake	Avid Elixir R Carbon SL	Rear Hub	DT Swiss 370 Disc Brake
Front Derailleur	Shimano SLX	Tires	Continental Mountain King, width = 2.4 in. (60 mm), tire pressure = 30 psi (207 kPa)
Rear Derailleur	SRAM X-0	Saddle	Specialized Phenom
Levers	SRAM X-9	Seatpost	Alloy Specialized

3.5.2 Data Processing Procedure

For this study, bicycle vibration is represented by the average acceleration measured in the direction normal to the ground. The following procedure was used to process the data and determine the bicycle vibration for any given road segment:

1. Synchronize the bicycle speed (from GPS) and vibration data (from accelerometer) using time stamps, and apply offsets to the time stamps of the vibration data when necessary.
2. Find the start and end times for a given test section using the GPS location.
3. Extract the bicycle speed and vibration data corresponding to a given test section (an example of the extracted data is shown in Figure 3.11).
4. Remove the portion of the data from when bicycle speed was less than 5 mph.
5. Divide the data into one-second long subsections and calculate the average vibration for each second as the average value of the absolute difference between vibration and gravity (1.0 *g*).
6. Normalize the average vibration for each second to 16 mph by dividing it by the average bicycle speed and multiplying it by 16 mph (26 km/h).
7. Take the weighted average vibration for the whole test section using travel length as the weight. Use this weighted average vibration to represent the overall bicycle vibration for the test section.

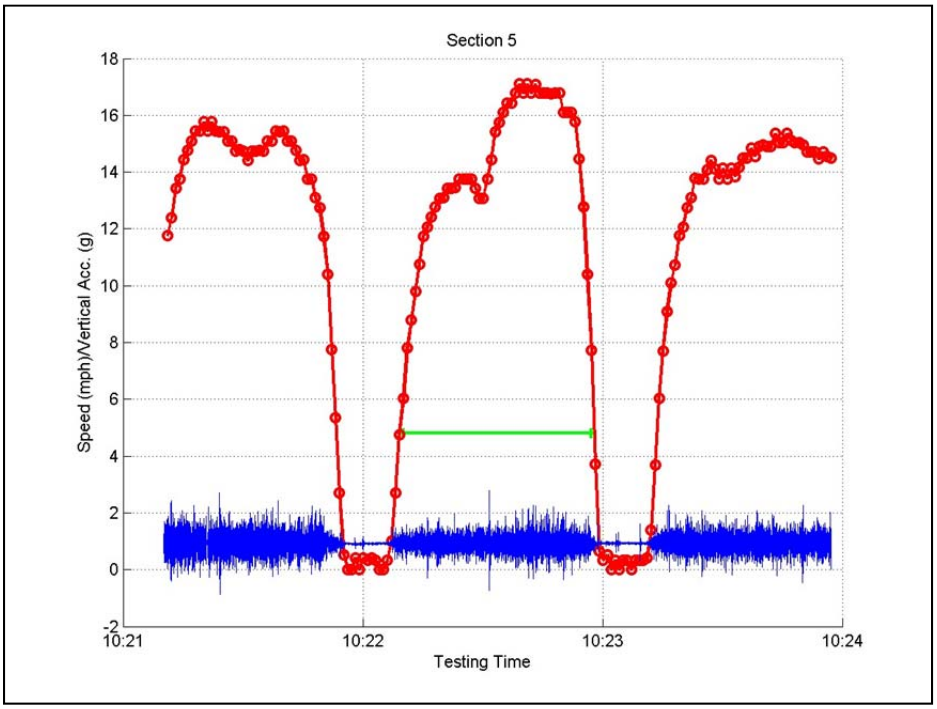

Figure 3.11: Example extract of bicycle speed with corresponding acceleration data.
(Note: **the red line with circles shows speed (mph), the blue line shows acceleration (*g*), and the green line shows the test section portion used for analysis where speed > 5 mph.)**

3.5.3 Development of Data Collection

A number of test rides were performed in the first study to evaluate the instrumentation system and develop the data analysis procedure before it was used for this study. No additional evaluation of the accelerometer instrumentation system was performed in this study.

3.6 Bicycle Ride Quality Survey Method

3.6.1 Survey Sample of Surface Treatments and Participants

Cyclists were given a survey to examine their experience riding on the urban pavement test sections in Davis, Richmond, Sacramento, Reno, and Chico on May 23, July 18, August 1, September 26, and October 18, 2015, respectively. The forms used in the survey—including the pre-ride, in-ride, and post-ride surveys—are presented in Appendix E. The pre-ride survey asked the participants demographic questions, such as their age, gender, and income, as well as questions about their bicycle and typical riding habits. The in-ride survey asked the riders to rate each section, first in terms of whether they considered it "acceptable" or "not acceptable" (with no further instructions given to define those terms), and second on a scale of 1 to 5 with 1 being the worst possible condition and 5 being the best. The post-ride survey asked questions similar to those in the pre- and in-ride surveys, as an aid for interpreting the results. The results of all the surveys and information regarding the volunteers and survey results are included in Chapter 4.

The in-ride survey questions and most of the pre- and post-ride survey questions asked in this study were the same as those asked in the first study, allowing the pooling of response data from both studies for modeling.

Volunteer cyclists were solicited in Davis through email and various social media outlets. Volunteer turnout at the initial Davis survey was less than expected and mostly consisted of people associated with the university. A $40 prepaid debit card was offered as an incentive in later surveys to widen the demographics of the people in the survey. Participants for Richmond, Sacramento, Reno, and Chico were solicited through local agencies and organizations, *Craigslist,* email, and various social media outlets. Altogether, 155 volunteers participated in these urban pavement surveys.

As required by the Institutional Research Board (IRB) of the University of California, Davis, which oversees all research involving human subjects, this was an anonymous survey and participants were identified only by a number, except on the liability waiver form, which was separated from the survey before the volunteers answered any questions.

3.6.2 Survey Method for City Surveys

Following are the approximate times and the tasks conducted on the days of the urban pavement surveys:

- 7:30 a.m. UCPRC staff and volunteers meet at start location.
- 9:00 a.m. Survey riders at survey start location.
- 9:00 a.m. to 9:30 a.m. Sign in, sign waivers, do first part of survey (pre-ride survey), safety talk, explain testing instructions.
- 9:30 a.m. to 11:00 a.m. Ride survey route using directions/map provided. Survey routes include 9 to 16 sections, depending on city. At the end of each section, riders stop to fill out in-ride rating form, then continue on to next section.
- 11:00 a.m. to 12:00 p.m. Survey riders proceed to end location to fill third part of survey (post-ride survey) and collect $40 incentive card (in Richmond, Sacramento, Reno, and Chico).

This entire process took two to three hours depending on the survey route length and survey rider speed.

Riders were given the following verbatim instructions:

1. Riders ride the survey route by following the marked cones, route arrows on the pavement, directions and map provided. Please stay to right side of the road and ride in the bicycle lane when possible.
2. Immediately rate each section (in-ride survey) with the help of UCPRC staff at the end of each section.
3. Once all sections are complete, continue along route to the end location.
4. Fill out the post-ride survey at the end location and proceed to collect $40 incentive prepaid card.

Riders agreed to follow these rules:

a. Ride at your normal speed on each section.
b. Complete the in-ride survey form at the end of each section.
c. Do NOT discuss your perceptions of the sections during the survey.

3.6.3 Participating Cycling Groups and Road Sections Used in the Survey

The urban pavement surveys were administered to different groups of cyclists at scheduled events coordinated by the UCPRC in the five cities of interest. The following groups assisted with the survey events:

- Richmond: City of Richmond Department of Engineering Services
- Sacramento: Franklin Neighborhood Development Corporation
- Reno: Washoe County Regional Transportation Commission and University of Nevada, Reno Department of Civil and Environmental Engineering
- Chico: Chico Velo Cycling Club and California State University, Chico Department of Civil Engineering

3.7 Macrotexture and Roughness Measurement Methods

The urban pavement survey sections were tested for macrotexture in terms of MPD and roughness in terms of IRI using vehicle-mounted, high-speed inertial profilers. Two profilers were used: one belonging to the UCPRC that was used in the earlier study, and a second, light-weight, high-speed profiler that was built by Surface Systems & Instruments Inc. specifically for this project and then rented for it. This second profiler was mounted on a lightweight vehicle (Smart Car) that, unlike the heavier UCPRC vehicle, would be capable of driving bicycle routes on state and local roads and bicycle-specific routes. The SSI/Smart Car system was also used to obtain raw elevation data at 3 mm intervals, less than the standard 1 inch (25.4 mm) sampling interval used for IRI, for use in mechanistic bicycle ride quality modeling.

The UCPRC vehicle and high-speed inertial profiler vehicle is shown in Figure 3.12, and the light-weight vehicle carrying the mounted SSI inertial profiler is shown in Figure 3.13 and Figure 3.14.

Figure 3.12: UCPRC intertial profiler vehicle with rear-mounted high-speed laser (red circle), in the right wheelpath, and GPS unit (orange oval).

Figure 3.13: SSI lightweight inertial profiler with rear-mounted high-speed lasers, one in each wheelpath (red circle, shows laser in right wheelpath) and GPS unit (orange oval).

Figure 3.14: SSI lightweight inertial profiler with rear-mounted high-speed lasers in both wheelpaths (red circles) and GPS unit (orange oval).

3.8 Distress Survey Method

A pavement condition survey was performed on all city survey sections in order to correlate pavement roughness (in IRI) to the extent of distresses found on the pavement. The specific distresses included patching, utility cuts, and cracking (determined as percent of the bicycle path with cracking: >10 percent, 10 to 50 percent, >50 percent). In determining the percentage of the bicycle path with cracking, all types of cracking were considered to be equal. Results of the survey are shown in Appendix E. Bicycle vibration data and distress survey correlations were performed using data from the inertial profilers.

An initial approach to a bicycle ride quality index (BQRI) was also established for correlating IRI to the percent of the bicycle path with cracking. The BRQI value was determined by summing the total acceleration events over a given threshold (2 *g*, 3 *g*, or 4 *g*) and normalizing the sum over the section length. The result, in the unit events per km (events/km), is used to characterize the index. Correlations were also performed by comparing rider survey feedback (on a scale of 1 to 5) and BQRI (events/km).

3.9 Methodology for Modeling Bicycle Ride Quality

The study's *repeated measures* sampling scheme (also called "longitudinal" or "clustered" data) resulted in a hierarchical data structure for ride quality (i.e., multiple participant quality scores from multiple segments within a city). Ride quality was modeled using a multilevel/hierarchical binomial regression model because it matched the data structure and because these types of models have been shown to increase out-of-sample prediction *(36)*. A Bayesian analysis framework was chosen to help guard against model overfitting (i.e., modeling noise in the sample instead of a predictable trend), and because Bayesian probabilities have simple interpretations that would help simplify the discussion *(37)*. The R statistical packages *rethinking* and *rstan* were used as an interface for the probabilistic statistical programming language *Stan*. A No-U-Turn (NUTS) sampler, a form of Hamiltonian Markov chain Monte Carlo (MCMC), was used to estimate the models *(38)*. The performance of each ride quality model was compared through the Widely Applicable Information Criteria (WAIC), a commonly accepted and suitable performance measure for multilevel models. Like all information criteria, WAIC is a relative measure based on model deviance, where lower WAIC values indicate greater theoretical out of sample prediction.

3.10 Methodology for Measuring and Modeling Physical Rolling Resistance

The local road sections to be analyzed for physical rolling-resistance modeling were tested between October 2015 and January 2016. It should be noted that although pavement-rolling resistance was not directly measured in this part of the study, for the purposes of this report the global coefficient of friction was attributed primarily to the pavement's rolling resistance.

To build a physical model for calculating a pavement rolling-resistance coefficient for a standard road bicycle, the model entitled Aerodynamic Drag Area Determined with Field-Based Measures *(27)* was used. The complete protocol is described in the same paper and a corresponding Microsoft *Excel* document *C_DA Calculator (27).* Power output by the rider is the best available estimate of effort by the cyclist and was used to measure total fatigue.

A summary of the test equipment used and the procedure followed, with modifications, are described below.

3.10.1 Test Equipment

The physical rolling resistance testing was performed using a road bicycle instrumented with a Garmin Edge 520 GPS computer, similar to the one used in the vibration analysis. A power meter was added to measure power output.

A power meter crank calculates a rider's power output by measuring the crank arm torque via four sets of strain gauges in the crank spindle. The crank arm (system lever arm) has a known length of 172.5 mm, and the speed of the pedal stroke is measured to find angular velocity. The power output is then calculated:

$$Torque\ x\ Angular\ Velocity = Power\ Output\ by\ Rider$$

where torque is measured in newton-meters (Nm), angular velocity in revolutions per minute (rpm), and power output in watts (W).

The Garmin Edge 520 bicycle computer collected power output values every second. The power meter from Manufacturer A is shown in Figure 3.15 and Figure 3.16.

3.10.2 Test Procedure

The beginning and end points for each test section were clearly established with cones and lines painted on the pavement. The weather station was placed at the midpoint of the section and set to a height relevant to the wind resistance experienced by the rider. The weather station collected wind speed, direction, humidity, atmospheric pressure, and temperature. Data were collected every minute. The weather station and test bicycle are shown in Figure 3.17.

Figure 3.15: Manufacturer A power meter crank, front.

Figure 3.16: Manufacturer A power meter crank, rear.

Localized weather condition data were sampled using a Davis Instruments™ Vantage Pro 2 weather station.

Figure 3.17: Bicycle instrumented with the Manufacturer A power meter (solid orange circle) and mobile weather station behind bicycle.

After an initial warm up, the test rider pedaled backwards to perform a zero-offset calibration of the power meter. This was necessary to account for environmental effects on the strain gauges and changes in mechanical drag in the bicycle drive train system. The test sequence is summarized in Table 3.12. A minimum of six tests were performed in each direction.

Table 3.12: Test Sequence Summary

Run	Direction	Power (watts)	Notes
Warm up	–	Various	
1	Out	350	Used for modeling
2	Back	350	
3	Out	300	–
4	Back	300	
5	Out	250	Used for modeling
6	Back	250	
7	Out	200	–
8	Back	200	
9	Out	150	Used for modeling
10	Back	150	
11	Out	350	Used for daily test validation
12	Back	350	
Warm down	–	Various	

For each replicate, the rider's power output was treated as the control variable; it was monitored in real time and displayed by the Garmin Edge 520. Final output speeds ranged from 15 to 26 mph (24 to 42 km/hr), depending on power sequence and pavement type. The 350 watt test interval was repeated in both directions to check for changes in rider position and/or environmental conditions during the test period. Riders took a standard position with head upright and hands upright and placed on the hoods of the bar *(26)*. The standard test cadence was set to 80+/-10 rpm to reduce the effects of pedaling style on aerodynamics. To minimize changes in aerodynamic drag area between tests, riders were issued a standard set of equipment including identical clothing, helmet, and sunglasses for each test. A test rider on the baseline HMA section is shown in Figure 3.18.

Figure 3.18: Test rider on baseline test section in upright riding position.

Assuming a constant coefficient of aerodynamic drag for each test section, the following data were input to Martin's model to backcalculate the coefficient of rolling resistance for the cyclist:

- Rider data: Bicycle weight + rider weight = system weight
- Section data: grade, direction
- Bicycle data: Power, initial velocity, final velocity, average velocity, time elapsed
- Environmental data: Temperature, humidity, atmospheric pressure, wind component calculated from wind velocity and wind direction relative to rider

The following data were also collected:

- Section data: Length
- Bicycle data: Cadence, heart rate

The calculated R-squared value for each test section had to meet or exceed the 98 percent threshold set by Martin.

3.10.3 Selection Criteria for Test Sections

Test sections were selected using the guidelines presented by Martin and included the following considerations:

- Uniform pavement surface
- Length: 0.33 to 1 mile
- Constant elevation grade with a slope less than 0.5 percent
- Straight with no traffic controls
- Minimal obstructions that would cause differences in local wind conditions (e.g., buildings and trees)
- Baseline sections: dense-graded HMA with IRI 90 to 120 inches/mile (1.42 to 1.89 m/km). Assume a global coefficient of friction of μ=0.004 for HMA baseline.

3.10.4 Expansion of Power Meter Measurement Systems

In order to explore additional methods of measuring rider power output values, a second power meter (shown in Figure 3.19 and Figure 3.20, including battery/strain gauges) was used on selected test sections. The data collected by both devices were compared for the validation. Like the power meter from Manufacturer A, the power meter from Manufacturer B consists of a series of strain gauges that are installed on the left crank arm; these gauges are used estimate the rider's total power output by measuring the torque applied to the crank arm. The unit from Manufacturer B also measures crank arm angular velocity.

Figure 3.19: Manufacturer B cycling power meter left crank arm, front.

Figure 3.20: Manufacturer B cycling power meter left crank arm, rear.

(This page left blank.)

4 MEASUREMENT AND SURVEY RESULTS AND ANALYSIS

Following the approach described in Section 3.2, cyclists were surveyed in different cities to obtain a larger sample of riders with broader demographic characteristics and a larger sample of pavement road sections. Using the methods described in Section 3.4 and Section 3.5, pavement macrotexture in terms of MPD, roughness in terms of IRI, and bicycle vibration were measured to characterize the pavement surface and dynamic response of bicycles.

4.1 Macrotexture Results Measured with the Laser Texture Scanner (LTS)

Pavement macrotexture was measured using the laser texture scanner method at different locations on each road section. The measurements were mainly performed at locations approximately 6 inches (150 mm) inside and outside the white edge of traveled way (ETW) stripes, where most bicyclists ride when there is traffic. The macrotexture results measured, in terms of MPD, from all the five cities are presented in Figure 4.1. The MPD values ranged from approximately 0.1 mm to 4.0 mm, with the median values ranging from 0.3 mm to 2.0 mm.

4.2 Macrotexture Measured by Inertial Profiler

Measurements taken with the inertial profiler (IP) followed a continuous line for the entire length of each section included in this study. The IP was run in the same direction and general location that the bicyclists rode for each survey section. Wherever possible for the group survey sections and most of the sections surveyed only for texture, the IP was run both inside (near the wheelpath) and outside the ETW stripe (on the shoulder) in the cyclist's direction of travel; but in some cases where the Caltrans sections were surveyed only for texture, the IP was run in both directions.

4.2.1 Continuous Macrotexture Results of Different Survey Sections Using IP

Figure 4.2 uses box plots to show the macrotexture measurements taken with the IP along the entire length of each pavement section in the five cities (see Table 3.1 for details of each section). The figure shows that the median MPD values across all the sections were in the approximate range of 0.3 mm to 1.9 mm, while the MPD values for several sections (Sections 6 and 7 in the Davis group and Sections 13 to 15 in the Richmond group) were around approximately 2.0 mm. The MPD values within most sections show small variations, while Chico Sections 3 and 15 show relatively larger variations within the sections. The MPD of each section measured by the IP for all the groups has been summarized in Table 4.1.

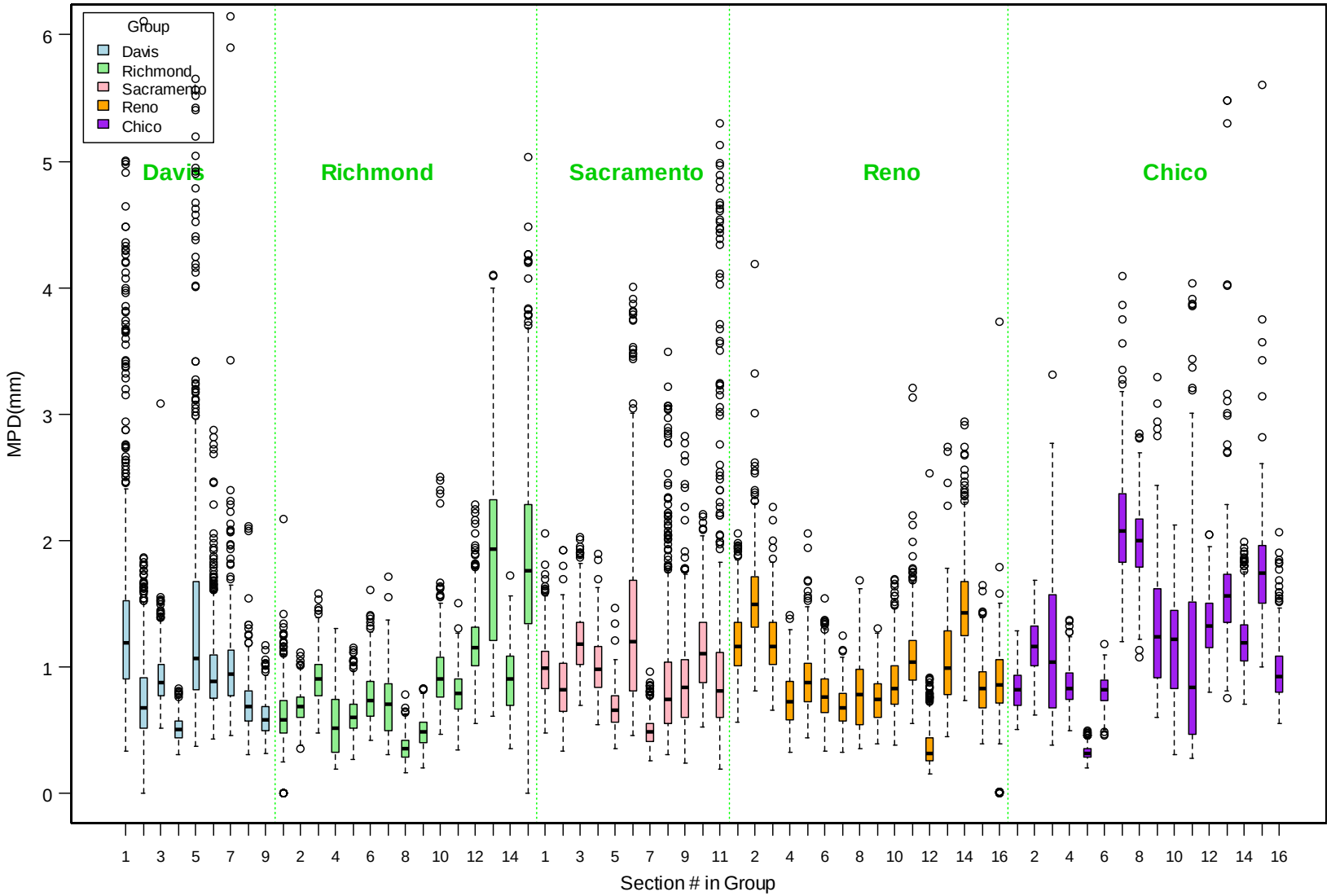

Figure 4.1: Box plots of MPD from LTS measurements for bicycle lanes or the inside of the edge of traveled way (ETW). *(Note:* 1 mm = 0.039 inches)

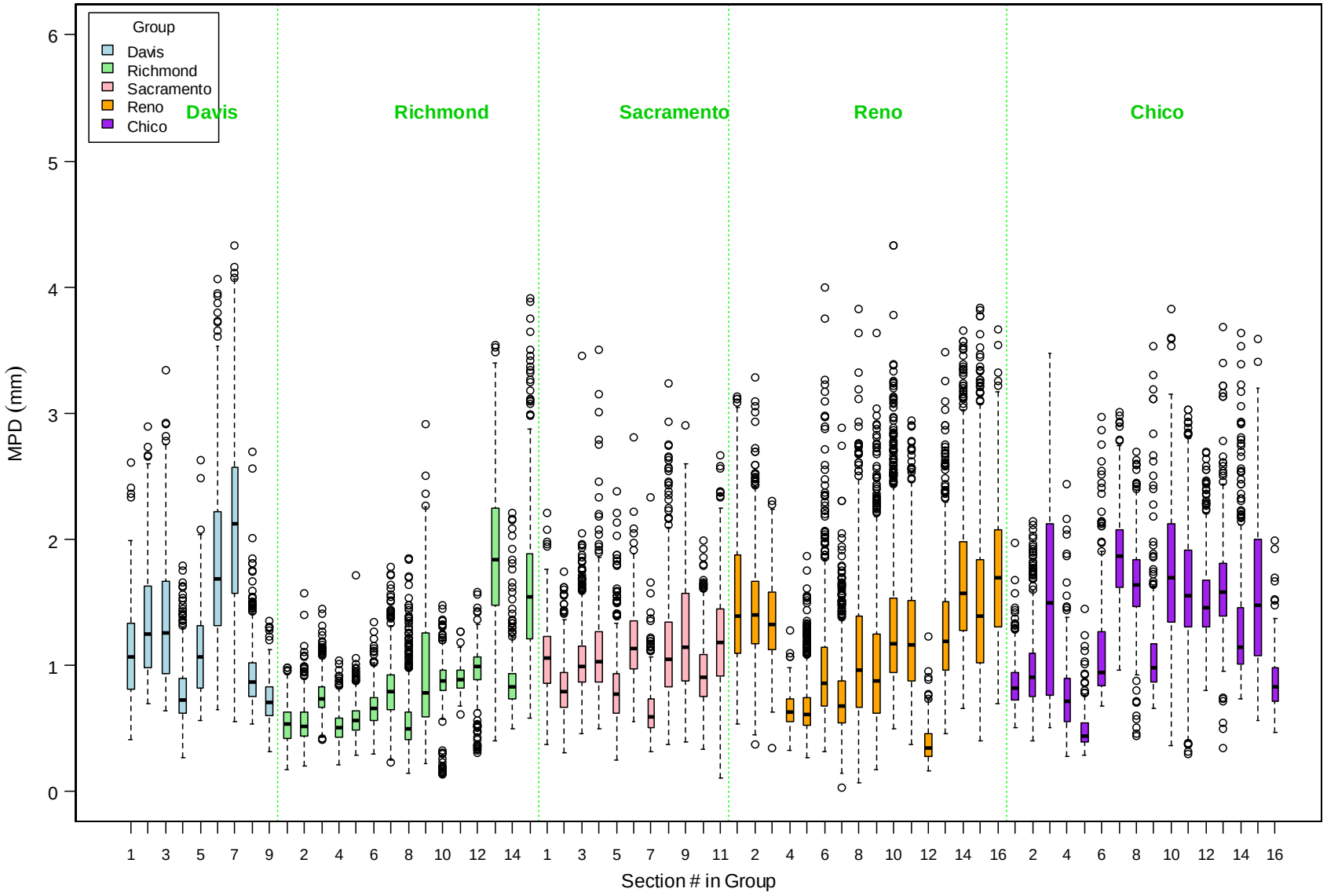

Figure 4.2: Summary box plots of macrotexture measured using the inertial profiler for all survey sections of all groups.
***(Note:* 1 mm = 0.039 inches)**

Table 4.1: Summary Macrotexture (MPD, mm) Measurements Using the Inertial Profiler for All Survey Sections

Group	Section	N	Mean	Std.Dev.	Min	Q1	Median	Q3	Max
Davis	1	380	1.11	0.36	0.40	0.81	1.07	1.33	2.61
	2	194	1.35	0.47	0.70	0.98	1.25	1.62	2.89
	3	215	1.36	0.54	0.63	0.93	1.25	1.67	3.34
	4	539	0.78	0.23	0.27	0.62	0.72	0.89	1.78
	5	174	1.12	0.36	0.56	0.82	1.06	1.31	2.63
	6	592	1.79	0.63	0.65	1.31	1.69	2.21	4.06
	7	583	2.09	0.73	0.55	1.57	2.12	2.57	4.33
	8	458	0.92	0.27	0.53	0.75	0.86	1.01	2.69
	9	197	0.73	0.19	0.31	0.60	0.70	0.82	1.35
Richmond	1	244	0.53	0.16	0.17	0.42	0.54	0.63	0.98
	2	430	0.55	0.16	0.20	0.44	0.52	0.62	1.57
	3	923	0.75	0.14	0.41	0.66	0.73	0.83	1.45
	4	793	0.51	0.12	0.20	0.42	0.50	0.58	1.04
	5	724	0.57	0.13	0.28	0.48	0.56	0.64	1.71
	6	827	0.66	0.14	0.29	0.56	0.65	0.74	1.34
	7	552	0.81	0.24	0.23	0.65	0.78	0.92	1.78
	8	630	0.57	0.26	0.14	0.40	0.49	0.63	1.84
	9	1001	0.95	0.47	0.21	0.59	0.78	1.26	2.91
	10	415	0.87	0.20	0.13	0.80	0.87	0.96	1.47
	11	247	0.90	0.11	0.61	0.82	0.88	0.96	1.27
	12	310	0.97	0.20	0.31	0.89	0.99	1.06	1.58
	13	669	1.83	0.63	0.40	1.47	1.83	2.24	3.54
	14	369	0.88	0.26	0.49	0.73	0.82	0.93	2.21
	15	721	1.62	0.56	0.57	1.21	1.54	1.89	3.91
Sacramento	1	393	1.06	0.28	0.37	0.86	1.06	1.23	2.21
	2	746	0.81	0.23	0.30	0.66	0.79	0.94	1.74
	3	894	1.03	0.25	0.45	0.86	0.99	1.15	3.45
	4	594	1.10	0.35	0.49	0.86	1.03	1.26	3.50
	5	535	0.82	0.30	0.24	0.62	0.77	0.93	2.38
	6	290	1.17	0.31	0.55	0.97	1.13	1.35	2.81
	7	329	0.65	0.23	0.31	0.51	0.59	0.74	2.33
	8	334	1.16	0.49	0.37	0.83	1.04	1.34	3.23
	9	373	1.23	0.47	0.39	0.88	1.14	1.57	2.90
	10	460	0.95	0.28	0.33	0.75	0.90	1.08	1.99
	11	578	1.21	0.42	0.11	0.91	1.18	1.45	2.67
Reno	1	236	1.53	0.58	0.53	1.09	1.39	1.87	3.13
	2	842	1.44	0.41	0.37	1.17	1.40	1.66	3.28
	3	191	1.34	0.32	0.34	1.12	1.32	1.58	2.30
	4	334	0.64	0.15	0.32	0.55	0.62	0.73	1.27
	5	1090	0.66	0.21	0.26	0.52	0.61	0.74	1.86
	6	864	0.98	0.48	0.31	0.68	0.85	1.14	4.00
	7	787	0.76	0.34	0.02	0.55	0.67	0.88	2.89
	8	1057	1.09	0.56	0.07	0.66	0.96	1.39	3.82
	9	1710	0.98	0.50	0.17	0.62	0.87	1.24	3.64
	10	2005	1.30	0.50	0.49	0.94	1.17	1.54	4.33
	11	738	1.24	0.49	0.37	0.88	1.16	1.51	2.94
	12	128	0.39	0.17	0.16	0.27	0.34	0.45	1.22
	13	1462	1.27	0.42	0.45	0.96	1.19	1.50	3.48
	14	2297	1.67	0.52	0.66	1.27	1.57	1.98	3.65
	15	2156	1.47	0.59	0.40	1.01	1.39	1.84	3.83
	16	362	1.75	0.59	0.69	1.31	1.69	2.07	3.66

Group	Section	N	Mean	Std.Dev.	Min	Q1	Median	Q3	Max
Chico	1	386	0.85	0.19	0.50	0.72	0.82	0.94	1.97
	2	974	0.94	0.28	0.39	0.75	0.90	1.09	2.14
	3	367	1.51	0.78	0.50	0.76	1.49	2.12	3.47
	4	619	0.75	0.27	0.27	0.55	0.71	0.89	2.44
	5	235	0.49	0.17	0.28	0.39	0.44	0.54	1.44
	6	425	1.10	0.40	0.68	0.84	0.94	1.26	2.97
	7	495	1.86	0.35	0.96	1.62	1.87	2.08	3.01
	8	584	1.65	0.32	0.44	1.46	1.63	1.83	2.70
	9	425	1.09	0.39	0.65	0.86	0.98	1.17	3.53
	10	520	1.67	0.65	0.36	1.34	1.69	2.12	3.82
	11	859	1.56	0.54	0.30	1.31	1.55	1.91	3.03
	12	831	1.51	0.29	0.79	1.30	1.46	1.67	2.69
	13	503	1.62	0.39	0.34	1.38	1.58	1.81	3.68
	14	482	1.31	0.48	0.73	1.01	1.14	1.45	3.63
	15	361	1.57	0.62	0.56	1.07	1.47	2.00	3.59
	16	155	0.88	0.26	0.47	0.71	0.82	0.97	1.99

4.3 Correlation of Macrotexture Measurements with Inertial Profiler and Laser Texture Scanner

The macrotexture (i.e., MPD) of all sections in the five cities was measured using both the IP and the LTS as independent checks on the measured values. The data from both devices was used to establish a correlation between their measurements. The median MPD data for each of the sections measured with the IP and the LTS are plotted in Figure 4.3 and, as can be seen, a very good linear relationship was found between them, although with relatively high scatter reflecting the fact that the IP measurements are mean values along the entire section while the LTS measurements are taken at a few discrete locations on each section. This relationship can be modeled with the following equation:

$$MPD_{IP} = 1.06 * MPD_{LTS} \quad (R^2 = 0.43) \qquad \textbf{(4.1)}$$

Where:

MPD_IP is the median macrotexture MPD value measured with IP (in mm) and
MPD_LTS is the macrotexture MPD value measured with LTS (in mm).

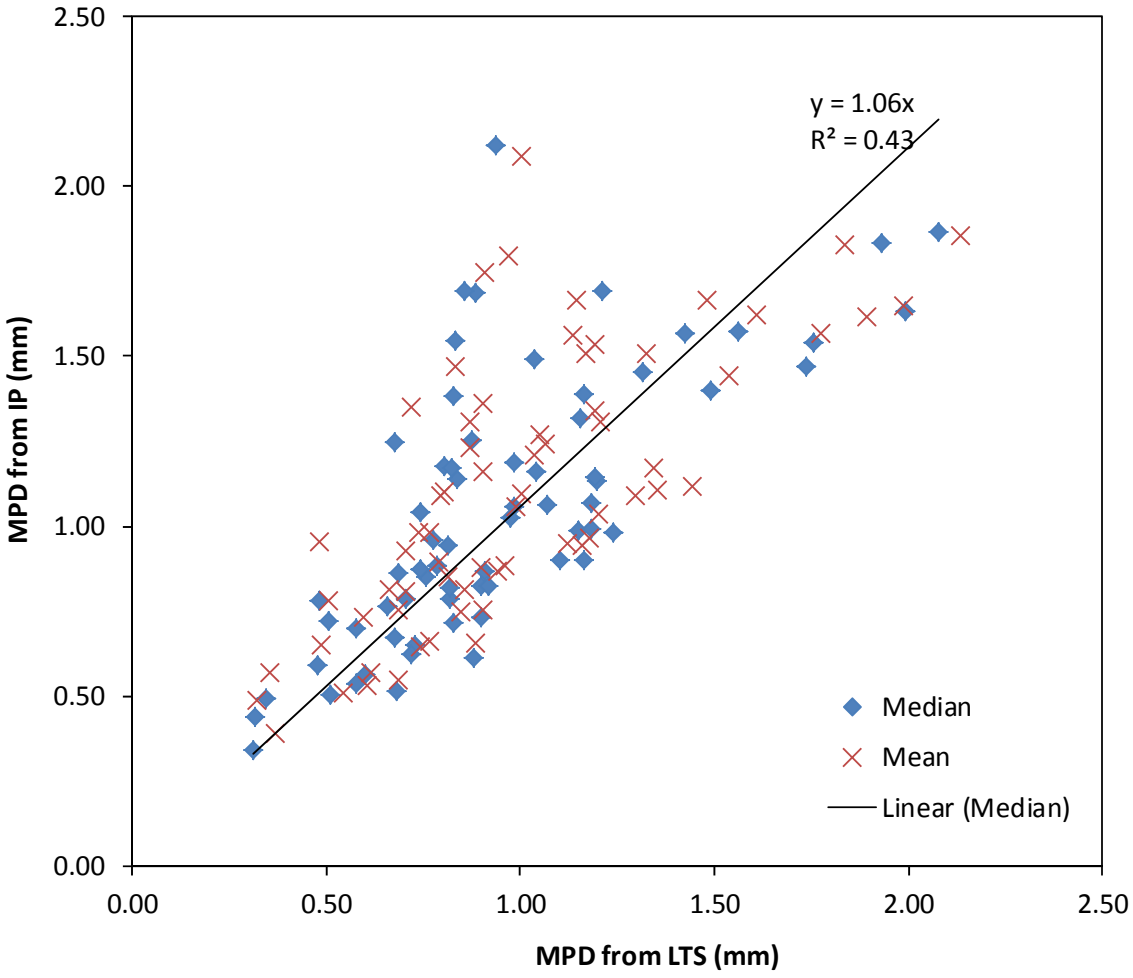

Figure 4.3: Correlation of macrotexture measurements with the inertial profiler and laser texture scanner.

4.4 IRI Measurement Results

Roughness measurements characterized in terms of IRI along the entire length of each pavement section in the five cities (see Table 3.1 for details of each section) are presented using box plots in Figure 4.4. It can be seen from the figures that the IRI values of most sections are in an approximate range of 63 inches/mile to 317 inches/mile (1.0 m/km to 5.0 m/km), but the IRI values of a few sections are larger than 5.0 m/km (317 inches/mile) and show even larger variations within the entire section. The IRI of each section for all the groups are summarized in Table 4.2. The section median IRI values across all the sections are in an approximate range of 76 inches/mile to 317 inches/mile (1.2 m/km to 5.0 m/km).

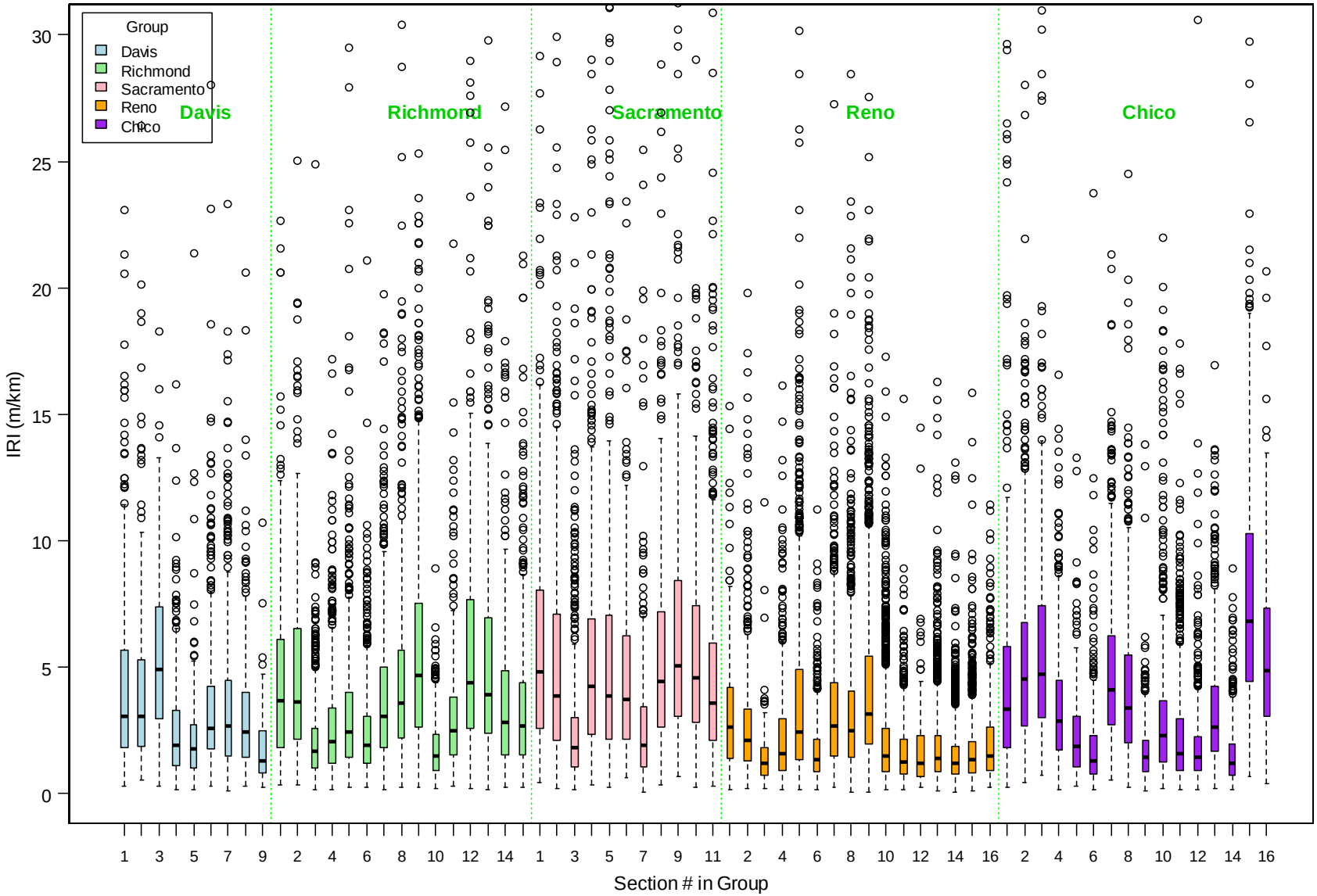

Figure 4.4: Summary box plots of IRI for all the survey sections in all groups.
***(Note:* 1 m/km = 63.4 inches/mile)**

Table 4.2: Summary Roughness (IRI, m/km) Measurements for All Survey Sections

Group	Section	N	Mean	Std.Dev.	Min	Q1	Median	Q3	Max
Davis	1	380	4.5	4.5	0.3	1.8	3.0	5.6	38.8
Davis	2	194	4.3	4.0	0.5	1.9	3.0	5.3	26.4
Davis	3	215	5.6	3.8	0.3	2.9	4.9	7.4	32.7
Davis	4	539	2.4	2.0	0.1	1.1	1.9	3.3	16.2
Davis	5	174	2.3	2.4	0.1	1.0	1.8	2.7	21.4
Davis	6	592	3.4	2.8	0.3	1.7	2.6	4.2	28.0
Davis	7	583	3.5	3.3	0.1	1.5	2.7	4.4	39.8
Davis	8	458	3.0	2.4	0.3	1.4	2.4	4.0	20.6
Davis	9	197	1.7	1.4	0.2	0.8	1.3	2.5	10.7
Richmond	1	244	4.6	3.8	0.3	1.8	3.7	6.0	22.6
Richmond	2	430	4.8	3.9	0.3	2.1	3.6	6.5	32.0
Richmond	3	922	2.0	1.6	0.1	1.0	1.6	2.6	24.9
Richmond	4	793	2.6	2.2	0.1	1.2	2.0	3.4	17.2
Richmond	5	724	3.3	3.4	0.2	1.4	2.4	4.0	43.9
Richmond	6	827	2.4	1.9	0.2	1.2	1.9	3.0	21.1
Richmond	7	552	3.9	3.0	0.1	1.8	3.0	5.0	19.7
Richmond	8	629	4.7	4.2	0.2	2.2	3.5	5.7	38.3
Richmond	9	1001	5.6	4.1	0.2	2.6	4.7	7.5	25.3
Richmond	10	415	1.8	1.2	0.2	0.9	1.5	2.3	8.9
Richmond	11	247	3.2	2.9	0.3	1.5	2.5	3.8	21.8
Richmond	12	310	6.3	6.3	0.2	2.6	4.4	7.7	43.0
Richmond	13	669	5.2	4.1	0.1	2.4	3.9	7.0	29.8
Richmond	14	368	3.8	3.6	0.2	1.5	2.8	4.8	27.2
Richmond	15	721	3.4	2.9	0.2	1.5	2.7	4.4	21.3
Sacramento	1	393	6.2	4.9	0.4	2.6	4.8	8.0	29.2
Sacramento	2	745	5.5	5.9	0.2	2.1	3.8	7.1	71.4
Sacramento	3	894	2.6	2.8	0.1	1.0	1.8	3.0	37.3
Sacramento	4	594	5.9	7.2	0.3	2.3	4.2	6.9	101.0
Sacramento	5	535	7.9	14.1	0.2	2.1	3.8	7.0	172.8
Sacramento	6	290	5.0	5.1	0.6	2.1	3.7	6.2	53.5
Sacramento	7	329	3.1	4.0	0.1	1.0	1.9	3.4	40.1
Sacramento	8	334	5.7	4.6	0.3	2.6	4.4	7.2	28.8
Sacramento	9	373	6.6	5.7	0.7	3.0	5.0	8.4	54.1
Sacramento	10	460	5.5	3.8	0.3	2.8	4.6	7.4	29.0
Sacramento	11	578	5.1	5.6	0.3	2.1	3.6	6.0	60.0
Reno	1	236	3.1	2.5	0.1	1.4	2.6	4.1	15.3
Reno	2	842	2.7	2.2	0.2	1.3	2.1	3.3	19.8
Reno	3	191	1.4	1.2	0.2	0.7	1.2	1.8	11.5
Reno	4	334	2.5	2.6	0.1	0.9	1.6	2.9	16.1
Reno	5	1089	3.8	4.0	0.2	1.3	2.4	4.9	44.9
Reno	6	864	1.7	1.3	0.1	0.8	1.3	2.1	11.2
Reno	7	787	3.4	2.9	0.2	1.5	2.7	4.4	27.3
Reno	8	1057	3.4	3.3	0.1	1.4	2.5	4.0	38.3
Reno	9	1710	4.1	3.3	0.1	1.9	3.2	5.4	27.6
Reno	10	2005	2.0	1.9	0.1	0.8	1.5	2.5	17.3
Reno	11	738	1.7	1.4	0.1	0.7	1.2	2.1	15.6
Reno	12	128	1.9	2.1	0.2	0.7	1.2	2.3	14.4
Reno	13	1462	1.9	1.7	0.1	0.9	1.4	2.3	16.3
Reno	14	2297	1.4	1.1	0.1	0.7	1.2	1.8	13.1
Reno	15	2156	1.6	1.2	0.1	0.8	1.3	2.0	15.8
Reno	16	362	2.1	2.0	0.2	0.9	1.5	2.6	11.4

Group	Section	N	Mean	Std.Dev.	Min	Q1	Median	Q3	Max
Chico	1	386	5.8	8.0	0.2	1.8	3.3	5.8	49.3
Chico	2	974	5.2	3.8	0.4	2.7	4.5	6.7	39.7
Chico	3	367	6.2	5.6	0.7	3.0	4.7	7.4	43.3
Chico	4	619	3.4	2.4	0.1	1.7	2.8	4.5	16.6
Chico	5	235	2.4	2.0	0.3	1.0	1.9	3.0	13.3
Chico	6	425	1.8	2.0	0.1	0.8	1.3	2.3	23.7
Chico	7	495	4.9	3.2	0.5	2.7	4.1	6.2	21.3
Chico	8	584	4.2	3.1	0.2	2.0	3.4	5.5	24.5
Chico	9	425	1.7	1.4	0.1	0.8	1.4	2.1	13.8
Chico	10	520	3.2	3.4	0.2	1.2	2.3	3.7	22.0
Chico	11	859	2.3	2.3	0.1	0.9	1.6	2.9	17.8
Chico	12	831	1.9	3.0	0.1	0.9	1.4	2.2	62.4
Chico	13	503	3.4	2.6	0.2	1.7	2.6	4.2	16.9
Chico	14	482	1.5	1.3	0.1	0.7	1.2	1.9	8.9
Chico	15	361	7.9	5.2	0.7	4.4	6.8	10.3	40.4
Chico	16	155	5.6	3.6	0.4	3.0	4.8	7.3	20.6

4.5 Bicycle Vibration Results

Bicycle vibration measurements (i.e., vertical acceleration) taken along the entire length of each pavement section (see Table 3.1 for details of each section) are summarized using box plots in Figure 4.5 through Figure 4.8 for road bicycles, commuter bicycles, mountain bicycles, and all three bicycle types together, respectively. The figures show that the vibration values for most of the sections were below 0.8 *g* and centered at approximately 0.5 *g,* except for a few sections where they were larger than 0.8 *g* and closer to 1.3 *g.* The vibration values of road bicycles show smaller variation but higher median values than those of commuter and mountain bicycles. As presented in Table 4.4, the median vibration values across all the three bicycle types for all the sections measured were in an approximate range of 0.2 *g* to 0.7 *g.*

The bicycle speeds on each survey section in the vibration measurements were calculated from GPS and accelerometer data. The speeds on each pavement section are summarized in Table 4.3. Testing speeds for the vibration measurements were set to 15 mph (24 km/h) for the road bicycles and 7.5 mph (12 km/h) for the commuter and mountain bicycles. Table 4.3 shows that the bicycle speed values for most sections were in the range of 7 mph to 20 mph (11 km/h to 32 km/h). The median bicycle speed values for all the sections in this study were in an approximate range of 7 mph to 12 mph (11 km/h to 19 km/h).

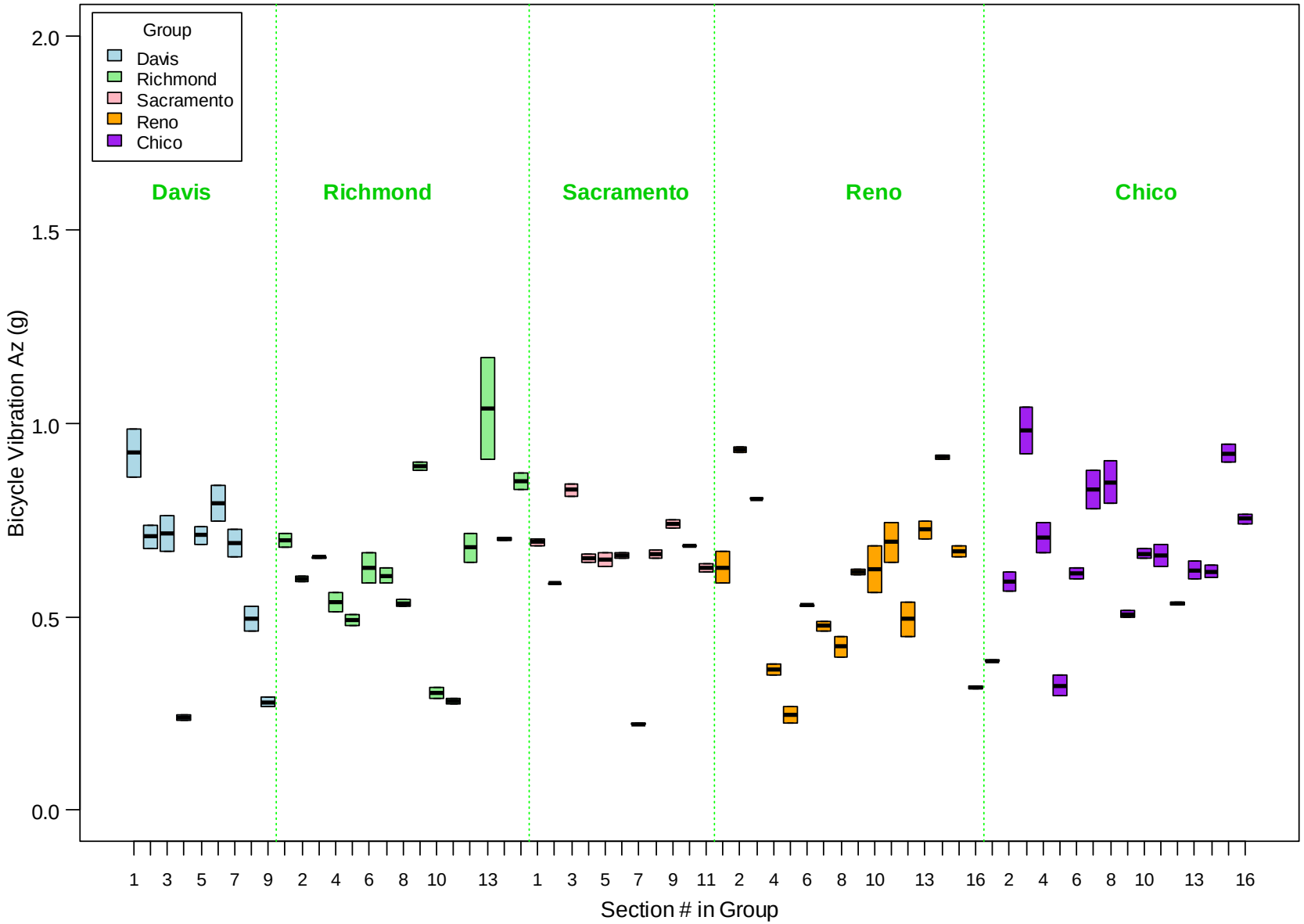

Figure 4.5: Summary box plots of road bicycle vibration for survey sections across all cities.

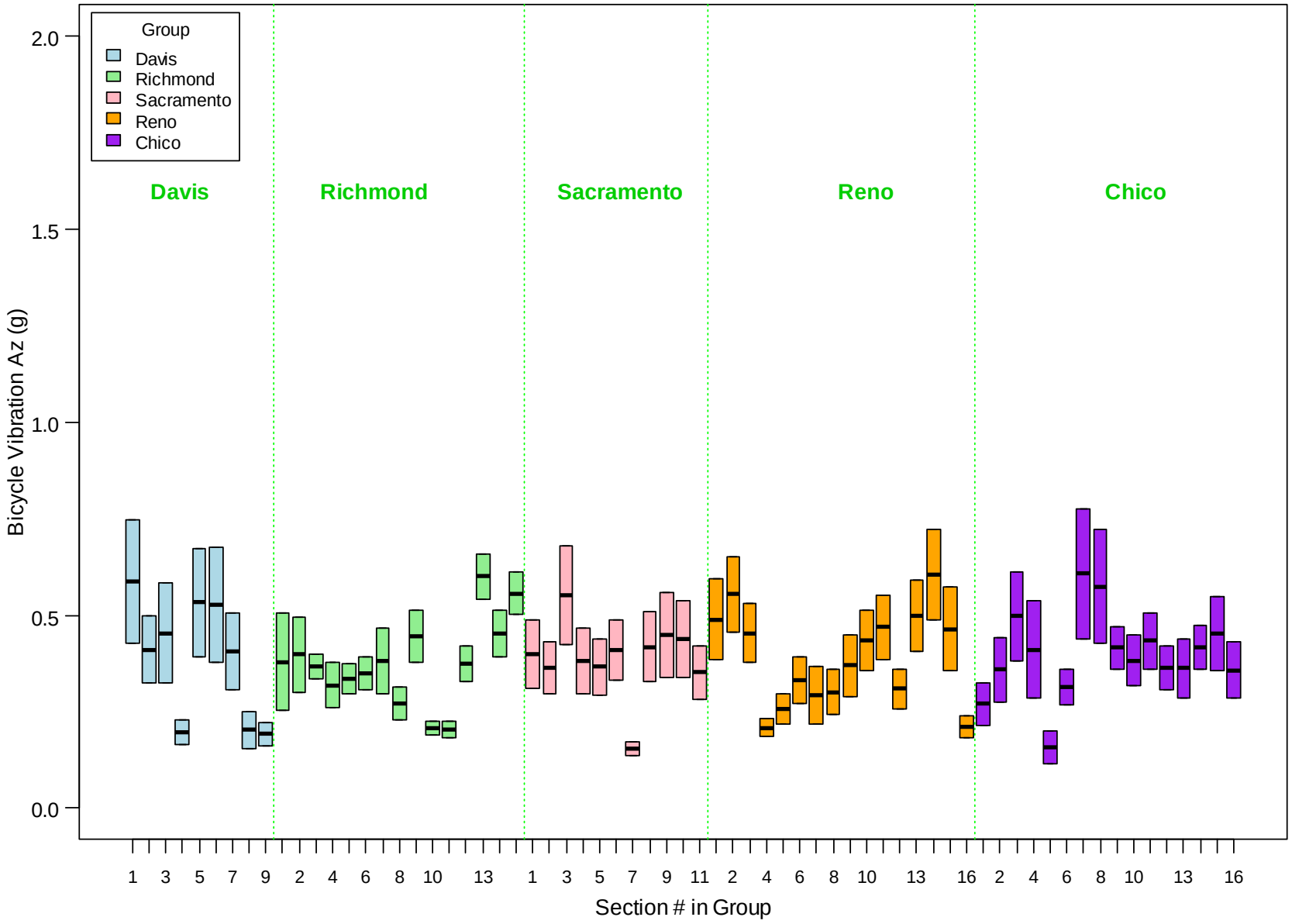

Figure 4.6: Summary box plots of commuter bicycle vibration for survey sections across all cities.

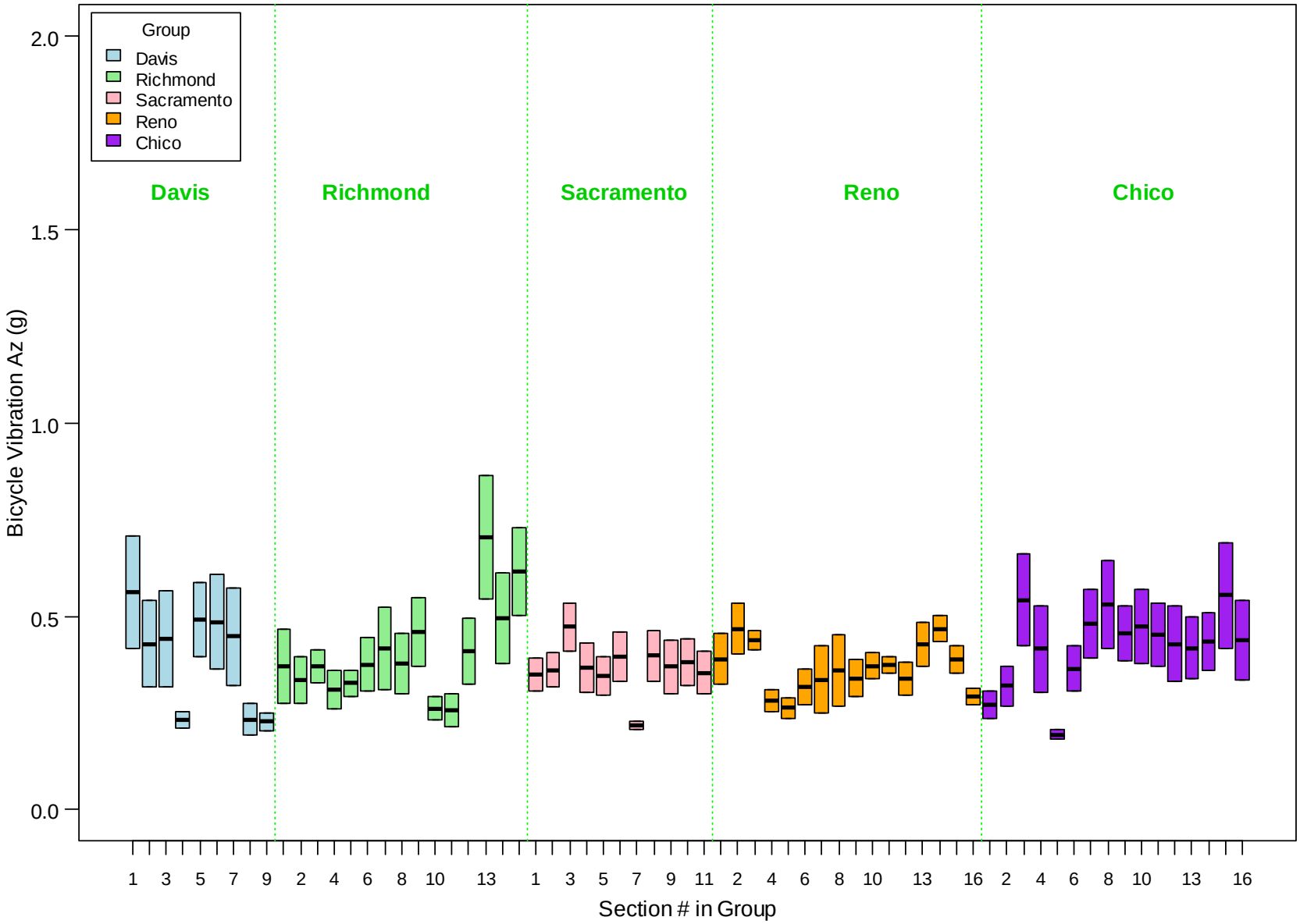

Figure 4.7: Summary box plots of mountain bicycle vibration for survey sections across all cities.

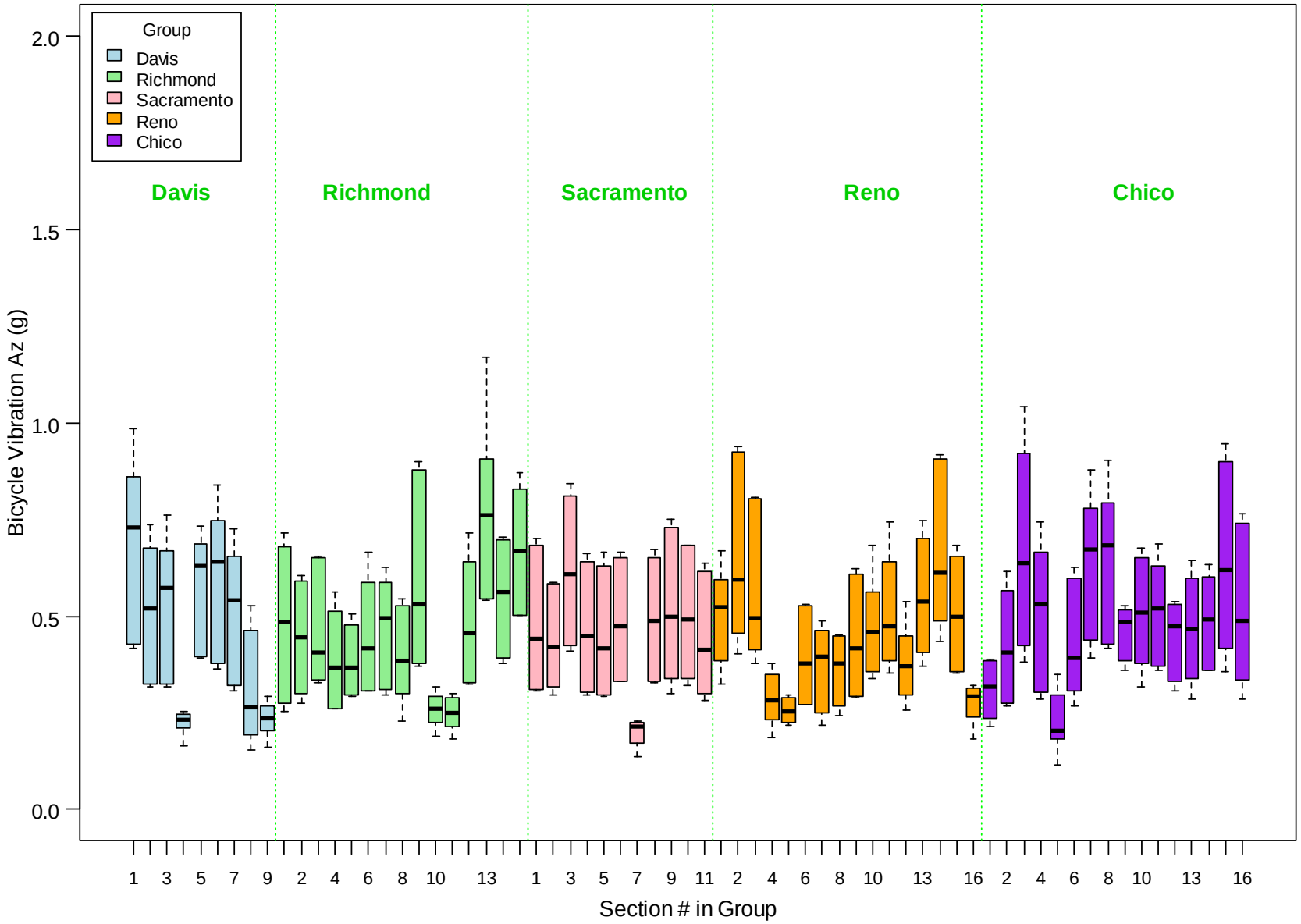

Figure 4.8: Summary box plot of bicycle vibration for all bicycle types together for survey sections across all cities.

Table 4.3: Summary Table of Bicycling Speed (mph) for Each Survey Section

Group	Section	N	Mean	Std.Dev.	Min	Q1	Median	Q3	Max
Davis	1	6	10.4	4.5	7.5	7.5	7.5	14.1	16.2
Davis	2	6	10.6	4.9	7.4	7.4	7.6	14.6	16.9
Davis	3	6	10.4	4.4	7.4	7.4	7.7	14.0	16.1
Davis	4	6	10.5	4.5	7.6	7.6	7.6	14.1	16.3
Davis	5	6	10.3	4.1	7.6	7.6	7.7	13.6	15.5
Davis	6	6	10.3	4.5	7.2	7.3	7.5	14.0	16.1
Davis	7	6	10.5	4.6	7.4	7.5	7.7	14.3	16.5
Davis	8	6	12.0	6.8	7.6	7.6	7.6	17.5	20.8
Davis	9	6	10.7	4.9	7.5	7.6	7.6	14.7	17.1
Richmond	1	6	10.2	3.9	7.6	7.6	7.7	13.3	15.2
Richmond	2	6	10.9	5.2	7.6	7.6	7.6	15.1	17.7
Richmond	3	6	10.6	4.7	7.6	7.6	7.6	14.5	16.8
Richmond	4	6	10.6	4.5	7.6	7.6	7.7	14.2	16.4
Richmond	5	6	10.5	4.6	7.5	7.5	7.6	14.3	16.5
Richmond	6	6	10.5	4.4	7.6	7.7	7.7	14.1	16.2
Richmond	7	6	10.5	4.7	7.4	7.4	7.4	14.3	16.6
Richmond	8	6	10.4	4.5	7.5	7.5	7.5	14.1	16.3
Richmond	9	6	10.3	4.5	7.3	7.4	7.4	14.0	16.2
Richmond	10	6	10.5	4.5	7.6	7.6	7.7	14.2	16.4
Richmond	11	6	10.6	4.3	7.7	7.7	7.8	14.1	16.2
Richmond	12	6	10.5	4.6	7.5	7.5	7.6	14.2	16.4
Richmond	13	6	10.5	4.6	7.5	7.5	7.5	14.2	16.4
Richmond	14	6	10.5	4.7	7.5	7.5	7.5	14.3	16.6
Richmond	15	6	10.9	4.8	7.8	7.8	7.9	14.8	17.1
Sacramento	1	6	10.1	4.0	7.5	7.5	7.5	13.3	15.3
Sacramento	2	6	10.4	4.5	7.4	7.4	7.6	14.1	16.3
Sacramento	3	6	10.5	4.6	7.4	7.5	7.5	14.2	16.5
Sacramento	4	6	10.4	4.8	7.3	7.3	7.4	14.4	16.7
Sacramento	5	6	10.5	4.7	7.4	7.5	7.6	14.3	16.5
Sacramento	6	6	10.4	4.5	7.4	7.4	7.5	14.0	16.2
Sacramento	7	6	10.8	4.9	7.6	7.6	7.6	14.7	17.1
Sacramento	8	6	10.2	4.2	7.5	7.5	7.5	13.6	15.6
Sacramento	9	6	10.2	4.4	7.3	7.3	7.4	13.8	15.9
Sacramento	10	6	10.2	4.3	7.4	7.4	7.5	13.7	15.8
Sacramento	11	6	10.1	4.1	7.4	7.4	7.6	13.5	15.4
Reno	1	6	10.9	4.0	7.4	7.9	9.3	14.3	15.9
Reno	2	6	10.8	3.8	7.5	8.0	9.5	14.0	15.5
Reno	3	6	10.2	3.7	7.3	7.5	8.4	13.2	14.8
Reno	4	6	10.7	3.6	7.5	8.0	9.4	13.8	15.3
Reno	5	6	10.6	3.4	7.8	8.1	9.1	13.5	15.0
Reno	6	6	10.6	3.6	7.5	7.9	9.1	13.7	15.2
Reno	7	4	11.4	4.0	7.8	8.3	10.0	14.8	16.4
Reno	8	4	10.8	3.8	7.5	7.9	9.2	14.0	15.6
Reno	9	6	11.5	3.4	8.7	9.0	9.9	14.3	15.8
Reno	10	6	11.0	3.6	7.6	8.1	9.9	14.1	15.5
Reno	11	4	10.7	3.4	7.5	8.1	9.8	13.6	14.9
Reno	12	4	10.2	3.4	7.3	7.7	8.9	13.1	14.5
Reno	13	4	10.8	3.7	7.5	8.0	9.5	13.9	15.4
Reno	14	6	11.0	3.7	7.7	8.2	9.7	14.2	15.7
Reno	15	4	10.9	3.7	7.7	8.1	9.4	14.1	15.6
Reno	16	4	11.0	3.5	7.6	8.2	10.0	14.0	15.3

Group	Section	N	Mean	Std.Dev.	Min	Q1	Median	Q3	Max
Chico	1	6	10.1	4.3	7.1	7.2	7.6	13.6	15.6
Chico	2	6	10.7	4.7	7.4	7.5	7.8	14.5	16.7
Chico	3	6	10.4	4.2	7.5	7.6	7.8	13.8	15.8
Chico	4	6	10.3	4.1	7.4	7.5	7.9	13.7	15.6
Chico	5	6	10.3	4.5	7.3	7.3	7.6	14.0	16.1
Chico	6	6	10.5	4.3	7.7	7.7	7.9	14.0	16.0
Chico	7	6	10.7	4.5	7.4	7.6	8.2	14.4	16.5
Chico	8	6	10.7	4.6	7.5	7.6	7.9	14.5	16.7
Chico	9	6	10.5	4.5	7.5	7.6	7.8	14.2	16.4
Chico	10	6	10.9	5.0	7.6	7.7	7.7	14.9	17.3
Chico	11	6	10.7	4.3	7.5	7.7	8.2	14.2	16.2
Chico	12	6	10.7	4.4	7.8	7.8	8.1	14.3	16.3
Chico	13	6	10.8	4.4	7.9	7.9	7.9	14.4	16.5
Chico	14	6	10.5	4.2	7.7	7.8	8.0	13.9	15.9
Chico	15	6	10.3	4.0	7.7	7.7	7.7	13.5	15.5
Chico	16	6	10.6	4.4	7.7	7.7	7.8	14.2	16.3

Table 4.4: Summary of Bicycle Vibration Data[a] (*g*) for Each Survey Section

Group	Section	N[b]	Mean	Std.Dev.	Min	Q1	Median	Q3	Max
Davis	1	6	0.69	0.23	0.42	0.50	0.73	0.83	0.98
Davis	2	6	0.52	0.17	0.32	0.37	0.52	0.64	0.74
Davis	3	6	0.54	0.18	0.32	0.38	0.57	0.65	0.76
Davis	4	6	0.22	0.03	0.16	0.21	0.23	0.24	0.25
Davis	5	6	0.58	0.15	0.39	0.44	0.63	0.68	0.73
Davis	6	6	0.60	0.19	0.36	0.43	0.64	0.73	0.84
Davis	7	6	0.51	0.17	0.31	0.37	0.54	0.63	0.72
Davis	8	6	0.31	0.15	0.15	0.21	0.26	0.42	0.53
Davis	9	6	0.23	0.05	0.16	0.21	0.24	0.26	0.29
Richmond	1	6	0.48	0.19	0.25	0.32	0.49	0.63	0.71
Richmond	2	6	0.44	0.14	0.27	0.32	0.45	0.57	0.61
Richmond	3	6	0.46	0.15	0.33	0.35	0.41	0.59	0.66
Richmond	4	6	0.39	0.13	0.26	0.29	0.37	0.48	0.56
Richmond	5	6	0.38	0.09	0.29	0.31	0.37	0.45	0.50
Richmond	6	6	0.45	0.15	0.31	0.33	0.42	0.55	0.66
Richmond	7	6	0.47	0.14	0.30	0.35	0.49	0.57	0.62
Richmond	8	6	0.39	0.13	0.23	0.30	0.38	0.51	0.55
Richmond	9	6	0.60	0.24	0.37	0.41	0.53	0.80	0.90
Richmond	10	6	0.26	0.05	0.19	0.23	0.26	0.29	0.32
Richmond	11	6	0.25	0.05	0.18	0.22	0.25	0.29	0.30
Richmond	12	6	0.49	0.16	0.32	0.35	0.46	0.60	0.71
Richmond	13	6	0.78	0.25	0.54	0.57	0.76	0.90	1.17
Richmond	14	6	0.55	0.15	0.38	0.42	0.56	0.68	0.70
Richmond	15	6	0.67	0.16	0.50	0.53	0.67	0.80	0.87
Sacramento	1	6	0.48	0.18	0.31	0.33	0.44	0.63	0.70
Sacramento	2	6	0.44	0.13	0.30	0.34	0.42	0.55	0.59
Sacramento	3	6	0.62	0.19	0.41	0.45	0.61	0.78	0.84
Sacramento	4	6	0.47	0.16	0.29	0.33	0.45	0.60	0.66
Sacramento	5	6	0.45	0.16	0.29	0.32	0.42	0.58	0.67
Sacramento	6	6	0.49	0.15	0.33	0.36	0.47	0.61	0.66
Sacramento	7	6	0.20	0.04	0.14	0.18	0.21	0.22	0.23
Sacramento	8	6	0.49	0.15	0.33	0.36	0.49	0.62	0.67
Sacramento	9	6	0.52	0.19	0.30	0.36	0.50	0.69	0.75
Sacramento	10	6	0.50	0.16	0.32	0.37	0.49	0.65	0.68
Sacramento	11	6	0.44	0.15	0.28	0.33	0.41	0.57	0.64

Group	Section	N[b]	Mean	Std.Dev.	Min	Q1	Median	Q3	Max
Reno	1	6	0.50	0.13	0.32	0.40	0.52	0.59	0.67
Reno	2	6	0.65	0.23	0.40	0.48	0.59	0.86	0.94
Reno	3	6	0.57	0.19	0.38	0.43	0.50	0.73	0.81
Reno	4	6	0.28	0.07	0.19	0.24	0.28	0.34	0.38
Reno	5	6	0.26	0.03	0.22	0.23	0.25	0.28	0.30
Reno	6	6	0.39	0.12	0.27	0.29	0.38	0.49	0.53
Reno	7	6	0.37	0.11	0.22	0.28	0.39	0.45	0.49
Reno	8	6	0.36	0.09	0.24	0.29	0.38	0.44	0.45
Reno	9	6	0.44	0.15	0.29	0.32	0.42	0.57	0.62
Reno	10	6	0.48	0.13	0.34	0.37	0.46	0.55	0.68
Reno	11	6	0.51	0.16	0.35	0.39	0.47	0.62	0.74
Reno	12	6	0.38	0.10	0.26	0.31	0.37	0.43	0.54
Reno	13	6	0.55	0.16	0.37	0.43	0.54	0.67	0.75
Reno	14	6	0.66	0.22	0.43	0.49	0.61	0.86	0.92
Reno	15	6	0.51	0.15	0.35	0.37	0.50	0.63	0.68
Reno	16	6	0.27	0.06	0.18	0.25	0.29	0.31	0.32
Chico	1	6	0.31	0.07	0.21	0.25	0.32	0.37	0.39
Chico	2	6	0.42	0.15	0.27	0.30	0.41	0.53	0.61
Chico	3	6	0.67	0.26	0.38	0.47	0.64	0.85	1.04
Chico	4	6	0.51	0.19	0.29	0.36	0.53	0.63	0.74
Chico	5	6	0.22	0.08	0.11	0.19	0.20	0.27	0.35
Chico	6	6	0.43	0.15	0.27	0.32	0.39	0.56	0.63
Chico	7	6	0.64	0.20	0.39	0.47	0.67	0.78	0.88
Chico	8	6	0.65	0.20	0.42	0.48	0.68	0.77	0.90
Chico	9	6	0.46	0.07	0.36	0.40	0.48	0.51	0.53
Chico	10	6	0.51	0.15	0.32	0.39	0.51	0.63	0.67
Chico	11	6	0.51	0.13	0.36	0.40	0.52	0.61	0.69
Chico	12	6	0.44	0.10	0.31	0.35	0.47	0.53	0.54
Chico	13	6	0.47	0.14	0.29	0.36	0.47	0.57	0.64
Chico	14	6	0.49	0.12	0.36	0.39	0.49	0.58	0.63
Chico	15	6	0.64	0.25	0.35	0.45	0.62	0.85	0.95
Chico	16	6	0.52	0.20	0.28	0.36	0.49	0.69	0.76

Notes:
[a.] Acceleration normalized at the speed of 26 km/h (16 mph); see Section 3.5.2 for details.
[b.] The number of processed vibration data, not the number of the initial measurement data.

4.6 Bicycle Survey Results

As shown in Table 3.2, the bicycle surveys collected data from a total of 155 participants who rode on 67 road sections distributed across the five cities in Northern California, resulting in a total of 2,194 observations. This section presents the main results, which pertain to ride quality, that were determined from the in-ride survey. The survey forms (pre-ride, in-ride, and post-ride) appear in Appendix A.

4.6.1 Acceptability

When each rider reached the end of a section, before moving on they filled out their in-ride survey, rating the just-completed section as either "Unacceptable" or "Acceptable." The overall acceptability (a rating of 0 or 1, with 0 = completely unacceptable and 1 = completely acceptable) of each section can be thought of as both the average acceptability rating of all the riders or of the percentage of riders that rated the pavement section

"Acceptable." The acceptability values for each pavement section are summarized in Figure 4.9 and in Table 4.5. It can be seen that the acceptability values for most of the sections were above 0.8, while only one of sixty-seven 67 sections (Richmond Section 9) obtained median ride quality acceptability values below 0.5. The reasons for the lower ride quality acceptability in some sections were higher MPD, higher IRI, or both, with the consequent greater higher bicycle vibration. The mean ride quality acceptability values for all the sections in this study covered the range of 0.4 to 1.0 (see Table 4.5).

4.6.2 Ride Quality

Riders reported on the bicycle ride quality (on a scale of 1 to 5, with 1 = poor and 5 = excellent) of each survey section through the in-ride survey. The values for each pavement section are summarized in Figure 4.10 and in Table 4.6. It can be seen that bicycle ride quality values for most of the sections were above 3.0, while the mean ride quality value was below 2.0 for only one out of 155 sections (Richmond Section 9). As with the acceptability ratings, the reason for the lower ride quality rating of some sections is due to either higher MPD, higher IRI, or both, and the consequent higher bicycle vibration. The mean bicycle ride quality values for all the sections in this study were in the approximate range of 2.0 to 4.9 (see Table 4.6).

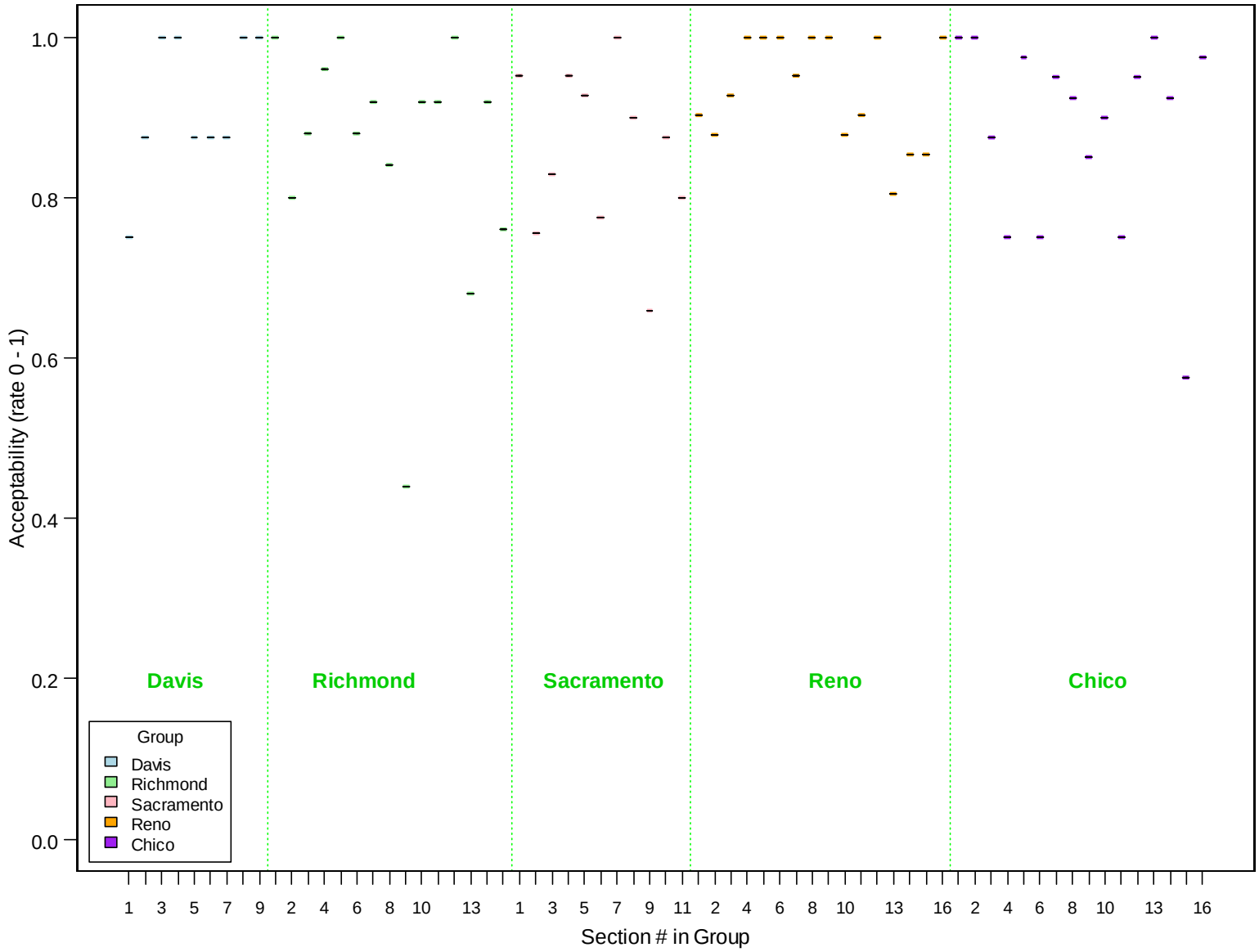

Figure 4.9: Summary plot of mean acceptability for each survey section across all cities.

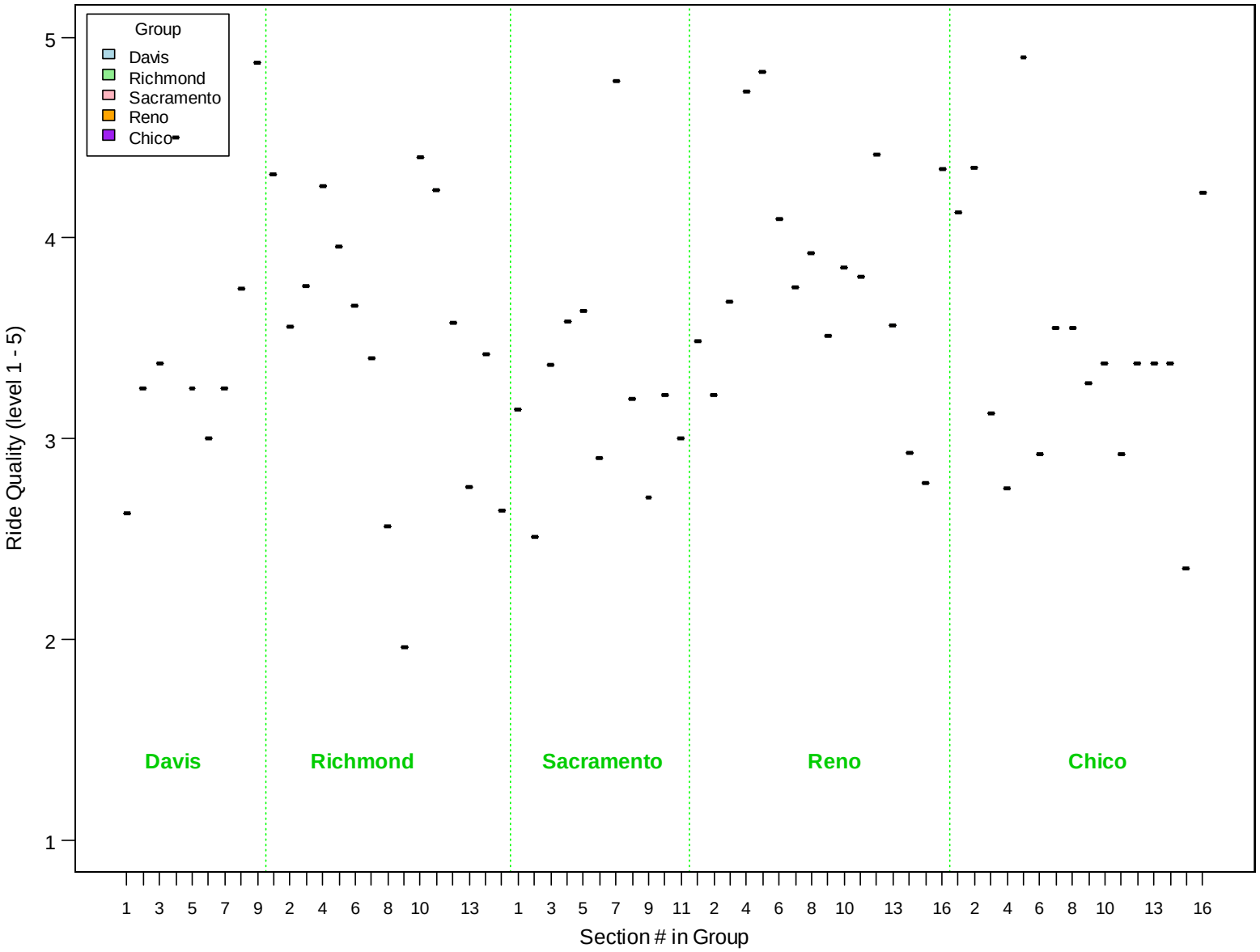

Figure 4.10: Summary box plot of mean ride quality for each survey section across all cities.

Table 4.5: Summary of Ride Quality Acceptability (0 or 1) for Each Survey Section Across All Cities

Group	Section	N	Mean	Std.Dev.	Min	Q1	Median	Q3	Max
Davis	1	8	0.8	0.5	0.0	0.8	1.0	1.0	1.0
Davis	2	8	0.9	0.4	0.0	1.0	1.0	1.0	1.0
Davis	3	8	1.0	0.0	1.0	1.0	1.0	1.0	1.0
Davis	4	8	1.0	0.0	1.0	1.0	1.0	1.0	1.0
Davis	5	8	0.9	0.4	0.0	1.0	1.0	1.0	1.0
Davis	6	8	0.9	0.4	0.0	1.0	1.0	1.0	1.0
Davis	7	8	0.9	0.4	0.0	1.0	1.0	1.0	1.0
Davis	8	8	1.0	0.0	1.0	1.0	1.0	1.0	1.0
Davis	9	8	1.0	0.0	1.0	1.0	1.0	1.0	1.0
Richmond	1	25	1.0	0.0	1.0	1.0	1.0	1.0	1.0
Richmond	2	25	0.8	0.4	0.0	1.0	1.0	1.0	1.0
Richmond	3	25	0.9	0.3	0.0	1.0	1.0	1.0	1.0
Richmond	4	25	1.0	0.2	0.0	1.0	1.0	1.0	1.0
Richmond	5	25	1.0	0.0	1.0	1.0	1.0	1.0	1.0
Richmond	6	25	0.9	0.3	0.0	1.0	1.0	1.0	1.0
Richmond	7	25	0.9	0.3	0.0	1.0	1.0	1.0	1.0
Richmond	8	25	0.8	0.4	0.0	1.0	1.0	1.0	1.0
Richmond	9	25	0.4	0.5	0.0	0.0	0.0	1.0	1.0
Richmond	10	25	0.9	0.3	0.0	1.0	1.0	1.0	1.0
Richmond	11	25	0.9	0.3	0.0	1.0	1.0	1.0	1.0
Richmond	12	25	1.0	0.0	1.0	1.0	1.0	1.0	1.0
Richmond	13	25	0.7	0.5	0.0	0.0	1.0	1.0	1.0
Richmond	14	25	0.9	0.3	0.0	1.0	1.0	1.0	1.0
Richmond	15	25	0.8	0.4	0.0	1.0	1.0	1.0	1.0
Sacramento	1	41	1.0	0.2	0.0	1.0	1.0	1.0	1.0
Sacramento	2	41	0.8	0.4	0.0	1.0	1.0	1.0	1.0
Sacramento	3	41	0.8	0.4	0.0	1.0	1.0	1.0	1.0
Sacramento	4	41	1.0	0.2	0.0	1.0	1.0	1.0	1.0
Sacramento	5	41	0.9	0.3	0.0	1.0	1.0	1.0	1.0
Sacramento	6	40	0.8	0.4	0.0	1.0	1.0	1.0	1.0
Sacramento	7	41	1.0	0.0	1.0	1.0	1.0	1.0	1.0
Sacramento	8	40	0.9	0.3	0.0	1.0	1.0	1.0	1.0
Sacramento	9	41	0.7	0.5	0.0	0.0	1.0	1.0	1.0
Sacramento	10	40	0.9	0.3	0.0	1.0	1.0	1.0	1.0
Sacramento	11	40	0.8	0.4	0.0	1.0	1.0	1.0	1.0
Reno	1	41	0.9	0.3	0.0	1.0	1.0	1.0	1.0
Reno	2	41	0.9	0.3	0.0	1.0	1.0	1.0	1.0
Reno	3	41	0.9	0.3	0.0	1.0	1.0	1.0	1.0
Reno	4	41	1.0	0.0	1.0	1.0	1.0	1.0	1.0
Reno	5	41	1.0	0.0	1.0	1.0	1.0	1.0	1.0
Reno	6	41	1.0	0.0	1.0	1.0	1.0	1.0	1.0
Reno	7	41	1.0	0.2	0.0	1.0	1.0	1.0	1.0
Reno	8	41	1.0	0.0	1.0	1.0	1.0	1.0	1.0
Reno	9	41	1.0	0.0	1.0	1.0	1.0	1.0	1.0
Reno	10	41	0.9	0.3	0.0	1.0	1.0	1.0	1.0
Reno	11	41	0.9	0.3	0.0	1.0	1.0	1.0	1.0
Reno	12	41	1.0	0.0	1.0	1.0	1.0	1.0	1.0
Reno	13	41	0.8	0.4	0.0	1.0	1.0	1.0	1.0
Reno	14	41	0.9	0.4	0.0	1.0	1.0	1.0	1.0
Reno	15	41	0.9	0.4	0.0	1.0	1.0	1.0	1.0
Reno	16	41	1.0	0.0	1.0	1.0	1.0	1.0	1.0

Group	Section	N	Mean	Std.Dev.	Min	Q1	Median	Q3	Max
Chico	1	40	1.0	0.0	1.0	1.0	1.0	1.0	1.0
Chico	2	40	1.0	0.0	1.0	1.0	1.0	1.0	1.0
Chico	3	40	0.9	0.3	0.0	1.0	1.0	1.0	1.0
Chico	4	40	0.8	0.4	0.0	0.8	1.0	1.0	1.0
Chico	5	40	1.0	0.2	0.0	1.0	1.0	1.0	1.0
Chico	6	40	0.8	0.4	0.0	0.8	1.0	1.0	1.0
Chico	7	40	1.0	0.2	0.0	1.0	1.0	1.0	1.0
Chico	8	40	0.9	0.3	0.0	1.0	1.0	1.0	1.0
Chico	9	40	0.9	0.4	0.0	1.0	1.0	1.0	1.0
Chico	10	40	0.9	0.3	0.0	1.0	1.0	1.0	1.0
Chico	11	40	0.8	0.4	0.0	0.8	1.0	1.0	1.0
Chico	12	40	1.0	0.2	0.0	1.0	1.0	1.0	1.0
Chico	13	40	1.0	0.0	1.0	1.0	1.0	1.0	1.0
Chico	14	40	0.9	0.3	0.0	1.0	1.0	1.0	1.0
Chico	15	40	0.6	0.5	0.0	0.0	1.0	1.0	1.0
Chico	16	40	1.0	0.2	0.0	1.0	1.0	1.0	1.0

Table 4.6: Summary of Ride Quality (1 to 5) for Each Survey Section Across All Cities

Group	Section	N	Mean	Std.Dev.	Min	Q1	Median	Q3	Max
Davis	1	8	2.6	0.9	2	2	2	3.25	4
Davis	2	8	3.3	0.7	2	3	3	4	4
Davis	3	8	3.4	0.5	3	3	3	4	4
Davis	4	8	4.5	1.1	2	4.75	5	5	5
Davis	5	8	3.3	1.2	2	2	3.5	4	5
Davis	6	8	3.0	0.5	2	3	3	3	4
Davis	7	8	3.3	0.7	2	3	3	4	4
Davis	8	8	3.8	0.7	3	3	4	4	5
Davis	9	8	4.9	0.4	4	5	5	5	5
Richmond	1	25	4.3	0.7	3	4	4	5	5
Richmond	2	25	3.6	1.0	2	3	4	4	5
Richmond	3	25	3.8	1.0	2	3	4	5	5
Richmond	4	25	4.3	0.8	3	4	4.5	5	5
Richmond	5	25	4.0	0.9	2	3	4	5	5
Richmond	6	25	3.7	0.9	1	3.5	4	4	5
Richmond	7	25	3.4	0.8	2	3	3	4	5
Richmond	8	25	2.6	0.7	1	2	3	3	4
Richmond	9	25	2.0	1.1	1	1	2	2	5
Richmond	10	25	4.4	0.9	2	4	5	5	5
Richmond	11	25	4.2	0.8	2	4	4	5	5
Richmond	12	25	3.6	0.7	2	3	4	4	5
Richmond	13	25	2.8	1.0	1	2	3	3	5
Richmond	14	25	3.4	0.8	2	3	4	4	5
Richmond	15	25	2.6	0.8	1	2	3	3	4
Sacramento	1	41	3.1	0.9	1	3	3	4	5
Sacramento	2	41	2.5	1.0	1	2	3	3	5
Sacramento	3	41	3.4	1.0	1	3	4	4	5
Sacramento	4	41	3.6	0.8	1	3	4	4	5
Sacramento	5	41	3.6	0.9	2	3	4	4	5
Sacramento	6	41	2.9	0.9	1	3	3	3	5
Sacramento	7	41	4.8	0.7	2	5	5	5	5
Sacramento	8	40	3.2	1.0	1	3	3	4	5
Sacramento	9	41	2.7	1.1	1	2	3	3	5
Sacramento	10	41	3.2	0.9	1	3	3	4	5
Sacramento	11	41	3.0	0.9	1	3	3	3	5
Reno	1	41	3.5	0.8	2	3	3	4	5
Reno	2	41	3.2	0.9	2	3	3	4	5
Reno	3	41	3.7	0.8	2	3	4	4	5
Reno	4	41	4.7	0.4	4	4	5	5	5
Reno	5	41	4.8	0.5	3	5	5	5	5
Reno	6	41	4.1	0.7	2	4	4	4	5
Reno	7	41	3.8	0.8	2	3	4	4	5
Reno	8	41	3.9	0.6	3	4	4	4	5
Reno	9	41	3.5	0.8	2	3	4	4	5
Reno	10	41	3.9	1.1	1	3	4	5	5
Reno	11	41	3.8	1.1	1	3	4	5	5
Reno	12	41	4.4	0.7	3	4	5	5	5
Reno	13	41	3.6	1.1	1	3	4	4	5
Reno	14	41	2.9	1.0	1	2	3	3	5
Reno	15	41	2.8	1.0	1	2	3	4	5
Reno	16	41	4.3	0.7	3	4	4	5	5

Group	Section	N	Mean	Std.Dev.	Min	Q1	Median	Q3	Max
Chico	1	40	4.1	0.7	3	4	4	5	5
Chico	2	40	4.4	0.8	2	4	5	5	5
Chico	3	40	3.1	0.8	1	3	3	3	5
Chico	4	40	2.8	0.9	1	2	3	3	5
Chico	5	40	4.9	0.6	1	5	5	5	5
Chico	6	40	2.9	0.9	1	2.75	3	3	5
Chico	7	40	3.6	0.8	2	3	4	4	5
Chico	8	40	3.6	0.8	1	3	3.5	4	5
Chico	9	40	3.3	1.0	1	3	3	4	5
Chico	10	40	3.4	1.0	1	3	3.5	4	5
Chico	11	40	2.9	1.2	1	2	3	3.25	5
Chico	12	40	3.4	0.9	1	3	4	4	5
Chico	13	40	3.4	0.8	1	3	3	4	5
Chico	14	40	3.4	0.8	2	3	3	4	5
Chico	15	40	2.4	1.0	1	2	2	3	5
Chico	16	40	4.2	0.8	2	4	4	5	5

4.7 Correlations between Texture, Vibration, and Ride Quality

The results from texture and roughness measurement, bicycle vibration, and the bicycle ride quality survey are summarized together in Table 4.7.

Correlation analysis included the average macrotexture (MPD, in mm) of each survey section measured using the IP, the average IRI (in m/km) of each survey section, the average bicycling speed (speed in mph), the average normalized vibration (vertical acceleration Az, in *g*) of each survey section measured using accelerometers on all the instrumented bicycles, the ride quality level (Ride Quality, Level 1 to 5) on each survey section, and the percentage of survey participants who rated the pavement "acceptable" (Acceptability, rating 0 or 1). Figure 4.11 through Figure 4.13 respectively present the correlation analysis for the first study (on rural and county roads and highways managed by Caltrans and local agencies), for this second study (of urban pavements), and the combined results of both studies. The correlation plots for the different bicycle types in this second study are presented in Appendix C.

The main observations from the correlation of the combined results from both studies (Figure 4.13) include the following:

a. Strong correlations were found between MPD, bicycle vibration, acceptability, and ride quality level.
b. Medium to weak correlations were found between IRI, bicycle vibration, acceptability, and ride quality level.
c. A relatively weak correlation was found between bicycle vibration and bicycle speed. No significant correlation was found between other variables and bicycle speed (small set of speeds).
d. Vibration appears to be somewhat more sensitive to MPD when MPD values are above 2 mm.

e. Vibration appears to be somewhat more sensitive to IRI when IRI values are above 317 inches/mile (5 m/km).
f. Stronger correlations were found between bicycle vibration with acceptability and ride quality than between MPD and IRI with acceptability and ride quality.
g. The relationship between MPD and ride quality is approximately linear.
h. The approximate range of MPD for bicycle ride quality "acceptability" is based on a straight line interpolation in Figure 4.13 for the percentage of participants who rated sections as "acceptable":
    - 80 percent found 1.8 mm MPD acceptable.
    - 60 percent found 2.1 mm MPD acceptable.
    - 50 percent found 2.3 mm MPD acceptable.
    - 40 percent found 2.5 mm MPD acceptable.
i. The average ride quality level rating (on a scale of 1 to 5) is approximately:
    - 3.5 for an MPD of 1.0 mm
    - 3.0 for an MPD of 1.8 mm
    - 2.5 for an MPD of 2.2 mm
    - 1.5 for an MPD of 3.0 mm
j. Most riders rated a pavement as "acceptable" when the ride quality rating was 3 or greater, and the percentage of riders finding a pavement "acceptable" decreased approximately linearly for ride quality ratings below 3 to a point where almost no one found a pavement acceptable when its ride quality rating was about 1.

Table 4.7: Summary of Values of Variables for Each Survey Section in All Groups

Group	Section	N [a]	MPD [b]	IRI [b]	Speed [b c]	Vibration [b c]	Acceptability [b]	Ride Quality [b]
Davis	1	8	1.07	3.0	7.5	0.73	0.75	2.6
Davis	2	8	1.25	3.0	7.6	0.52	0.88	3.3
Davis	3	8	1.25	4.9	7.7	0.57	1.00	3.4
Davis	4	8	0.72	1.9	7.6	0.23	1.00	4.5
Davis	5	8	1.06	1.8	7.7	0.63	0.88	3.3
Davis	6	8	1.69	2.6	7.5	0.64	0.88	3.0
Davis	7	8	2.12	2.7	7.7	0.54	0.88	3.3
Davis	8	8	0.86	2.4	7.6	0.26	1.00	3.8
Davis	9	8	0.70	1.3	7.6	0.24	1.00	4.9
Richmond	1	25	0.54	3.7	7.7	0.49	1.00	4.3
Richmond	2	25	0.52	3.6	7.6	0.45	0.80	3.6
Richmond	3	25	0.73	1.6	7.6	0.41	0.88	3.8
Richmond	4	25	0.50	2.0	7.7	0.37	0.96	4.3
Richmond	5	25	0.56	2.4	7.6	0.37	1.00	4.0
Richmond	6	25	0.65	1.9	7.7	0.42	0.88	3.7
Richmond	7	25	0.78	3.0	7.4	0.49	0.92	3.4
Richmond	8	25	0.49	3.5	7.5	0.38	0.84	2.6
Richmond	9	25	0.78	4.7	7.4	0.53	0.44	2.0
Richmond	10	25	0.87	1.5	7.7	0.26	0.92	4.4
Richmond	11	25	0.88	2.5	7.8	0.25	0.92	4.2
Richmond	12	25	0.99	4.4	7.6	0.46	1.00	3.6
Richmond	13	25	1.83	3.9	7.5	0.76	0.68	2.8
Richmond	14	25	0.82	2.8	7.5	0.56	0.92	3.4
Richmond	15	25	1.54	2.7	7.9	0.67	0.76	2.6
Sacramento	1	41	1.06	4.8	7.5	0.44	0.95	3.1
Sacramento	2	41	0.79	3.8	7.6	0.42	0.76	2.5
Sacramento	3	41	0.99	1.8	7.5	0.61	0.83	3.4
Sacramento	4	41	1.03	4.2	7.4	0.45	0.95	3.6
Sacramento	5	41	0.77	3.8	7.6	0.42	0.93	3.6
Sacramento	6	40	1.13	3.7	7.5	0.47	0.78	2.9
Sacramento	7	41	0.59	1.9	7.6	0.21	1.00	4.8
Sacramento	8	40	1.04	4.4	7.5	0.49	0.90	3.2
Sacramento	9	41	1.14	5.0	7.4	0.50	0.66	2.7
Sacramento	10	40	0.90	4.6	7.5	0.49	0.88	3.2
Sacramento	11	40	1.18	3.6	7.6	0.41	0.80	3.0
Reno	1	41	1.39	2.6	9.3	0.52	0.90	3.5
Reno	2	41	1.40	2.1	9.5	0.59	0.88	3.2
Reno	3	41	1.32	1.2	8.4	0.50	0.93	3.7
Reno	4	41	0.62	1.6	9.4	0.28	1.00	4.7
Reno	5	41	0.61	2.4	9.1	0.25	1.00	4.8
Reno	6	41	0.85	1.3	9.1	0.38	1.00	4.1
Reno	7	41	0.67	2.7	10.0	0.39	0.95	3.8
Reno	8	41	0.96	2.5	9.2	0.38	1.00	3.9
Reno	9	41	0.87	3.2	9.9	0.42	1.00	3.5
Reno	10	41	1.17	1.5	9.9	0.46	0.88	3.9
Reno	11	41	1.16	1.2	9.8	0.47	0.90	3.8
Reno	12	41	0.34	1.2	8.9	0.37	1.00	4.4
Reno	13	41	1.19	1.4	9.5	0.54	0.80	3.6
Reno	14	41	1.57	1.2	9.7	0.61	0.85	2.9
Reno	15	41	1.39	1.3	9.4	0.50	0.85	2.8
Reno	16	41	1.69	1.5	10.0	0.29	1.00	4.3

Group	Section	N [a]	MPD [b]	IRI [b]	Speed [b c]	Vibration [b c]	Acceptability [b]	Ride Quality [b]
Chico	1	40	0.82	3.3	7.6	0.32	1.00	4.1
Chico	2	40	0.90	4.5	7.8	0.41	1.00	4.4
Chico	3	40	1.49	4.7	7.8	0.64	0.88	3.1
Chico	4	40	0.71	2.8	7.9	0.53	0.75	2.8
Chico	5	40	0.44	1.9	7.6	0.20	0.98	4.9
Chico	6	40	0.94	1.3	7.9	0.39	0.75	2.9
Chico	7	40	1.87	4.1	8.2	0.67	0.95	3.6
Chico	8	40	1.63	3.4	7.9	0.68	0.93	3.6
Chico	9	40	0.98	1.4	7.8	0.48	0.85	3.3
Chico	10	40	1.69	2.3	7.7	0.51	0.90	3.4
Chico	11	40	1.55	1.6	8.2	0.52	0.75	2.9
Chico	12	40	1.46	1.4	8.1	0.47	0.95	3.4
Chico	13	40	1.58	2.6	7.9	0.47	1.00	3.4
Chico	14	40	1.14	1.2	8.0	0.49	0.93	3.4
Chico	15	40	1.47	6.8	7.7	0.62	0.58	2.4
Chico	16	40	0.82	4.8	7.8	0.49	0.98	4.2

Notes: MPD (mm), IRI (m/km), Speed (mph), vibration (g)

[a]: Number of participants in survey.

[b]: Median values of each variable are listed here.

[c]: For all bicycle types.

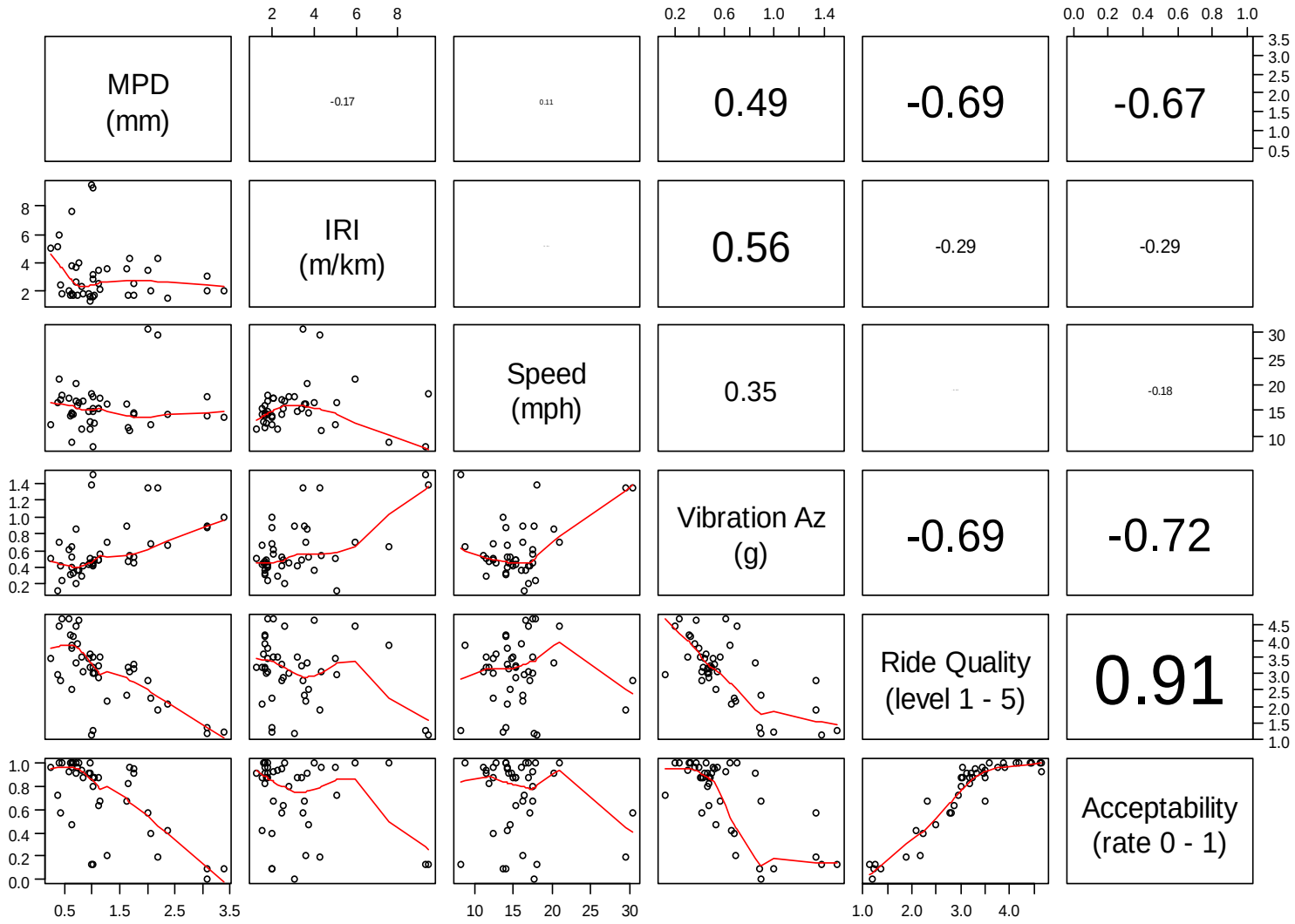

Figure 4.11: Correlations between MPD, IRI, speed, vibration, ride quality level, and acceptability rate (first study [Phases I and II] on rural pavements). *(Note:* scatterplots and smooth fitted lines are shown in lower panels. Correlations between variables are shown in upper panels, with the size of the type within the box proportional to absolute correlation.)

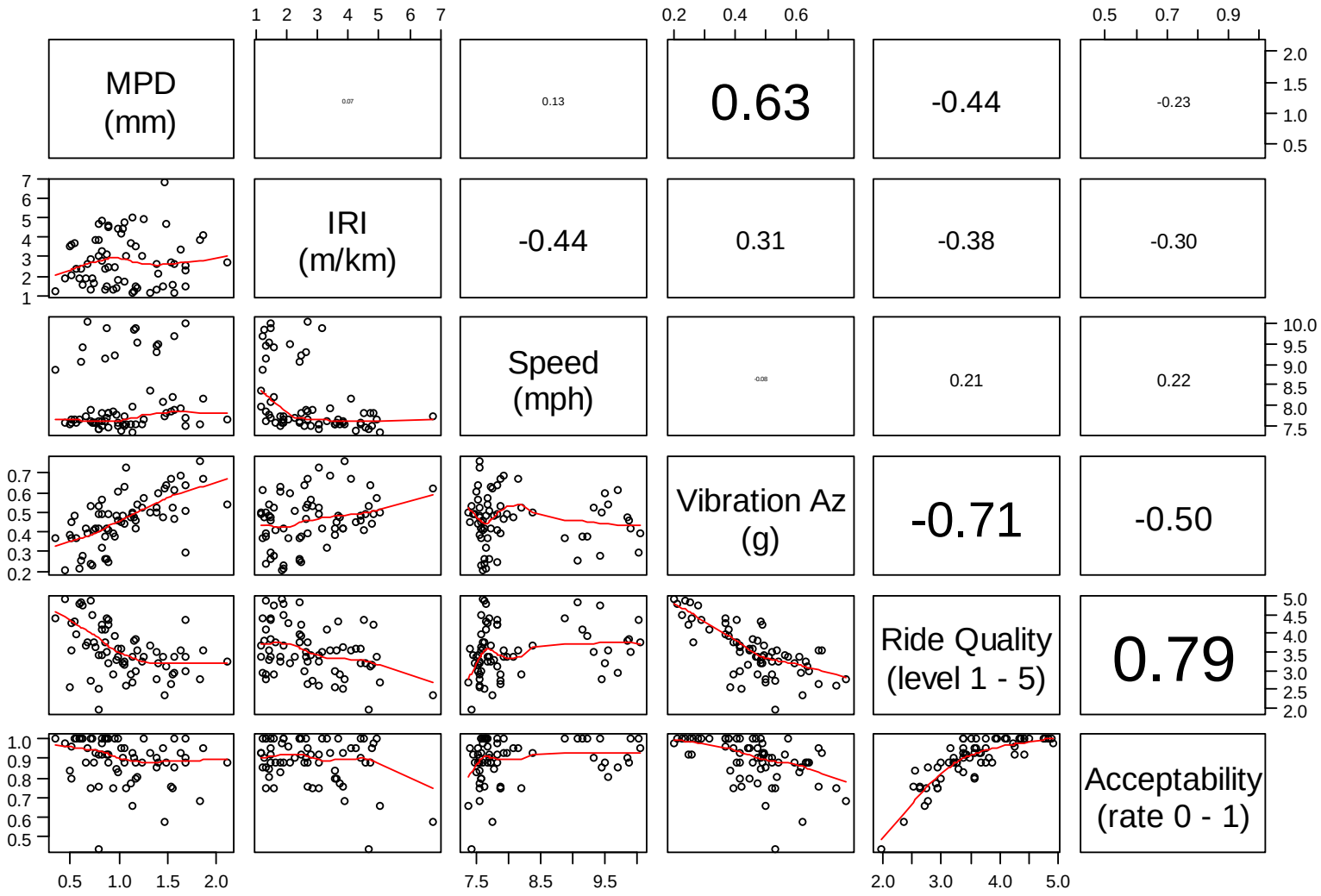

Figure 4.12: Correlations between MPD, IRI, speed, vibration, ride quality level, and acceptability rate (second study on urban pavements). *(Note:* scatterplots and smooth fitted lines are shown in lower panels. Correlations between variables are shown in upper panels, with the size of the type within the box proportional to absolute correlation.)

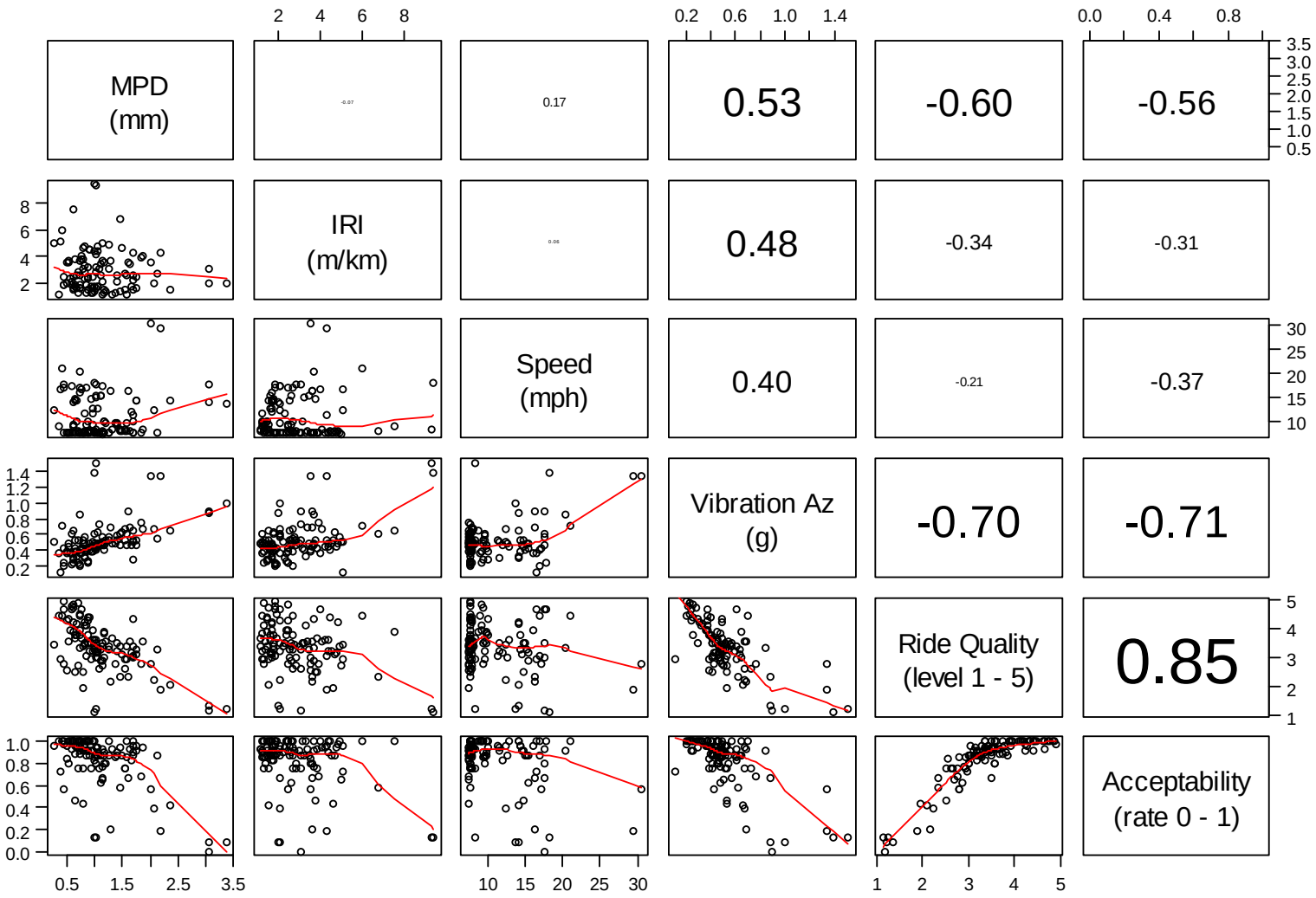

Figure 4.13: Correlations between MPD, IRI, speed, vibration, ride quality level, and acceptability rate (first and second studies combined). *(Note:* scatterplots and smooth fitted lines are shown in lower panels. Correlations between variables are shown in upper panels, with the size of the type within the box proportional to absolute correlation.)

(This page left blank)

5 TRENDS BETWEEN PAVEMENT TEXTURE AND ROUGHNESS WITH PRESENCE OF DISTRESSES

In order to establish basic correlations between pavement roughness and distress, a distress survey was performed and a basic bicycle ride quality index established. When defining cracking, one of the distresses considered, the crack type was identified in the raw distress survey only for informational purposes and was not used in the correlation calculations. A summary of the results and correlations are included in this chapter. The full results of the pavement distress survey are shown in Appendix E.

5.1 City Section Distress Survey

5.1.1 Distress Results

The average pavement distress profile for each city, across all sections, from the pavement distress survey is shown in Table 5.1.

Table 5.1: Summary of Average Pavement Distress Survey Results by City

City	Patches	Utility Cuts	Less than 10% Cracked	10% to 50% Cracked	Greater than 50% Cracked
Davis	33%	22%	44%	56%	0%
Richmond	27%	80%	53%	20%	27%
Sacramento	64%	55%	36%	55%	9%
Reno	44%	11%	69%	25%	6%
Chico	63%	7%	56%	38%	6%

5.2 Relationships between Pavement Roughness and Distresses

5.2.1 IRI and Distresses

Table 5.2 shows the correlations between average IRI and pavement distress, by city. Trends were found between the measured values. On average, the median IRI was 26.3 percent higher on sections with patches and 6.2 percent higher on sections with utilities located in the bicycle traveled way compared with sections that had neither of those distresses. On average, IRI was 10.9 percent higher on sections with 10 to 50 percent of the section having cracking than in those sections with less than 10 percent cracking. On average, IRI was 24.6 percent higher on sections with greater than 50 percent of the section showing cracking compared to sections with less than 10 percent of the section showing cracking. These correlation trends did not match for Reno sections with greater than 50 percent cracking.

Table 5.2: Average IRI Results for Varying Conditions of Pavement

City	Average IRI (m/km)						
	Patching	No Patching	Utility Cuts	No Utilities	Greater than 50% Cracked	10% to 50% Cracked	Less than 10% Cracked
Davis	4.08	3.08	3.40	3.42	-	4.05	2.62
Richmond	5.67	4.30	4.51	5.76	4.98	4.79	5.52
Sacramento	4.13	3.65	4.46	3.35	5.23	3.62	4.14
Reno	2.98	1.99	2.49	2.16	1.61	3.51	2.11
Chico	3.99	3.49	4.28	3.33	6.01	3.87	3.51
Average (m/km)	**4.17**	**3.30**	**3.83**	**3.60**	**4.46**	**3.97**	**3.58**
Average (inches/mile)	**264**	**209**	**243**	**228**	**283**	**252**	**227**

5.2.2 MPD and Distresses

The correlations between MPD and pavement distress are shown in Table 5.3. Conflicting trends were found between the measured values. On average, the median MPD was 7.3 percent lower on patched sections and 21.2 percent higher on sections with utilities located in the traveled way compared with sections that had neither of those distresses. On average, the median MPD was 1.2 percent lower on sections of 10 to 50 percent cracking compared to those with less than 10 percent cracking. On average, the median MPD was 28.5 percent higher in sections with greater than 50 percent cracking compared with those with less than 10 percent cracking. In Davis and Richmond there was a trend between patching, utilities, and increases in cracking with increases in measured MPD. In Sacramento there was a correlation between increased cracking with increases in measured MPD, but no trend between patching and utilities with increases in measured MPD. In Reno and Chico there was no trend between patching, utilities, and increases in cracking with increases in measured MPD.

Table 5.3: Median MPD Results (mm) for Varying Conditions of Pavement

City	Median MPD (mm)						
	Patching	No Patching	Utilities	No Utilities	Greater than 50% Cracked	10% to 50% Cracked	Less than 10% Cracked
Davis	1.32	1.04	1.81	0.83	-	1.25	0.99
Richmond	0.92	0.79	0.88	0.66	1.16	0.83	0.69
Sacramento	0.95	0.96	0.93	0.98	1.10	1.03	0.80
Reno	0.86	1.24	1.06	1.14	1.38	0.93	1.10
Chico	1.06	1.48	1.20	1.24	1.48	0.88	1.41
Median	**1.02**	**1.10**	**1.17**	**0.97**	**1.28**	**0.99**	**1.00**

5.2.3 Correlations between Bicycle Vibration and Distresses

The correlations between measured bicycle vibration for the commuter, mountain, and road bicycle types and pavement distress are shown in Table 5.4. The distresses were defined in terms of percent of the section with cracking. Across all sections, the correlation R^2 ranged from 0.01 to 0.09. The correlations were highly dependent on which city was being considered. These results show correlations of 0.35 or greater in Davis, Richmond, and Chico between the vibrations experienced by the cyclist and the amount of cracking. In Richmond and Sacramento, the correlation between the vibrations experienced by the cyclist and the amount of cracking are all below 0.08, indicating that roughness was due to causes other than cracking.

Table 5.4: Summary of Correlations (R^2) between Vibration and Percent of Sections with Cracking

City	Commuter Bicycle	Mountain Bicycle	Road Bicycle
Davis	0.45	0.54	0.46
Richmond	0.56	0.35	0.43
Sacramento	0.03	0.01	0.08
Reno	0.00	0.00	0.00
Chico	0.36	0.44	0.75
All sections	**0.01**	**0.02**	**0.09**

Based on the results shown in this chapter, the relationships between distresses and MPD are unclear. On the other hand, a relationship between IRI and distresses was found, but how this affects cyclists is unknown as IRI was developed as a measure of vehicle ride quality. In three of the five cities examined, correlations were found between vibration and the amount of cracking in the sections for all bicycle types. When correlating vibration and the percent of each section with cracking across all cities, the R^2 values ranged from 0.01 (for commuter bikes) up to 0.09 (for road bikes) which both indicate almost no correlation.

5.3 Preliminary Exploration of a Bicycle Ride Quality Index

5.3.1 Correlation of Bicycle Ride Quality Index and Rider Survey

Correlations were explored between a preliminary bicycle ride quality index (BRQI) based on the number of acceleration events above a threshold and bicycle ride quality.

For each test section, the number of acceleration events greater than 3 *g* and 2 *g* were summed for the commuter and mountain bicycles, respectively, and those greater than 4 *g* and 3 *g* for road bicycles. The number of events was then normalized to section length to produce a bicycle ride quality index unit of acceleration events per kilometer (events/km). The BRQI was then correlated with the mean rider survey feedback (1 to 5 scale) from

the bicycle ride quality survey. Results are shown for the commuter, mountain, and road bicycles in Table 5.5, Table 5.6, and Table 5.7, respectively.

Table 5.5: Summary of Correlations (R^2) between BRQI and Mean Survey Results (1 to 5) for Commuter Bicycle by City

City	Commuter Bicycle			
	Events/km greater than 3 *g*		Events/km greater than 2 *g*	
	Front	Rear	Front	Rear
Davis	0.14	-	0.20	0.02
Richmond	0.50	0.31	0.60	0.45
Sacramento	0.11	0.03	0.18	0.06
Reno	0.00	0.04	0.31	0.01
Chico	0.58	0.27	0.47	0.37
All Sections	**0.26**	**0.10**	**0.33**	**0.17**

Table 5.6: Summary of Correlations (R^2) between BRQI and Mean Survey Results (1 to 5) for Mountain Bicycle by City

City	Mountain Bicycle			
	Events/km greater than 3 *g*		Events/km greater than 2 *g*	
	Front	Rear	Front	Rear
Davis	0.06	-	0.32	0.02
Richmond	0.59	0.23	0.61	0.48
Sacramento	0.15	0.16	0.12	0.18
Reno	0.10	0.18	0.23	0.15
Chico	0.62	0.36	0.56	0.55
All Sections	**0.30**	**0.12**	**0.33**	**0.26**

Table 5.7: Summary of Correlations (R^2) between BRQI and Mean Survey Results (1 to 5) for Road Bicycle by City

City	Road Bike			
	Events/km greater than 3 *g*		Events/km greater than 4 *g*	
	Front	Rear	Front	Rear
Davis	0.44	0.41	0.30	0.32
Richmond	0.24	0.34	0.28	0.48
Sacramento	0.30	0.29	0.28	0.37
Reno	0.48	0.61	0.39	0.70
Chico	0.54	0.41	0.52	0.59
All Sections	**0.30**	**0.32**	**0.30**	**0.41**

The results show that there are correlations (R^2) ranging from 0.00 to 0.60 for the commuter bicycle, from 0.02 to 0.62 for the mountain bicycle, and from 0.24 to 0.70 for the road bicycle. The correlations were performed for each city and also across all sections in all cities. The results show that the road bicycle has the strongest correlation between ride quality survey results (1 to 5 scale) and the events/km in BQRI. This is likely due to the fact that a road bicycle has smaller tires, at a higher pressure, and is therefore more sensitive to the pavement conditions than commuter and mountain bicycles. It should be noted that overall, the correlation coefficients are

low, indicating that there are other factors that are not considered in the index that are important to explaining bicycle ride quality.

In addition to correlating the BRQI between all the sections in each survey city, correlations were also performed by surface type. All the sections were sorted according to basic surface type characteristics, that is, chip seal, HMA, and slurry seal, and the correlations are shown for each bicycle type in Table 5.8, Table 5.9, and Table 5.10.

Table 5.8: Summary of Correlations (R^2) between BRQI (events/km) and Mean Survey Results (1 to 5) for Commuter Bicycle by Surface Type

Surface Type	Commuter Bike			
	Events/km greater than 3 *g*		Events/km greater than 2 *g*	
	Front	Rear	Front	Rear
All	0.26	0.10	0.33	0.17
Chip seal	0.06	0.02	0.01	0.00
HMA	0.46	0.28	0.53	0.30
Slurry seal	0.22	0.08	0.30	0.16

Table 5.9: Summary of Correlations (R^2) between BRQI (events/km) and Mean Survey Results (1 to 5) for Mountain Bicycle by Surface Type

Surface Type	Mountain Bike			
	Events/km greater than 3 *g*		Events/km greater than 2 *g*	
	Front	Rear	Front	Rear
All	0.30	0.12	0.33	0.26
Chip seal	0.01	0.09	0.09	0.07
HMA	0.53	0.30	0.47	0.40
Slurry seal	0.30	0.15	0.30	0.27

Table 5.10: Summary of Correlations (R^2) between BRQI (events/km) and Mean Survey Results (1 to 5) for Road Bicycle by Surface Type

Surface Type	Road Bike			
	Events/km greater than 3 *g*		Events/km greater than 4 *g*	
	Front	Rear	Front	Rear
All	0.30	0.32	0.30	0.41
Chip seal	0.35	0.02	0.13	0.13
HMA	0.56	0.53	0.56	0.55
Slurry seal	0.26	0.28	0.21	0.37

The comparisons of BRQI and mean survey results among pavement surface types show the strongest correlations between the HMA surface and road bicycle (R^2 = 0.53 to 0.56), commuter bicycle (R^2 = 0.30 to 0.53), and mountain bicycle (R^2 = 0.30 to 0.53). The comparisons between BRQI and mean survey results showed lower R^2 correlations for both the chip seal and slurry seal surface types. The low correlations between the BRQI based on vibration events per kilometer and the survey results indicate that there are likely other characteristics of the pavement surface that can be better correlated to the mean survey results.

5.3.2 Correlation of Bicycle Ride Quality Index and Distress

The correlation between BRQI and distress was checked for the two accelerometer mounting locations (stem and seatpost) and for each bicycle type. The results showed that the strongest correlations of events/km and the percent of the section with cracking were as follows:

- Commuter bicycle in the rear mounting position with a 2 *g* event threshold (R^2=0.164),
- Mountain bicycle at the front mounting position with a 3 *g* event threshold (R^2=0.220), and
- Road bicycle in the rear mounting position with a 4 *g* event threshold (R^2=0.207).

As an example, the results for the road bicycle with a rear mounting position are illustrated in Figure 5.1. The amount of cracking was defined from the pavement distress survey: <10 percent (minimal), 10 to 50 percent (moderate), >50 percent (severe).

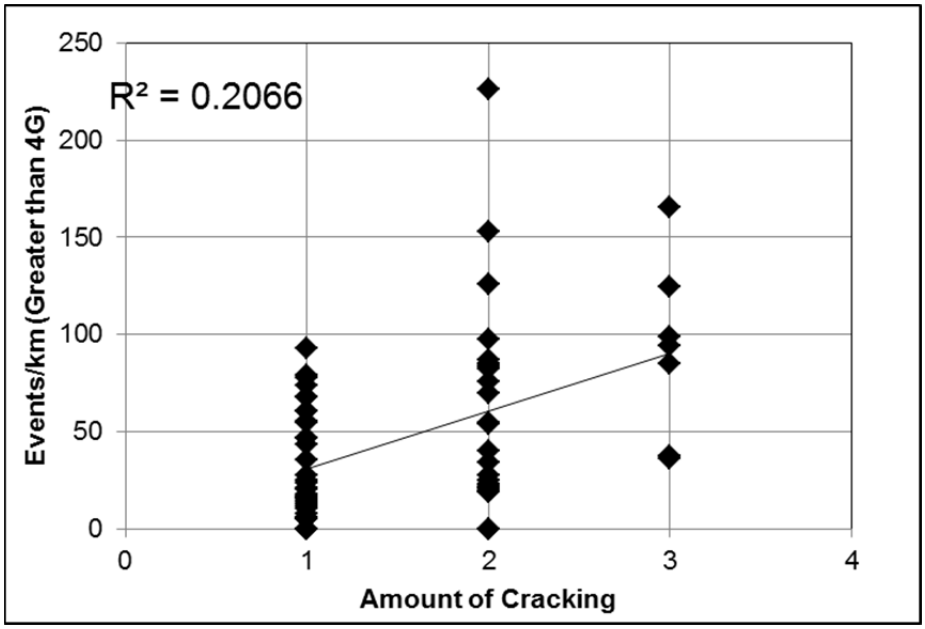

Figure 5.1: Acceleration BQRI (events/km) versus severity of cracking (1 to 3 scale), road bike, rear mount, 4 *g* event threshold.

(This page left blank)

6 CORRELATIONS BETWEEN PAVEMENT MACROTEXTURE AND TREATMENT SPECIFICATIONS

Correlations were identified between pavement texture measured in terms of MPD and surface treatment specifications. The data used to develop the correlations came from state highway sections selected especially because specification information was available, and from those city and county sections used for the rider survey analysis for which specifications were also available.

6.1 Macrotexture Measurement Results from Caltrans Highway Sections

Table 6.1, Table 6.2, and Table 6.3 respectively summarize the results of macrotexture measurement results (in terms of MPD) on Caltrans state highway sections with chip seals, slurry seals, and microsurfacing treatments. Figure 6.1 shows the geographic locations of the state highway sections tested. Plots of the MPD ranges measured on each chip seal, slurry seal, and microsurfacing test section appear in Figure 6.2, Figure 6.3, and Figure 6.4, respectively. A simple average of the median, standard deviation, and Q1 and Q3 values was taken for comparisons between specification types throughout this report. For specifications that have only one tested section, the statistical values were obtained from the complete, raw data set.

Table 6.1: Summary of MPD (mm) Results: Chip Seals

EA #	Location	Construction Year	Specification Year	Specification Binder Type	Specification Aggregate Type	Median MPD	Avg. of Median MPDs	Avg. of Std. Dev.
06-0N2804	06-Kin-33-8.0/19/0	2012	2006	Asphaltic emulsion (polymer-modified)	3/8" medium screenings	1.30	1.15	0.19
06-0N2804	06-Kin-41-33.0/28.5	2012				1.10		
06-0N2804	06-Mad-145-6.8/0.2	2012				1.04		
11-2M2104	11-Imp-78-62.9/80.7	2012	2006	Asphalt rubber binder	1/2" medium precoated screenings	4.13	2.44	0.29
02-3E9004	02-Sis-97-34.5/40.0	2012				0.74		
09-354504	09-Mno-395-40.1/44.9	2013	2006	Asphalt rubber binder	3/8" precoated screenings	1.47	1.47	0.85
06-0P7504	06-Ker-46-37.5/49.0	2014	2010	Asphaltic emulsion (polymer-modified)	Coarse 1/2" max. precoated screenings	2.07	2.23	0.32
06-0S2404	06-Fre-33-72.8/R83.0	2015				2.36		
06-0S2404	06-Fre-33-R63.0/69.1	2015				2.26		
03-0G1404	03-Yol-16-0.0/18.9	2015	2010	Asphaltic emulsion (polymer-modified)	3/8" medium maximum screenings	1.11	1.27	0.33
06-0Q8404	06-Ker-223-10.9/20.0	2014				1.34		
06-0Q8404	06-Ker-223-1.9/4.0	2014				1.45		
06-0Q8404	06-Ker-58-15.4/27.2	2014				1.36		
06-0Q8404	06-Ker-43-16.3/24.1	2014				1.49		
06-0S2304	06-Mad-49-1.3/9.3	2015				1.56		
06-0S2304	06-Mad,Mpa-41-40.9/45.7,0.0/4.9	2015				2.09		
03-4M5504	03-Gle-162-76.3/84.6	2013				0.58		
03-4M5504	03-Gle-162-67.2/76.3	2013				0.75		
06-0Q8504	06-Ker-119-0.0/r9.5	2014				1.21		
08-0Q5004	08-SBd,Riv-62-66.0/91.0	2015				1.01		

EA #	Location	Construction Year	Specification Year	Specification Binder Type	Specification Aggregate Type	Median MPD	Avg. of Median MPDs	Avg. of Std. Dev.
07-2W8304	07-LA-2-26.4/82.3-WB	2012	2010	Asphalt rubber binder	1/2" medium maximum screenings	4.00	3.41	0.44
07-2W8304	07-LA-2-26.4/82.3-EB	2012				3.97		
03-0G1904	03-Sac-104-4.6/17.7	2015				2.27		
06-0Q7904	06-Ker-46-54.0/57.	2014	2010	Asphalt rubber binder	Coarse 1/2" max. precoated screenings	1.41	1.23	0.28
06-0Q7904	06-Ker-65-0.7/6.1	2014				1.04		
06-0S2504	06-Ker-166, 178-9.0/24.5, 27.2/57.1	2015				0.94		
06-0S2504	06-Ker-178-27.2/57.1-WB	2015				1.4		
06-0S2504	06-Ker-178-27.2/57.1-EB	2015				1.36		
02-4E9604	02-Teh-172-0.0/8.9	2013	2010	Asphalt rubber binder	Fine 3/8" max. screenings	1.78	1.31	0.27
02-4F1604	02-Sis-3-R48.3/53.1	2013				0.91		
02-4G1704	02-Mod-395-23.3/40.0	2014				1.27		
02-4E9704	02-Teh-36-55.2/67.5	2013				1.54		
02-4F1304	02-Sha-44-46.3/43.2	2013				1.18		
02-4F1304	02-Sha-44-57.0/48.2	2013				1.29		
02-4F1304	02-Las-139-40.0-30.0	2013				1.56		
02-4F1504	02-Sis-97-0.5/R11.5	2013				1.06		
02-4F1504	02-Sis-3-27.0/36.0	2013				0.8		
02-4F1804	02-Tri-3-69.0/74.5	2013				1.56		
02-4F1804	02-Teh-36-11.5/6.0	2013				1.41		
02-4G9704	02-Sis-3-6.9/23.0	2014				1.3		
09-358504	09-Mno-6-26.5/32.3	2014				1.38		

Table 6.2: Summary of MPD (mm) Results: Slurry Seals

EA	Location	Construction Year	Specification Year	Aggregate Type	Median MPD	Avg. of Median MPDs	Avg. of Std. Dev.
02-3E9404	02-Plu-70-0.0/33.0	2012	2006	Type III	0.73	0.75	0.18
06-0N3004	06-Tul-201-0.0/14.0	2012			0.80		
08-0P7904	08-Riv-95-L0.0/36.2	2013			0.71		
07-1W7004	07-LA-66-0.0/3.0	2015	2010	Type II	0.96	0.82	0.21
03-0G1804	03-Yol-128-7.8/10.0	2015			0.67		
11-2M4104	11-SD-94, 188-30.0	2013	2010	Type III	2.45	2.45	0.52

Table 6.3: Summary of MPD (mm) Results: Microsurfacings

EA	Location	Construction Year	Specification Year	Aggregate Type	Median MPD	Avg. of Median MPDs	Std. Dev. of Median MPDs
03-4M3404	03-ED-49-15.7/24.0	2012	2006	Microsurfacing Type II	0.57	0.65	0.31
03-4M3404	03-ED-153-0.0/0.6	2012			0.72		
08-0P3804	08-SBd-83, 210-R0.0/7.2, R30.2/R33.2	2013	2006	Microsurfacing Type III	0.81	0.81	0.17
02-4E9804	02-Plu-70-37.5/46.2	2013	2010	Microsurfacing Type III	0.64	0.71	0.15
03-0G1704	03-Pla-28-0.8/5.9	2015			0.69		
03-0G1704	03-Pla-28-10.5/11.1	2015			0.66		
03-4M8004	03-ED-89-0.0/8.6	2013			0.86		

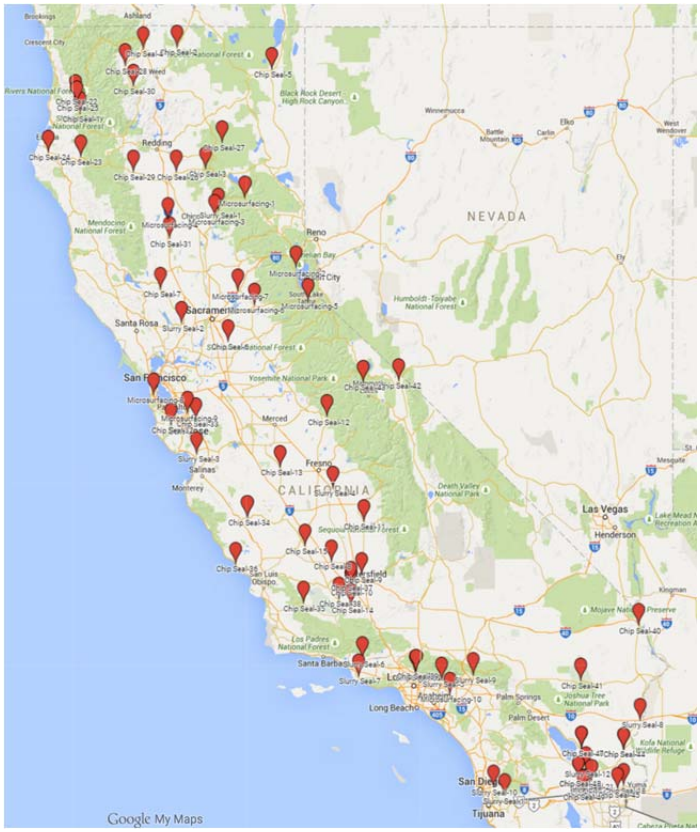

Figure 6.1: Summary of state highway sections for comparison of specifications and MPD.

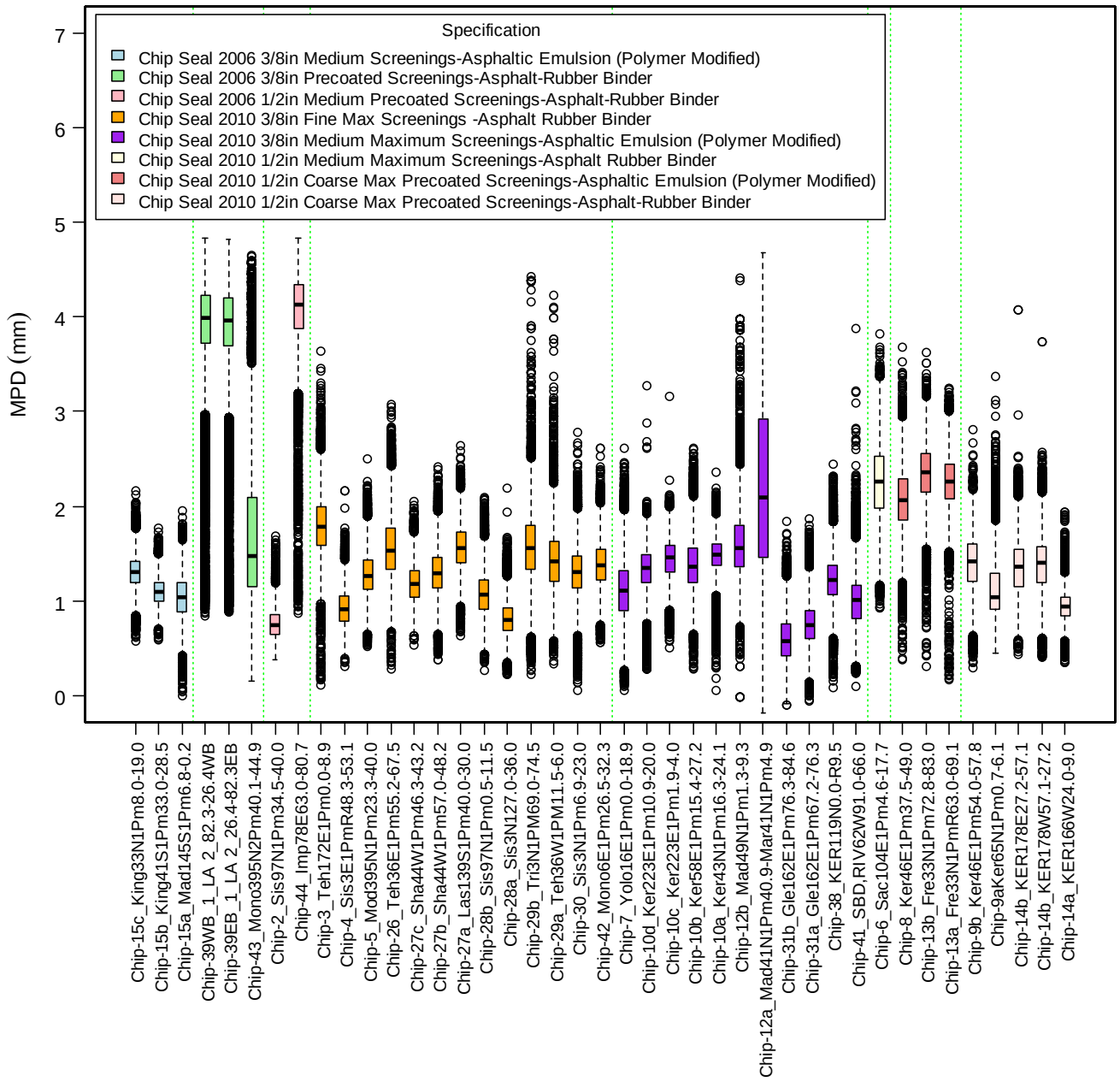

Figure 6.2: Ranges of MPD measured on chip seal sections.

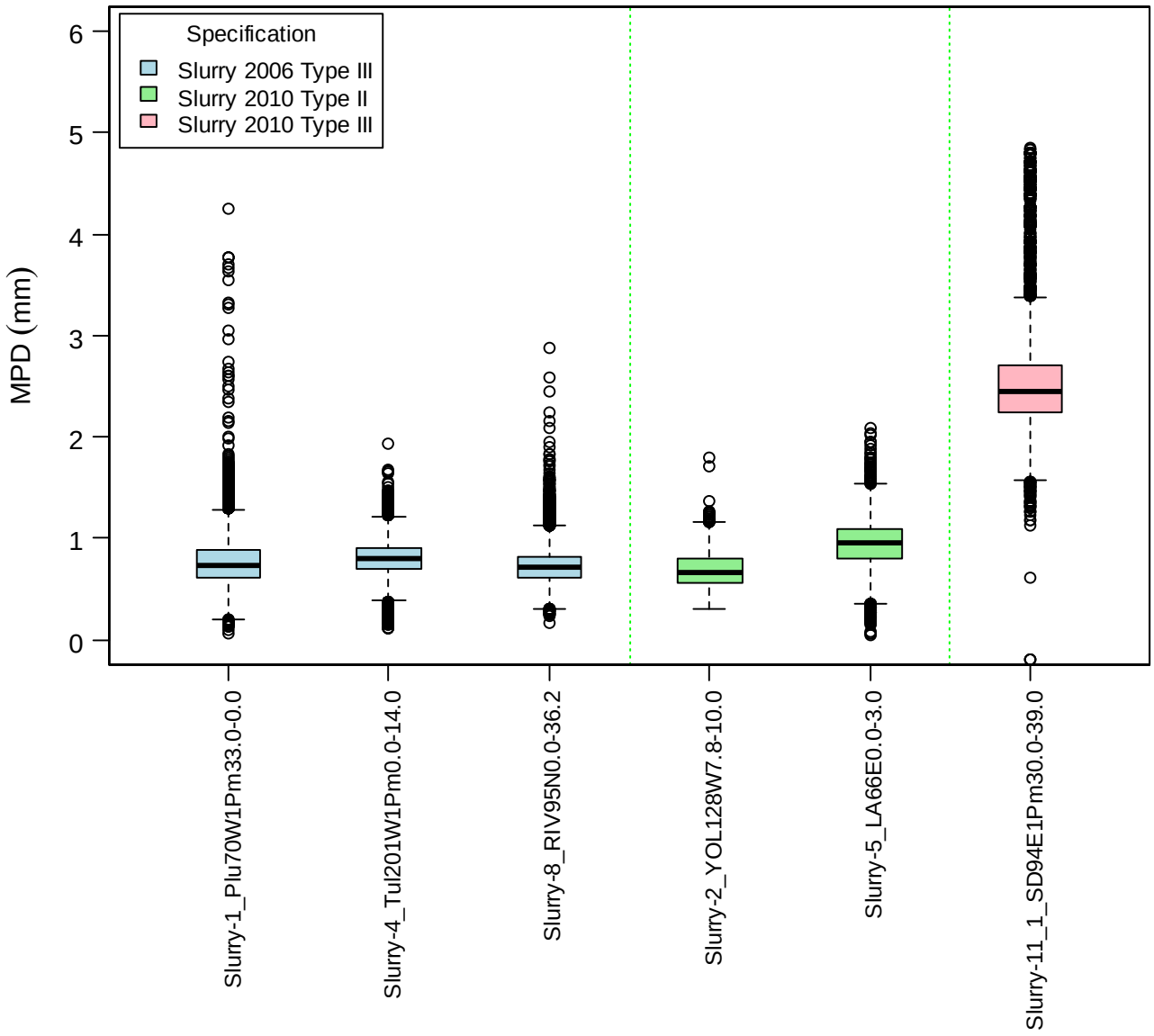

Figure 6.3: Ranges of MPD measured on slurry seal sections.

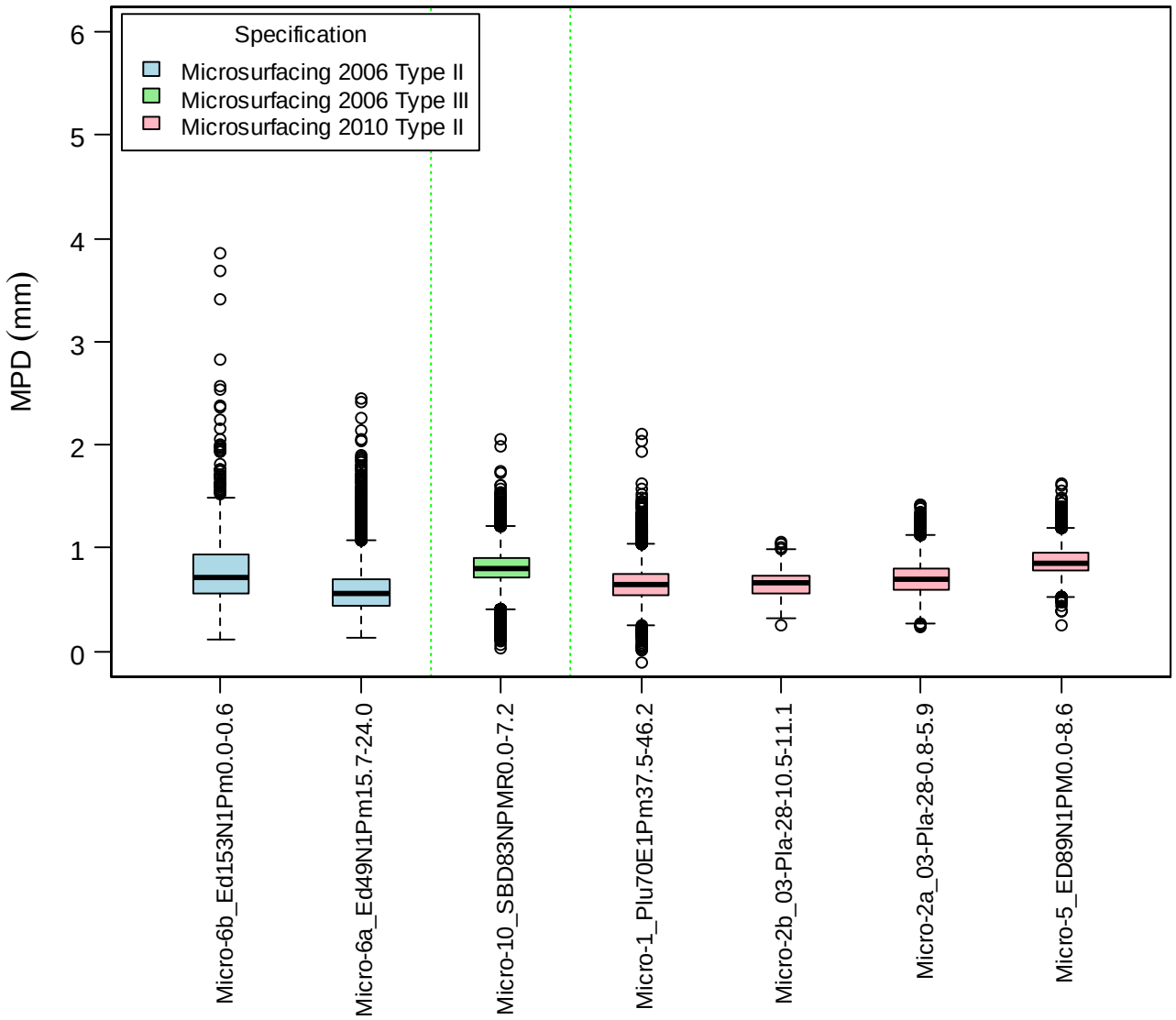

Figure 6.4: Ranges of MPD measured on microsurfacing sections.

6.2 Analysis of Chip Seal Projects

Table 6.4 shows the median values for chip seal treatment specification types tested in this study. Project data going back to 2012 were accessed from the website of the Division of Engineering Services, Office Engineer database. Information collected included treatment specifications, project plans, and project award dates. Material gradation information was unavailable for the state highway projects. The UCPRC attempted to obtain this data from Caltrans but those as-built gradation results were stored in a format that was beyond the resources of this project to retrieve for analysis.

Table 6.4: Summary of Median MPD Results: Chip Seals

Specification Year	Specification Binder Type	Specification Aggregate Type	Average of Median MPD	Average of Std. Dev.	Average of Q1	Average of Q3
2006	Asphaltic emulsion (polymer-modified)	3/8" medium screenings	1.15	0.19	1.02	1.27
2006	Asphalt rubber binder	1/2" medium precoated screenings	2.44	0.29	2.26	2.60
2006	Asphalt rubber binder	3/8" precoated screenings	1.47	0.85	1.15	2.09
2010	Asphaltic emulsion (polymer-modified)	Coarse 1/2" max. precoated screenings	2.23	0.32	2.03	2.43
2010	Asphaltic emulsion (polymer-modified)	3/8" medium maximum screenings	1.27	0.33	1.06	1.49
2010	Asphalt rubber binder	1/2" medium maximum screenings	3.41	0.44	3.13	3.65
2010	Asphalt rubber binder	Coarse 1/2" max. precoated screenings	1.23	0.28	1.06	1.41
2010	Asphalt rubber binder	Fine 3/8" max screenings	1.31	0.27	1.15	1.48

The distribution of median MPD results for all chip seal projects is shown in plotted in Figure 6.5. The average median MPD values for each chip seal specification type is shown in Figure 6.6.

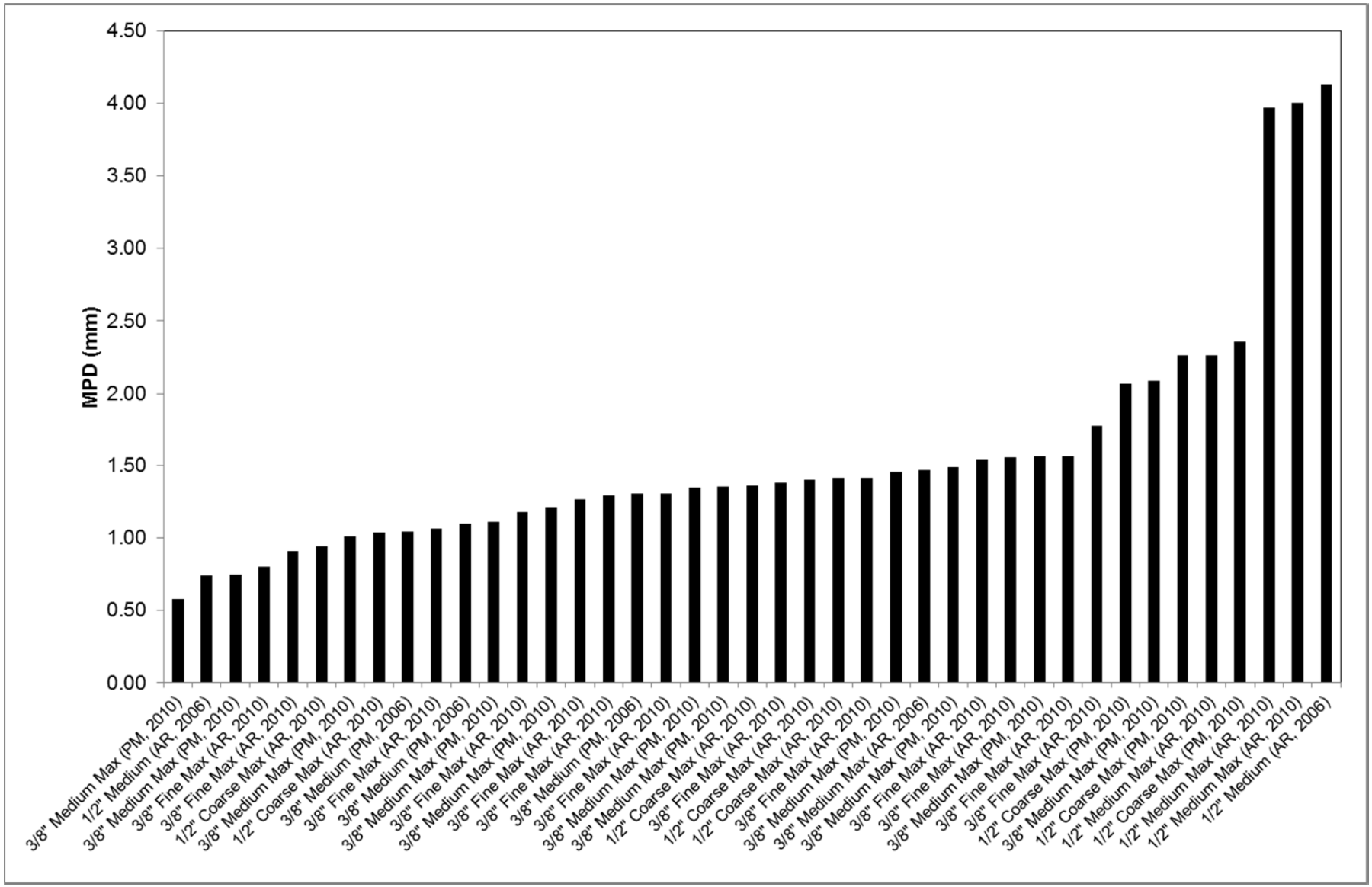

Figure 6.5: Distribution of median MPD results for all projects, chip seals.

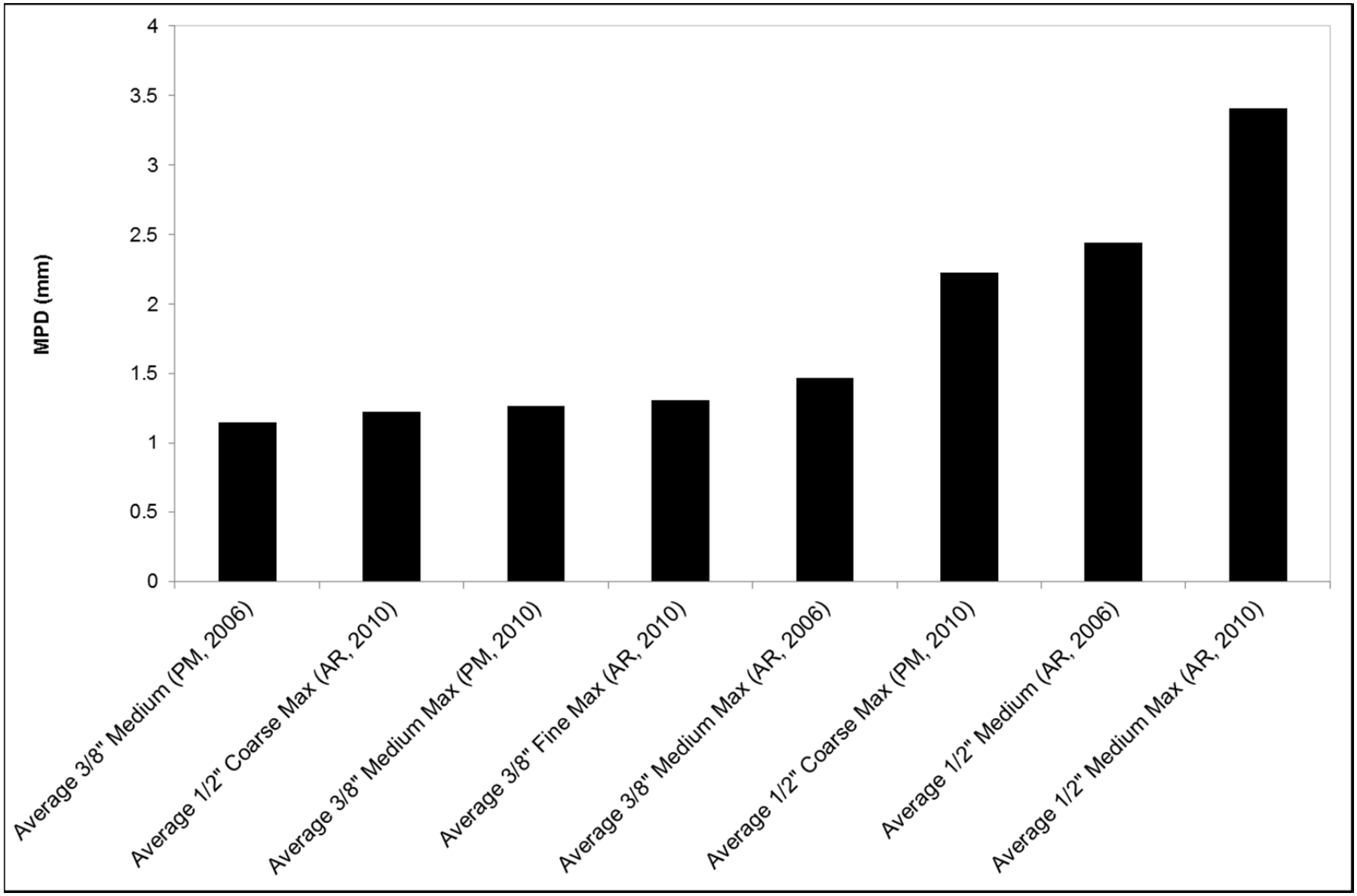

Figure 6.6: Chip seal average of median MPD results by specification type.

6.2.1 Correlation of Macrotexture and Chip Seal Aggregate Gradation Specifications

Correlations between macrotexture and aggregate gradation specifications were evaluated for state highway chip seal sections. The gradation bands as stated on the standard specifications were identified for each chip seal project. All available data was considered for correlations, but because most of the screening material is concentrated among a few sieve sizes, moving to the next sieve size did not improve correlation. Ideally UCPRC would have used actual laboratory test results for the aggregate screenings from quality control testing, but this information was unavailable. The following chip seal treatment types were tested and the key aggregate gradation properties as found in the specifications for each project are summarized in Table 6.5.

Table 6.5: Chip Seal Standard Specification Maximum Aggregate Size (first sieve with 100 percent passing) and #4 Sieve Bounds

Specification Year	Binder Type	Aggregate Type	Maximum Aggregate Size (inches)	#4 Upper Bound (% passing)	#4 Lower Bound (% passing)
2006	Asphaltic emulsion (polymer-modified)	3/8" medium screenings	1/2	15	0
2006	Asphalt rubber binder	1/2" medium precoated screenings	3/4	5	0
2006	Asphalt rubber binder	3/8" max. precoated screenings	3/4	15	0
2010	Asphaltic emulsion (polymer-modified)	Coarse 1/2" max. precoated screenings	1/2	5	0
2010	Asphaltic emulsion (polymer-modified)	3/8" medium maximum screenings	3/8	15	0
2010	Asphalt rubber binder	1/2" medium maximum screenings	3/4	5	0
2010	Asphalt rubber binder	Coarse 1/2" max. precoated screenings	3/4	2	0
2010	Asphalt rubber binder	Fine 3/8" max. screenings	3/4	15	0

The maximum aggregate size shown in Table 6.5 was defined as the smallest sieve with 100 percent passing allowed in the specification. The #8 (2.36 mm) standard sieve size was not considered because it is not always included as a specified size. When the maximum aggregate size and the average median MPD for each specification type are compared, as shown in Figure 6.7, the correlation R^2 value is 0.09. For the #4 sieve size upper specification limit, Figure 6.8 shows a correlation R^2 value of 0.33.

When the specified maximum aggregate size and median MPD for all projects are compared without averaging them by specification type, the R^2 value is 0.03. For the #4 sieve size, the R^2 value is 0.17. Figure 6.9 and Figure 6.10 show results of the correlations. The trend for the maximum aggregate size is as expected, with generally increasing MPD versus increasing maximum aggregate size, however there is very large variability of MPD for each maximum aggregate size.

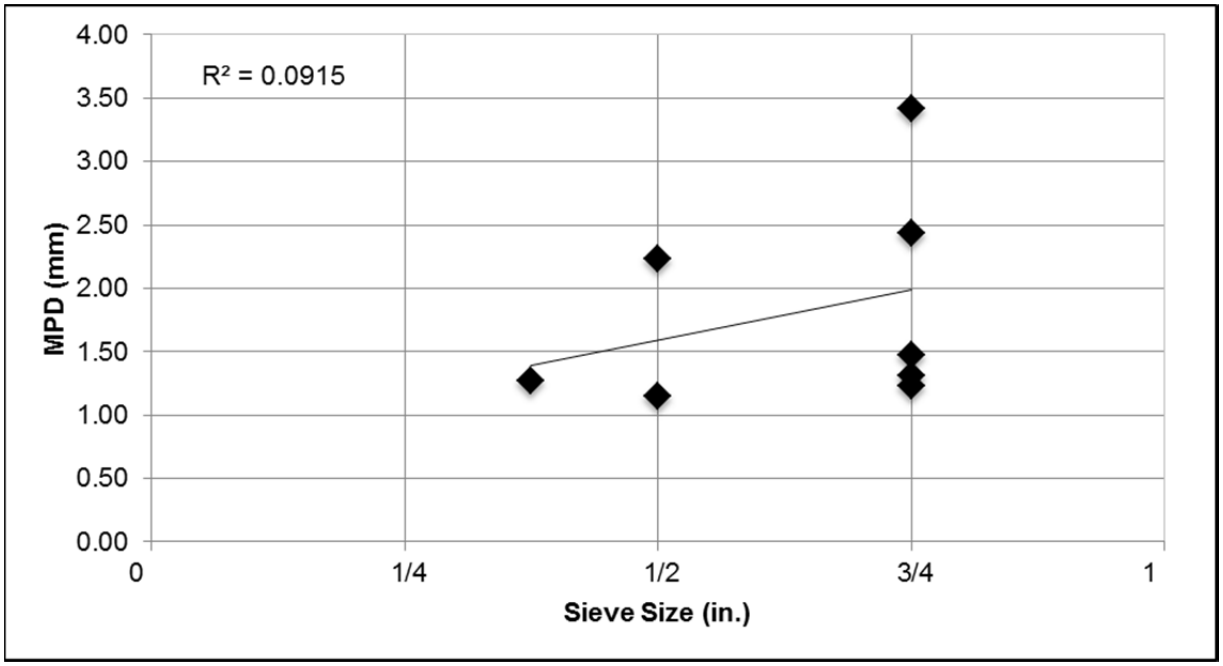

Figure 6.7: Maximum aggregate size (smallest sieve with 100 percent passing allowed in the specification) versus average median MPD for each chip seal specification type.

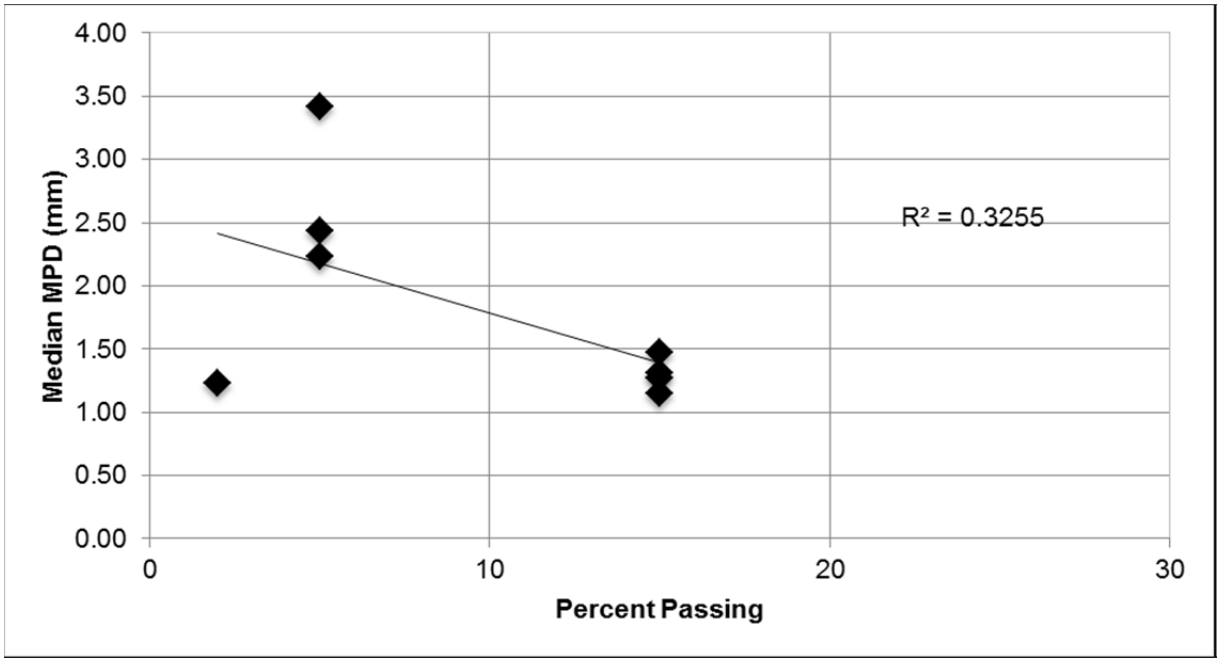

Figure 6.8: Percent passing #4 sieve upper bound versus average median MPD for chip seal specification types.

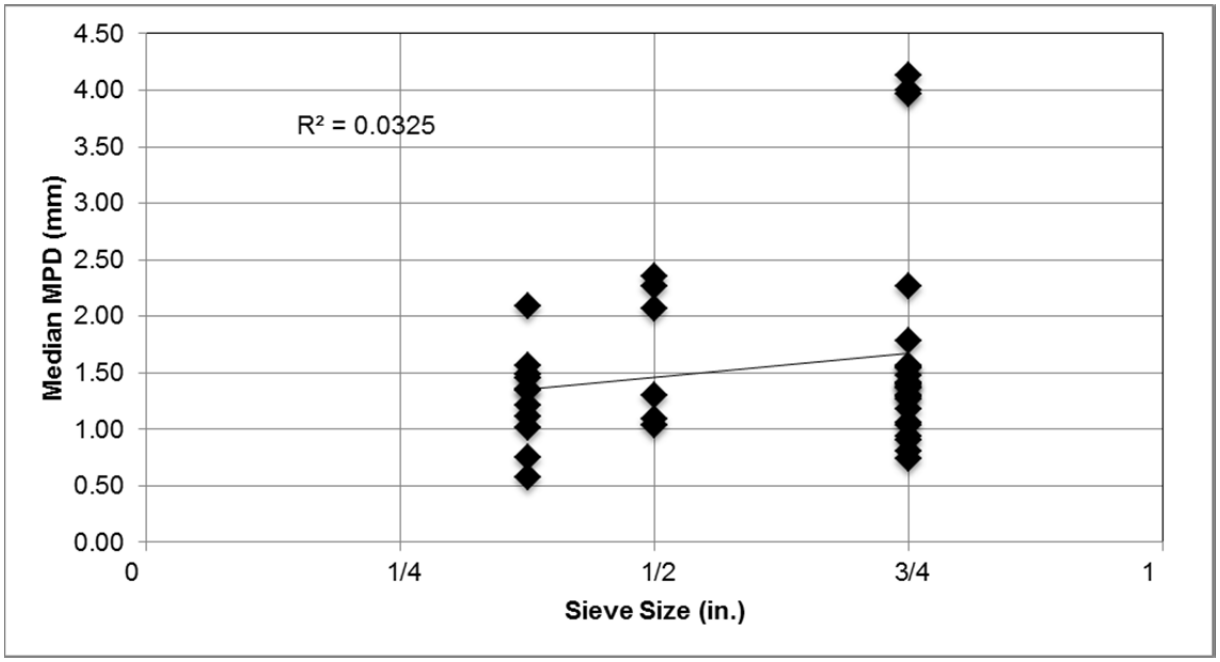

Figure 6.9: Maximum aggregate size (smallest sieve with 100 percent passing allowed in the specification) versus median MPD for all chip seal sections.

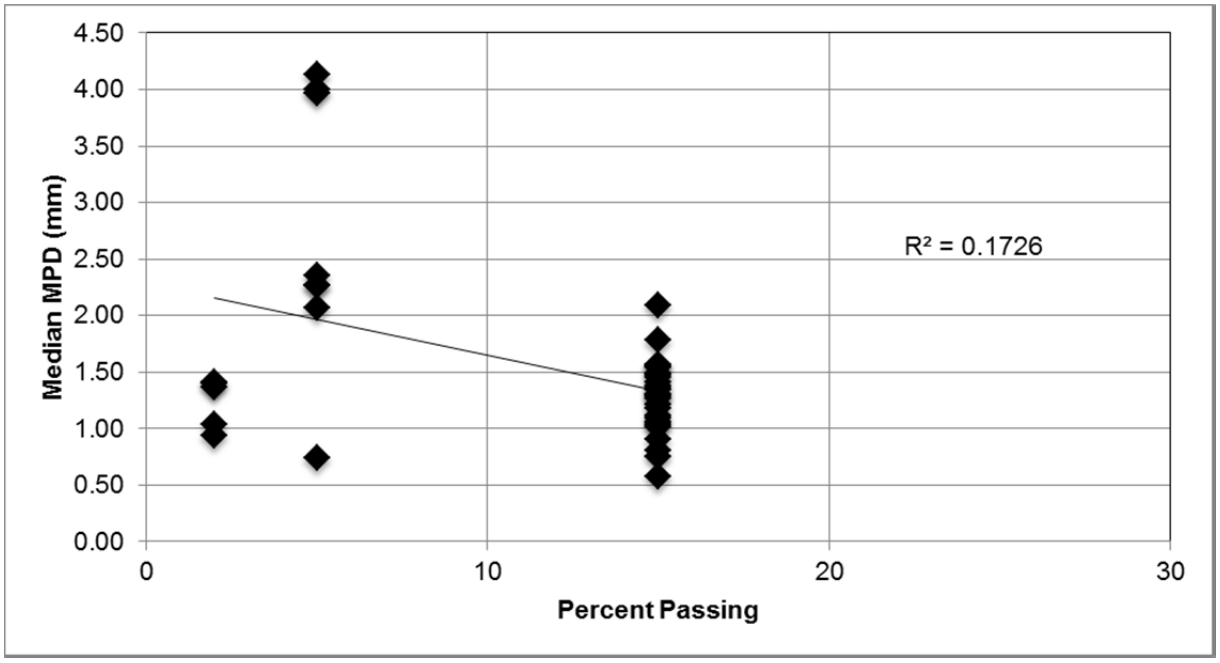

Figure 6.10: Percent passing #4 sieve upper bound versus median MPD for all chip seal sections.

6.2.2 *Macrotexture versus Time*

The median MPD values of the state highway chip seal sections were plotted versus their construction date for all of the seals placed with different specifications, as shown in Figure 6.11. The actual project completion date was not available for all projects, and the available information regarding the construction date found for all projects was the project award date.

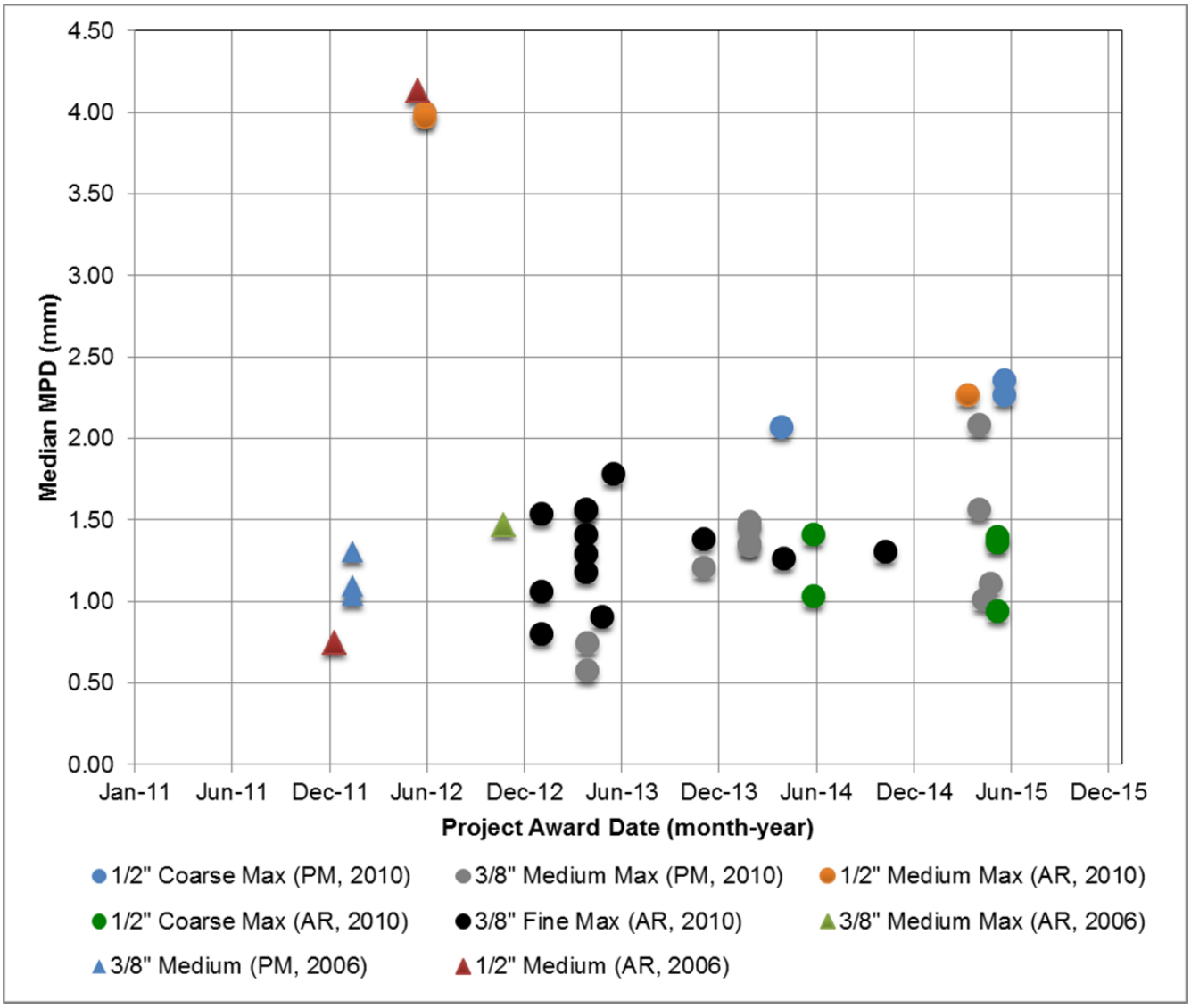

Figure 6.11: MPD results measured in fall 2015 plotted by project award date.
***(Note:* Asphalt rubber binder [AR], polymer-modified binder [PM], 2006 Standard CT Specification [2006], 2010 Standard CT Specification [2010])**

6.3 Analysis of Slurry Seal Sections

6.3.1 Correlation of Macrotexture and Slurry Seal Aggregate Gradation Specifications

Slurry seal as-built aggregate gradation data was available for the sections in Reno, as provided by the Washoe County RTC. Specifications and/or material gradation information was not available from the other cities or from Caltrans. Table 6.6 summarizes gradation values for Type II and Type III slurry seal aggregates obtained from laboratory testing by Lumos and Associates. Aggregate sizes used for comparison were the #4 and #8 standard sieve sizes. Figure 6.12 and Figure 6.13 show results of the correlations between MPD and percent passing the critical size. For the #4 sieve size, the R^2 value was 0.46. For the #8 sieve size, the R^2 value was 0.38. The results show, as expected, the median MPD decreasing as the percentage passing the critical aggregates sizes (#4 and #8) increases.

Table 6.6: Summary of Laboratory Gradation Results for Reno Slurry Seal Treatments

City	Section	Maximum Aggregate Size (inch)[3]	Percent Passing #4 Sieve	Percent Passing #8 Sieve
Reno	1	3/8	78	48
Reno	2	3/8	81	56
Reno	3	3/8	81	56
Reno	4	3/8	96	67
Reno	5[1]	–		–
Reno	6	3/8	86	55
Reno	7	3/8	96	72
Reno	8	3/8	96	72
Reno	9	3/8	96	72
Reno	10	3/8	97	70
Reno	11	3/8	90	63
Reno	12[2]	–	–	–
Reno	13	3/8	97	70
Reno	14	3/8	80	55
Reno	15	3/8	89	59
Reno	16[1]	–	–	–

Notes:
[1] : HMA section
[2] : no laboratory test results available.
[3] : smallest sieve with 100 percent passing.

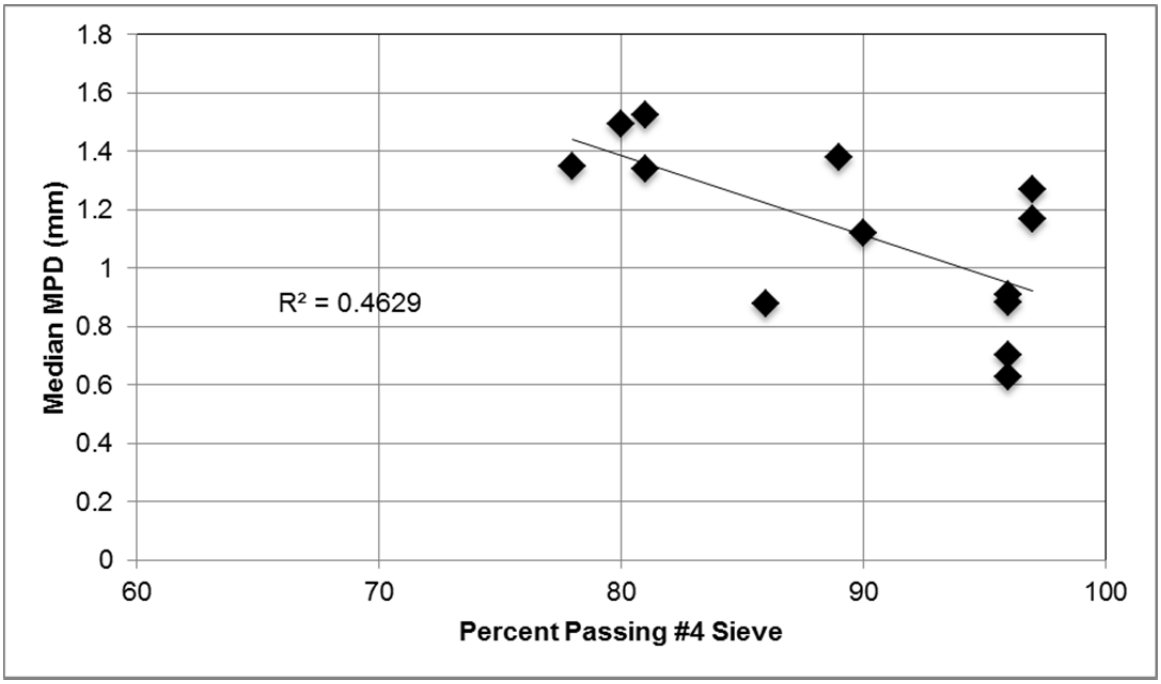

Figure 6.12: Correlations of percent passing the #4 sieve and median MPD (mm).

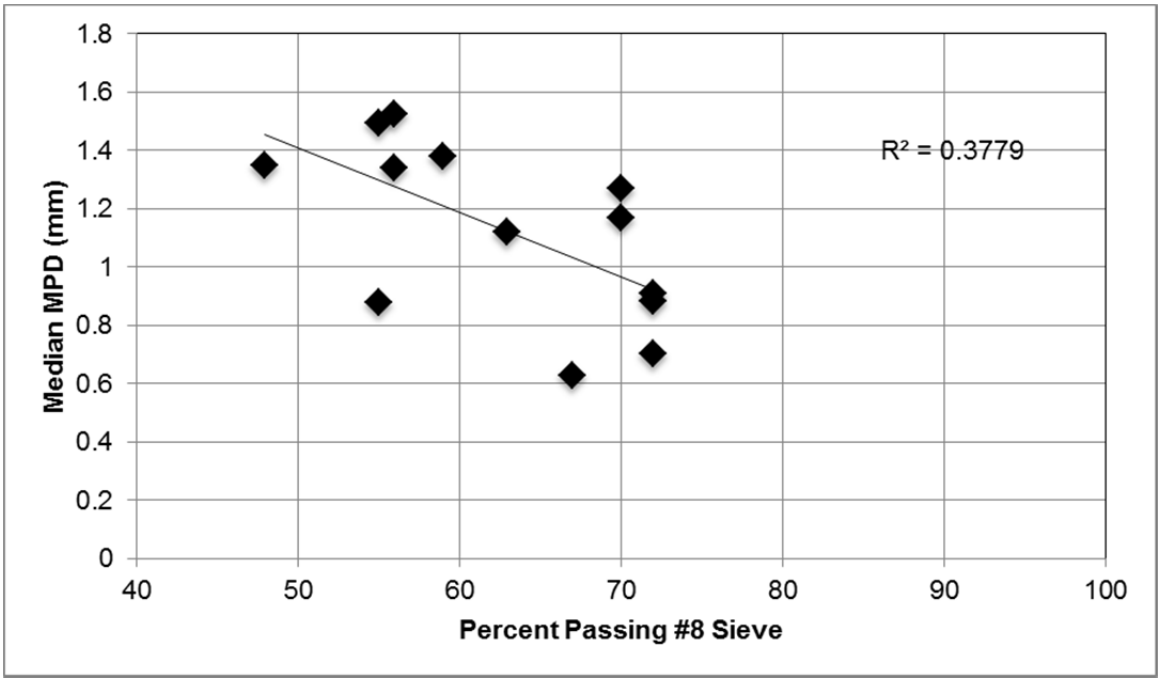

Figure 6.13: Correlations of percent passing the #8 sieve and median MPD (mm).

(This page left blank)

7 MODELING FOR BICYCLE RIDE QUALITY

The results of the bicycle ride quality surveys, including riders' opinions of the sections and their demographic information, and the measurements of MPD and IRI were used to develop models for predicting pavement ratings (1 to 5) and the acceptability of the pavement to cyclists.

7.1 Data Exploration

The scatterplot matrix from the rural highway survey in the first study, shown in Figure 7.1, provided valuable information about potential significant explanatory variables and possible multicollinearity between variables. Since both IRI and MPD are measures of pavement condition, one concern is that the two variables might be highly correlated. With a correlation coefficient of only -0.17, this was found not to be the case for this study and allowed for the inclusion of both IRI and MPD in the modeling efforts. As far as explanatory variables for acceptability ratings, MPD was found to be highly correlated with acceptability given its correlation of -0.66, while IRI had much smaller value of -0.30. Vibration was found to be highly correlated with acceptability (-0.72), so given that both IRI and MPD are highly correlated with vibration, one can expect the inclusion of these two condition variables in the model to effectively serve as a proxy for much of the vibration experienced by a bicycle rider.

7.2 Modeling the Acceptability of Pavement

The first model specified was a simple varying intercept-only model. Three additional models were specified with predetermined groups of variables thought to influence acceptability (see Table 7.1). These models are nested models starting with parsimony and then adding complexity. All models were specified with the same general form (i.e., the only differences were the addition of predictor variables).

7.2.1 Varying Intercept Model

The varying intercept model serves as a baseline and provides information about the significance of the variability among people and among segments. The large amount of variation among individuals is expected, given that people have different experiences and therefore different expectations for what is acceptable. The large variability among segments is also expected, since the segments have different attributes such as pavement condition, lane configurations, etc.

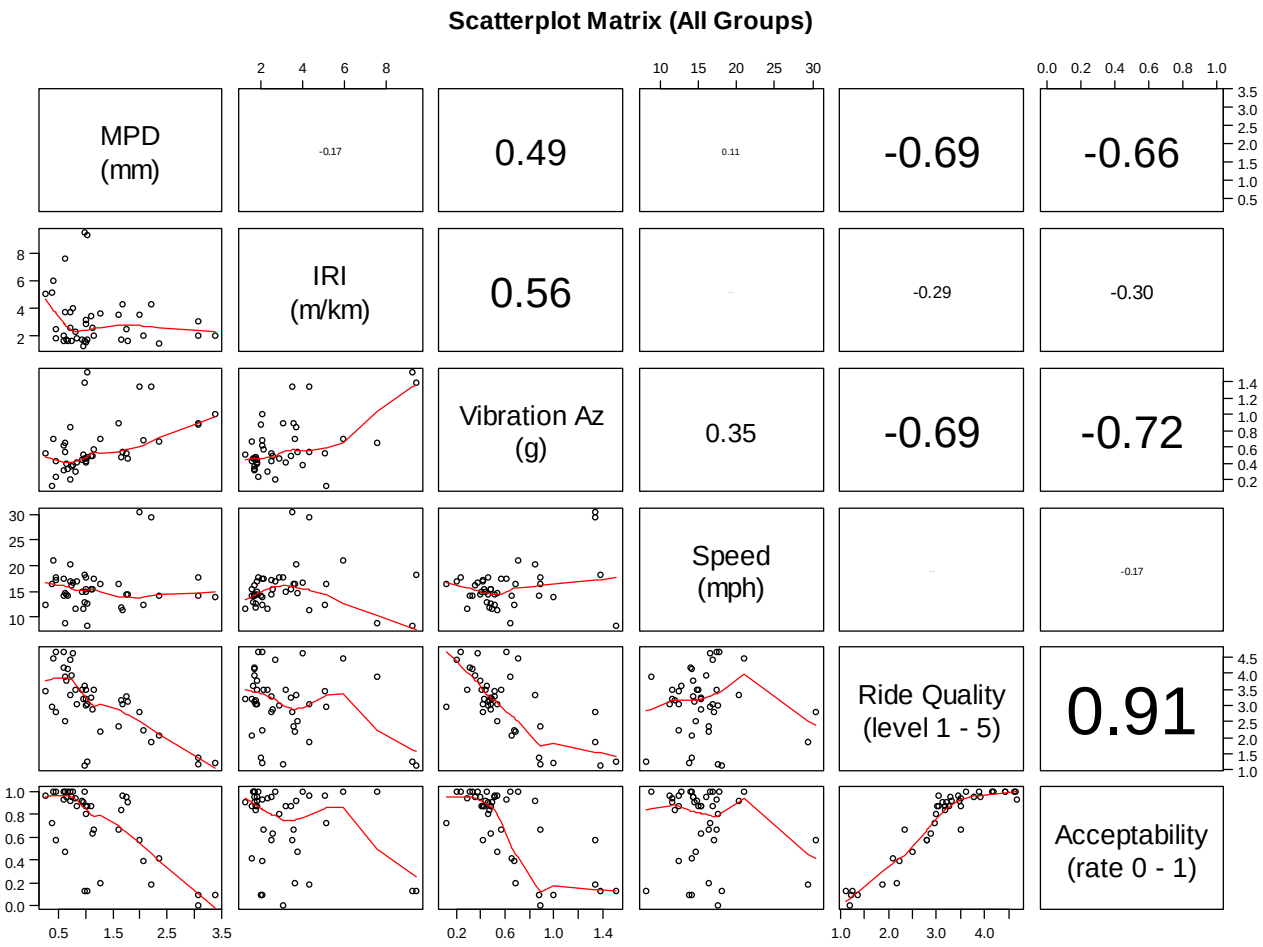

Figure 7.1: Correlations between MPD, IRI, vibration, speed, ride quality level, and acceptability level (all groups) from the first study.
***(Note:* scatterplots and smooth fitted lines are shown in lower panels. Correlations between variables are shown in upper panels, with the size of the type within the box proportional to absolute correlation.)**

7.2.2 Pavement Characteristic Model

To try to capture some of the within-segment variance, the mean and standard deviation for IRI and MPD were added to the model. The coefficients for the mean MPD and mean IRI were both found to be significant and negative. This is intuitive since it shows that as MPD and IRI increase, the likelihood that an individual will rate the section as acceptable decreases. The standard deviation for MPD was found to be insignificant although the standard deviation for IRI was found to be significant and positive, indicating that riders are more likely to rate a segment acceptable as the IRI becomes more variable. It is possible that this means that riders are willing to accept riding on segments where there are sections of the segment that have a high IRI as long as there are also sections of the segment with a low IRI where they feel comfortable. It may also be that cyclists are able to maneuver more freely (using rider discretion, the slower speed and the bicycle's thinner wheels) than the vehicle carrying the IRI measuring device (which conducts measurements in the same path on the pavement), and this

allows them to avoid the sections of the segment that have high IRI. The bicycles have smaller tires and a rider can adjust their lane position if they see small bumps or holes ahead of time. The WAIC improves moving from the intercept-only model to consideration of pavement characteristics, suggesting that the new model is better for prediction.

7.2.3 Bicycle/Personal Characteristics Model

To attempt to capture some of the variance among people, information about the riders and their bicycles were included. The effects of gender, bicycling frequency, age, education, and tire pressure were investigated. None of these variables were found to be significant with 90 percent confidence, however, gender was found to be significant with a confidence of about 80 percent. Previous studies have found that female riders tend to be more concerned with traffic interactions and with having adequate bicycle infrastructure such as separated bike lanes, so it is likely that they may also be more sensitive to pavement condition. Bicycling frequency is over-represented in the sample, given that 70 percent of the riders in the survey said that they bicycled at least every other day. This means that although age and tire pressure were found to be insignificant in this study, this may not hold true for the larger population, which includes people who do not bicycle as often. Bicycle type and frame material were also considered but found to be insignificant. It should be noted that the sample size is different for models that include personal characteristics since those 66 out of 2,886 survey respondents who chose not to answer this section of the survey were removed from the sample before fitting the model.

7.2.4 Full Model

The full model combines the pavement characteristics model and the personal characteristics model. As expected, the WAIC for the full model is the lowest out of all the models, indicating that it is the model that fits the data the best. It can be seen that the mean intercept and the varying intercepts among the individuals and segments are still significant, showing that there is still explanatory information that was not captured in the survey and modeling process. This information could include the person's bicycling history and experience, and features of the road that are not captured by MPD and IRI, such as drains or many other factors.

By simulating riders and pavement conditions and holding all other aspects constant, the full model can be used to predict the percentage of the population that would rate a given segment as acceptable. Two example simulations are shown in Figure 7.2 and Figure 7.3. The first figure is for a simulated rider independent of gender and other personal characteristics that influence opinion, and the second figure is a simulation for the type of user most likely to rate a section as unacceptable, which is a female rider who bikes often and has at least a BA degree. When using a plot to try to guide decision making for treatment choice, it is important to first consider what the population of interest is.

These plots show that it is the combination of MPD and IRI which determines acceptability. For example, it is predicted that when IRI is less than 129 inches/mile (2 m/km), 90 percent of the simulated riders would still find the segment acceptable up to an MPD of 1.7 mm. However, if IRI reaches 258 inches/mile (4 m/km), then the MPD at which 90 percent of the simulated riders would feel it is acceptable is 1.4 mm. For high levels of IRI, such as 380 inches/mile (6 m/km), in order to satisfy 90 percent of the simulated riders, MPD would need to be less than 1 mm. For frequent-biking, educated, female riders, the thresholds for acceptability are somewhat lower. For example, to have 90 percent of the simulated riders from this population deem a segment acceptable when the IRI is 258 inches/mile (4 m/km), MPD would need to be 1.3 mm, which is 0.1 mm lower than for the combined male and female population.

It should be mentioned that since pavement condition is not the only factor that influences segment acceptability, it is possible that there are certain segments which will never be acceptable to bicyclists because of a perceived lack of safety due to interactions with vehicles. It is also important to mention that even if a segment is found acceptable by 95 percent of its riders, if the riding population is large enough, there will still be people who will find the segment unacceptable, for example 25 out of every 500 riders who use a section each month.

Table 7.1: Coefficients Resulting from the Modeling for Acceptability

		Varying Intercepts			Macrotexture and Roughness			Personal Characteristics			Full Model		
	Model Parameter	**Mean**	**90% interval**		**Mean**	**90% interval**		**Mean**	**90% interval**		**Mean**	**90% interval**	
Mean Intercept	**Constant**	3.87	3.29	4.48	6.12	4.6	7.58	4.83	3.83	5.86	7.26	5.43	9.17
Varying Intercepts (constants), Deviations from Mean Intercept	**st.dev. (σ) Person**	2.32	1.94	2.68	1.4	0.47	2.3	2.4	2.01	2.79	1.83	0.95	2.77
	st.dev. (σ) Segment	2.27	1.82	2.69	2.04	1.61	2.44	2.3	1.85	2.75	2.09	1.64	2.51
Varying Slopes	**st.dev. (σ) Person MPD**				1.92	1.18	2.62				1.58	0.69	2.43
	st.dev. (σ) Person IRI				0.13	0	0.25				0.14	0	0.27
Main Pavement Effects	**Mean MPD**				-1.29	-2.41	-0.22				-1.53	-2.69	-0.39
	st.dev. MPD				1.05	-1.33	3.4				0.82	-1.64	3.16
	Mean IRI				-0.72	-1.12	-0.32				-0.67	-1.09	-0.27
	st.dev. IRI				0.43	0.06	0.79				0.39	0	0.74
Main Personal Characteristic Effects	**Female**							-0.59	-1.25	0.14	-0.57	-1.25	0.14
	Bicycle Often (>= every other day)							-0.56	-1.32	0.22	-0.45	-1.21	0.34
	Age (centered and scaled by 2σ)							0	-0.71	0.77	-0.09	-0.86	0.66
	Education (>= BA degree)							-0.21	-0.91	0.5	-0.17	-0.91	0.54
	Bicycle Tire Pressure (centered and scaled by 2σ)							-0.33	-1.1	0.4	-0.27	-1.03	0.48
Number of Observations		2,886			2,886			2,820			2,820		
Widely Applicable Information Criteria (WAIC)		1,336.6			1,304.6			1,270.2			1,248.9		

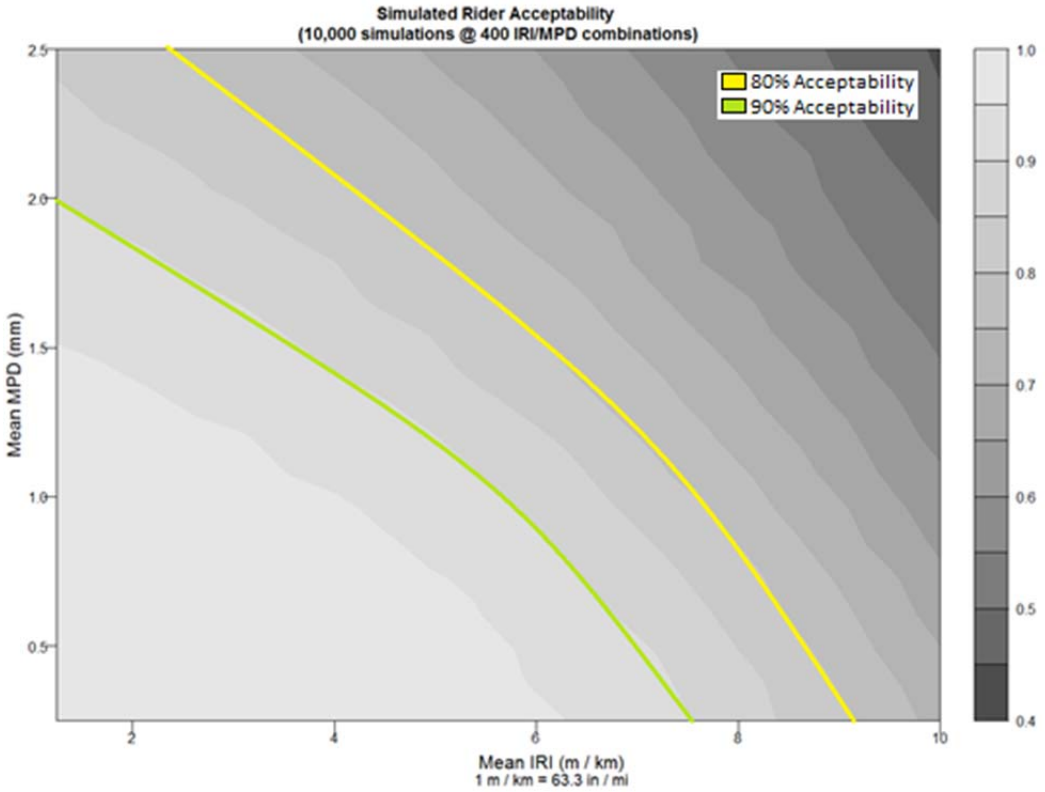

Figure 7.2: Counterfactual plot of the simulated predicted probability of acceptance for a simulated rider independent of gender and other influencing personal characteristics.
***(Note:* the yellow line represents the conditions where 80 percent of simulated riders would find the section acceptable, holding all other variables constant. The green line represents the 90 percent boundary.)**

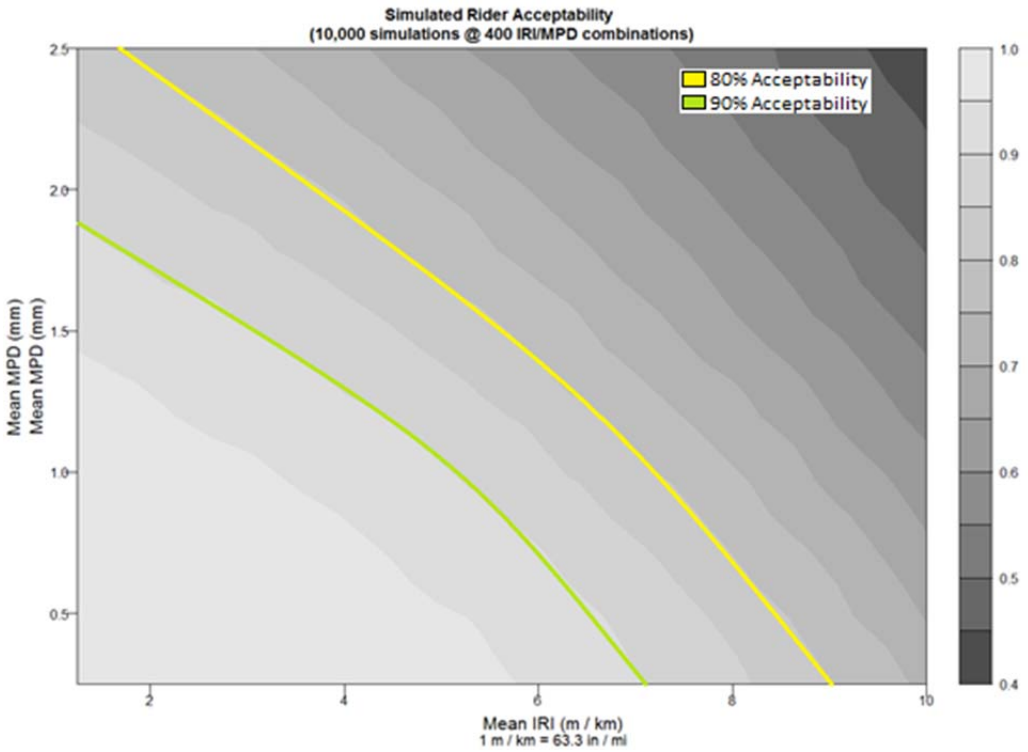

Figure 7.3: Counterfactual plot of the simulated predicted probability of acceptance for the most discriminating rider (a female rider, with at least a BA in education level, who bicycles often).
***(Note:* the yellow line represents the conditions where 80 percent of simulated riders would find the section acceptable, holding all other variables constant. The green line represents the 90 percent boundary.)**

(This page left blank)

8 MODELING FOR BICYCLE ROLLING RESISTANCE

Developing a physical model for bicycle rolling resistance, as discussed in Section 2.6, involved estimating the global coefficient of friction and relative changes in μ between various pavement surface types. The findings discussed in this chapter include the effects of various pavement surfaces on cyclist efficiency, which infers that pavement rolling resistance influences the bicycle and the rider. Two conclusions can be drawn from the results: first, if a cyclist rides with a similar effort on two pavements, the pavement with the higher μ value will result in an increase in the time required to travel the same distance; and, second, if a cyclist chooses to travel at the same speed on the pavement with a higher μ, it will require an increase in effort to overcome the additional forces resulting from the change in μ. The effects of vibration were not considered in this model.

8.1 Comparing Power Meters

To further examine the role of power meters in measuring rider power output and explore various types of measuring systems, a second power meter was included in the study and fastened to the left side of the crankset on Section 1. The two power meters were designated as coming from either Manufacturer A or Manufacturer B, and the results of measurements by each are summarized in Table 8.1. The correlation of the measurements taken by the two meters was R^2= 0.988, and the average difference between the two measured values was 4.5 percent. It should be noted that different calibration techniques were applied to each meter type based on the manufacturers' specifications.

Table 8.1: Comparison of Power Meter Testing Results

Target Power (watts)	Average Measured Power Output (watts)		Difference (%)	Number of Values Recorded
	Manufacturer A	Manufacturer B		
350	366	348	4.9	144
350	365	337	7.7	140
300	313	286	8.6	161
300	296	289	2.4	151
250	258	249	3.5	152
250	251	249	0.8	161
200	214	204	4.7	176
200	217	203	6.5	169
150	175	160	8.6	201
150	161	159	1.2	186
350	348	333	4.3	147
350	350	345	1.4	146
		Average	**4.5**	

The different power meter types were validated in order to explore various methods of measuring the power output of the rider. The comparative data shown in Table 8.1 reveal that the power meter from Manufacturer A

produced consistently higher values than the one from Manufacturer B for the sections tested, and this may reflect differences in how the two units operate. However, because the relative values of the two systems were consistent, it was therefore recommended that either measuring system could be used—but not a combination of the two—throughout the entire field-testing program.

8.2 Establishing a Baseline Aerodynamic Drag Area for Modeling

A baseline HMA section (Section 1 in Figure 8.2) was used to establish the aerodynamic drag area of the test rider following the procedure set forth by Martin et al. *(27)* with the following modifications. The baseline test section was 0.95 miles (1,528 m), longer than the length of the track 0.29 mi. (460 m) used by Martin. Testing was performed by controlling the value of power input to the system (power output of the rider) instead of by maintaining a constant velocity. The rider began each test section at the estimated velocity for the power sequence to minimize the effect of kinetic energy. This resulted in the speed generally being constant throughout each test section.

The baseline section had a measured IRI of 94.3 inches/mile (1.49 m/km) and a median MPD of 0.58 mm, as measured by the SSI Lightweight inertial profiler and UCPRC inertial profiler vehicle, respectively. The baseline global coefficient of friction was set to 0.004 based upon previously used average values *(27)*. As noted previously, the global coefficient of friction is defined as the sum of the rolling resistance (C_{rr}) and the bearing friction of the system. With the bicycle system and rider velocity constant throughout the testing, the bearing friction was generally constant.

The wind speed, direction, humidity, atmospheric pressure, and temperature were collected by the weather station located at the midpoint of the section. Data readings were collected every minute. Wind speed and direction values were used to find the wind component normal to the test rider's direction. All sections were tested in both directions to normalize the wind speed and direction. Humidity, atmospheric pressure, and temperature values were used to calculate air density *(27)*. All calculations for air density were performed in the Microsoft *Excel* document provided by Martin et al.

A standard riding position was used throughout the study. Riders were instructed to complete all tests in a similar upright position *(26)*, with hands on the brake hoods.

For baseline calculations, the 350 watt, 250 watt, and 150 watt test runs were used. A summary of the testing sequence is shown in Table 3.12. The calculated R^2 values for the test section met the 98 percent threshold set by Martin et al. The calculated aerodynamic drag area coefficient was 0.383 m^2. This value was used for comparative tests to backcalculate changes in the global coefficient of friction.

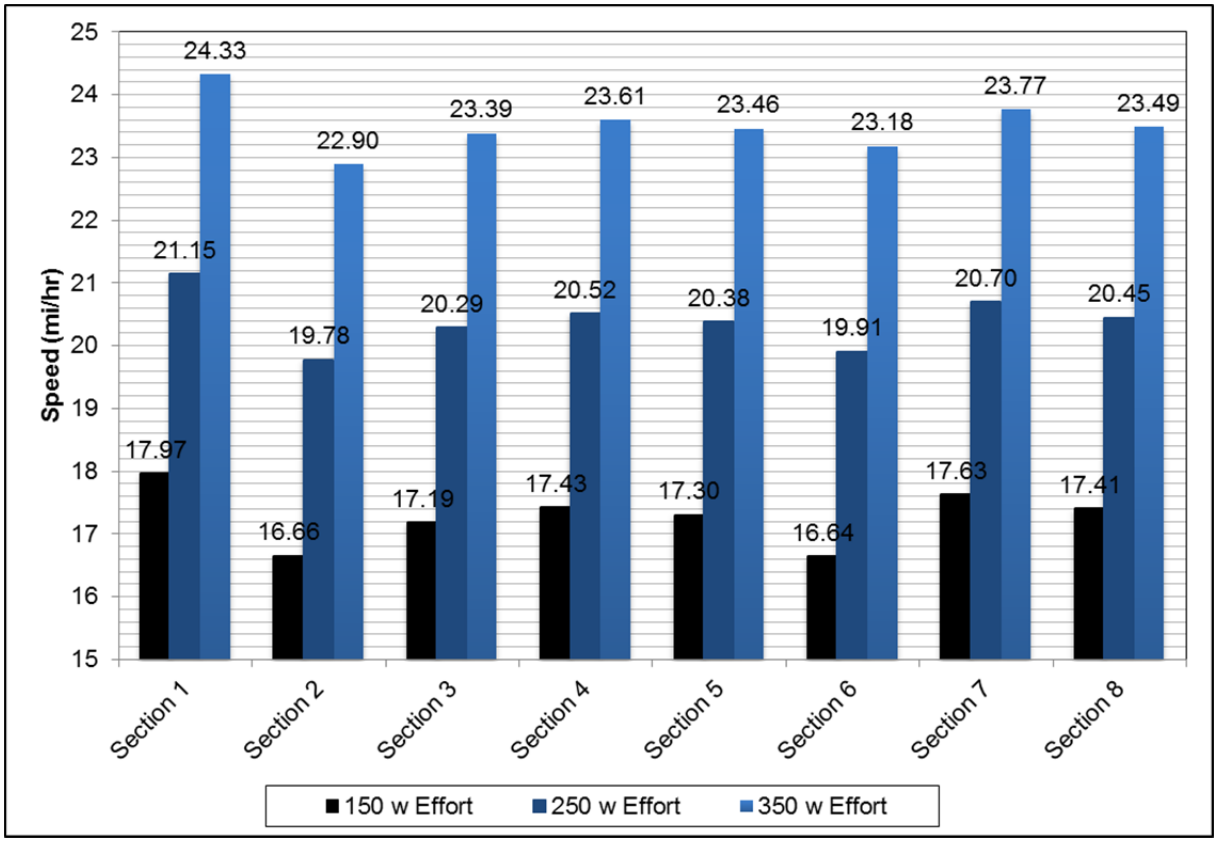

Figure 8.1: Normalized plotted output speeds for three different riding efforts (150 watts, 250 watts, 350 watts).

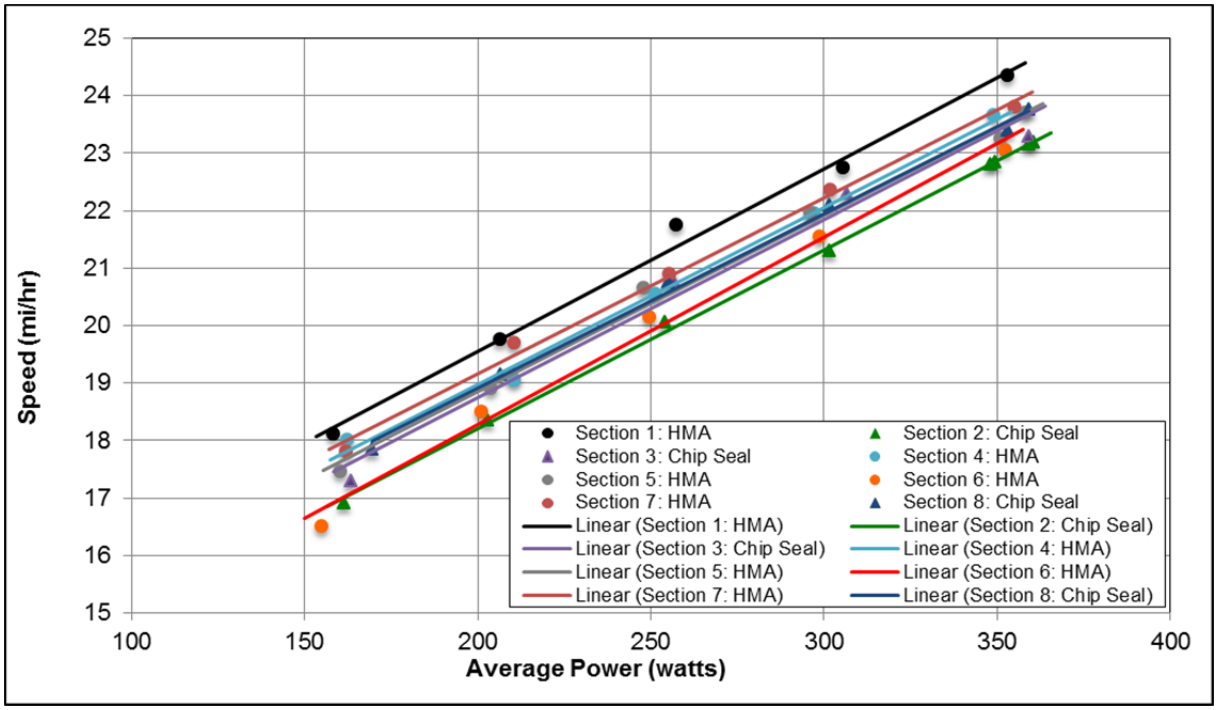

Figure 8.2: Road bicycle power and speed plot of recorded data, given C_DA=0.383 m^2 and a similar standard road bicycle.

8.3 Field Backcalculated Coefficient of Rolling Resistance

Utilizing the same testing procedure and test sequence described above, seven sections of varying pavement conditions and types were tested. Test section routes and beginning and end points are shown in Table 3.7, and inertial profiler results for MPD and IRI are shown in Table 8.2.

Table 8.2: Summary of Inertial Profiler Testing Results

Section	Route	IRI (inches/mile)	Median MPD (mm)
1	Yol-RD98*	94	0.58
2	Yol-RD90	236	2.12
3	Sol-Sievers Rd	132	2.25
4	Sol-Sparlng Rd	95	1.18
5	UCD-Hopkins Rd	265	0.96
6	UCD-Levee Rd	327	1.79
7	Sol-Putah Creek Rd	222	0.53
8	Sol-Putah Creek Rd	150	1.06

Note: * indicates baseline section

This study did not intend to characterize the aerodynamic effects on the rider and bicycle system, but rather on the contribution of pavement macrotexture to ride quality as measured by the power meter. The normalized average power and speed recorded for each test sequence is plotted in Figure 8.1. These values are not fully corrected for weather using the methods described by Martin et al., however, some correction has been included by averaging the test results of both directions on a flat, straight road. The changes in output speed shown on the y-axis can be primarily attributed to variations of μ. Normalized bicycle speeds given three riding efforts, characterized by power outputs of 150, 250, and 350 watts, are also shown in Figure 8.1.

The results of the field tests are shown in Figure 8.2 for all pavement surface types. The speed output is plotted by the average power recorded for each test sequence. Generally, a linear relationship is shown between increases in power and speed. For the purposes of this report, 150 watts can be considered as a recreational cycling effort and 350 watts can be considered as a competitive or sportive cycling effort.

The value of μ was backcalculated assuming a constant coefficient of drag area for all sections. The C_DA calculator model yielded R^2 values for each test section that met or exceeded the 98 percent threshold set by Martin et al. Results of backcalculated μ and R^2 values are shown in Table 8.3.

Table 8.3: Summary of Backcalculated Global Coefficient of Friction (μ) Values

Section	Location	Pavement Description	Martin Model			# of Test Runs Performed
			C_DA (m^2)	μ	R^2	
1	Yol-RD98	HMA	0.382	0.0040	98%	12
2	Yol-RD90	Chip seal	0.383	0.0096	99%	16
3	Sol-Sievers	Chip seal	0.383	0.0085	99%	12
4	Sol-Sparlng	HMA	0.383	0.0075	99%	12
5	UCD-Hopkins	HMA	0.383	0.0071	99%	12
6	UCD-Levee	HMA	0.383	0.0098	99%	12
7	Sol-Putah Creek	HMA	0.383	0.0066	99%	12
8	Sol-Putah Creek	Chip seal	0.383	0.0068	99%	12

Correlations between pavement macrotexture measured in MPD (mm) and the backcalculated μ results are shown in Figure 8.3. The R^2 value is 0.70.

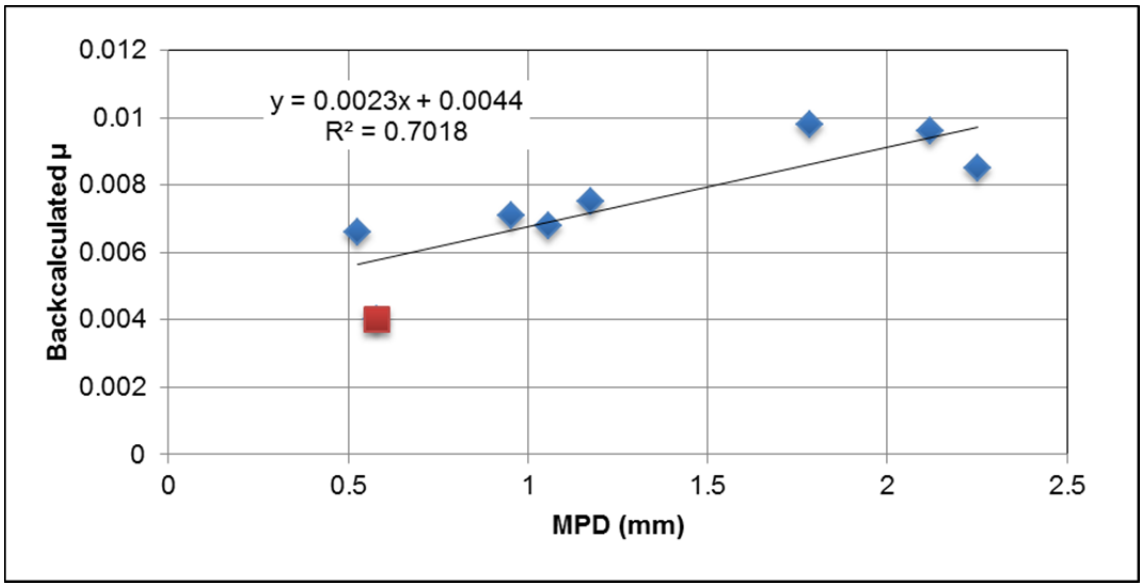

Figure 8.3: Backcalculated global coefficient of friction, μ, correlations to MPD (mm) with baseline value denoted in red.

Correlations between pavement profile measured in IRI (inches/mile) and the backcalculated μ results are shown in Figure 8.4. The R^2 value is 0.34.

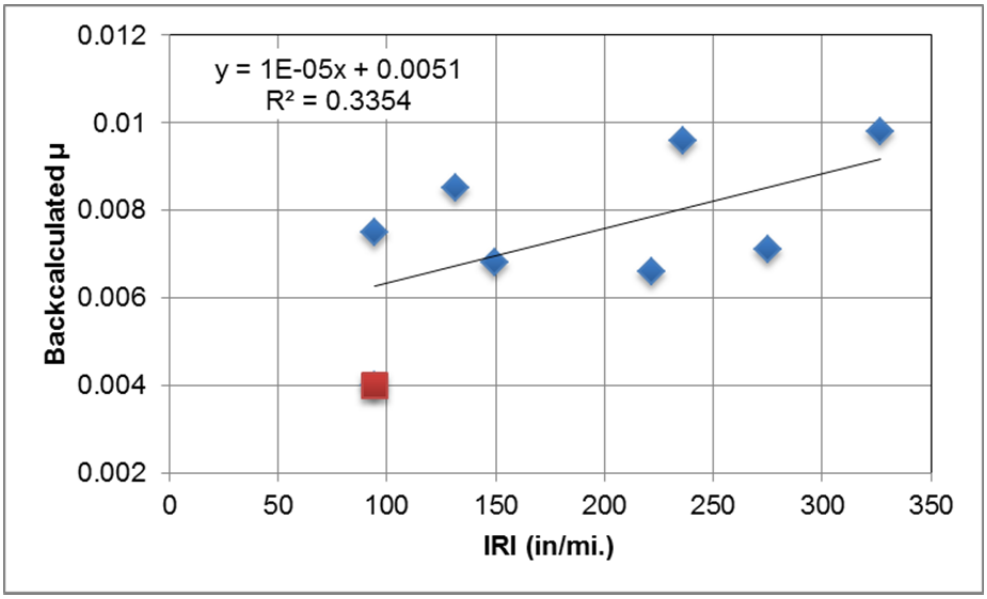

Figure 8.4: Backcalculated global coefficient of friction, μ, correlations to IRI (inches/mile) with baseline value denoted in red.

Based on these results, the μ experienced by the cyclist is more correlated to the MPD of a pavement ($R^2 = 0.70$) than to IRI ($R^2 = 0.34$). Results from Section 3 and Section 5 illustrate these relationships. Section 3 (a chip seal), which has a relatively low IRI value and high MPD value, resulted in a 113 percent increase in the backcalculated μ compared to the baseline HMA section (Section 1). Section 5 (HMA), which has a relatively high IRI value and low MPD value, resulted in a 78 percent increase in the value of μ compared with the baseline.

Two conclusions can be drawn from the results presented here. First, if a cyclist rides at a similar effort level on two pavements of similar grade, the pavement with the higher (μ) value will likely result in an increase in the time required to travel the same distance given similar environmental conditions. Second, if a cyclist chooses to travel at the same speed on a pavement with a higher μ, given similar grade and environmental conditions, it will require an increase in effort to overcome the additional forces resulting from the change in (μ). The effects of vibration were not considered in this model.

Factors likely affecting the backcalculated μ include the following:

1. Road surface
    a. Pavement macrotexture (MPD)
    b. Pavement profile (IRI)
    c. Pavement megatexture, although the effect is unknown and there is currently no known parameter for characterizing megatexture (wavelengths between 0.164 and 1.46 ft [0.05 and 0.5 m]).

2. Tire pressure and construction
3. Changes in combined cyclist and bicycle mass
4. Changes of bearing friction as the system's velocity changes

Since the second, third, and fourth items were held constant or were controlled, it can be assumed that changes in μ were attributable to road surface characteristics, including the unmeasured effects of megatexture.

While the model allows backcalculation of μ-values, there are many external variables that must be considered, including:

- Accurately accounting for wind, primarily wind gusts
- Vehicles that pass a rider during a test, producing wind conditions similar to gusts
- Changes in rider position during the test primarily associated with fatigue
- The ability of a rider to complete each run at a steady speed to avoid changes in kinetic energy
- Power meter measurement errors
- Changes of bearing friction as the system's velocity increases and temperature changes

Tests that were performed when wind speeds were high or conditions were gusty were discarded because of the potential variance they might cause in the test results.

8.4 Effects on Rider Fatigue

As a rider experiences variations in μ, the effects on his or her fatigue can be characterized by the changes in the output speed for similar power efforts. Between the baseline HMA section, with its MPD of 0.58 mm and IRI of 94 inches/mile (1.48 m/km), and the chip seal on Section 2, with its MPD of 2.12 mm and IRI of 236 inches/mile (3.72 m/km), the following changes were measured:

- At 350 watts, a 1.43 mph decrease in speed
- At 250 watts, a 1.37 mph decrease in speed
- At 150 watts, a 1.31 mph decrease in speed

Generally, given the same level of effort, a bicyclist would expect to travel at a similar speed on a variety of pavement types. And, as this report shows, there is a large range of pavement surface conditions on California's state and local networks. However, between various pavement conditions, there are measurable changes in μ that will likely result in a reduction of speed with a similar power output. To account for these changes in μ and adapt their power output level, a bicyclist has two options: to pedal with greater power output effort to overcome the additional forces or to lower their speed and maintain the same pedaling power output effort. As expected, an increased effort by the rider to overcome the additional forces will increase the rider's fatigue. It should also be noted that similar μ values were measured on sections of HMA and on chip seals, showing that μ is likely dependent on the surface characteristics in terms of macrotexture and roughness and not on the generic surface types.

These results provide evidence that the effects of a pavement's μ may affect bicyclists' perceptions of pavement ride quality and acceptability, not only through increased vibration, which produces discomfort, but also through increases in the pedaling power effort required of riders.

9 LONG-TERM MONITORING OF MACROTEXTURE CHANGE FOR DIFFERENT TREATMENTS

Long-term monitoring was conducted on three highway sections—LA-2, SLO-1, and Mon-198—to examine changes in macrotexture over time for different pavement surface treatments.

9.1 LA-2

The details of the chip placed on LA-2 are shown in Reference *(2)*. The macrotexture of LA-2 was measured in both directions in November 2013 as part of the previous project and in September 2015 as part of this project. The results are presented in Figure 9.1. In 2013, approximately 0.5 ft (0.15 m) inside the edge of traveled way (ETW), the median MPD was 2.06 mm in one direction and 2.13 mm in the other. When measured again in 2015 the median MPD was 4.0 mm in both directions. It is uncertain why the measured MPD increased between the two years of measurement. Potential explanations include changes to testing location and the amount of debris on the pavement. The path taken by the vehicle and laser profiler on the 56 mile long section of winding mountain road may have been closer to the ETW in 2013. If the testing in 2015 was performed in a different location outside the ETW and in an area with less traffic compaction of the chip seal, there would likely be a higher measured MPD. This is a likely outcome due to the limitations of the positioning control of the MPD laser on test section. Another possible explanation of the higher MPD is that there was an increase in the number of loose stones near the ETW in 2015. Initial testing was performed on November 20, 2013, during a time of year that historically experiences higher rainfall. Follow-up testing was performed on September 5, 2015, at the end of a long dry season. A recent rainfall could have cleaned loose debris from the pavement surface. A close-up photo of the pavement surface on LA-2 is shown in Figure 9.2.

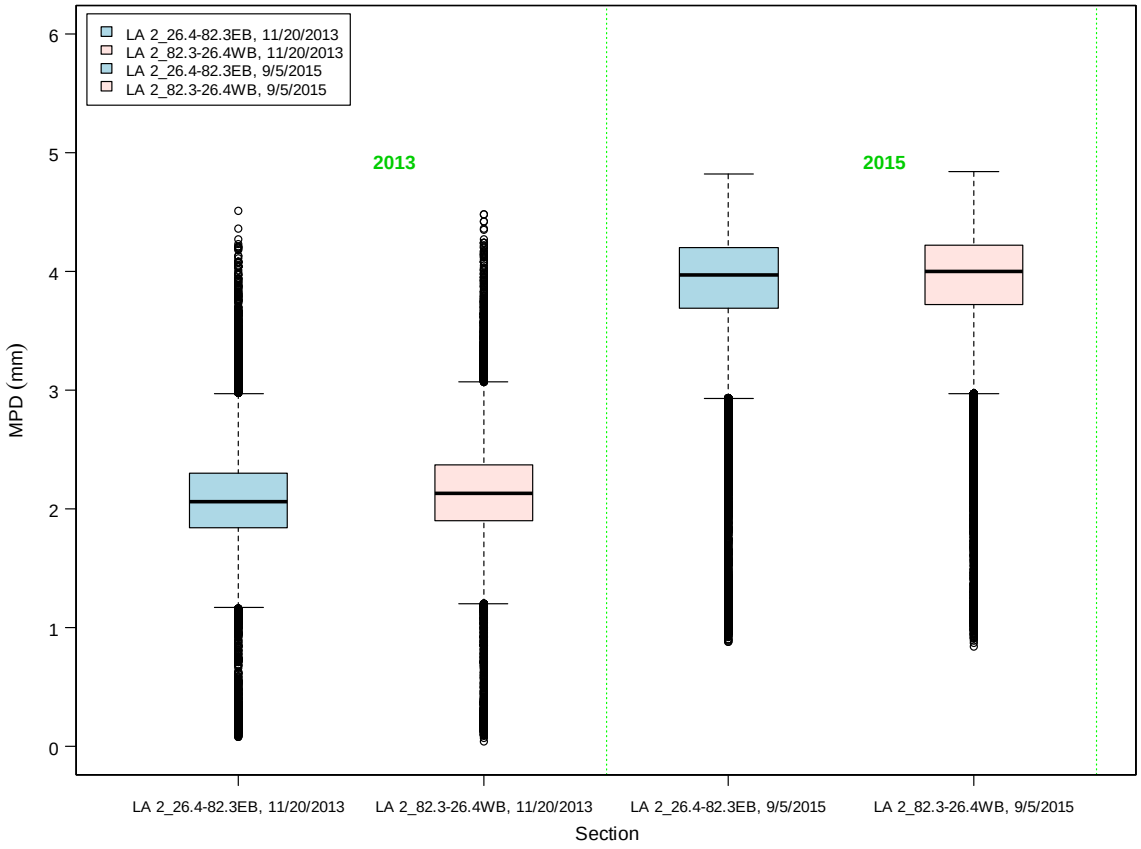

Figure 9.1: MPD over time on LA-2 by direction.

Figure 9.2: Close-up photo of pavement on LA-2.

9.2 SLO-1

On three different occasions, the macrotexture of SLO-1 was measured on the shoulder near the ETW and in the right wheelpath in two directions. The first measurements were taken on the chip seal in April 2013; in November 2013, a second set of measurements were taken on the sand seal applied on top of the chip seal as part of the previous project; and in August 2015, a third set of measurements were taken as part of this project. The results are presented in Figure 9.3. The median macrotexture of the chip seal on the shoulder and in the wheelpath decreased from 3.0 mm to 2.0 mm over the two-year period, and for the sand seal it decreased from 2.5 mm to 1.5 mm. By 2015, the median macrotexture of the sand seal on SLO-1 had been further reduced to approximately 1.5 mm on the shoulder and approximately 1.0 mm in wheelpath.

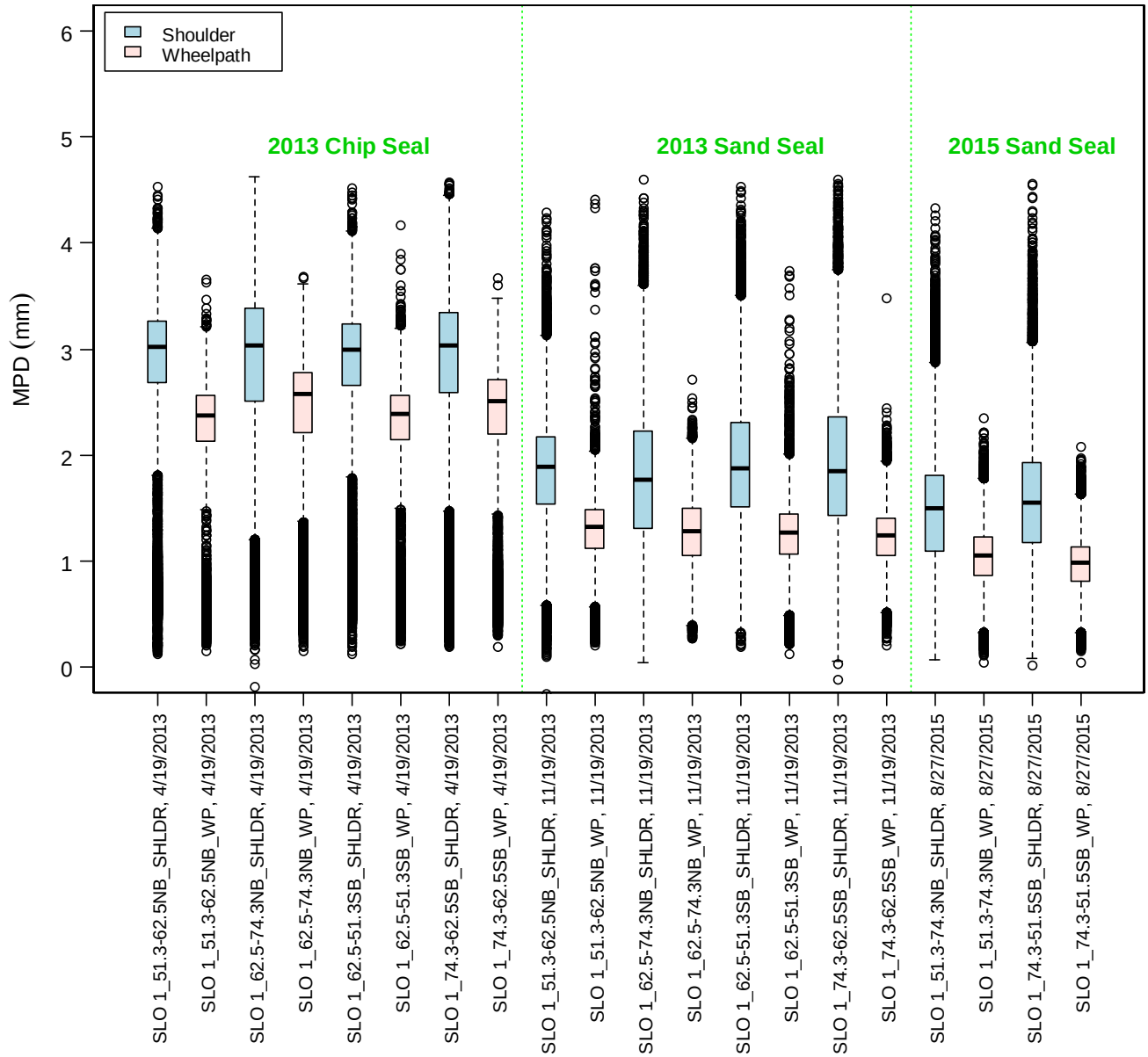

Figure 9.3: MPD over time on the SLO-1 subsections (by post mile and direction) on the shoulder (SHLD) and in the wheelpath (WP).

9.3 Mon-198

Macrotexture on the twenty Mon-198 test sections from the previous study was measured in the wheelpath in both directions in October 2013, as part of the previous project, and in August 2015, as part of this project. The results are presented in Figure 9.4. On sixteen of these test sections the median macrotexture decreased during this time period, most likely due to the effects of traffic pushing protruding stones to a flatter position and/or deeper into the binder. Sections 7 and 16 (cinder seal), Sections 9 and 14 (a 1/4 inch PME seal coat with a second application of a double chip seal), and Sections 11 and 12 (slurry seal) showed an increase in macrotexture from 2013 to 2015. Although it is not certain why, it was likely due to some raveling loss.

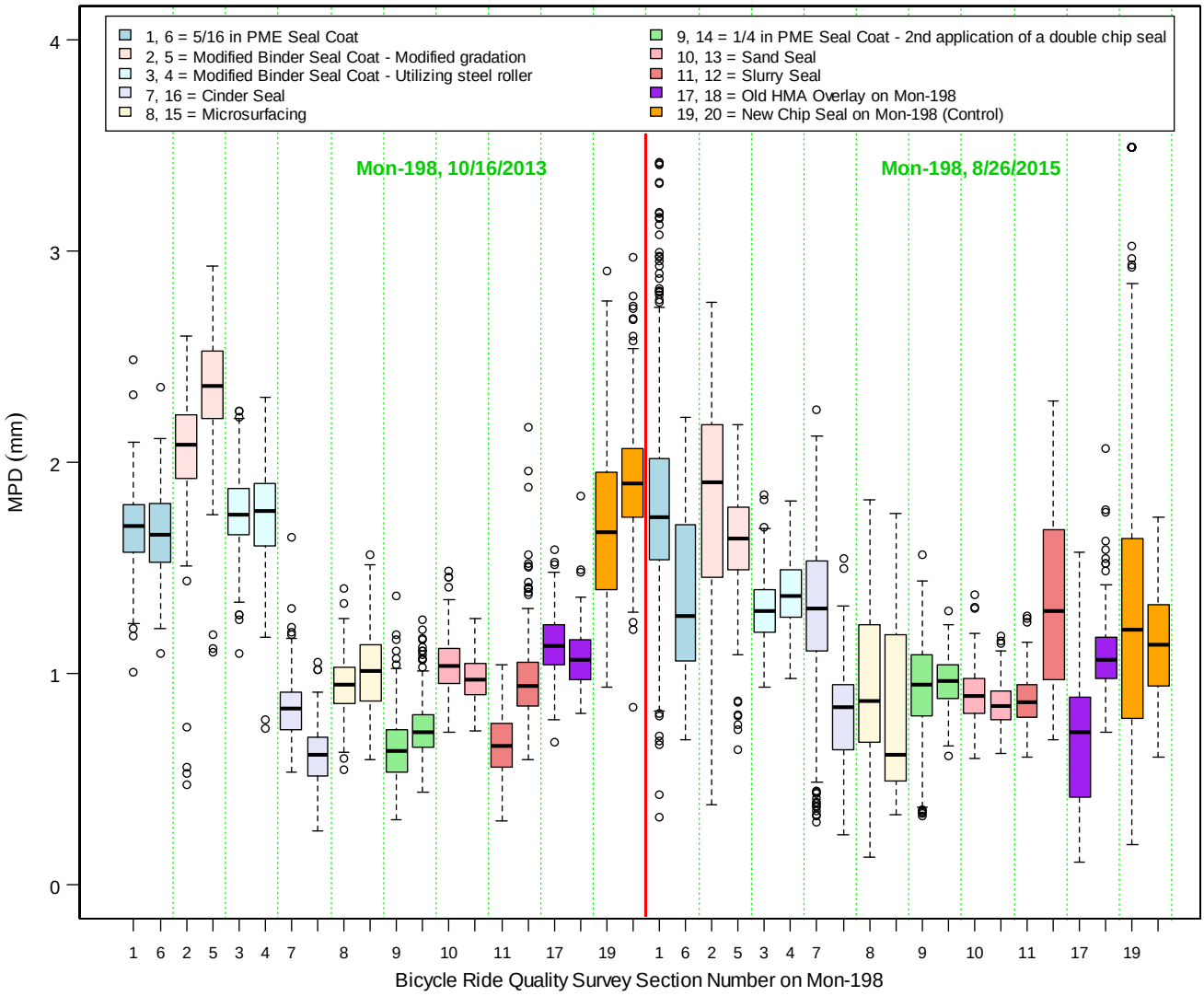

Figure 9.4: MPD over time on Mon-198.

9.4 Summary of Long-Term Monitoring Results

The long-term monitoring results are summarized in Table 9.1.

Table 9.1: Summary of Long-Term Macrotexture Measurements on Test Sections

Group	Section	Mean	Std. Dev.	Min.	Q1	Median	Q3	Max.
LA-2 2013	LA 2_26.4-82.3EB, 11/20/2013	2.08	0.38	0.08	1.84	2.06	2.30	4.51
LA-2 2013	LA 2_82.3-26.4WB, 11/20/2013	2.14	0.39	0.04	1.90	2.13	2.37	4.49
LA-2 2015	LA 2_26.4-82.3EB, 9/5/2015	3.90	0.45	0.88	3.69	3.97	4.20	4.82
LA-2 2015	LA 2_82.3-26.4WB, 9/5/2015	3.92	0.46	0.84	3.72	4.00	4.22	4.84
2013 Chip Seal	SLO 1_51.3-62.5NB_SHLDR, 4/19/2013	2.70	0.95	0.13	2.68	3.02	3.27	4.53
2013 Chip Seal	SLO 1_51.3-62.5NB_WP, 4/19/2013	2.12	0.73	0.15	2.13	2.37	2.56	3.65
2013 Chip Seal	SLO 1_62.5-74.3NB_SHLDR, 4/19/2013	2.76	0.95	-0.19	2.51	3.03	3.39	4.62
2013 Chip Seal	SLO 1_62.5-74.3NB_WP, 4/19/2013	2.33	0.73	0.15	2.22	2.58	2.78	3.68
2013 Chip Seal	SLO 1_62.5-51.3SB_SHLDR, 4/19/2013	2.70	0.91	0.12	2.66	2.99	3.24	4.51
2013 Chip Seal	SLO 1_62.5-51.3SB_WP, 4/19/2013	2.13	0.73	0.21	2.14	2.38	2.57	4.17
2013 Chip Seal	SLO 1_74.3-62.5SB_SHLDR, 4/19/2013	2.77	0.91	0.19	2.59	3.03	3.34	4.57
2013 Chip Seal	SLO 1_74.3-62.5SB_WP, 4/19/2013	2.29	0.69	0.19	2.20	2.51	2.72	3.66
2013 Sand Seal	SLO 1_51.3-62.5NB_SHLDR, 11/19/2013	1.80	0.60	-0.25	1.53	1.89	2.17	4.29
2013 Sand Seal	SLO 1_51.3-62.5NB_WP, 11/19/2013	1.27	0.35	0.21	1.12	1.32	1.49	4.41
2013 Sand Seal	SLO 1_62.5-74.3NB_SHLDR, 11/19/2013	1.79	0.68	0.04	1.31	1.76	2.23	4.60
2013 Sand Seal	SLO 1_62.5-74.3NB_WP, 11/19/2013	1.27	0.33	0.27	1.06	1.29	1.50	2.71
2013 Sand Seal	SLO 1_62.5-51.3SB_SHLDR, 11/19/2013	1.89	0.68	0.19	1.51	1.88	2.31	4.53
2013 Sand Seal	SLO 1_62.5-51.3SB_WP, 11/19/2013	1.23	0.34	0.12	1.06	1.27	1.44	3.74
2013 Sand Seal	SLO 1_74.3-62.5SB_SHLDR, 11/19/2013	1.90	0.72	-0.13	1.43	1.84	2.36	4.60
2013 Sand Seal	SLO 1_74.3-62.5SB_WP, 11/19/2013	1.22	0.28	0.21	1.05	1.24	1.41	3.47
2015 Sand Seal	SLO 1_51.3-74.3NB_SHLDR, 8/27/2015	1.46	0.54	0.06	1.09	1.49	1.81	4.33
2015 Sand Seal	SLO 1_51.3-74.3NB_WP, 8/27/2015	1.05	0.28	0.04	0.87	1.06	1.23	2.34
2015 Sand Seal	SLO 1_74.3-51.5SB_SHLDR, 8/27/2015	1.57	0.58	0.01	1.17	1.56	1.93	4.56
2015 Sand Seal	SLO 1_74.3-51.5SB_WP, 8/27/2015	0.98	0.24	0.05	0.81	0.98	1.14	2.07
Mon-198 in 2013	1	1.69	0.19	1.01	1.57	1.70	1.80	2.49
Mon-198 in 2013	2	1.66	0.19	1.10	1.53	1.66	1.80	2.36

Group	Section	Mean	Std. Dev.	Min.	Q1	Median	Q3	Max.
Mon-198 in 2013	3	2.06	0.27	0.47	1.92	2.08	2.23	2.60
Mon-198 in 2013	4	2.36	0.26	1.10	2.21	2.36	2.53	2.93
Mon-198 in 2013	5	1.76	0.18	1.10	1.66	1.75	1.88	2.25
Mon-198 in 2013	6	1.76	0.22	0.74	1.60	1.77	1.90	2.31
Mon-198 in 2013	7	0.83	0.14	0.53	0.74	0.83	0.91	1.65
Mon-198 in 2013	8	0.61	0.13	0.25	0.51	0.62	0.70	1.05
Mon-198 in 2013	9	0.94	0.13	0.54	0.86	0.94	1.03	1.40
Mon-198 in 2013	10	1.01	0.18	0.59	0.87	1.01	1.14	1.56
Mon-198 in 2013	11	0.64	0.16	0.31	0.53	0.63	0.73	1.37
Mon-198 in 2013	12	0.74	0.13	0.44	0.65	0.72	0.80	1.26
Mon-198 in 2013	13	1.04	0.13	0.72	0.95	1.04	1.12	1.49
Mon-198 in 2013	14	0.97	0.11	0.73	0.90	0.97	1.05	1.26
Mon-198 in 2013	15	0.66	0.14	0.30	0.56	0.66	0.76	1.04
Mon-198 in 2013	16	0.97	0.20	0.59	0.85	0.94	1.05	2.17
Mon-198 in 2013	17	1.14	0.14	0.67	1.04	1.13	1.23	1.58
Mon-198 in 2013	18	1.07	0.14	0.81	0.97	1.06	1.16	1.84
Mon-198 in 2013	19	1.69	0.36	0.93	1.40	1.67	1.95	2.91
Mon-198 in 2013	20	1.91	0.29	0.84	1.74	1.90	2.06	2.97
Mon-198 in 2015	1	1.81	0.53	0.32	1.54	1.74	2.02	3.42
Mon-198 in 2015	2	1.36	0.37	0.69	1.06	1.27	1.70	2.21
Mon-198 in 2015	3	1.79	0.52	0.38	1.46	1.90	2.18	2.76
Mon-198 in 2015	4	1.63	0.24	0.64	1.49	1.64	1.79	2.18
Mon-198 in 2015	5	1.30	0.15	0.94	1.20	1.30	1.40	1.85
Mon-198 in 2015	6	1.38	0.16	0.98	1.27	1.37	1.49	1.82
Mon-198 in 2015	7	1.28	0.35	0.29	1.11	1.31	1.53	2.25
Mon-198 in 2015	8	0.79	0.24	0.23	0.64	0.84	0.95	1.54
Mon-198 in 2015	9	0.93	0.37	0.13	0.67	0.87	1.23	1.82
Mon-198 in 2015	10	0.81	0.38	0.33	0.49	0.61	1.19	1.76
Mon-198 in 2015	11	0.91	0.26	0.32	0.80	0.95	1.09	1.57
Mon-198 in 2015	12	0.96	0.12	0.61	0.88	0.96	1.04	1.30
Mon-198 in 2015	13	0.90	0.13	0.60	0.81	0.89	0.98	1.37
Mon-198 in 2015	14	0.85	0.10	0.62	0.78	0.85	0.92	1.18
Mon-198 in 2015	15	0.87	0.11	0.61	0.79	0.87	0.95	1.28
Mon-198 in 2015	16	1.33	0.40	0.69	0.97	1.30	1.68	2.29
Mon-198 in 2015	17	0.68	0.33	0.11	0.42	0.72	0.89	1.57
Mon-198 in 2015	18	1.09	0.18	0.72	0.97	1.06	1.17	2.06
Mon-198 in 2015	19	1.30	0.72	0.19	0.79	1.21	1.64	3.49
Mon-198 in 2015	20	1.14	0.24	0.60	0.94	1.14	1.33	1.74

(This page left blank)

10 RECOMMENDED GUIDELINES FOR SELECTING PRESERVATION TREATMENT SPECIFICATIONS FOR BICYCLE RIDE QUALITY

The test methods and results presented in the preceding chapters were used to develop recommended guidelines for specifications for current surface treatments that can be applied on routes that bicyclists use.

10.1 Approach Used to Develop Recommended Guidelines

A number of factors affect whether a bicycle rider considers a given pavement section to be "acceptable" or "unacceptable." To deal with the broad variability among riders and among sections, the model presented in Chapter 7 focused on determining the likelihood that a given rider under certain conditions would find a pavement "acceptable." The results of that rider survey model revealed that both MPD and IRI play a role in cyclists' perceptions of ride comfort and acceptability, and that each added unit of IRI or MPD lessened the likelihood that a pavement would receive an "acceptable" rating. The model also showed that the increases in MPD and IRI are cumulative, meaning that there may be a level of MPD so high that no acceptable level of IRI can be found, and vice versa.

The models also revealed that there are particular personal characteristics that influence whether a rider is less likely to rate a section as "acceptable." For example, a rider's opinion about what they consider acceptable may also be affected by their riding experience and by their gender. To develop guidance for selection of surface treatments, simulations were performed using the model and using 10,000 riders with characteristics randomly selected from the ranges in the surveys and 400 randomly selected combinations of MPD and IRI. The simulations were performed using two groups of riders, one group (Group 1) which was sampled across all ranges of personal characteristics and one group representing riders with the personal characteristics associated with the most discriminating opinions about section acceptability (Group 2). Ranges of acceptable MPD are given in the recommended guidelines, spanning the results of the simulations for Group 1 and Group 2.

Controlling the level of IRI on chip seals, surface seals, and microsurfacing treatments as part of construction quality control is beyond an agency's or contractor's capacity, but an agency can chose a particular specification for MPD, as different surface treatments have been shown to yield different MPD ranges. Therefore, the results of the simulations were used to recommend a level of MPD that would result in an acceptable value of IRI for a segment. To make the recommended guidelines workable, the desired IRI values were broken into three categories: <190 inches/mile, 190 to 380 inches/mile, and >380 inches/mile [<3 m/km, 3 to 6 m/km, and >6 m/km]).

10.2 Use of the Recommended Guidelines

Following are the steps to use the recommended guidelines (the decision tree for this process appears in Figure 10.1):

1. Determine the starting point on the section by using its measured or estimated IRI value in one of the three established categories—less than 190 inches/mile, between 190 and 380 inches/mile, or greater than 380 inches/mile—and follow the next consideration laid out in the decision tree (Figure 10.1).
2. Determine the desired level of acceptability (that is, to either 80 or 90 percent of bicycle riders) and follow the decision tree to the next step.
3. Based on the level of acceptability desired for the project, select one of the allowable MPD values for the treatment. The acceptability level for Group 1 (all riders) is the higher MPD value shown and the acceptability level for Group 2 (most sensitive riders) is the lower value.
4. Depending on whether a chip seal, slurry seal, or microsurfacing will be applied to the pavement section, use the acceptable MPD value determined in Step 3 and the data in either Table 10.1, or Figure 10.2, Figure 10.3, or Figure 10.4, respectively, to select the specification that is likely to produce an acceptable MPD value.
    a. It is recommended that the specification selected have a median MPD value that is less than or equal to the acceptable MPD value determined in Step 3. The median values are listed in Table 10.1 and are shown as a solid line in the middle of each colored box in Figure 10.2, Figure 10.3, and Figure 10.4.
    b. If it is desired to increase the certainty that the acceptable MPD value will not be exceeded, it is recommended that the specification selected have a 25^{th} percentile MPD value that is less than or equal to the acceptable MPD value chosen in Step 3. The 25^{th} percentile values are listed under the heading Q1 in Table 10.1 and are shown as the bottom line of the colored boxes in Figure 10.2, Figure 10.3, and Figure 10.4.
5. The scope of these recommended guidelines for choosing a surface treatment specification only considers bicycle ride quality. Users of these recommended guidelines must also consider other criteria when selecting a surface treatment specification, including motor vehicle safety in terms of skid resistance under wet conditions and preservation of the pavement structure considering the life-cycle cost of the treatment. Other guidance regarding those criteria and decision-making processes must be satisfied before making final decisions regarding the appropriate surface treatment.

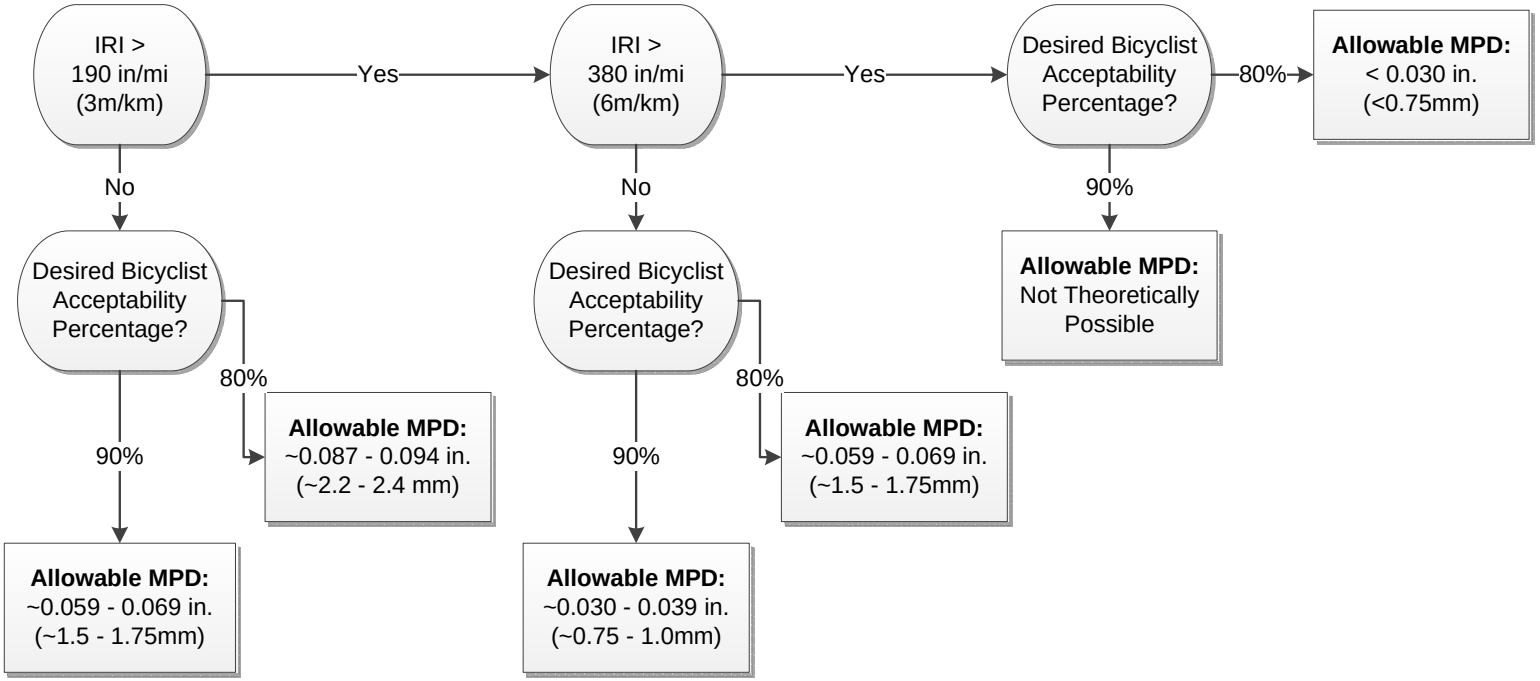

Figure 10.1: Decision tree for MPD values.

Table 10.1: Median and 25th Percentile (Q1) MPD Values for Each Treatment Specification

Type	Specification Year	Specification Binder Type	Specification Aggregate Type	Average of Median MPD (mm)	Average of Std. Dev. (mm)	Average of 25th Percentile Q1 (mm)	Average of 75th Percentile Q3 (mm)
Chip seal	2006	Asphaltic emulsion (polymer-modified)	3/8" medium screenings	1.15	0.19	1.02	1.27
	2006	Asphalt rubber binder	1/2" medium precoated screenings	2.44	0.29	2.26	2.60
	2006	Asphalt rubber binder	3/8" precoated screenings	1.47	0.85	1.15	2.09
	2010	Asphaltic emulsion (polymer-modified)	Coarse 1/2" max. precoated screenings	2.23	0.32	2.03	2.43
	2010	Asphaltic emulsion (polymer-modified)	3/8" medium maximum screenings	1.27	0.33	1.06	1.49
	2010	Asphalt rubber binder	1/2" medium maximum screenings	3.41	0.44	3.13	3.65
	2010	Asphalt rubber binder	Coarse 1/2" max. precoated screenings	1.23	0.28	1.06	1.41
	2010	Asphalt rubber binder	Fine 3/8" max. screenings	1.31	0.27	1.15	1.48
Slurry seal	2006	-	Slurry Type III	0.75	0.18	0.64	0.87
	2010	-	Slurry Type II	0.82	0.21	0.68	0.95
	2010	-	Slurry Type III	2.45	0.52	2.25	2.70
Microsurfacing	2006	-	Microsurfacing Type II	0.65	0.31	0.51	0.82
	2006	-	Microsurfacing Type III	0.81	0.17	0.71	0.91
	2010	-	Microsurfacing Type III	0.71	0.15	0.62	0.81

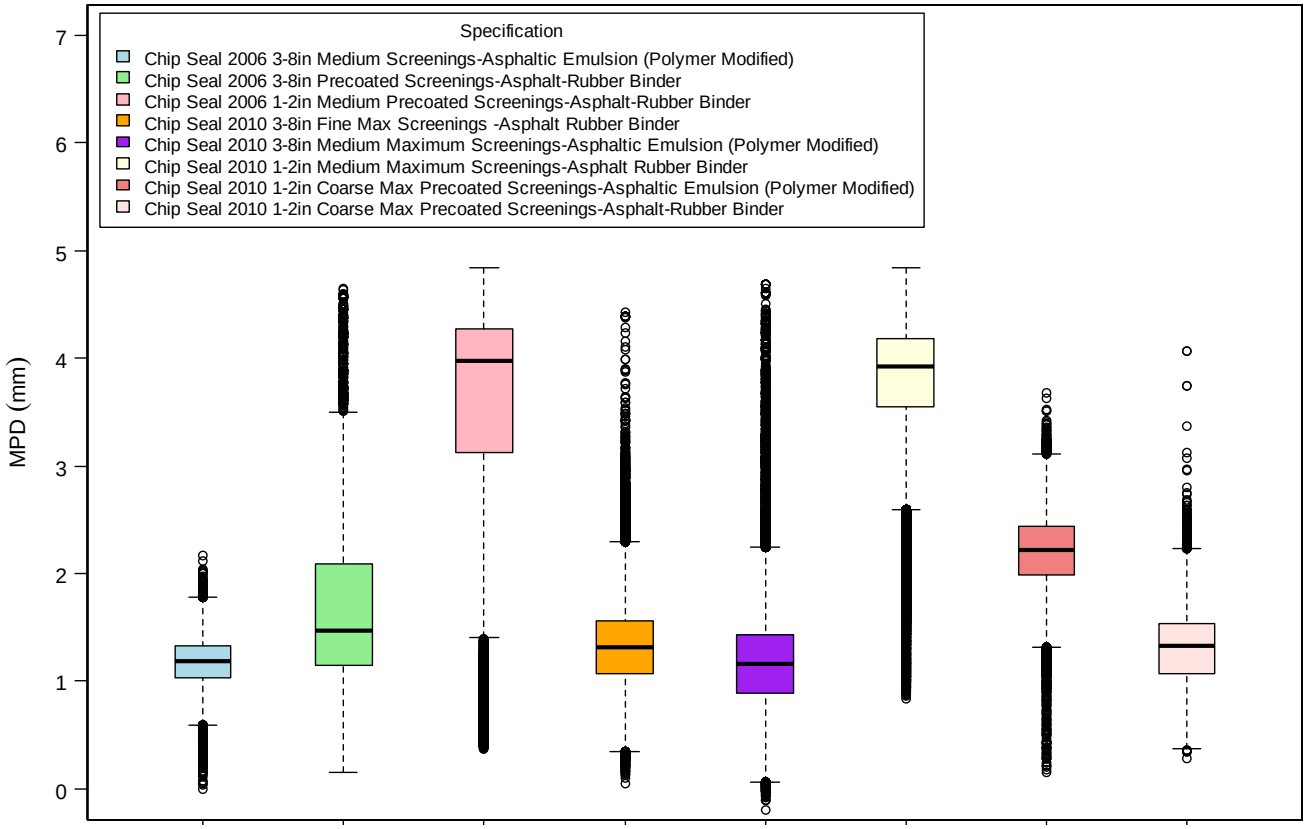

Figure 10.2: MPD values of chip seals with different specifications.

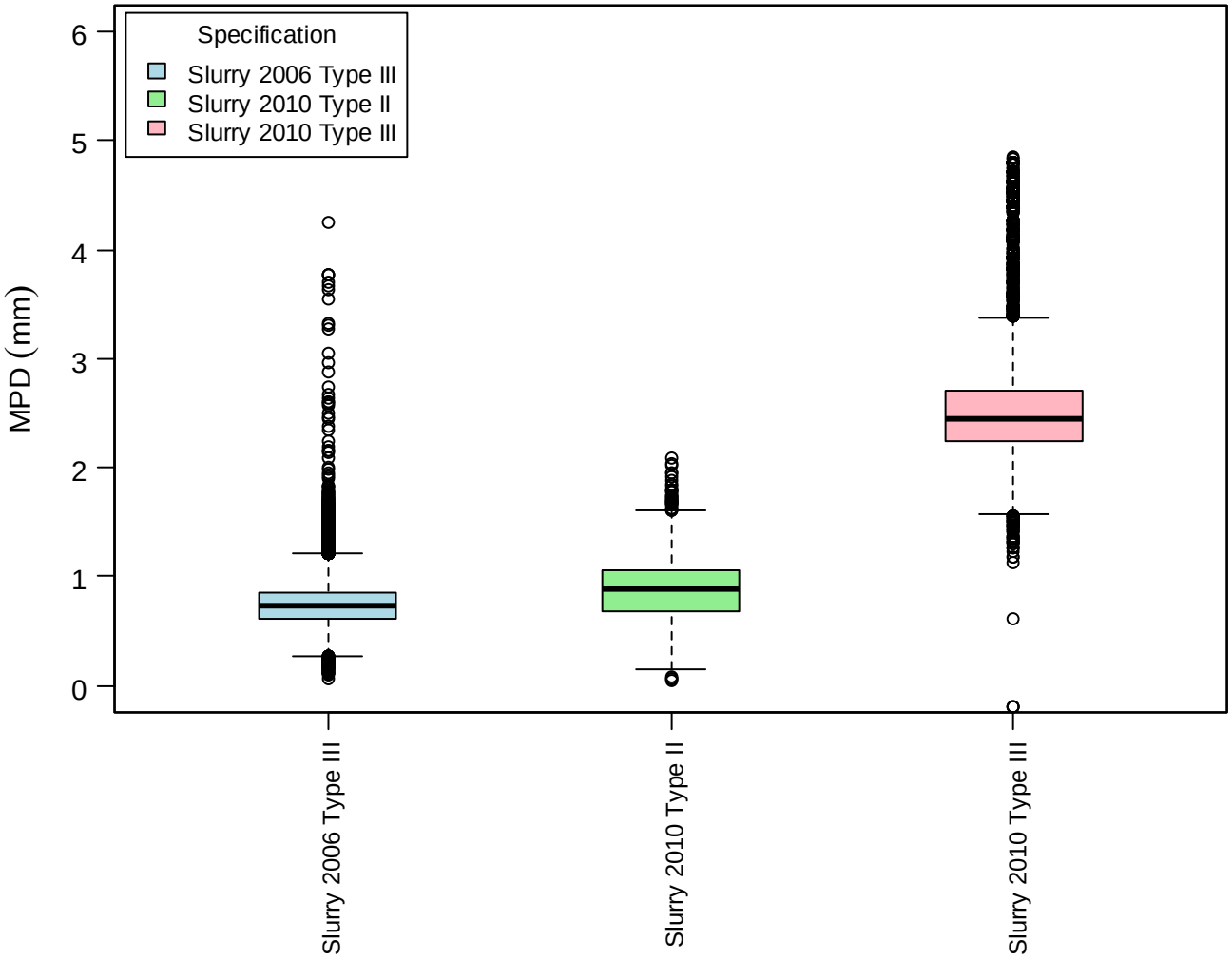

Figure 10.3: MPD values of slurry seals with different specifications.

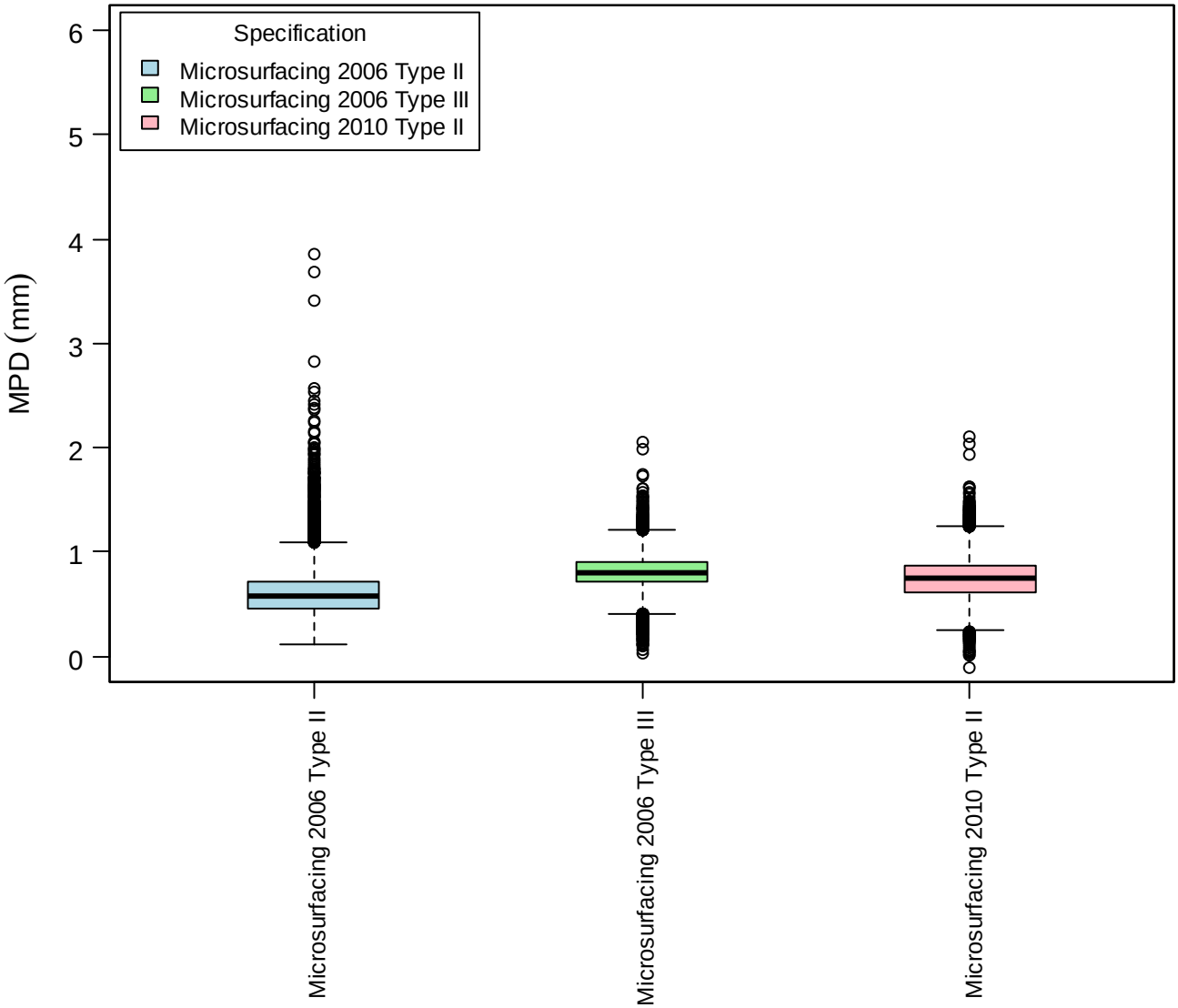

Figure 10.4: MPD values of microsurfacings with different specifications.

(This page left blank)

11 CONCLUSIONS AND RECOMMENDATIONS

11.1 Summary

The objective of this continued project was to prepare recommended guidelines for the design of preservation treatments suitable for bicycle routes on state highways and local streets in California. This was achieved by first measuring macrotexture and roughness on different local government and state highway treatments; and then measuring the subjective responses of bicycle riders through surveys conducted as part of group rides in five cities; and measuring bicycle vibration and the power required of riders on a number of those treatments using instrumented bicycles. The bicyclist surveys and vibration measurements were then correlated with the macrotexture and roughness measurements. Macrotexture was measured on additional sections and ranges of macrotexture were identified for specific treatment specifications. Models were then created that related pavement surface conditions to bicyclist response, and all of the assembled information was used to create recommended guidelines for the selection of specifications for chip seals, slurry seals, and microsurfacings to meet cyclists' expectations for acceptable ride quality.

11.2 Conclusions

The following conclusions have been drawn from the results and analyses presented:

- Both IRI and MPD are important parameters to determine whether bicycle riders find a particular section acceptable, and MPD is more important than IRI.
- The perception of bicycle ride quality appears to depend on the interaction of MPD and IRI; the MPD threshold at which riders will find a given segment unacceptable decreases as the IRI increases.
- Considering simple rider demographics or pavement condition variables such as those used in this study does not completely capture the considerable variability among people and among sections that influences what riders consider acceptable or unacceptable pavement condition.
- Increased MPD and to a lesser extent increased IRI were found to correlate with the increased vibration and additional power required to move a bicycle, which matches the rider survey results.
- From the measurements and surveys completed in this study and its predecessor and without considering IRI, 80 percent of riders rated pavements with MPD values of 1.8 mm or less as acceptable and 50 percent rated pavements with MPD values of 2.3 mm or less as acceptable.
- Most treatments used in urban areas produced high acceptability across cities, however, there are some specifications that have a high probability of resulting in high percentages of "unacceptable" ratings from bicyclists.
- Pavement macrotexture generally tends to decrease over time under trafficking, with less reduction outside the wheelpaths than in the wheelpaths.

- The research was successful in identifying ranges of MPD for current Caltrans specifications for chip seals, slurry seals and microsurfacings, however, it was not possible to find useful correlations between MPD and individual sieve sizes within the gradations.
- From laboratory gradation data on aggregate screenings used on slurry seal sections in Reno, Nevada, correlations were found between the median MPD of a pavement surface and the percent passing the #4 (4.75 mm) and #8 (2.36 mm) screen sizes in the constructed gradation.
- The research was successful in developing recommended guidelines that allow pavement treatment designers and pavement managers to select treatment specifications for bicycle routes that will result in a high probability of being found "acceptable" by bicyclists. The scope of the recommended guidelines presented in this report for choosing a surface treatment specification only considers bicycle ride quality. The recommended guidelines also state that other criteria must be considered when selecting a surface treatment specification, including motor vehicle safety in terms of skid resistance under wet conditions, for which minimum MPD requirements should be considered, and the life-cycle cost of the treatment.

11.3 Recommendations

Based on the results of this study, the following recommendations are made regarding pavement surfaces that will be used by bicyclists:

- Begin use of the recommended guidelines included in this report as part of the surface treatment selection process along with existing guidance that considers criteria other than bicycle ride quality, such as motorist safety and treatment life-cycle cost, and improve them as experience is gained. The recommendations are for the selection of existing surface treatment specifications based on different levels of bicycle ride quality satisfaction.
- In the recommended guidelines, consider using the 90 percent acceptable MPD level on routes with higher bicycle use as opposed to the 80 percent acceptable MPD level that is also included. Further confidence that the treatment will have an acceptable MPD level can be obtained by selecting treatments based on the 25^{th} percentile MPD of the gradation in the specification instead of the median MPD.
- As new treatment specifications are developed, collect MPD data on them so that they can be included in updated versions of the recommended guidelines.
- If greater precision in developing specifications is desired than is currently possible, consider additional research to develop methods of estimating MPD from gradations and aggregate shape (such as flakiness index).

REFERENCES

1. H. Li, J. Harvey, R. Wu, C. Thigpen, S. Louw, Z. Chen, J. D. Lea, D. Jones, and A. Rezaie. 2013. *Preliminary Results: Measurement of Macrotexture on Surface Treatments and Survey of Bicyclist Ride Quality on Mon-198 and SLO-1 Test Sections.* Univ. of California Pavement Research Center, Davis and Berkeley. UCPRC-TM-2013-07.
2. H. Li, J. Harvey, C. Thigpen, and R. Wu. 2013. *Surface Treatment Macrotexture and Bicycle Ride Quality.* Univ. of California Pavement Research Center, Davis and Berkeley. UCPRC-RR-2013-07.
3. Sandberg, U., and J.A. Ejsmont. 2002. *Tyre/Road Noise Reference Book*. INFORMEX, Harg, SE-59040 Kisa, Sweden.
4. Anderson, D.A., R.S. Huebner, J.R. Reed, J.C. Warner, and J.J. Henry. 1998. *NCHRP Web Document 16: Improved Surface Drainage of Pavements. Project 1-29*. Transportation Research Board, National Research Council: Washington, D.C.
5. Flintsch, G., E. de León, K. McGhee, and I. Al-Qadi. 2003. "Pavement Surface Macrotexture Measurement and Applications." *Transportation Research Record: Journal of the Transportation Research Board* Vol. 1860 (1): 168-177.
6. Panagouli, O.K., and A.G. Kokkalis. 1998. "Skid Resistance and Fractal Structure of Pavement Surface." *Chaos, Solitons & Fractals* 9 (3): 493-505.
7. Rezaei, A., J.T. Harvey, and Q. Lu. 2012. *Investigation of Noise and Ride Quality Trends for Asphaltic Pavement Surface Types: Five-Year Results*. Univ. of California Pavement Research Center, Davis and Berkeley, CA. UCPRC-RR-2012-04.
8. Bu, Y., T. Huang, Z. Xiang, X. Wu, and C. Chen. 2010. "Optimal Design of Mountain Bicycle Based on Biomechanics." *Transactions of Tianjin University* 16 (1): 45-49.
9. Lorenzo, D.S.D., and M.L. Hull. "Quantification of Structural Loading During Off-Road Cycling." 1999. *Journal of Biomechanical Engineering* 121 (4): 399-405.
10. McKenna, S., M. Hill, and M. Hull. 2003. "Methods for Fatigue Testing Off-Road Bicycle Handlebars Based on Assembly Effects Using Two Different Stem Designs." *Journal of Testing and Evaluation* 31 (2): 10.
11. McKenna, S.P., M.R. Hill, and M.L. Hull. 2002. "A Single Loading Direction for Fatigue Life Prediction and Testing of Handlebars for Off-Road Bicycles." *International Journal of Fatigue* 24 (11): 1149-1157.
12. Wilczynski, H., and M.L. Hull. 1994. "A Dynamic System Model for Estimating Surface-Induced Frame Loads During Off-Road Cycling." *Journal of Mechanical Design* 116 (3): 816-822.
13. Pucher, J., J. Dill, and S. Handy. 2010. "Infrastructure, Programs, and Policies to Increase Bicycling: An International Review." *Preventive Medicine* 50: S106-S125.

14. Tal, G., and S. Handy. 2008. “Children's Biking for Nonschool Purposes: Getting to Soccer Games in Davis, California.” *Transportation Research Record* 2074: 40-45.
15. Xing, Y., S.L. Handy, and P.L. Mokhtarian. 2010. “Factors Associated with Proportions and Miles of Bicycling for Transportation and Recreation in Six Small U.S. Cities.” *Transportation Research Part D-Transport and Environment* 15 (2): 73-81.
16. Henault, J., and J. Bliven. *Characterizing the Macrotexture of Asphalt Pavement Designs in Connecticut.* 2011. Report No. CT-2243-2-10-3, Connecticut Department of Transportation.
17. Winters, M., G. Davidson, D. Kao, and K. Teshke. 2011. “Motivators and Deterrents of Bicycling: Comparing Influences on Decisions to Ride.” *Transportation* 38 (1): 153-168.
18. Landis, B.W., V.R. Vattikuti, and M.T. Brannick. 1997. “Real-Time Human Perceptions: Toward a Bicycle Level of Service.” In *Transportation Research Record: Journal of the Transportation Research Board* 1578: 119-126. . *trrjournalonline.trb.org/doi/pdf/10.3141/1578-15* (Accessed July 25, 2014).
19. Heinen, E., B. van Wee, and K. Maat. 2010. “Commuting by Bicycle: An Overview of the Literature.” *Transport Reviews* 30 (1):59-96.
20. Pucher, J., J. Dill, and S. Handy. 2010. “Infrastructure, Programs, and Policies to Increase Bicycling: An International Review.” *Preventive Medicine* 50: S106-S125.
21. Parkin, J., Wardman, M., and Page, M. 2007. “Models of Perceived Cycling Risk and Route Acceptability.” *Accident Analysis & Prevention* 39: 364–371.
22. Martin, J.C., D.L. Milliken, J.E. Cobb, K.L. McFadden, and A.R. Coggan. 1998. “Validation of a Mathematical Model for Road Cycling Power.” *Journal of Applied Biomechanics* 14: 276-291.
23. Kyle, C.R. 1988. “The Mechanics and Aerodynamics of Cycling.” In *Medical and Scientific Aspects of Cycling,* edited by E.D. Burke and M.M. Newsom, 235-251. Champaign, IL.: Human Kinetics.
24. Dahn, K., L. Mai, J. Poland, and C. Jenkins. 1991. “Frictional Resistance in Bicycle Wheel Bearings.” *Cycling Science* 1: 28-32.
25. Martin, J.C., A.S. Gardner, M. Barras, and D.T. Martin. 2006. “Modeling Sprint Cycling Using Field-derived Parameters and Forward Integration.” *Medicine & Science in Sports & Exercise* 38: 592-597.
26. Grappe, F., R. Candau, A. Belli, and J. D. Rouillon. 1997. “Aerodynamic Drag in Field Cycling with Special Reference to the Obree’s Position.” *Ergonomics* 40 (12): 1299-1311.
27. Martin, J.C., A.S. Gardner, M. Barras, and D.T. Martin. 2006. “Aerodynamic Drag Area of Cyclists Determined with Field-based Measures.” *Sportscience* 10: 68-69.
28. Fox, R. W., and A.T. McDonald. 1973. *Introduction to Fluid Mechanics* (2nd ed.). New York: Wiley.
29. Ryschon, T.W. 1994. “Physiologic Aspects of Bicycling.” *Clinics in Sports Medicine* 13 (1): 15-38.
30. Jeukendrup, A.E., and J. Martin. 2001. “Improving Cycling Performance: How Should We Spend Our Time and Money.” *Sports Medicine* 31: 559-569.

31. Wang, Y., J. Moss, and R. Thisted. 1992. "Predictors of Body Surface Area." *Journal of Clinical Anesthesia* 4: 4-10.
32. Gardner, A.S., S. Stephens, D.T. Martin, E. Lawton, H. Lee, and D. Jenkins. 2004. "Accuracy of SRM and Power Tap Power Monitoring Systems for Bicycling." *Medicine & Science in Sports & Exercise*. 36: 1252-1258.
33. Vijayakumar D.A., O. Prakash, R.K. Sharma. 2012. "Estimation of Air Density and Its Importance in Barometric Pressure Measurements." Paper presented at AdMet 2012, the 2nd National Conference on Advances in Metrology. Metrology Society of India. Pune, India.
34. Picard A., R.S. Davis, M. Glaser, K. Fujii. 2008. "Revised Formula for Air Density of Moist Air." *Metrologia* 45: 149-155.
35. Brower M. 2003. *Wind Resource Maps of Northern New England*. TrueWind Solutions, LLC.
36. Goldstein, H. 1999. *Multilevel Statistical Models.* Institute of Education, London.
37. McElreath, R. 2015. *Statistical Rethinking.* Chapman & Hall/CRC.
38. Stan Development Team. *Stan: A C++ Library for Probability and Sampling,* Version 2.5. *http://mc-stan.org/.* (Accessed Jan. 5, 2016)

APPENDIX A: EXAMPLE SURVEY FORM (RENO)

Caltrans/UCPRC Bicyclist Comfort Survey

Pre-ride Survey: General Information *(Please fill out and return it **BEFORE** riding)*

*Date: **09/26/2015** (mm/dd/yyyy) Participant #_ City: **Reno, NV***

1. What is your gender? _____

2. What year were you born? _____ (yyyy)

3. How often do you ride your bicycle?
   □ Every day □ About once a week □ Once a month or less
   □ About every other day □ About twice a month

4. How often do you engage in any physical activity of at least 20 minutes?
   □ Every day □ About once a week □ Once a month or less
   □ About every other day □ About twice a month

5. For what purposes do you ride your bicycle (check ALL that apply)?
   □ Recreation or fitness □ Getting to and from work or school
   □ Visiting friends □ Shopping or running errands
   □ Competitive sporting events □ Other: _____

6. How many times did you ride your bicycle last *week*? _____ times

7. How many times did you ride your bicycle last *month*? _____ times

8. How many times do you ride your bicycle *on average every month*? _____ times

Please allow UCPRC staff to complete this section

9. Bicycle Type:
   □ Road □ Touring □ Mountain □ Recumbent
   □ Hybrid □ Cruiser □ Folding □ Other: _____

10. What materials are the bicycle frame, fork, and wheels made of and what is the tire pressure?

A. Frame: □ Aluminum □ Carbon □ Don't know
□ Titanium □ Steel □ Other: _____

B. Fork: □ Aluminum □ Carbon □ Don't know
□ Titanium □ Steel □ Other: _____

C. Wheels: □ Aluminum □ Carbon □ Don't know
□ Steel □ Other: _____

D. Tire pressure: **Front** _____ (psi) **Rear** _____ (psi) *(measure via pump/gauge)*

E. Tire width: _____ (mm of inch) *(measure via calipers or visual inspection)*

Caltrans/UCPRC Bicyclist Comfort Survey

In-ride Survey: (*Please fill out at the end of **EACH** section*)

Section#: **1** Street: Sinclair St. to Holocomb Ave. on Mill St.

1. How do you rate the surface of the road? □ Acceptable □ Unacceptable

2. Compared to all of the roads on which you bicycle, please indicate your level of comfort (1-5):
   Uncomfortable Comfortable

1	2	3	4	5

Section#: **2** Street: E Liberty St St. to Burns St. on Holocomb Ave

1. How do you rate the surface of the road? □ Acceptable □ Unacceptable

2. Compared to all of the roads on which you bicycle, please indicate your level of comfort (1-5):
   Uncomfortable Comfortable

1	2	3	4	5

Section#: **3** Street: Burns St. to Vassar St. on Holocomb Ave.

1. How do you rate the surface of the road? □ Acceptable □ Unacceptable

2. Compared to all of the roads on which you bicycle, please indicate your level of comfort (1-5):
   Uncomfortable Comfortable

1	2	3	4	5

Section#: **4** Street: Mt Rose St. to W Plumb Ln. on Lakeside Dr.

1. How do you rate the surface of the road? □ Acceptable □ Unacceptable

2. Compared to all of the roads on which you bicycle, please indicate your level of comfort (1-5):
   Uncomfortable Comfortable

1	2	3	4	5

Section#: **5** Street: W Plumb Ln. to Brinky Ave. on Lakeside Dr.

1. How do you rate the surface of the road? □ Acceptable □ Unacceptable

2. Compared to all of the roads on which you bicycle, please indicate your level of comfort (1-5):
   Uncomfortable Comfortable

1	2	3	4	5

Caltrans/UCPRC Bicyclist Comfort Survey

In-ride Survey: (*Please fill out at the end of **EACH** section*)

Section#: **6** Street: Berrum Ln. to Urban Rd. on Plumas St.

1. How do you rate the surface of the road? □ Acceptable □ Unacceptable

2. Compared to all of the roads on which you bicycle, please indicate your level of comfort (1-5):
   Uncomfortable Comfortable

1	2	3	4	5

Section#: **7** Street: Urban Rd. to Mt Rose St. on S Arlington Ave.

1. How do you rate the surface of the road? □ Acceptable □ Unacceptable

2. Compared to all of the roads on which you bicycle, please indicate your level of comfort (1-5):
   Uncomfortable Comfortable

1	2	3	4	5

Section#: **8** Street: Mt Rose St. to California Ave. on S Arlington Ave.

1. How do you rate the surface of the road? □ Acceptable □ Unacceptable

2. Compared to all of the roads on which you bicycle, please indicate your level of comfort (1-5):
   Uncomfortable Comfortable

1	2	3	4	5

Section#: **9** Street: S Arlington Ave. to Memory Ln on California Ave.

1. How do you rate the surface of the road? □ Acceptable □ Unacceptable

2. Compared to all of the roads on which you bicycle, please indicate your level of comfort (1-5):
   Uncomfortable Comfortable

1	2	3	4	5

Section#: **10** Street: Hunter Lake Dr. to S McCarran Blvd on Mayberry Dr.

1. How do you rate the surface of the road? □ Acceptable □ Unacceptable

2. Compared to all of the roads on which you bicycle, please indicate your level of comfort (1-5):
   Uncomfortable Comfortable

1	2	3	4	5

Caltrans/UCPRC Bicyclist Comfort Survey

In-ride Survey: (*Please fill out at the end of **EACH** section*)

Section#: **11** Street: S McCarran Blvd. to Idlewild Dr. on Mayberry Dr.

3. How do you rate the surface of the road? □ Acceptable □ Unacceptable

4. Compared to all of the roads on which you bicycle, please indicate your level of comfort (1-5):
   Uncomfortable Comfortable

1	2	3	4	5

Section#: **12** Street: Idlewild Dr. to Livermore Dr. on Mayberry Dr.

3. How do you rate the surface of the road? □ Acceptable □ Unacceptable

4. Compared to all of the roads on which you bicycle, please indicate your level of comfort (1-5):
   Uncomfortable Comfortable

1	2	3	4	5

Section#: **13** Street: Livermore Dr. to Aspen Glen Dr.. on Mayberry Dr.

3. How do you rate the surface of the road? □ Acceptable □ Unacceptable

4. Compared to all of the roads on which you bicycle, please indicate your level of comfort (1-5):
   Uncomfortable Comfortable

1	2	3	4	5

Section#: **14** Street: Mayberry Dr. to 1500' before S McCarran Blvd. on W 4th St.

3. How do you rate the surface of the road? □ Acceptable □ Unacceptable

4. Compared to all of the roads on which you bicycle, please indicate your level of comfort (1-5):
   Uncomfortable Comfortable

1	2	3	4	5

Section#: **15** Street: S McCarran Blvd. to Stoker Ave on W 4th St.

3. How do you rate the surface of the road? □ Acceptable □ Unacceptable

4. Compared to all of the roads on which you bicycle, please indicate your level of comfort (1-5):
   Uncomfortable Comfortable

1	2	3	4	5

Caltrans/UCPRC Bicyclist Comfort Survey

In-ride Survey: (*Please fill out at the end of **EACH** section*)

Section#: **16** Street: Vine St. to Ralson St. on W 1st St.

1. How do you rate the surface of the road? □ Acceptable □ Unacceptable

2. Compared to all of the roads on which you bicycle, please indicate your level of comfort (1-5):
   Uncomfortable Comfortable

1	2	3	4	5

Caltrans/UCPRC Bicyclist Comfort Survey

Post-ride Survey *(please fill out and return it at the end of all sections)*

Date: ***09/26/2015*** *(mm/dd/yyyy) Participant #* *City:* ***Reno, NV***

1. **Today's Ride:** Identify your favorite section of road from all the sections you just bicycled on. _____ (section #)

2. **Today's Ride:** What is the biggest reason that section was your favorite (select one)?
   - ☐ Scenery/greenery
   - ☐ Topography (e.g. hilly, flat)
   - ☐ Bicycle facilities (e.g. a bicycle lane or path)
   - ☐ Pavement ride quality (e.g. bumpy, smooth)
   - ☐ Traffic conditions/safety
   - ☐ Wind
   - ☐ Safety from crime
   - ☐ Who you ride with
   - ☐ Other: _____

3. **Today's Ride:** Identify your least favorite section of road from all the sections you just bicycled on. _____ (section #)

4. **Today's Ride:** What is the biggest reason that section was your least favorite (select one)?
   - ☐ Scenery/greenery
   - ☐ Topography (e.g. hilly, flat)
   - ☐ Bicycle facilities (e.g. a bicycle lane or path)
   - ☐ Pavement ride quality (e.g. bumpy, smooth)
   - ☐ Traffic conditions/safety
   - ☐ Wind
   - ☐ Safety from crime
   - ☐ Who you ride with
   - ☐ Other: _____

5. Are you of Hispanic/Latino origin?
   - ☐ No, not of Hispanic, Latino
   - ☐ Yes, Mexican, Mexican American, or Chicano
   - ☐ Yes, Puerto Rican
   - ☐ Yes, Cuban
   - ☐ Yes, another Hispanic, Latino, or Spanish origin (please write in): _____

6. What is your race?
   - ☐ White
   - ☐ Black or African American
   - ☐ Asian (If yes, write in name of country/ethnicity): _____
   - ☐ Pacific Islander (If yes, write in name of country/ethnicity): _____
   - ☐ American Indian or Alaska Native (If yes, write in name of principal tribal identity): _____
   - ☐ Other race: _____

7. What is your educational background? (Check the highest level attained)

   □ Some grade school or high school □ 4-year college/technical school degree

   □ High school diploma □ Some graduate school

   □ Some college or technical school □ Completed graduate degree(s)

8. What is your current employment status?

   □ Full-time □ Non-employed student □ Unemployed □ Retired

   □ Part-time □ Self-employed □ Homemaker

9. Your approximate annual *household* income before taxes:

   □ Less than $15,000 □ $35,000 to $54,999 □ $75,000 to $94,999

   □ $15,000 to $34,999 □ $55,000 to $74,999 □ $95,000 or more

10. **Overall:** Based on your experience, what factors influence your enjoyment of a ride the most? Circle one on scale of 1 to 5, from *1 being the 'least influential'* to *5 being the 'most influential',*

Least		***Neutral***		***Most***	
1	2	3	4	5	Scenery/Greenery
1	2	3	4	5	Topography (e.g. hilly, flat)
1	2	3	4	5	Bicycle facilities (e.g. a bicycle lane or path)
1	2	3	4	5	Pavement ride quality (e.g. bumpy, smooth)
1	2	3	4	5	Traffic conditions/safety
1	2	3	4	5	Wind
1	2	3	4	5	Safety from crime
1	2	3	4	5	Who you ride with
1	2	3	4	5	Other: _____

APPENDIX B: MACROTEXTURE MEASURED USING IP ON SURVEY SECTIONS

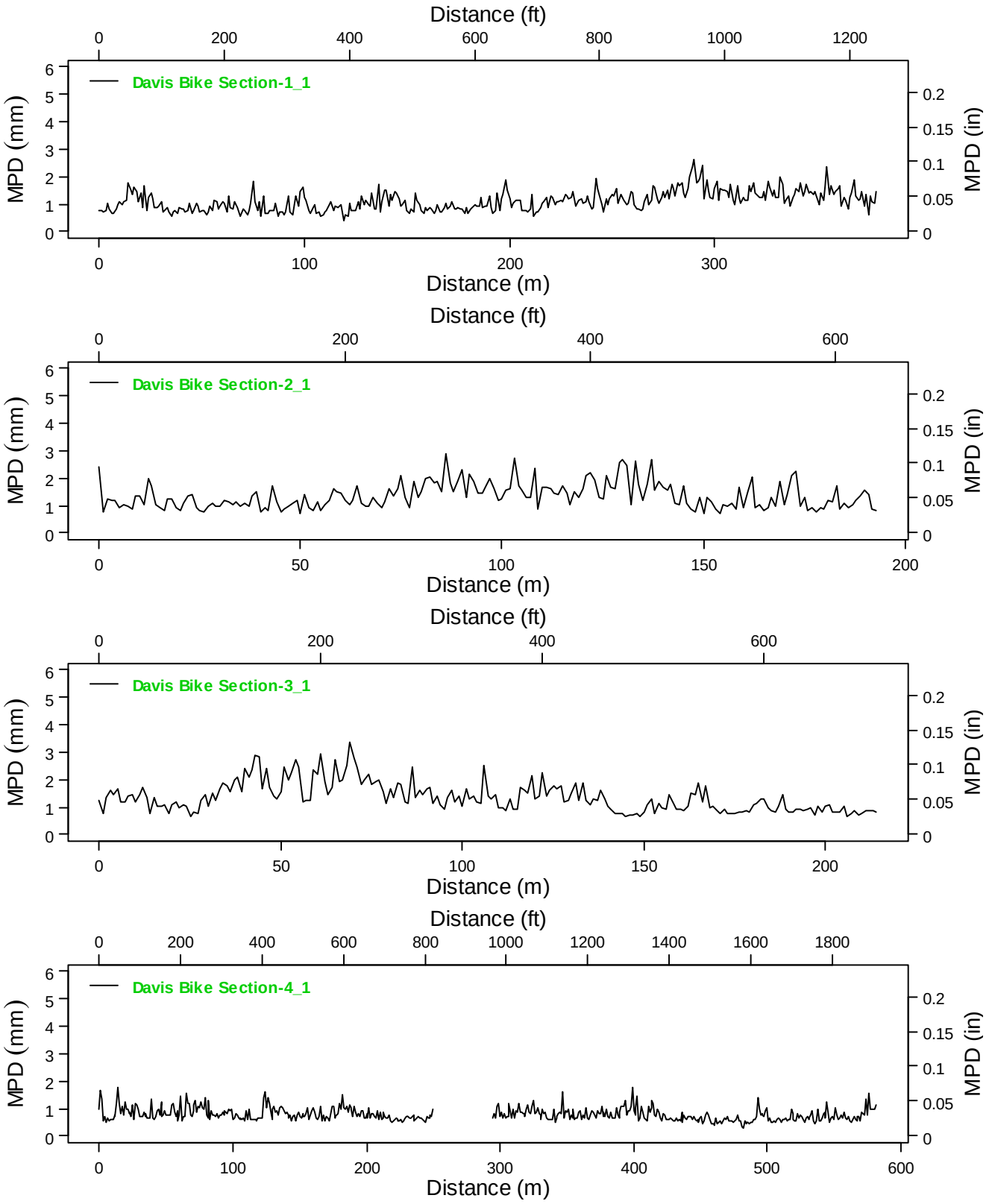

Figure B.1: Macrotexture measured using IP on Davis survey Sections 1 to 4.

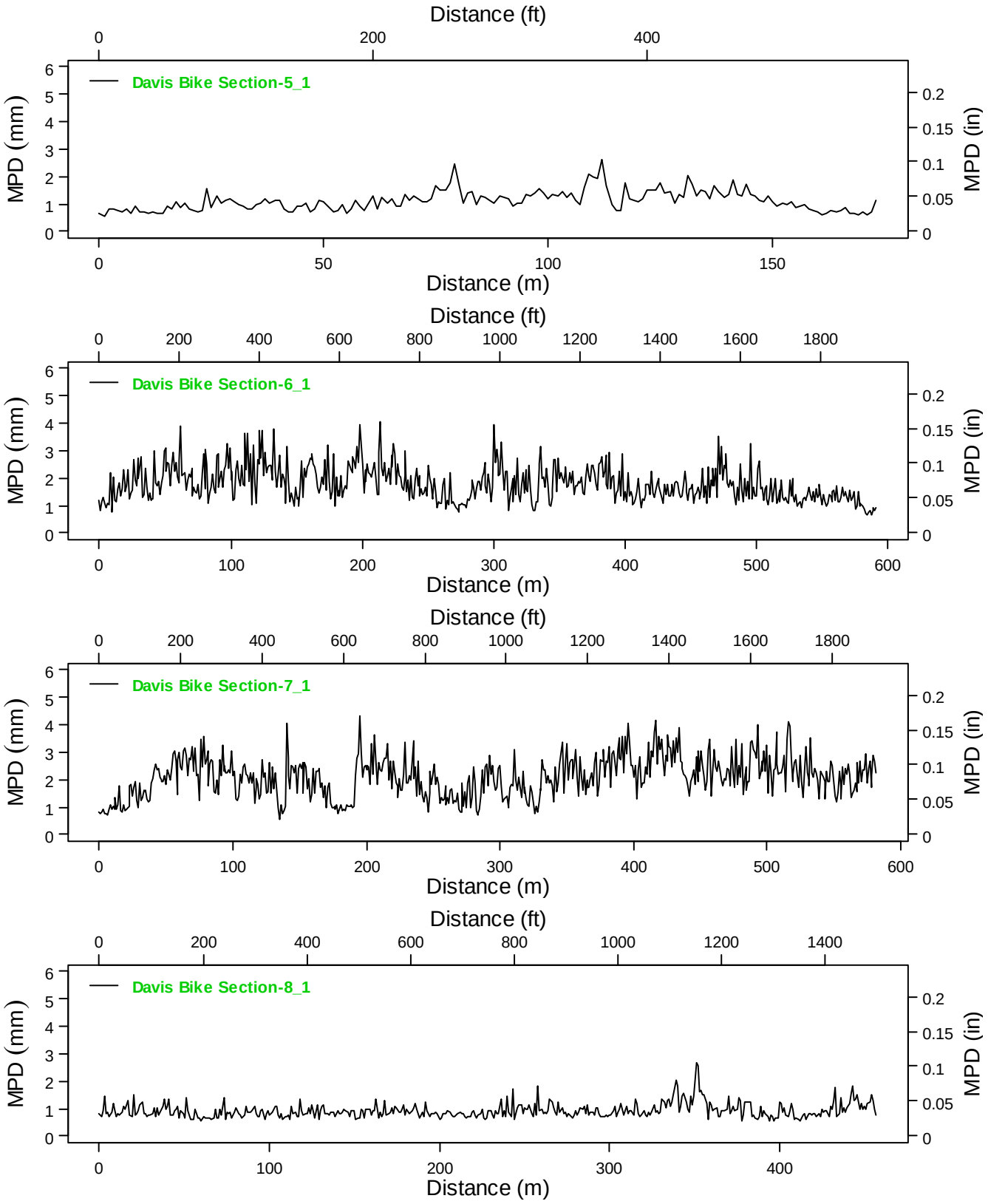

Figure B.2: Macrotexture measured using IP on Davis survey Sections 5 to 8.

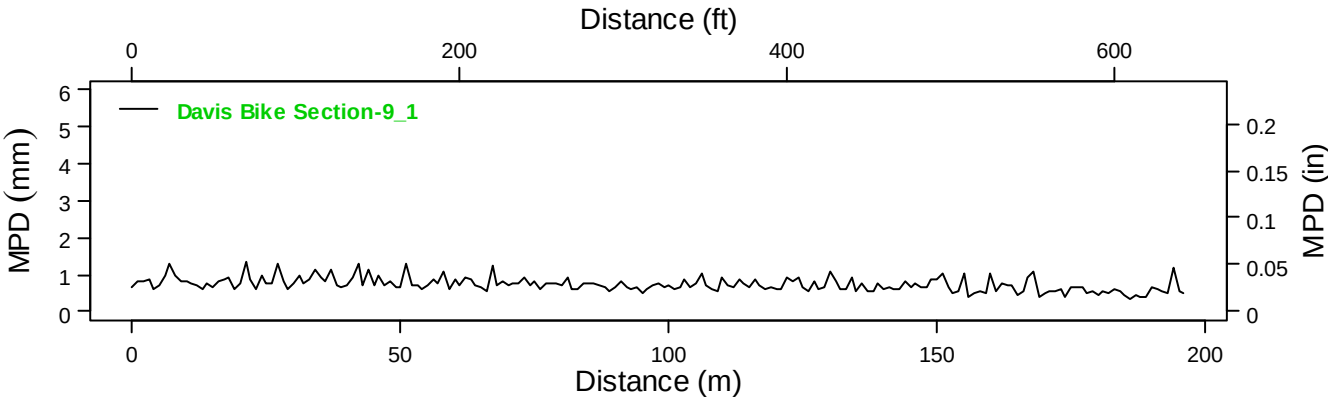

Figure B.3: Macrotexture measured using IP on Davis survey Section 9.

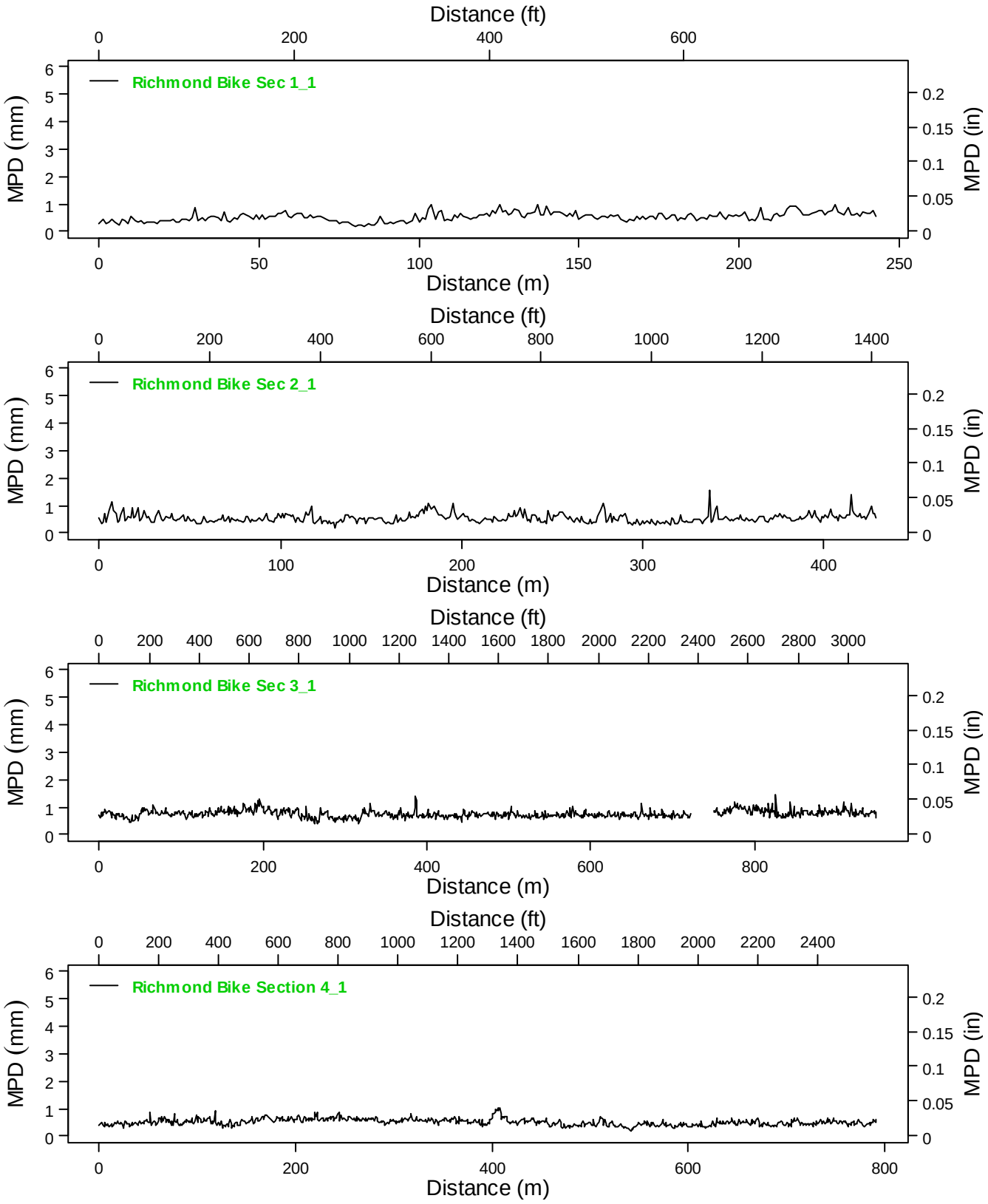

Figure B.4: Macrotexture measured using IP on Richmond survey Sections 1 to 4.

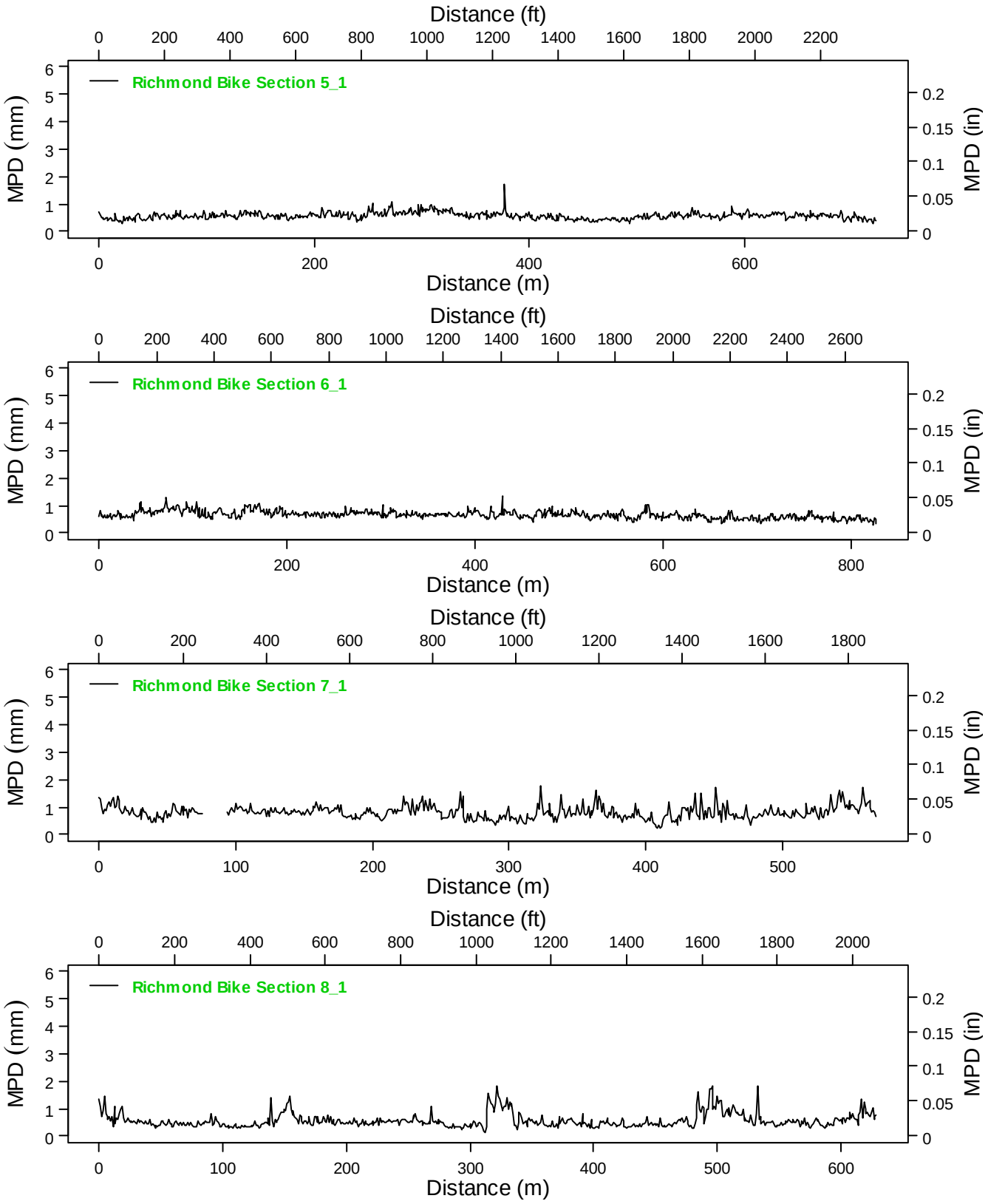

Figure B.5: Macrotexture measured using IP on Richmond survey Sections 5 to 8.

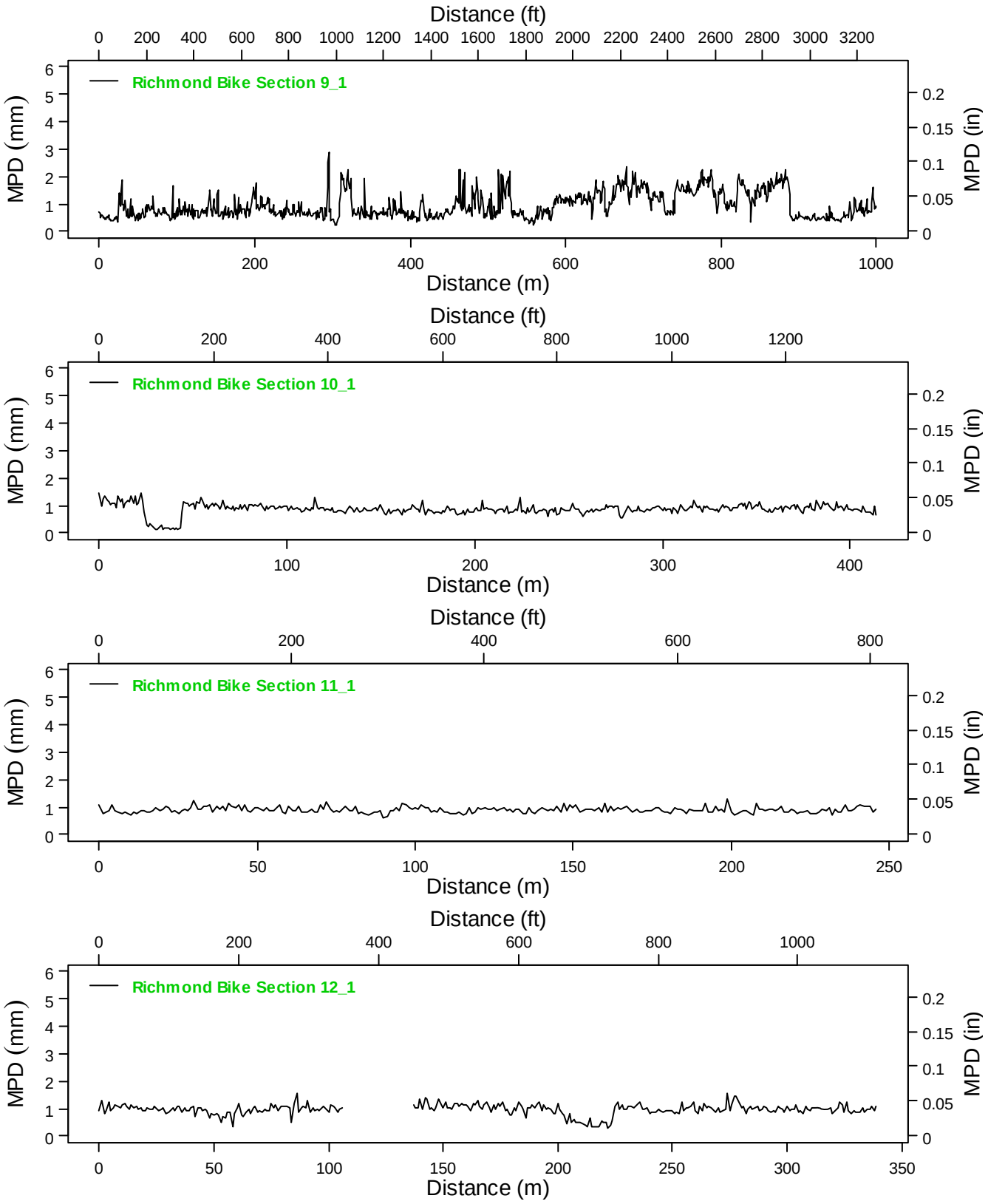

Figure B.6: Macrotexture measured using IP on Richmond survey Sections 9 to 12.

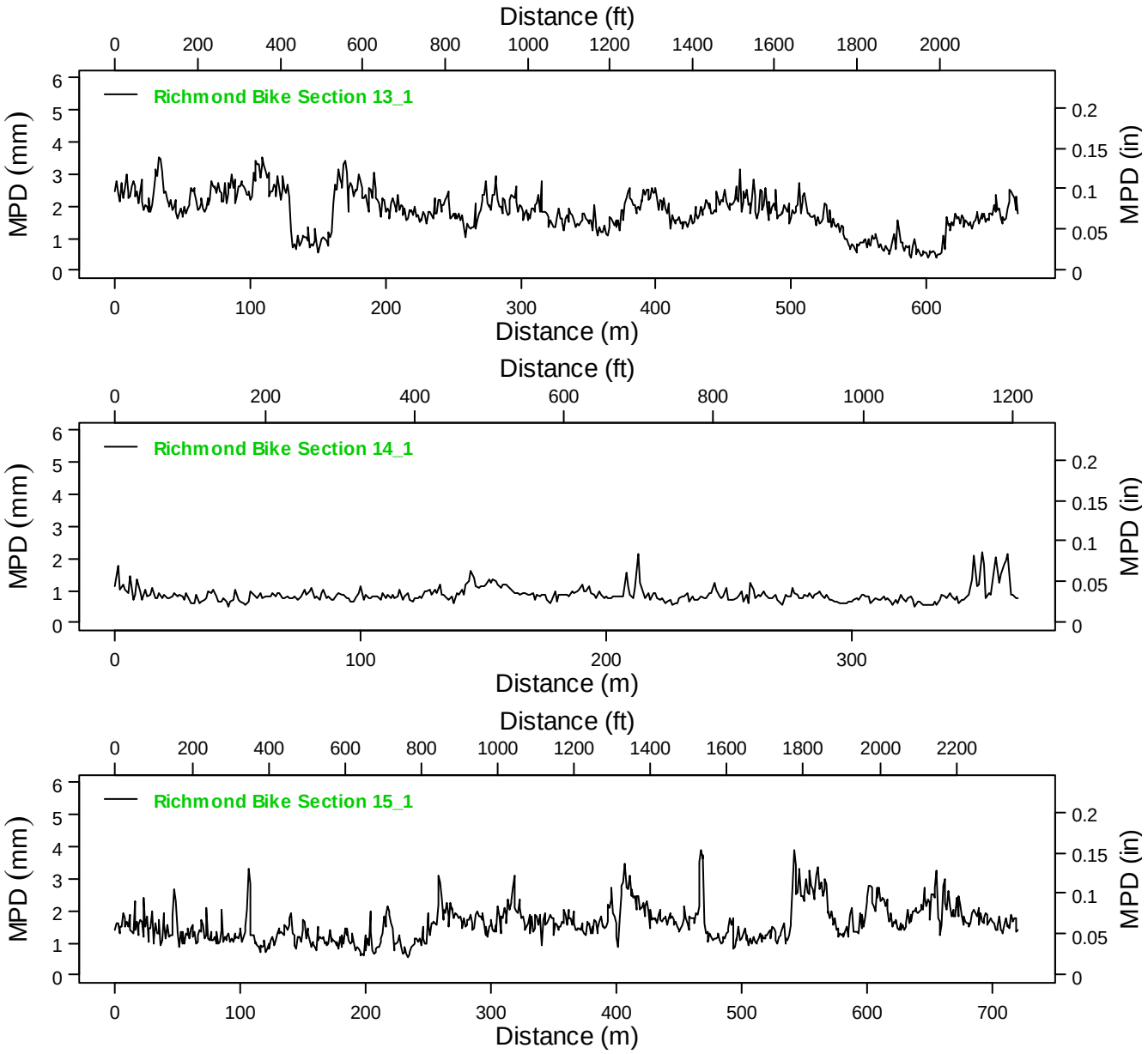

Figure B.7: Macrotexture measured using IP on Richmond survey Sections 13 to 15.

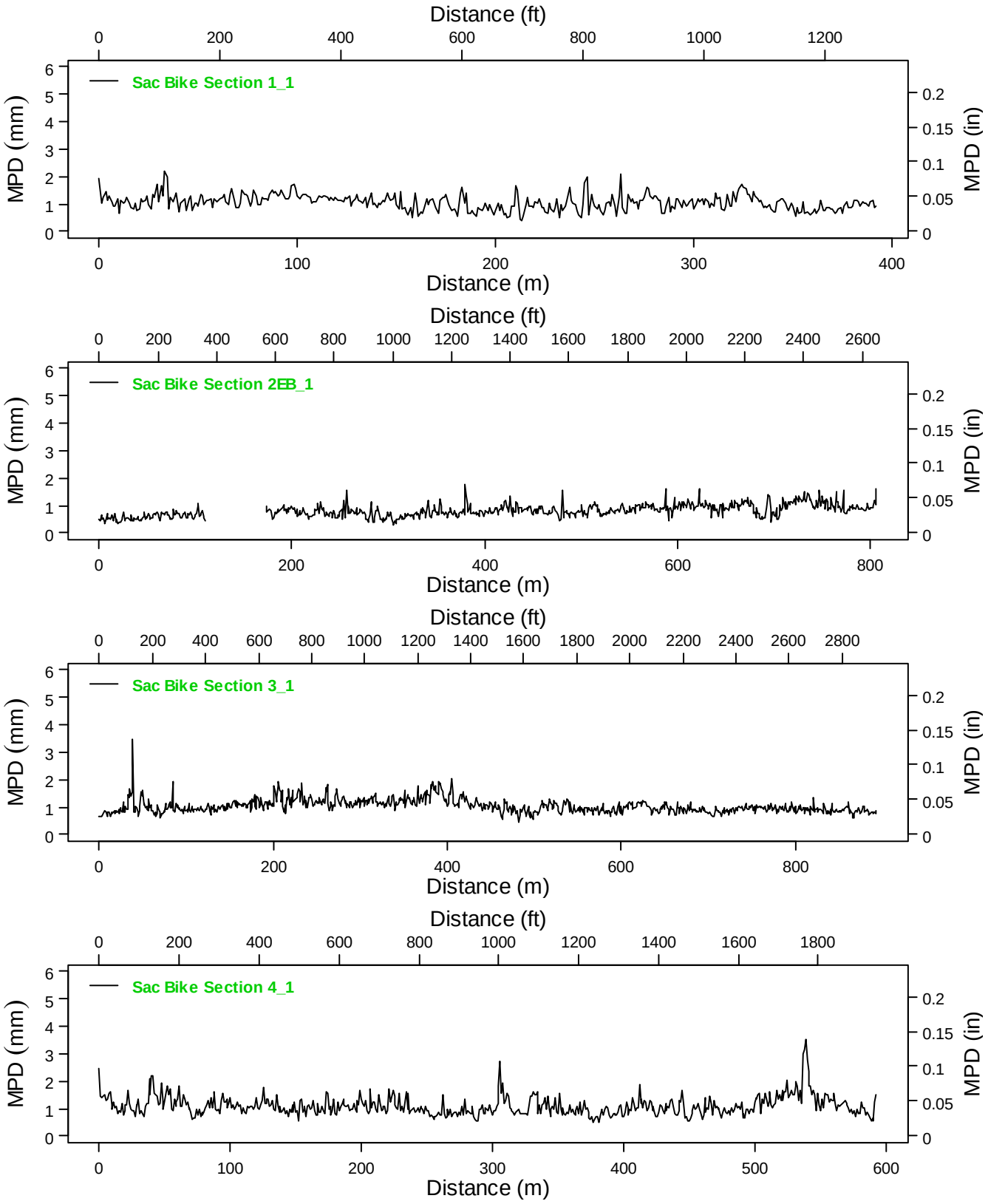

Figure B.8: Macrotexture measured using IP on Sacramento survey Sections 1 to 4.

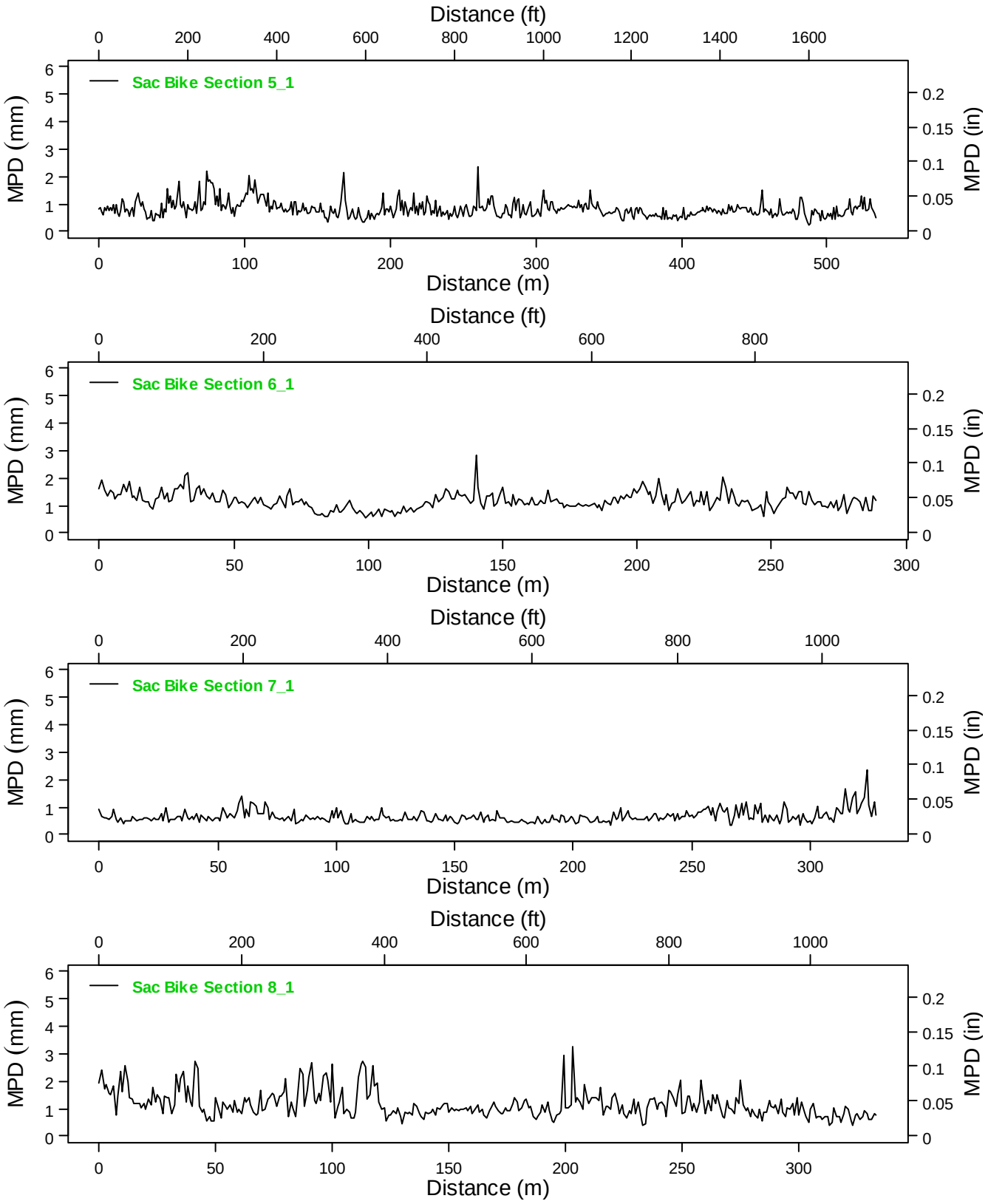

Figure B.9: Macrotexture measured using IP on Sacramento survey Sections 5 to 8.

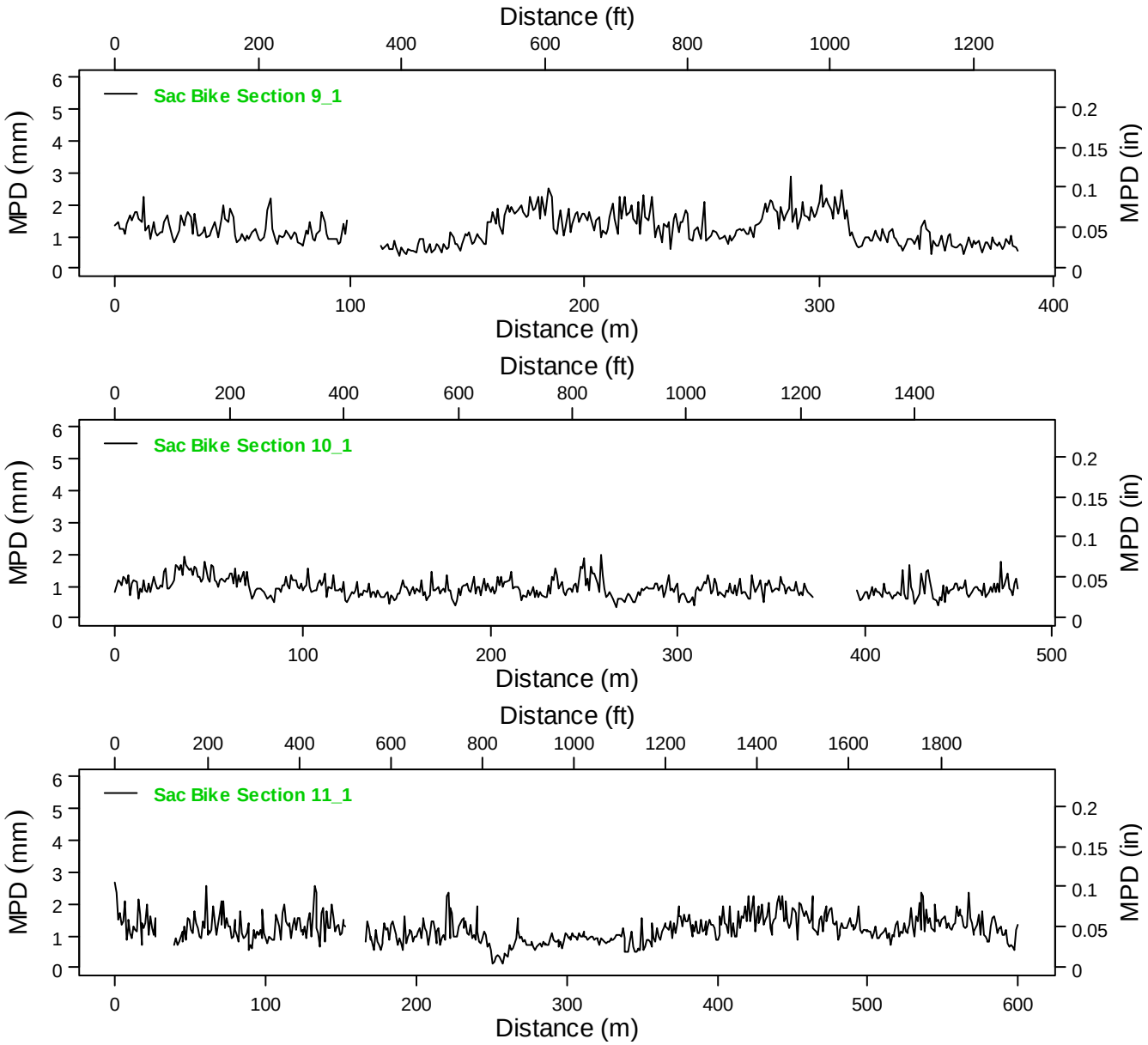

Figure B.10: Macrotexture measured using IP on Sacramento survey Sections 9 to 11.

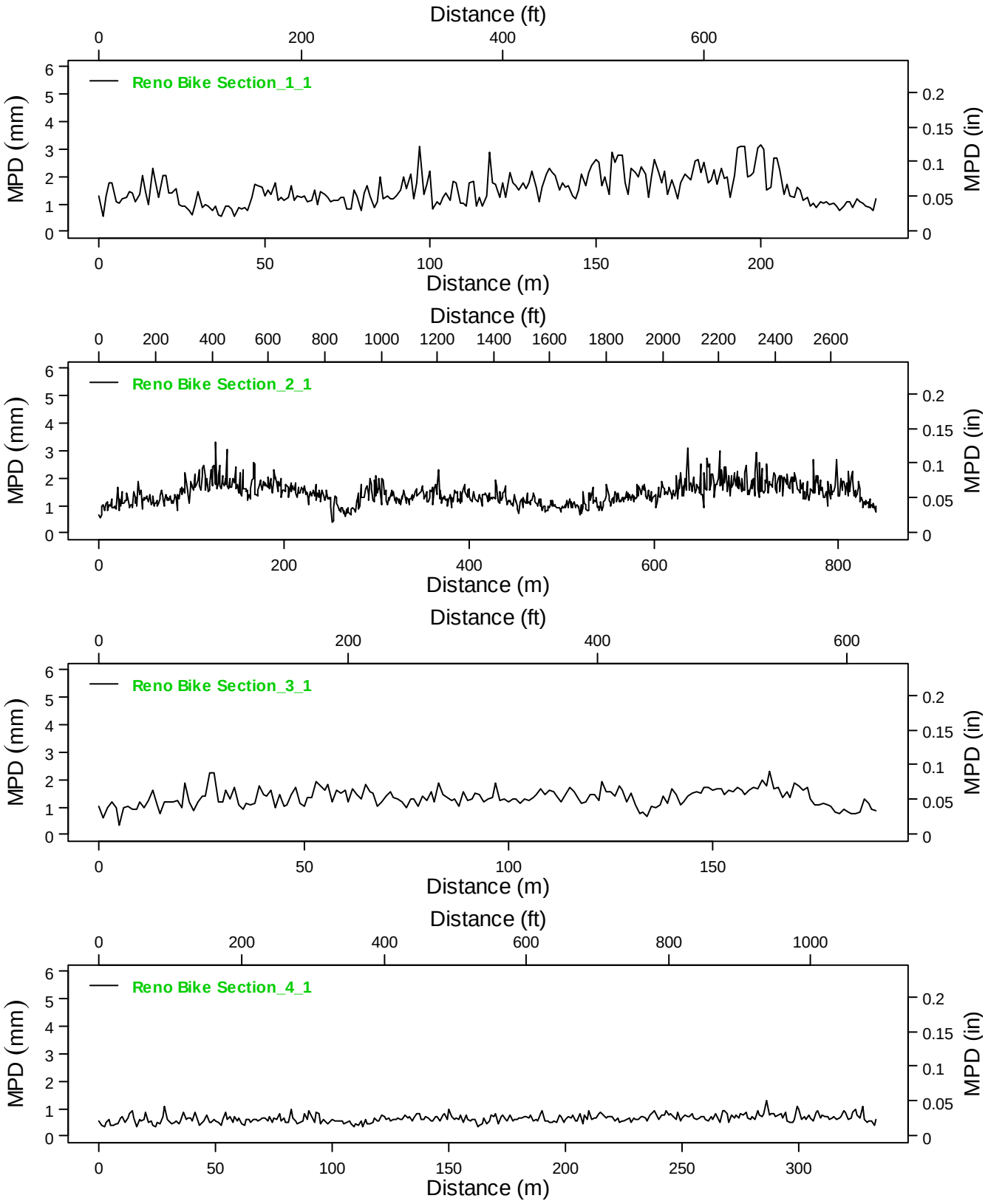

Figure B.11: Macrotexture measured using IP on Reno survey Sections 1 to 4.

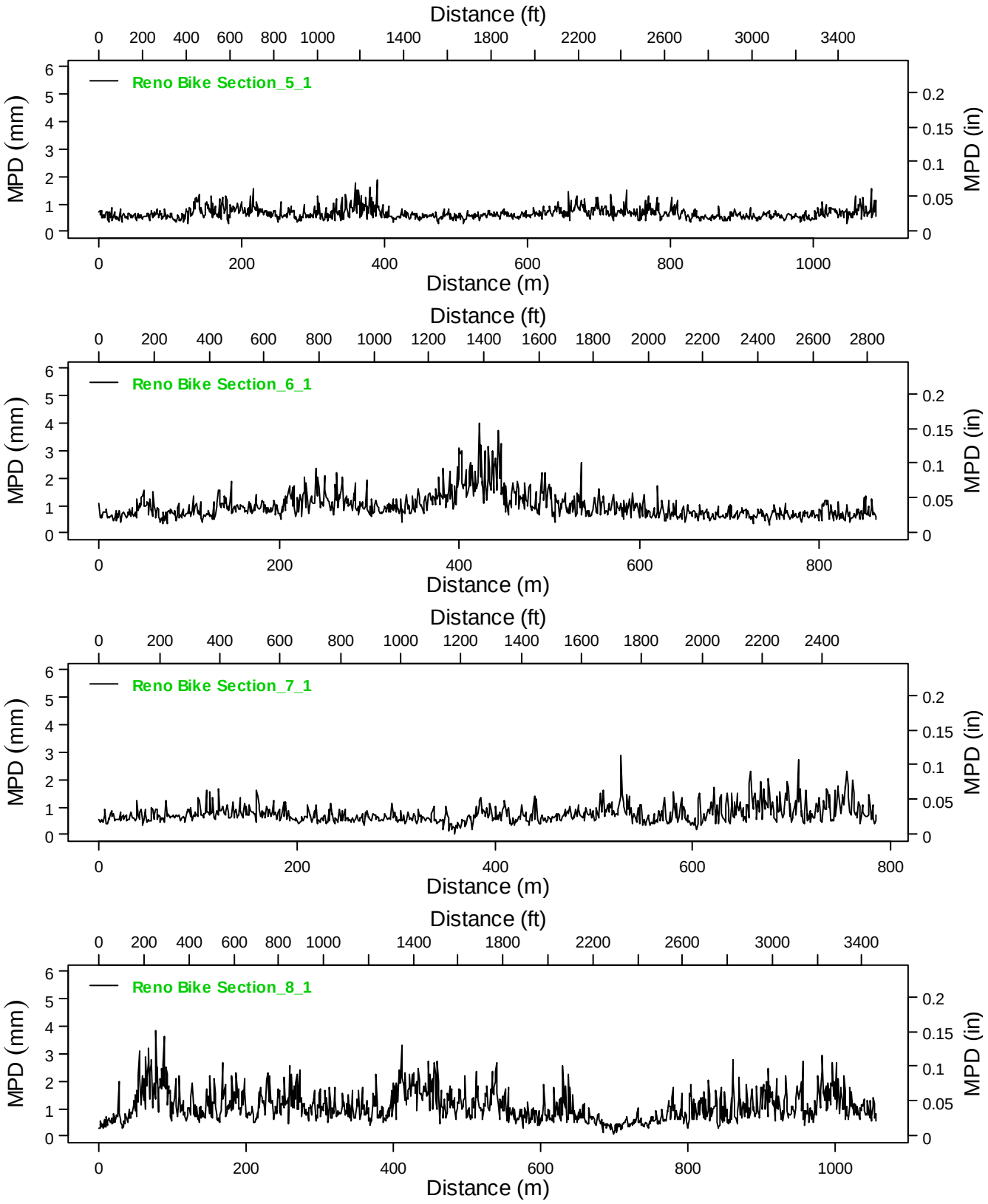

Figure B.12: Macrotexture measured using IP on Reno survey Sections 5 to 8.

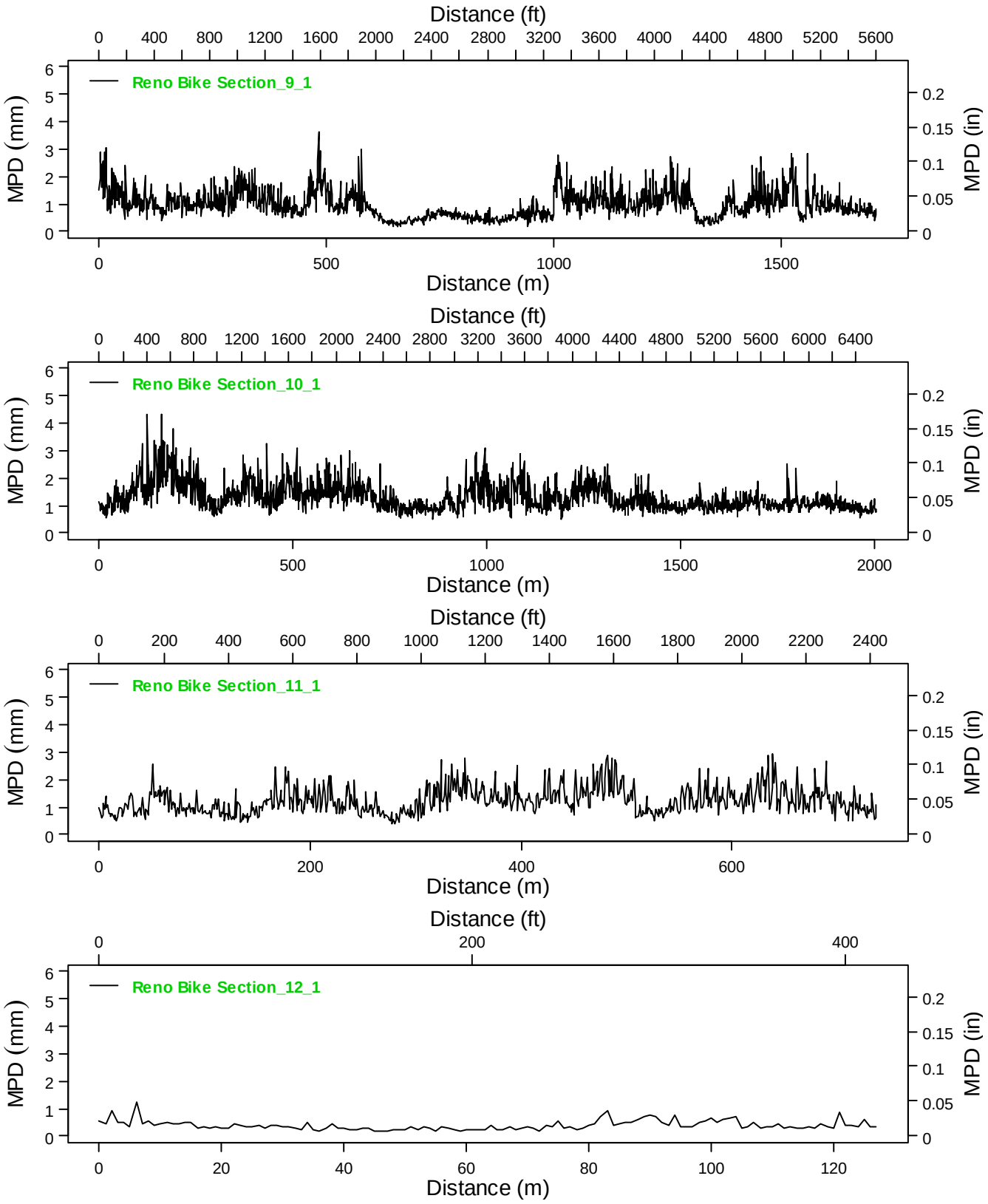

Figure B.13: Macrotexture measured using IP on Reno survey Sections 9 to 12.

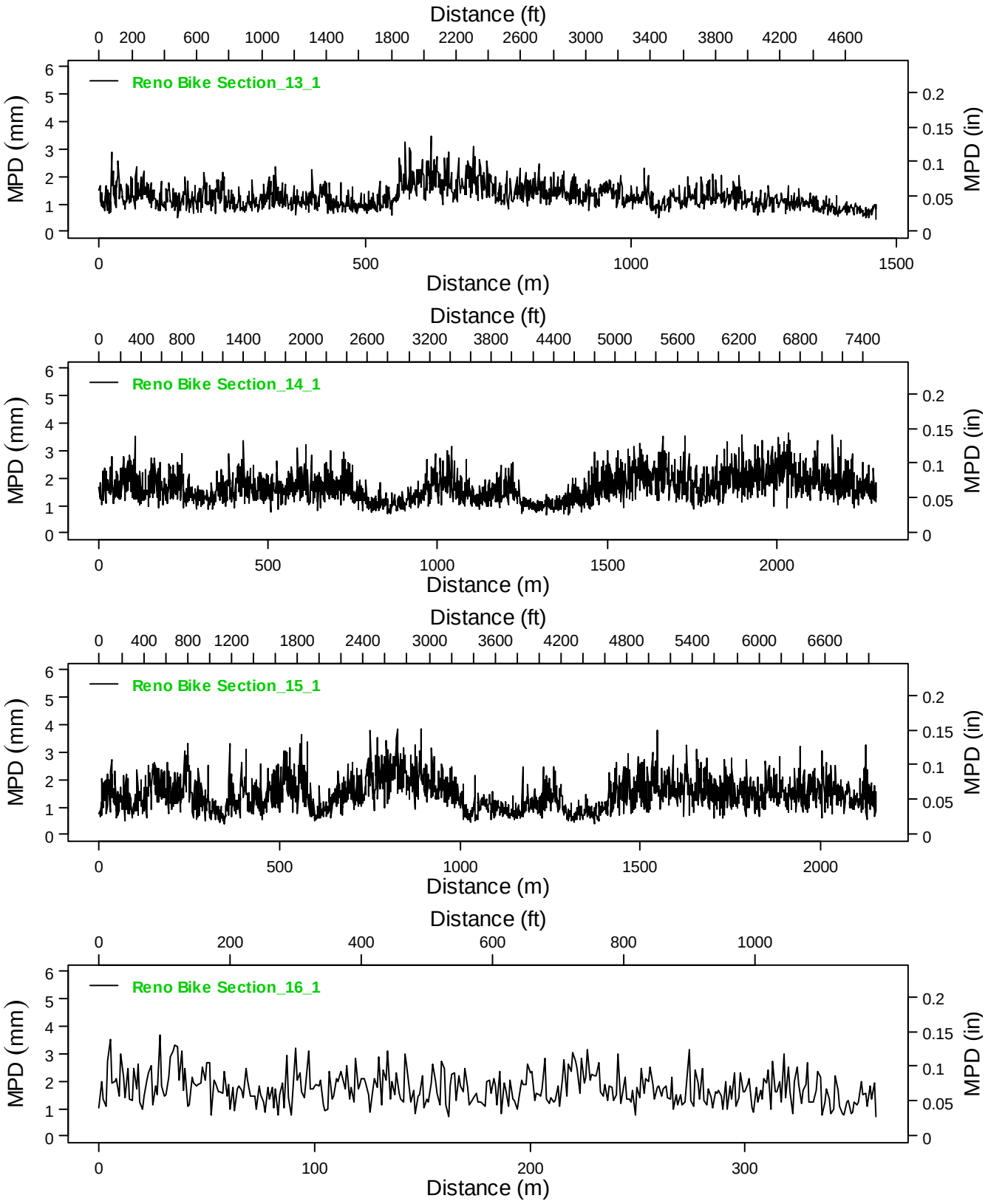

Figure B.14: Macrotexture measured using IP on Reno survey Sections 13 to 16.

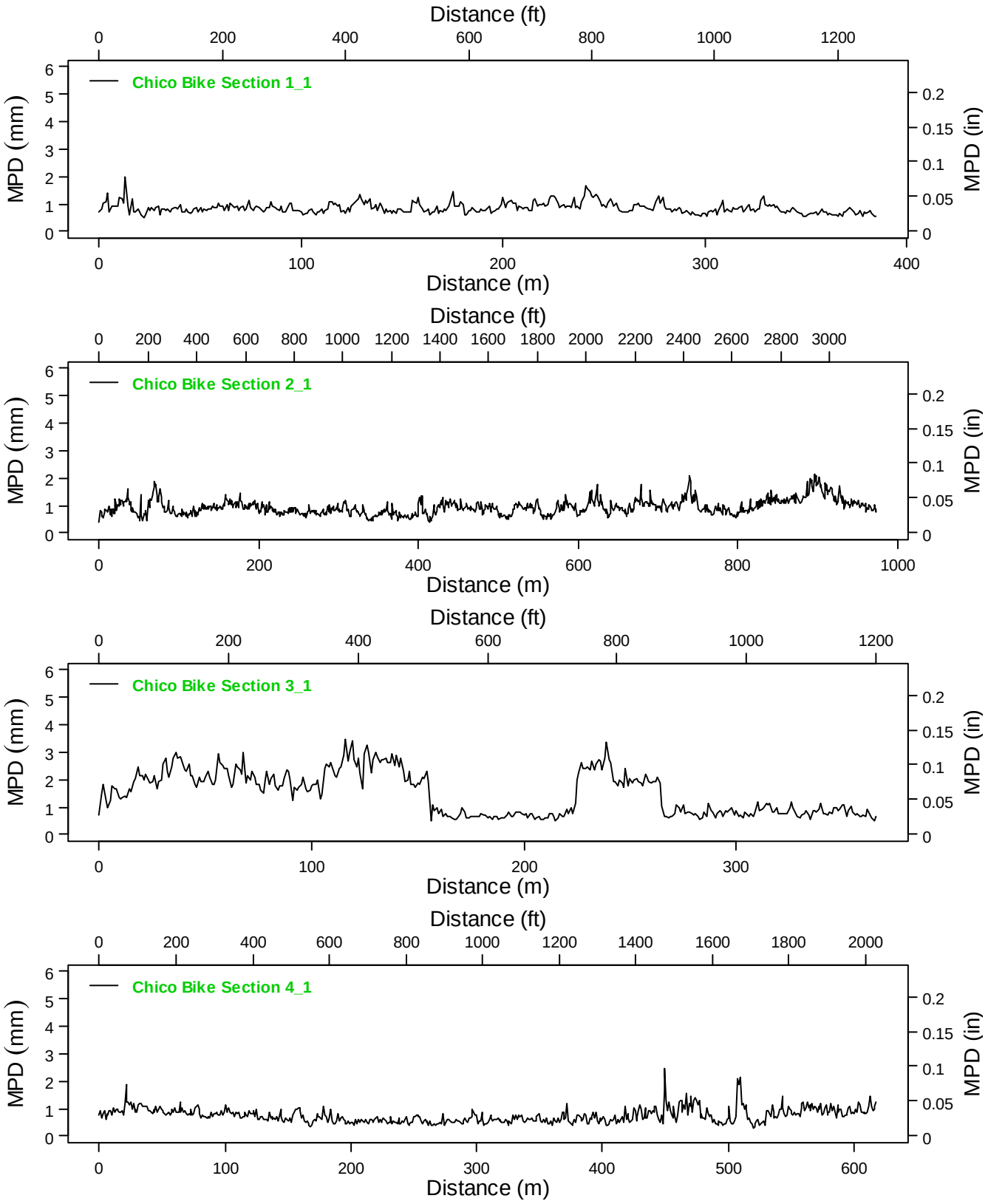

Figure B.15: Macrotexture measured using IP on Chico survey Sections 1 to 4.

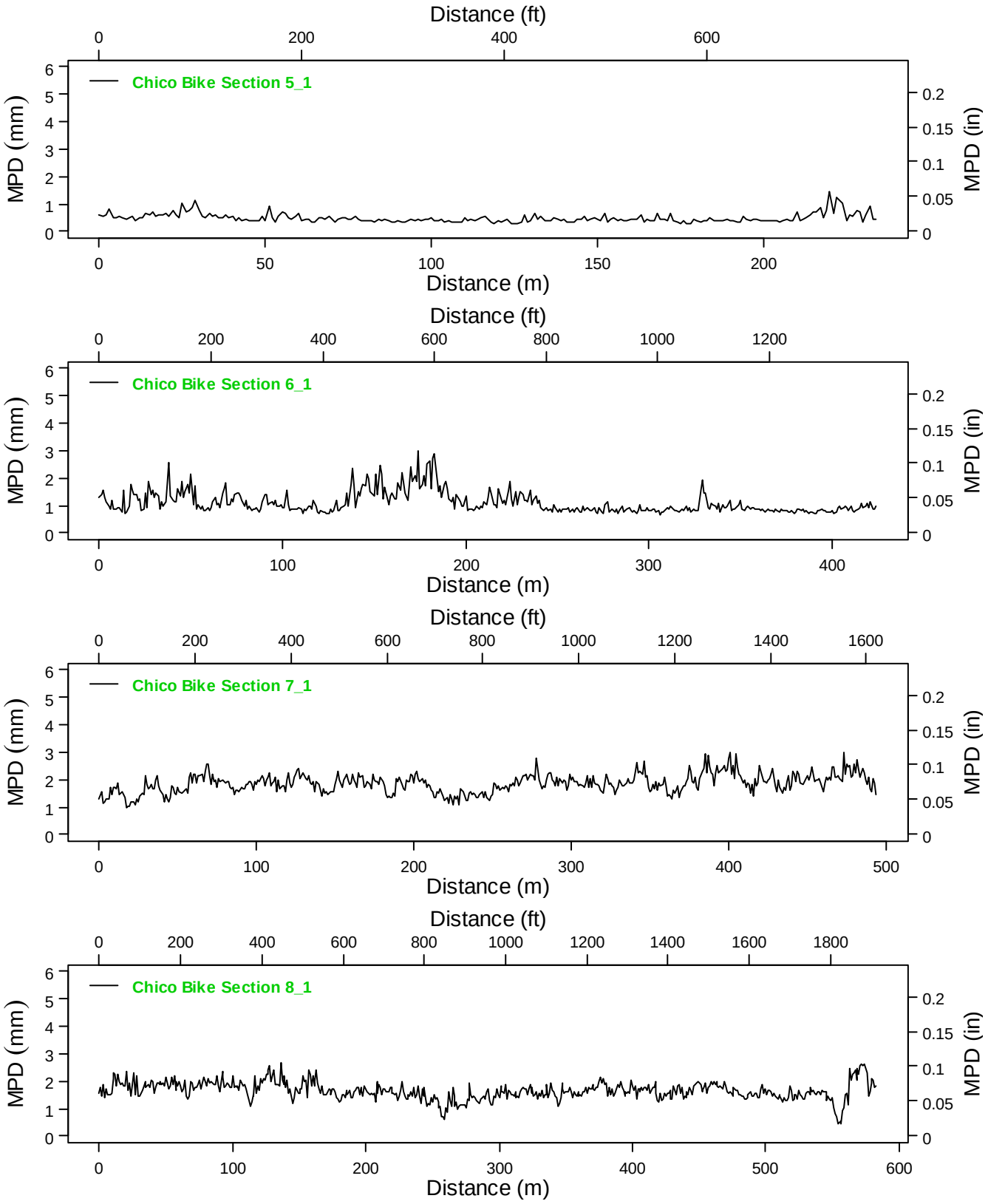

Figure B.16: Macrotexture measured using IP on Chico survey Sections 5 to 8.

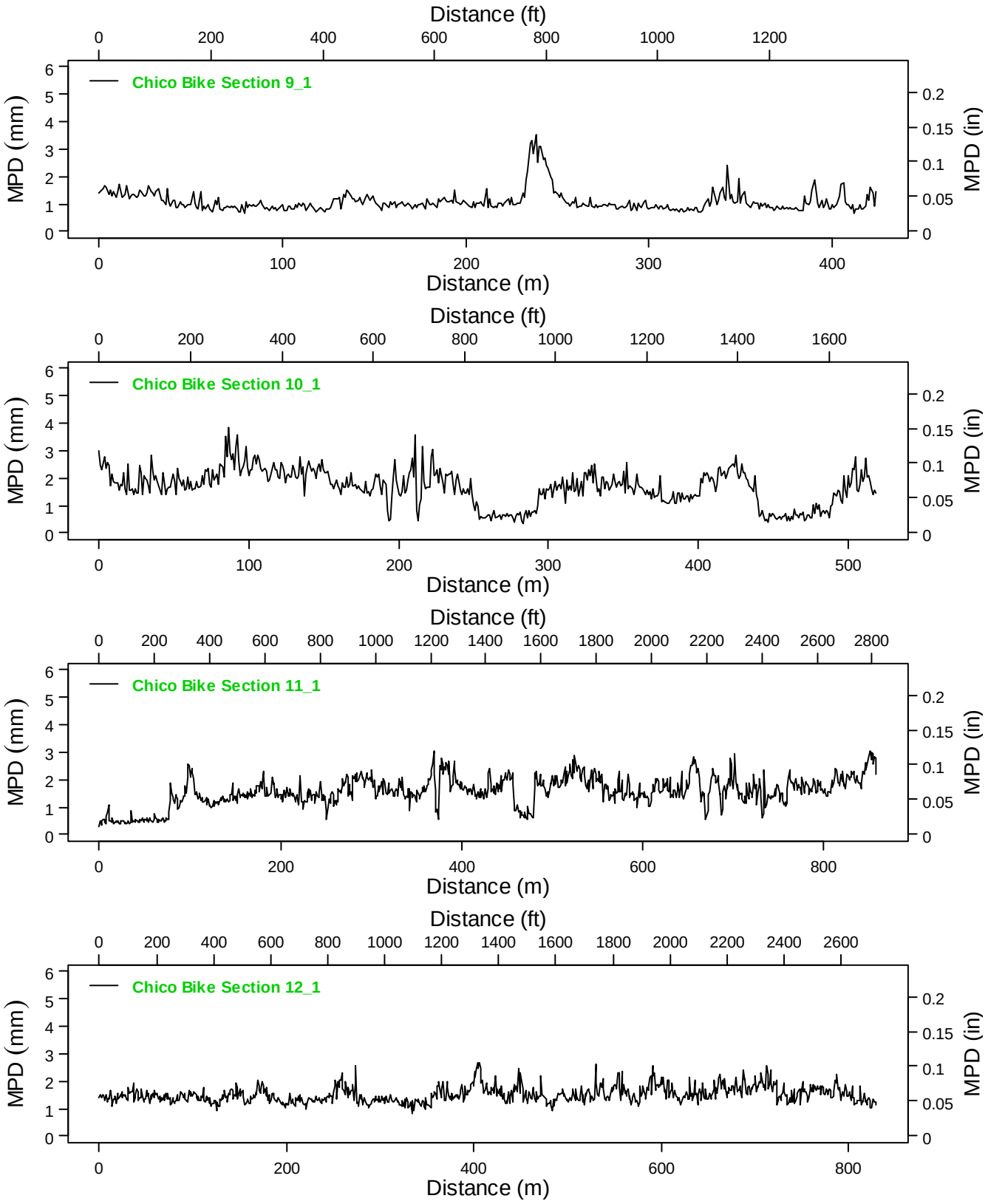

Figure B.17: Macrotexture measured using IP on Chico survey Sections 9 to 12.

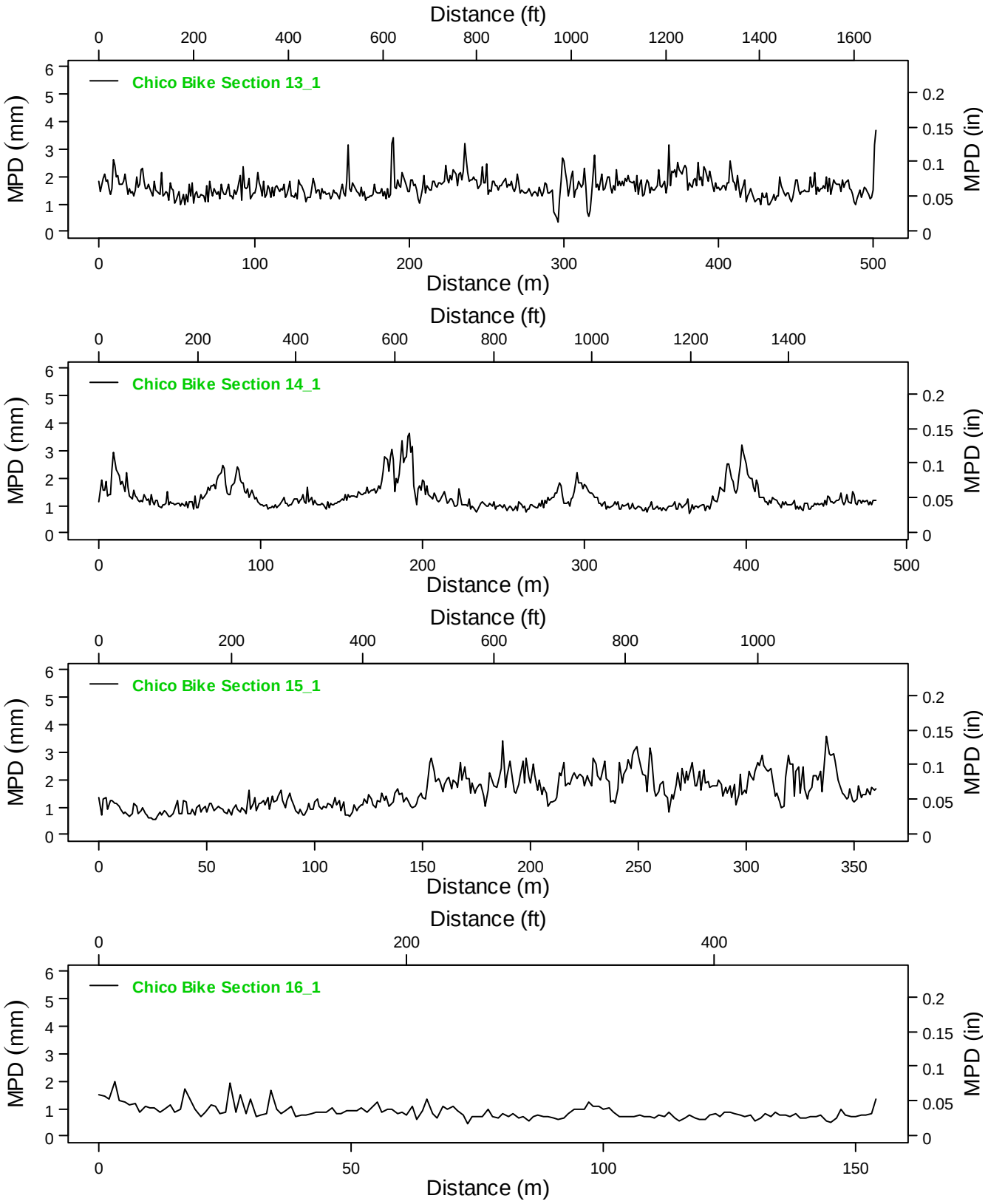

Figure B.18: Macrotexture measured using IP on Chico survey Sections 13 to 16.

APPENDIX C: PLOTS OF CORRELATIONS BETWEEN TEXTURE, VIBRATION, AND RIDE QUALITY BY BICYCLE TYPE FOR THIS STUDY

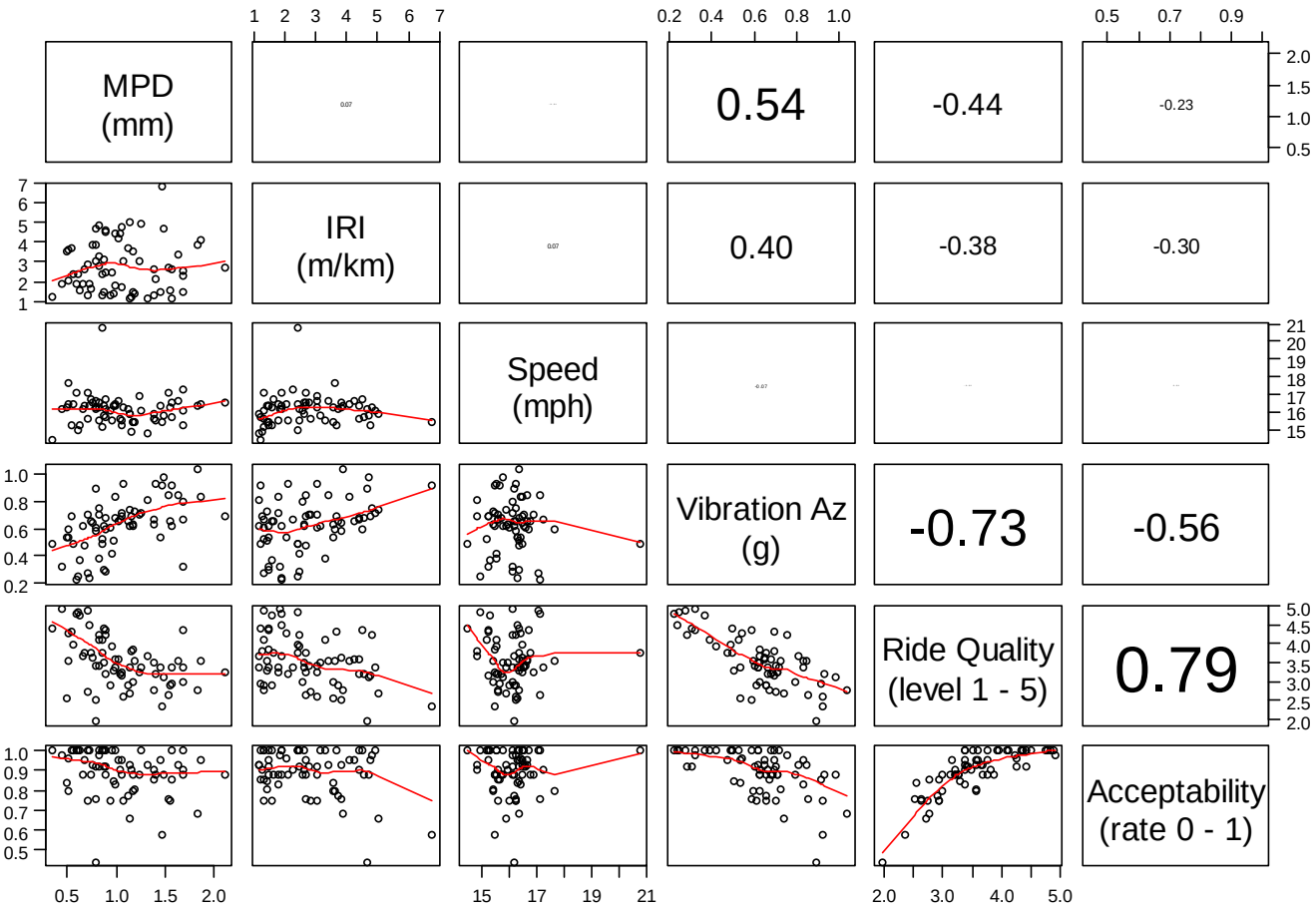

Figure C.1: Correlations between MPD, IRI, speed, vibration, ride quality level, and acceptability rate (second study, road bicycles).
(Note: **scatterplots and smooth fitted lines are shown in lower panels. Correlations between variables are shown in upper panels, with the size of the type within the box proportional to absolute correlation.)**

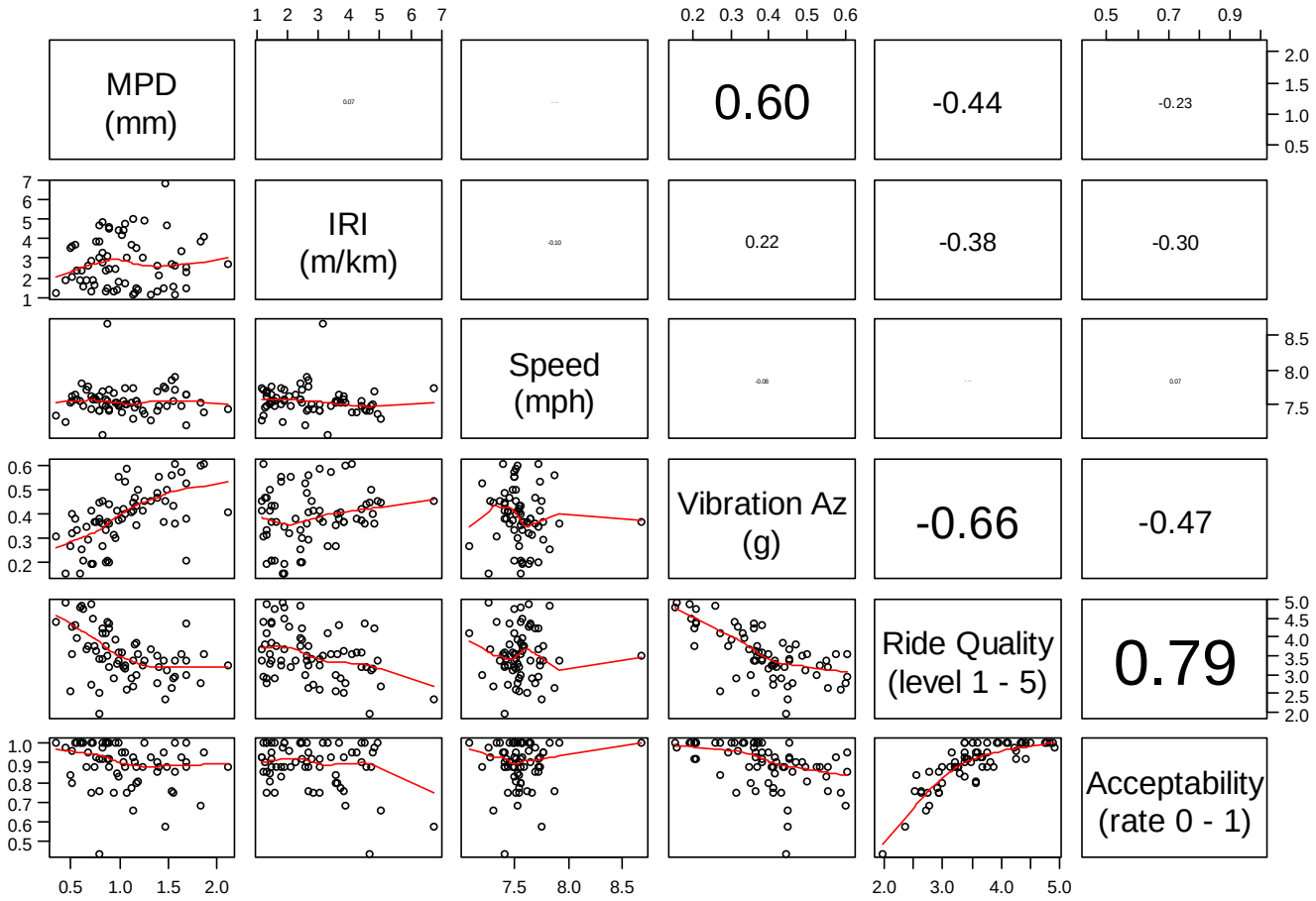

Figure C.2: Correlations between MPD, IRI, speed, vibration, ride quality level, and acceptability rate (second study, commuter bicycles).
(Note: **scatterplots and smooth fitted lines are shown in lower panels. Correlations between variables are shown in upper panels, with the size of the type within the box proportional to absolute correlation.)**

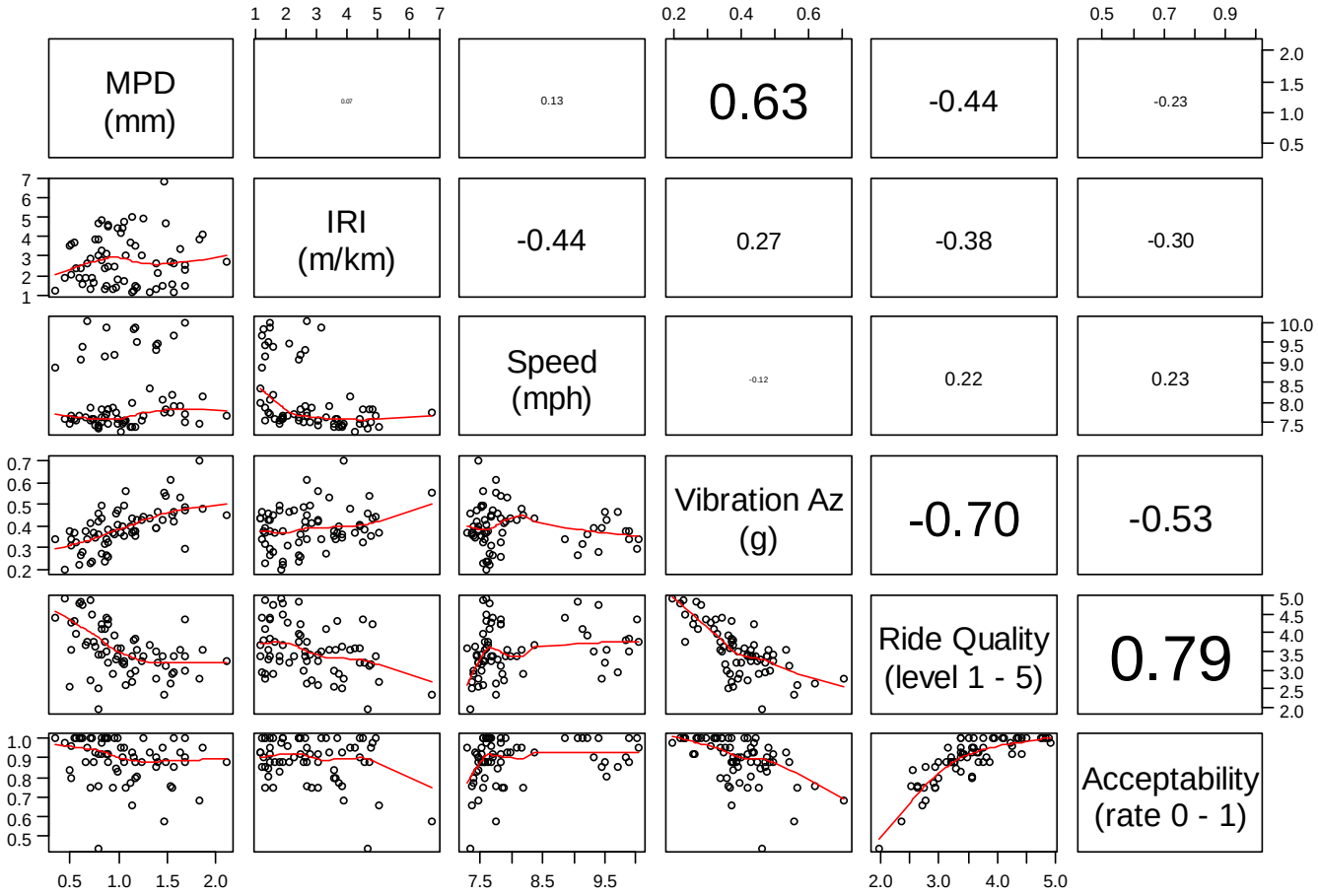

Figure C.3: Correlations between MPD, IRI, speed, vibration, ride quality level, and acceptability rate (second study, mountain bicycles).

(Note: **scatterplots and smooth fitted lines are shown in lower panels. Correlations between variables are shown in upper panels, with the size of the type within the box proportional to absolute correlation.)**

APPENDIX D: TEXTURE RESULTS OF STATE HIGHWAY SECTIONS

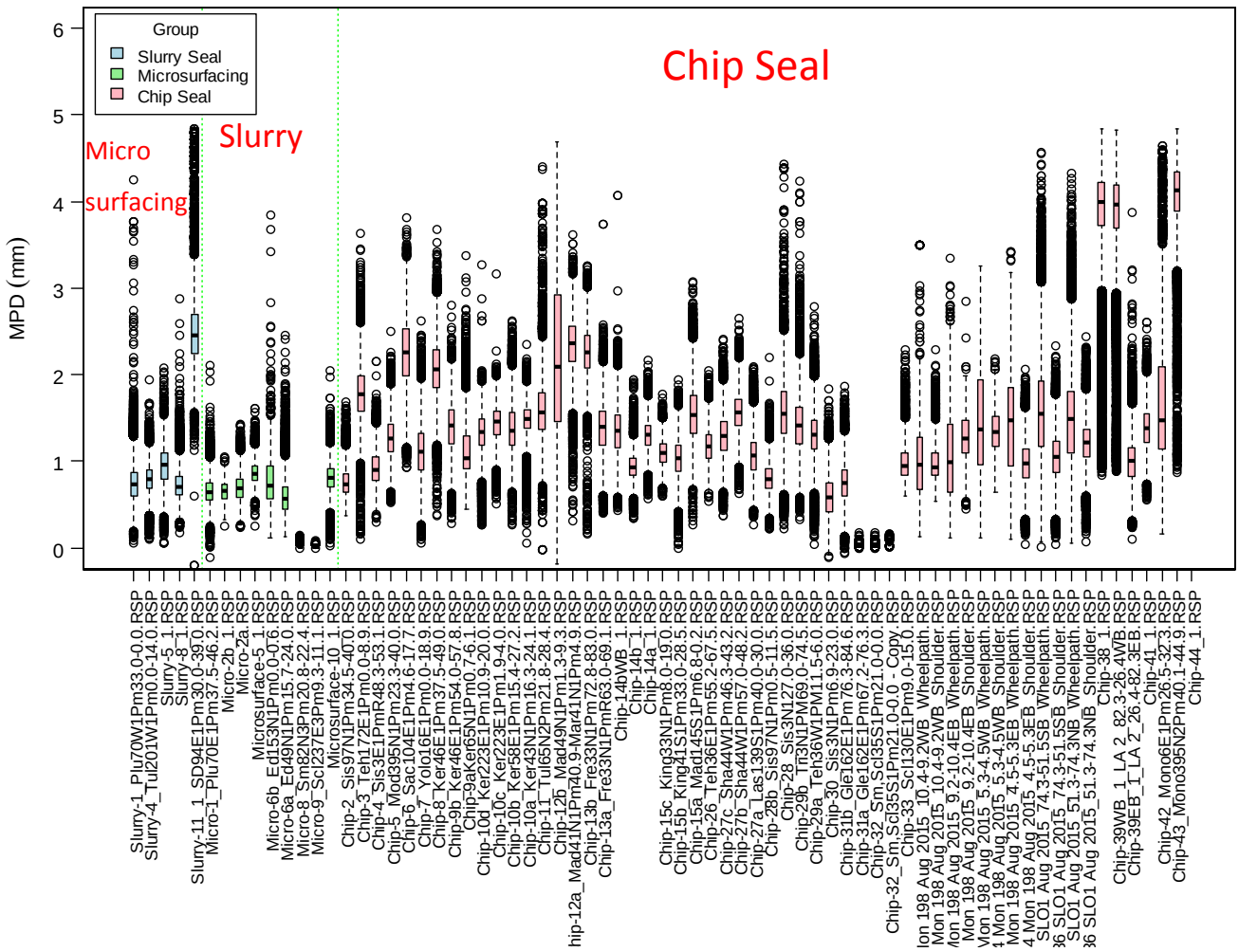

Figure D.1: Summary of MPD of state highway sections.

APPENDIX E: PAVEMENT DISTRESS SURVEY RESULTS

Location		Distress Type				Cracking Detail					
City	Section	Patching	Utility Cuts	Utilities	Cracking	Longitudinal	Fatigue	Transverse	Reflective	Block	Edge
Davis	1	0	0	0	2	1	1	2	1	1	1
Davis	2	0	0	0	2	1	1	2	1	1	1
Davis	3	1	0	0	2	1	1	2	2	1	1
Davis	4	0	0	0	1	1	1	1	1	1	1
Davis	5	0	0	0	2	1	1	3	1	1	1
Davis	6	0	0	1	1	1	1	1	1	1	1
Davis	7	1	0	1	2	1	1	2	2	1	1
Davis	8	1	1	0	1	2	1	2	1	1	2
Davis	9	0	0	0	1	1	1	1	1	1	1
City	Section	Patching	Utility Cuts	Utilities	Cracking	Longitudinal	Fatigue	Transverse	Reflective	Block	Edge
Richmond	1	1	0	0	1	1	1	1	1	1	1
Richmond	2	0	0	1	1	1	2	1	1	1	1
Richmond	3	0	0	1	2	1	1	2	1	1	1
Richmond	4	0	0	1	1	1	1	1	1	1	1
Richmond	5	0	0	0	1	1	1	1	1	1	1
Richmond	6	0	0	1	1	1	1	1	1	1	1
Richmond	7	0	0	1	2	2	2	2	1	1	1
Richmond	8	1	0	1	3	2	2	3	1	1	1
Richmond	9	1	0	1	3	2	2	3	1	1	1
Richmond	10	0	0	1	1	1	1	1	1	1	1
Richmond	11	0	0	0	1	1	1	1	1	1	1
Richmond	12	1	0	1	1	1	1	2	1	1	1
Richmond	13	1	1	1	3	1	3	2	1	1	1
Richmond	14	0	0	1	2	1	2	2	1	1	1
Richmond	15	0	0	1	3	2	2	3	1	1	1
City	Section	Patching	Utility Cuts	Utilities	Cracking	Longitudinal	Fatigue	Transverse	Reflective	Block	Edge
Sacramento	1	0	0	1	2	1	3	2	1	1	1
Sacramento	2	1	1	1	2	1	1	2	1	1	1
Sacramento	3	1	0	0	1	1	1	2	1	1	1
Sacramento	4	1	0	0	2	2	1	2	1	2	1
Sacramento	5	1	0	1	1	2	1	1	1	1	1
Sacramento	6	0	1	0	2	2	2	2	1	1	1
Sacramento	7	0	0	0	1	1	1	1	1	1	1
Sacramento	8	0	0	1	2	2	1	2	1	1	1
Sacramento	9	1	1	1	3	1	3	2	1	1	1
Sacramento	10	1	1	1	1	1	2	1	1	1	1
Sacramento	11	1	1	0	2	1	2	2	1	1	1
City	Section	Patching	Utility Cuts	Utilities	Cracking	Longitudinal	Fatigue	Transverse	Reflective	Block	Edge
Reno	1	0	0	1	1	1	1	2	1	1	1
Reno	2	0	0	1	2	2	1	2	1	1	1
Reno	3	0	0	0	1	1	1	1	1	1	1
Reno	4	1	0	1	1	1	1	1	1	1	1
Reno	5	1	0	1	2	2	1	2	1	1	1
Reno	6	0	0	1	1	1	1	1	1	1	1
Reno	7	1	0	0	2	1	1	2	1	1	1
Reno	8	1	0	1	1	1	1	2	1	1	1
Reno	9	1	0	1	2	1	1	2	1	1	1
Reno	10	1	1	1	1	1	1	1	1	1	1
Reno	11	1	0	1	1	1	1	1	1	1	1
Reno	12	0	0	1	1	1	1	1	1	1	1
Reno	13	0	0	1	1	1	1	1	1	1	1
Reno	14	0	0	1	1	2	1	1	1	1	1
Reno	15	0	0	0	3	3	1	2	1	1	1
Reno	16	0	0	1	1	1	1	1	1	1	1
City	Section	Patching	Utility Cuts	Utilities	Cracking	Longitudinal	Fatigue	Transverse	Reflective	Block	Edge
Chico	1	1	0	1	1	1	1	1	1	1	1
Chico	2	1	0	1	1	1	1	1	1	1	1
Chico	3	1	0	0	3	1	3	1	1	1	1
Chico	4	0	0	0	2	1	3	1	1	1	1
Chico	5	1	1	0	2	1	3	1	1	1	1
Chico	6	1	0	1	2	1	2	2	1	1	1

Location		Distress Type				Cracking Detail					
City	Section	Patching	Utility Cuts	Utilities	Cracking	Longitudinal	Fatigue	Transverse	Reflective	Block	Edge
Chico	7	0	0	0	1	1	1	1	1	1	1
Chico	8	0	0	0	1	1	1	1	1	1	1
Chico	9	1	0	0	2	1	1	2	1	1	1
Chico	10	0	1	1	1	1	1	2	1	1	1
Chico	11	1	0	0	1	1	1	2	1	1	1
Chico	12	0	0	1	1	1	1	1	1	1	1
Chico	13	0	0	1	1	1	1	2	1	1	1
Chico	14	1	0	0	1	1	1	2	1	1	1
Chico	15	1	0	1	2	1	2	2	1	1	1
Chico	16	1	0	1	2	1	2	2	1	1	1